การพัฒนาโซลิดลิปิดนาโนพาร์ทิเคิลของเอเซียติก แอซิด สำหรับนำส่งทางจมูก

นางสาวพิไลพร คุณธรรม

วิทยานิพนธ์นี้เป็นส่วนหนึ่งของการศึกษาตามหลักสูตรปริญญาเภสัชศาสตรมหาบัณฑิต
สาขาวิชาเภสัชอุตสาหกรรม ภาควิชาวิทยาการเภสัชกรรมและเภสัชอุตสาหกรรม
คณะเภสัชศาสตร์ จุฬาลงกรณ์มหาวิทยาลัย
ปีการศึกษา 2554

DEVELOPMENT OF ASIATIC ACID SOLID LIPID NANOPARTICLES FOR NASAL DELIVERY

Miss Pilaiporn Khunathum

A Thesis Submitted in Partial Fulfillment of the Requirements
for the Degree of Master of Science in Pharmacy Program in Industrial Pharmacy
Department of Pharmaceutics and Industrial Pharmacy
Faculty of Pharmaceutical Sciences
Chulalongkorn University
Academic Year 2011

Thesis Title	DEVELOPMENT OF ASIATIC ACID SOLID LIPID NANOPARTICLES FOR NASAL DELIVERY
By	Miss Pilaiporn Khunathum
Field of Study	Industrial Pharmacy
Thesis Advisor	Professor Garnpimol C. Ritthidej, Ph.D.
Thesis Co-advisor	Associate Professor Vimolmas Lipipun, Ph.D.

Accepted by the Faculty of Pharmaceutical Sciences, Chulalongkorn University in Partial Fulfillment of the Requirements for the Master's Degree

...…….. Dean of the Faculty of Pharmaceutical Sciences

(Associate Professor Pintip Pongpech, Ph.D.)

THESIS COMMITTEE

……. Chairman

(Associate Professor Uthai Suvanakoot, Ph.D.)

……. Thesis Advisor

(Professor, Garnpimol C. Ritthidej, Ph.D.)

……. Thesis Co-advisor

(Associate Professor Vimolmas Lipipun, Ph.D.)

…….. Examiner

(Associate Professor Kraisri Umprayn, Ph.D.)

…….. Examiner

(Associate Professor Parkpoom Tengamnuay, Ph.D.)

…….. External Examiner

(Saraporn Harikarnpukdee , Ph.D.)

พิไลพร คุณธรรม : การพัฒนาโซลิดลิปิดนาโนพาร์ทิเคิลของเอเซียติก แอซิด สำหรับนำส่งทางจมูก. (DEVELOPMENT OF ASIATIC ACID SOLID LIPID NANOPARTICLES FOR NASAL DELIVERY) อ.ที่ปรึกษาวิทยานิพนธ์หลัก: ศ. ดร.กาญจน์พิมล ฤทธิเดช, อ.ที่ปรึกษาวิทยานิพนธ์ร่วม: รศ. ดร. วิมลมาศ ลิปิพันธ์, 209 หน้า.

การศึกษานี้มีวัตถุประสงค์เพื่อเตรียมสูตรตำรับโซลิดลิปิดนาโนพาร์ทิเคิล (เอสแอลเอ็น) ของเอเซียติก แอซิด เพื่อใช้ในการนำส่งยาเข้าสู่สมองผ่านทางจมูก ในเบื้องต้นเอสแอลเอ็นถูกเตรียมโดยวิธีโฮโมจีไนเซชันอุณหภูมิสูง ซึ่งประกอบด้วยไขมันแข็งหกชนิด ได้แก่ ไตรมัยริสติน, ไตรสเตียริน, คอมพลิทอล 888, ไฮโดรจิเนตปาล์มออยล์, ปาล์มมิติก แอซิด และ สเตียริก แอซิด ทวีน 80 ถูกใช้เป็นสารลดแรงตึงผิวหลัก พอลอกซาเมอร์ 188, สแปน 80, สแปน 85 และ โซลูทอล เอ็ช เอส 15 ถูกใช้เป็นสารลดแรงตึงผิวร่วม หลังจากเตรียมสูตรตำรับเอสแอลเอ็นที่ปราศจากยาแล้วนำไปทดสอบในสภาวะเร่งพบว่ามี 25 สูตรตำรับที่มีความคงตัวและเอสแอลเอ็นซึ่งประกอบด้วยปาล์มมิติก แอซิด และ สเตียริก แอซิด ไม่สามารถเตรียมและให้ความคงตัวภายหลังจากเก็บในสภาวะเร่งได้ จากนั้นนำสูตรตำรับที่ได้ไปเตรียมเอส แอลเอ็นของเอเซียติก แอซิดและประเมินคุณสมบัติทางกายภาพและทางเคมี รวมทั้งศึกษาความคงตัวของสูตรตำรับที่อุณหภูมิ 4 องศาเซลเซียส, อุณหภูมิห้องและ 45 องศาเซลเซียส เป็นระยะเวลาหกเดือน เอสแอลเอ็นของเอเซียติก แอซิด มีขนาดอนุภาคเฉลี่ยอยู่ในช่วง 34.53±0.81 ถึง 186.50±2.23 นาโนเมตรและมีขนาดเพิ่มขึ้นเมื่อถูกหุ้มด้วยไคโตซาน ค่าความต่างศักย์ระหว่างพื้นผิวอนุภาคมีค่าเป็นลบเล็กน้อยและมีค่าเป็นบวกเล็กน้อยเมื่อถูกหุ้มด้วยไคโตซาน ค่าความเป็นกรด-เบส อยู่ในช่วง 4.5-6.5 ซึ่งเหมาะสมต่อการใช้สำหรับในการนำส่งยาทางจมูกและมีค่าลดลงเล็กน้อยเมื่อถูกหุ้มด้วยไคโตซาน เอสแอลเอ็นของเอเซียติก แอซิด แสดงคุณสมบัติในการเก็บกักยาสูงมากกว่าร้อยละ 95 ค่าความหนืดอยู่ในช่วง 0.8967 ± 0.07 ถึง 1.3853 ± 0.07 เซนติป้วส์ และแสดงคุณสมบัติการไหลเป็นแบบนิวโตเนียนเช่นเดียวกับสูตรตำรับที่ถูกหุ้มด้วยไคโตซาน ซึ่งความหนืดมีค่าคงที่ไม่แปรผันกับแรงที่ให้ต่อหน่วยเวลา การประเมินคุณสมบัติของยาในไขมันแข็งโดยวิธีดีเอสซีและเอกซเรย์ดิฟแฟลกชันพบว่า เอเซียติก แอซิดกระจายตัวอยู่ในเอสแอลเอ็นในรูปแบบอะมอฟัส การศึกษาการยึดเกาะของเอสแอลเอ็นของเอเซียติก แอซิดเมื่อเปรียบเทียบกับสูตรตำรับที่ถูกหุ้มด้วยไคโตซานพบว่าไคโตซานจะช่วยเพิ่มคุณสมบัติในการยึดเกาะได้ดีกว่า โดยแปรผันตามความเข้มข้นของไคโตซานที่ใส่ในสูตรตำรับ การศึกษาการส่งผ่านของเอสแอลเอ็นไม่พบความแตกต่างระหว่างก่อนและหลังทำการทดลองของค่าคงที่ความต้านทานทางไฟฟ้าผ่านชั้นเดี่ยวของเซลล์ซีซีแอล 30 ค่าเปอร์เซ็นต์การรอดชีวิตของซีซีแอล 30 ภายหลังการทดลองมากกว่าร้อยละ 90 ซึ่งสอดคล้องกับการทดลองความเป็นพิษต่อเซลล์โดยวิธีเอ็มทีที สูตรตำรับที่ประกอบด้วยไตรมัยริสตินเป็นไขมันแข็งโดยใช้ทวีน 80 และ สแปน 85 เป็นสารลดแรงตึงผิวพบว่าสามารถนำส่งยาเข้าในเซลล์และส่งผ่านเซลล์มากกว่าตำรับที่ประกอบด้วยไฮโดรจิเนตปาล์มออยล์เป็นไขมันแข็งโดยใช้ ทวีน 80 และ สแปน 85 เป็นสารลดแรงตึงผิว แต่หลังจากถูกหุ้มด้วยไคโตซานพบว่าสูตรตำรับสามารถนำส่งยาเข้าในเซลล์มากกว่าแต่ส่งผ่านเซลล์น้อยกว่าเมื่อเปรียบเทียบกับสูตรที่ไม่ถูกหุ้มซึ่งสอดคล้องกับการศึกษาการส่งผ่านของยาในเซลลูโลส แอซีเตท 0.2 นาโนเมตร

ภาควิชา วิทยาการเภสัชกรรมและเภสัชอุตสาหกรรม ลายมือชื่อนิสิต .....

สาขาวิชา เภสัชอุตสาหกรรม ลายมือชื่อ อ.ที่ปรึกษาวิทยานิพนธ์หลัก .....

ปีการศึกษา 2554 ลายมือชื่อ อ.ที่ปรึกษาวิทยานิพนธ์ร่วม .....

5176575633 : MAJOR INDUSTRIAL PHARMACY
KEYWORDS : asiatic acid/ solid lipid nanoparticles / high pressure homogenizer / chitosan / human nasal epithelial carcinoma cell line

PILAIPORN KHUNATHUM: DEVELOPMENT OF ASIATIC ACID SOLID LIPID NANOPARTICLES FOR NASAL DELIVERY. ADVISOR: PROF. GARNPIMOL C. RITTHIDEJ, Ph.D., CO-ADVISOR: ASSOC. PROF. VIMOLMAS LIPIPUN, Ph.D., 209 pp.

The purpose of this study was to prepare asiatic acid solid lipid nanoparticles (AA-SLN) for nasal delivery to brain. The SLN were preliminary prepared by hot high-pressure homogenization method composed of six solid lipids referred to trimyristin (TM), tistearin (TS), glyceryl behenate (GB), hydrogenated palm oil (SOF), palmitic acid (PA) and stearic acid (SA). Tween80 (TW80) was used as surfactant and poloxamer 188 (PL188), span80 (SP80), span85(SP85) and solutol HS15 (SL) were used as co-surfactants. After storage at accelerated condition, 25 formulations were maintained stabilized products. Palmitic acid and stearic acid could not produced stabilized formulations at all. Then asiatic acid was loaded SLN (AA-SLN) were prepared to determine physicochemical properties and stability at 4° C, room temperature and 45° C for 6 months. The particle size range from 34.53 $\pm$ 0.81 to 186.50 $\pm$ 2.23 nm. Larger sizes were obtained after coating with by chitosan. The zeta potential showed slightly negative charged and tended to slightly positive charged after coating with chitosan. The pH values were in the range of 4.5-6.5 which are suitable for used in nasal delivery route, they were slightly decreased when coating with chitosan. The entrapment efficiency of AA-SLN demonstrated high % entrapment efficiency of more than 95% w/w. Viscosity were in the range of 0.90 $\pm$ 0.07 to 1.39 $\pm$ 0.07 cps. The formulations showed newtonian flow characteristic that consistently exists between viscosity and shear rate as same as in CT/AA-SLN. The results of DSC and X-ray diffractions were corresponding similar that after AA was incorporated into SLN, the drug was not in crystalline state but in amorphous state. CT/AA-SLN displayed to enhance mucoadhesion property when compared with AA-SLN correlating to the concentration of added chitosan. The TEER values were not different after permeation experiments in all fomulations compared with initial. The % cell viability was more than 90% which correlated in cytotoxicity by MTT assay. TM TW80:SP85 5:5 was shown higher cellular uptake and permeation into human nasal epithelial carcinoma cell line than SOF TW80:SP85 5:5. CT/ AA-SLN that showed higher cellular uptake but lower permeation than AA-SLN which was agreement with in vitro permeation study thruogh 0.2 µm cellulose acetate membrane.

Department : Pharmaceutics and Industrial Pharmacy Student's Signature .....
Field of Study : Industrial Pharmacy Advisor's Signature .....
Academic Year : 2011 Co-advisor's Signature .....

ACKNOWLEDGEMENTS

I would like to express my sincere thanks and gratitude to my thesis advisor, Professor Garnpimol C. Ritthidej, Ph.D., and my thesis co-advisor, Associate Professor Vimolmas Lipipun, Ph.D., for their invaluable advice, guidance, and encouragement throughout my investigation. Their kindness and cheerfulness are also deeply appreciated.

I thank most sincerely the reviewers of this thesis, Associate Professor Uthai Suvanakoot, Ph.D., the chairman of my thesis examination committee, I am grateful to committee members; Associate Professor Kraisri Umprayn, Ph.D., Associate Professor Parkpoom Tengamnuay, Ph.D. and Saraporn Harikarnpukdee , Ph.D. for their valuable suggestion and comment.

The acknowledgement is given to all staffs of Department of Pharmaceutics and Industrial Pharmacy especially Mr. Prasong Changmai and Mr. Samrerng Thienyen for their helpful in providing facilities and instrument for my thesis experiment, Department of Pharmacology and Physiology, Department of Biochemistry and Microbiology, Faculty of Pharmaceutical Sciences, Chulalongkorn University, for their constructive criticism and for giving me valuable suggestions for improvement.

I wish to thank to my lovely friends for their friendship and other people whose names have not been mentioned for their great help and support.

Ultimately, I would like to thank my father, my mother and my sister for their assistance, encouragement, cheerfulness, continued support during the course of my education and endless love throughout my life.

CONTENTS

LIST OF TABLES

LIST OF FIGURES

FIGURE PAGE

LIST OF ABBREVIATIONS

ANOVA	=	analysis of variance
AA	=	asiatic acid
° C	=	degree Celsius
CC_{50}	=	50% cytotoxicity concentration
cm	=	centrimeter
conc	=	concentration
cps	=	centipoise
CV	=	coefficient variation
DMSO	=	dimethyl sulfoxide
DSC	=	differential scanning calorimetry
et al.	=	et aliti, ‘and others’
FBS	=	fetal bovine serum
g	=	gram
HBSS	=	Hank’s balance salt solution
hrs	=	hours
mg	=	milligram
min	=	minute
ml	=	milliliter
MTT	=	3-(4,5-dimethylthazol-2-yl)-2,5-diphenyl tetrazolium bromide
MW	=	molecular weight
nm	=	nanometer
PBS	=	phosphate buffered saline
pH	=	the negative logarithm of the hydrogen ion concentration
PI	=	polydispersity index
R^2	=	coefficient of determination
HPH	=	high pressure homogenizer

LIST OF ABBREVIATIONS (CONT.)

HPLC	=	high performance liquid chromatography
hr	=	hour
rpm	=	revolution per minute
µg	=	microgram
SD	=	standard deviation
SLN	=	solid lipid nanoparticle
TEER	=	transepithelial electrical resistence
TEM	=	Transmission electron microscopy
µl	=	microliter
µm	=	micrometer
w/v	=	weight by volume
v/v	=	volume by volume
%	=	percentage
<	=	less than
>	=	more than

CHAPTER I

INTRODUCTION

Nowadays, enormous progress has been made regarding our understanding of the pathogenic mechanisms of neurological disorders that there are only a small number of effective agents for treating of illnesses. A key barrier of developing such agents for use in neurological disorders is the blockage of drug entrance into central nervous system (CNS) by the blood brain barrier (BBB). Intranasal administration has generated widespread interest among the scientific community as an alternative route for the administration of many therapeutic agents. The advantages of nasal delivery are the avoidance of drug degradation in gastrointestinal tract from acidic or enzymatic environment and from hepatic first pass metabolism, rapid absorption and onset of effect, higher bioavailability thus uses lower doses of drug. Nasal delivery is easily accessible via non-invasive route, thus self-medication is possible (Priyanka, Shringi, and Sanjay, 2002). In addition, intranasal route can transport therapeutic agents to CNS bypassing the blood brain barrier by the unique connection, which the olfactory and trigeminal nerves provide between the brain and external environments (Yashpal, Pragati, and Kapoor, 2009). Thus the intranasal delivery is found suitable for the transport of therapeutic agents to the CNS.

Currently, there has been an increasing interest in the biochemical functions of natural contained in vegetables, fruits and medicinal plants, which could be candidates for the prevention of oxidative damage (neuroprotective effects) and improving memory. Asiatic acid (2, 3, 23-trihydroxyurs-12-en-28-oic acid) has a common structure of pentacyclic triterpenes and belongs to the amyrin ursolic acid group. It is a main active compound in *Centella asiatica (Linn.) Urban*, a medicinal plant in a family of Apiaceae which is found almost all over the world including in India, China, Indonesia, Australia, the South Pacific, Madagascar, Thailand and southern and middle Africa. *Centella asiatica* is claimed to be benefit in effect to the brain, for instance, managing the central nervous system disorders, possessing memory enhancing effect, improving the general mental ability of mentally retarded.

The plant plays a significant role of neuroprotective effects by its antioxidant properties which may reduce free radical in the patients with neurodegenerative disorders like ischemia, epilepsy and Alzheimer' s disease (Ramanathan et al., 2007). In the Ayurvedic system of medicine it is also recommended in chronic diseases and as a "brain tonic" in various mental disorders. The extract of *Centella asiatica* has been patented as a dementia treating agent and cognitive enhancer. Recently, *Centella asiatica* products are widely available in market as cognitive booster (Wattanathorn et al., 2008). Therefore, development of suitable carrier system of asiatic acid needs to be investigated in order to be used as effective neuroprotective agent.

Solid lipid nanoparticles (SLN) have been reported as an alternative drug delivery system. Solid lipid nanoparticles are in the submicron size range (50–1000 nm) and are composed of physiologically tolerated lipid components; at room temperature the particles are in the solid state (YiFan et al, 2006). Ingredients in SLN have to be approved for pharmaceutical application in humans. Their solid matrix protects active ingredients against chemical degradation and allows modulation of drug release profiles. SLN can be produced without the use of toxic solvents and even large scale production is possible (Carsten et al, 2001). Many methods have been developed to prepare SLN, such as high pressure homogenization, solvent emulsification or evaporation, high speed stirring, ultrasonication and solvent diffusion method. The high pressure homogenization technique has emerged as a reliable and powerful technique for preparation of SLN. In contrast to other techniques, scaling up has no problem in most cases. Two general approaches of the homogenization step, the hot and the cold homogenization technique, can be used for the production of SLN (Nagi et al., 2008). In general, hot homogenization technique obtaining higher temperatures results in lower particle sizes and narrow size distribution when compared with cold homogenization technique due to the decreased viscosity of the inner phase. For temperature-sensitive compounds the cold homogenization technique can be applied (Muller, Karsten, and Sven, 2000). Therefore, hot homogenization method was chosen in this study to prepare SLN containing asiatic acid.

Chitosan, a cationic polysaccharide, exists abundantly in nature and shows potential for safe use in healthcare field. It is derived from chitin by alkaline deacetylation and consists of 2-amino-2-deoxy-(1-4b)-d glucopyranose residues (d-glucosamine units) and N-acetyl-d-glucosamine units. Chitosan is a biodegradable natural polymer with great potential for pharmaceutical applications due to its biocompatibility, high charge density, non-toxicity and mucoadhesive properties. Chitosan has been used as a drug carrier for sustained release preparations and improvement of bioavailability for hydrophobic drugs. It has been shown to possess mucoadhesive properties due to molecular attractive forces formed by electrostatic interaction between positively charged chitosan oligosaccharide and negatively charged mucosal surfaces. Chitosan nanospheres are used to improve the uptake of hydrophilic substances across the epithelial layers. Chitosan nanosphere can be prepared by reacting chitosan with controlled amounts of multivalent anion resulting in cross-linking between chitosan molecules. The cross-linking may be achieved in acidic, neutral, or basic environments depending on the method applied. The ability of chitosan to increase epithelial permeability is due to its disruption of tight junctions by transiently open intercellular tight junction in agreement with previous study where they described that chitosan nanoparticles are attractive protein carriers as the polymer is mucoadhesive and enhances paracellular permeability by opening the tight junctions between epithelial cells and as the tight junctions open (Ward et al., 2000).

Thus, the aim of this study was to prepare SLN containing asiatic acid by hot homogenization method and to improve its stability and obtain small particle size (nanosizes) for enhance absorption of SLN for poorly soluble drugs. The obtained SLN were also investigated for their physicochemical characteristics such as particle size, zeta potential, surface morphology, drug entrapment efficiency and polymorphism properties. In addition, improving mucoadhesive properties of asiatic acid SLN by chitosan to increase adhesion time on nasal area for enhance nasal absorption. Finally, the in vitro behavior in cell culture of resulted SLN such as cell viability, cellular uptake and permeation properties was assessed.

The specific objectives of this investigation were as follows:

1. To develop dispersed formulations of solid lipid nanoparticles (SLN) containing asiatic acid for nasal delivery.

2. To study the effects of solid lipid type and amount of single emulsifier : tween 80, poloxamer 188, span80, span85 and solutol HS 15 and combined emulsifiers on the stability of SLN formulations.

3. To study the polymorphism properties of solid lipid.

4. To study the mucoadhesive properties of chitosan-coated asiatic acid loaded SLN.

5. To study the cell viability, cellular uptake and permeation properties of asiatic acid loaded SLN by using human nasal epithelial carcinoma cell line.

The overall aim of this study was to assess the potential of SLN containing asiatic acid for use as a novel neuroprotective agent delivery system.

CHAPTER II

LITERATURE REVIEW

Centella asiatica (Linn.) Urban

Centella asiatica (Linn.) Urban (synonym Hydrocotyle asiatica Linn.) belongs to the family Umbelliferae or Apiaceae, locally known as Bua-bok, is widely distributed in open or damp shaded places in Thailand. It is a prostate stoloniferous plant, a small creping herb with rooting of the nodes. The leaves are kidney-shapes about 1.3 – 3.6 cm diameter, leaf stalk 2 – 5 cm long. The flowers are of a light violet color (Figure 1). The gray to brownish-green plant has a smell that is reminiscent of tobacco leaves, and a mildly bitter taste. The leaves have long petioles arising rosette-like from a common base, embracing the flowers; inflorescence is in a single umble, bearing 1 – 5 flowers and stalks are 3 – 6 inches long (Channarong, 2007).

Leave

Leave, stalk and flower

Figure 1 *Centella asiatica (Linn.) Urban*.

Asiatic acid, a triterpene of *Centella asiatica (L.) Urban* (Umbelliferae), has been patented as a treatment for dementia and an enhancer of cognition by the Hoechst Aktiengesellschaft (EP 0 383 171 A2), modified the chemical structure of asiatic acid and obtained 36 derivatives of asiatic acid in an attempt to prepare neuroprotective compounds that were more efficacious than asiatic acid itself. The neuroprotective activities of these derivatives were evaluated using primary cultures of rat cortical neurons insulted with the neurotoxin, glutamate, as an in vitro screening system. Among the semi-synthesized derivatives, three derivatives significantly mitigated the neurotoxicity induced by glutamate in this screening system. The neuroprotective activities of these 3 derivatives appeared to be more powerful than that of asiatic acid itself. These 3 derivatives significantly attenuated decreases in the levels of glutathione, glutathione peroxidase and other enzymes, which participate in the cellular defense mechanisms blunting oxidative stress. Furthermore, they significantly reduced the overproduction of no induced by glutamate. These results showed that these derivatives of asiatic acid exerted significant neuroprotective effects on cultured cortical cells by their potentiation of the cellular oxidative defense mechanism. Therefore, these agents may prove to be efficacious in protecting neurons from the oxidative damage caused by exposure to excess glutamate (Lee et al., 2000).

Axonal regeneration is important for functional recovery following nerve damage. *Centella asiatica Urban* herb, also known as *Hydrocotyle asiatica L*., has been used in Ayurvedic medicine for centuries as a nerve tonic. Here, we show that *Centella asiatica* ethanolic extract (100 microg mL-1) elicits a marked increase in neurite outgrowth in human SHSY5Y cells in the presence of nerve growth factor (NGF). However, a water extract of *Centella asiatica* was ineffective at 100 µg/ml. Sub-fractions of *Centella asiatica* ethanolic extract, obtained through silica-gel chromatography, were tested (100 µg/ml) for neurite elongation in the presence of NGF. Greatest activity was found with a non-polar fraction (GKF4). Relatively polar fractions (GKF10 to GKF13) also showed activity, albeit less than GKF4. Thus, *Centella asiatica* contains more than one active component. Asiatic acid (AA), a triterpenoid compound found in *Centella asiatica* ethanolic extract and GKF4, showed marked activity at 1 microM (µg/ml). AA was not present in GKF10 to

GKF13, further indicating that other active components must be present. Neurite elongation by AA was completely blocked by the extracellular-signal-regulated kinase (ERK) pathway inhibitor PD 098059 (10 microM). Male Sprague-Dawley rats given *Centella asiatica* ethanolic extract in their drinking water (300-330 mg kg-1 daily) demonstrated more rapid functional recovery and increased axonal regeneration (larger calibre axons and greater numbers of myelinated axons) compared with controls, indicating that the axons grew at a faster rate. Taken together, our findings indicate that components in *Centella asiatica* ethanolic extract may be useful for accelerating repair of damaged neurons (Soumyanath et al., 2005).

The effect of chloroform : methanolic 80:20 extract of *Centella asiatica* (CA: 100 and 200 mg/kg) was evaluated on the course of free radical generation and exitotoxicity in monosodiumglutamate (MSG) treated female Sprague Dawley rats. The extract showed significant improvement in catalase, super oxide dismutase and lipid peroxides levels in hippocampus and striatum regions. Glutathione level was not altered with CA treatment. Similar observation was made with dextromethrophan. The general behavior, locomotor activity and CA1 a region of hippocampus was significantly protected by CA indicating neuroprotective effect of CA in MSG induced exitotoxic condition. Hence it can be concluded that CA protected MSG induced neurodegeneration attributed to its antioxidant and behavioural properties. This activity of CA can be explored in epilepsy, stroke and other degenerative conditions in which the role of glutamate is known to play vital role in the pathogenesis (Ramanathan et al., 2007).

Parkinson's disease (PD) is a progressive neurodegenerative disorder with a prevalence of 1–2% in people over the age of 50. Mitochondrial dysfunction occurred in PD patients showing a 15–30% loss of activity in complex I. Asiatic acid (AA), a triterpenoid, is an antioxidant and used for depression treatment, but the effect of AA against PD-like damage has never been reported, investigated the protective effects of AA against H_2O_2 or rotenone-induced cellular injury and mitochondrial dysfunction in SH-SY5Y cells. Mitochondrial membrane potential (MMP) and the expression of voltage-dependent anion channel (VDAC) were detected with or without AA

pretreatment following cellular injury to address the possible mechanisms of AA neuroprotection. The results showed that pre-treatment of AA (0.01–100 nM) protected cells against the toxicity induced by rotenone or H_2O_2. In addition, MMP dissipation occurred following the exposure of rotenone, which could be prevented by AA treatment. More interestingly, pre-administration of AA inhibited the elevation of VDAC mRNA and protein levels induced by rotenone(100 nM) or H_2O_2 (300 μM).These data indicate that AA could protect neuronal cells against mitochondrial dysfunctional injury and suggest that AA might be developed as an agent for PD prevention or therapy (Xiong et al., 2009).

The neuroprotective effect of asiatic acid in a mouse model of permanent cerebral ischemia. Various doses of asiatic acid (30, 75, or 165 mg/kg) were administered orally at 1 hr pre and 3, 10, and 20 hr postischemia, and infarct volume and behavioral deficits were evaluated at day 1 or 7 postischemia. IgG (blood-brain barrier integrity) and cytochrome c (apoptosis) immunostaining was carried out at 24 hr postischemia. The effect of asiatic acid on stress-induced cytochrome c release was examined in isolated mitochondrial fractions. Furthermore, its effects on cell viability and mitochondrial membrane potential were studied in HT-22 cells exposed to oxygen-glucose deprivation. Asiatic acid significantly reduced the infarct volume by 60% at day 1 and by 26% at day 7 postischemia and improved neurological outcome at 24 hr postischemia. Our studies also showed that the neuroprotective properties of asiatic acid might be mediated in part through decreased blood-brain barrier permeability and reduction in mitochondrial injury. The present study suggests that asiatic acid may be useful in the treatment of cerebral ischemia (Krishnamurthy et al., 2009).

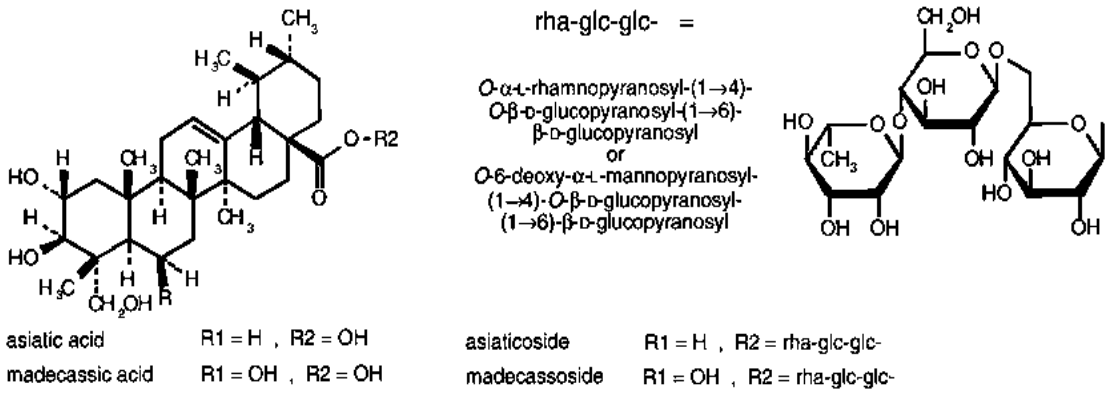

Figure 2 Structural of triterpenoid compounds of asiatic acid**.**

Transport drug from nasal to brain

The brain is one of the best protected organs of the body, to the outside by the skull and towards the blood circulation by the blood brain barrier (BBB). The purpose of BBB is to maintain the homeostasis of the brain, and to allow the creation of a unique extracellular fluid environment within the CNS, whose composition can as a consequence be precisely controlled (Begly, 2004). The presence of the tight junctions and the lack of aqueous pathways between cell greatly restricts the movement of polar solutes across the cerebral endothelium. Certain substances may diffuse passively across the brain endothelial cells. The diffusion is dependent on lipophilicity and molecular weight. Drugs with a molecular weight above 500 Da are normally excluded from passive diffusional transport across BBB. However, a large number of drugs that would possess a flavorable lipophilicity and molecular weight, which should normally enable an easy transport across BBB, are rapidly pumped back into the blood stream by extremely effective effect pumps (Begly, 1996 , Kreuter, 2002). As a consequence, the BBB presents a huge challenge for the effective delivery of a large number of therapeutics to the brain, and, therefore, many attempts have been made to overcome this barrier. For instance, these attempts include the osmotic opening of tight junctions (Gummerloch and Neuwelt, 1992), use of prodrugs or carrier system such as antibodies, liposome and nanoparticle. The employment of

prodrugs may yield a higher lipophilicity, enabling a better permeation and transport into and across the lipophilicity endothelial barrier. Colloidal carrier also can take advantage of these carrier systems present in the BBB.

By intranasal route a wide variety of therapeutic agents including both small molecules and macromolecules can be successfully delivered to the CNS. Thus, it is feasible to deliver challenging drugs to the CNS efficiently such as small polar molecules, peptides and proteins, and even the large proteins and polysaccharides such as vaccines or DNA plasmids exploited for DNA vaccines. Besides, intranasal delivery neither require any modification of the therapeutic agents nor require that drugs be coupled with any carrier (Illum, 2003).

The nasal cavity is subdivided along the centre into two halves by the nasal septum. The two cavities open to the facial side through the anterior nasal apertures and to the rhinopharynx via the posterior nasal apertures. The total surface area of the nasal cavity in man is about 150 cm^2 and the total volume about 15 ml. Each of the two nasal cavities can be subdivided into three regions; namely the nasal vestibule, the olfactory region and the respiratory region. The olfactory region in man covers an area of about 10 cm and is positioned on the superior turbinate and opposite the septum. The respiratory region is dominated by the presence of the large inferior turbinate, the middle turbinate, which has similarities to a polyp and further back in the nose, the superior turbinate.

In the respiratory region, which is considered the major site for drug absorption into the systemic circulation, the mucosa consists of an epithelium resting on a basement membrane and a lamina propria. The anterior part of the respiratory region is covered with squamous epithelium, which changes to a transitional epithelium and converts in the posterior part of the cavity to a pseudostratified columnar epithelium. The pseudostratified epithelium, also named the respiratory epithelium, consists of four dominant cell types; ciliated columnar cells, non-ciliated columnar cells, goblet cells and basal cells. Of these the basal cells are situated on the basal membrane and do not extend to the apical epithelial surface, as do the other

three cell types. A total of 15–20% of the respiratory cells is covered by a layer of long cilia of size 2–4 mm. The cilia move in a coordinated way to propel mucus across the epithelial surface towards the pharynx. The respiratory cells are also covered by about 300 microvilli per cell. Microvilli increase the surface area of the cell considerably, which in turn promotes the transport of substances and water between the cells. Goblet cells are interspersed between the columnar cells and are the main entities responsible for the secretion of the mucus covering the epithelial cell layer. The mucus layer consists of a low viscosity sol layer that surrounds the cilia and a more viscous gel layer forming a layer on top of the sol layer and covering the tips of the cilia. The blood supply to the respiratory region of the nasal cavity comes from the external and the internal carotid arteries through a dense network of capillaries in the lamina propria. The blood from the main part of the nasal pseudocavity is drained via the sphenopalatine foramen into the pterygoid plexus or via the superior ophthalmic vein, whereas blood from the anterior part of the nose is drained via the facial vein.

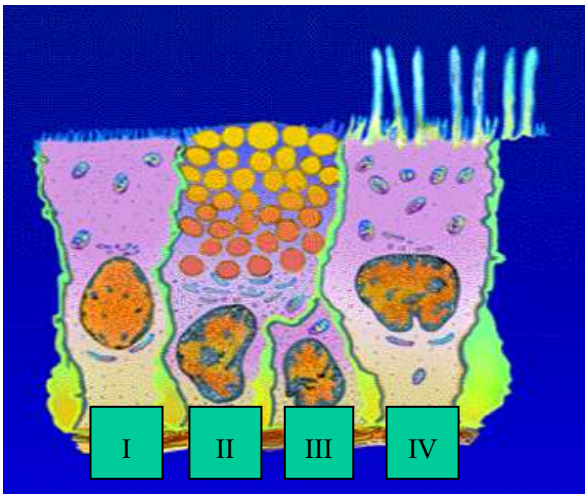

Figure 3 : Schematic illustration of the various cell types in the nasal respiratory epithelium. (I) Non-ciliated columnar epithelial cell with microvilli; (II) goblet cell with mucus granules and Golgi apparatus; (III) basal cell; (IV) ciliated columnar cell with mitochondria (Illum, 2000).

The olfactory epithelium is dedicated to the detection of smells and both the cellular composition and organisation of the epithelial layers maximise the accessibility of air to epineuronal structures bearing odorant detectors. In man the epithelium is restricted to a small area in the roof of the nasal cavity of about 10 cm as compared to an area of about 150 cm in dogs, which reflects the major importance of the sense of smell to the dog. The olfactory region is situated between the nasal septum and the lateral wall of each of the two nasal cavities and just below the cribriform plate of the ethmoid bone separating the cranial cavity from the nasal cavity. Since the olfactory mucosa is above the normal path of the airflow, odorants normally reach the sensitive receptors by diffusion. The process of sniffing enhances the diffusion process by drawing air currents upward within the nasal cavity so that a greater percentage of the molecules comes into contact with the receptor neurones. The olfactory epithelium is a modified form of respiratory epithelium in that it is a pseudostratified epithelium that consists of three cell types; the olfactory receptor cells, supporting epithelial (sustentacular) cells and basal cells. Beneath the basement membrane is the lamina propria, which contains blood vessels, olfactory axon bundles, trigeminal and autonomic nerve fibres and Bowman's glands, which secrete the mucus, that cover, the epithelial surface. Fig. 3 shows an outline of the olfactory epithelium indicating the various types of cells present and the connection of neurones to the olfactory bulb (Illum, 2000).

Two mechanisms are involved in the nasal delivery of drugs to the CNS. First, a fast rate that depends on lipophilicity. Second, a slower rate that depends on molecular weight. The transport of drugs across the nasal membrane and into the blood stream may involve either the passive diffusion of drug molecules through the pores in the nasalmucosa or some form of non-passive transport. Thus, the transport mechanism of substances such as insulin, mannitol or propranolol across the nasal mucosa occurs by a passive transport mechanism. The addition of deoxycholate (0.1%) enhances the transport of insulin and mannitol. Regarding transport of tyrosine and phenylalanine across rat nasal mucosa it has been shown that both these amino acids are absorbed by an active transport process and requires energy.The neuronal connections between the nasal mucosa and brain provide a unique pathway for the

non-invasive delivery of the therapeutic agents to the CNS, even to those drugs which do not cross BBB (Mathison, Nagilla, and Kompella, 2007). The olfactory epithelium is the major path for substances entering the CNS and the peripheral circulation. The olfactory neuronal pathway provides both an intraneuronal and extraneuronal pathway into the brain (Thorne, 1995). The intraneuronal pathway involves axonal transport and requires longer time for drugs to reach different brain regions. While the extraneuronal pathway involves bulk fl ow transport through perineural channels thus delivering drugs directly to the brain parenchymal tissues and/or CSF. The extraneuronal pathway allows therapeutic agents to reach CNS within minutes (Chen et al., 1998). Besides, the trigeminal neural pathway may also be involved in rapid delivery of protein therapeutic agents, such as insulin-like growth factor-1 to the brain and spinal cord following intranasal administration (Frey, Thorne, and Pronk, 2000).

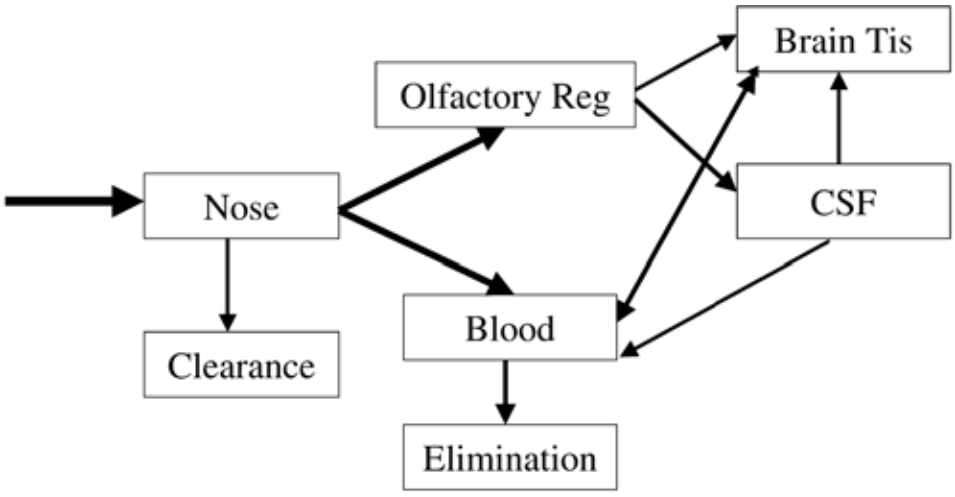

Figure 4 The nose to brain transport routes (Yashpal, Pragati, and Kapoor, 2009).

The mechanism of the delivery of drugs with the nanoparticle across BBB: (i) increased retention of the nanoparticles in the brain blood capillaries combined with and adsorbtion to the capillary walls which could create a higher concentration gradient that would enhance the transport across the endothelial cell layer (ii) could lead to an opening of the tight junctions in free, or together with nanoparticles, in bound form (iii) may be endocytosed by endothelial cells, followed by the release of

drug within these cells and delivery to the brain (iv) the nanoparticles with bound drugs could be transcytosed through the endothelial cell layer (v) a general surfactant effect characterized by a solubilization of the endothelial cell membrane lipids that would lead to membrane fluidization and an enhanced drug permeability through the BBB (vi) the polysorbate 80 used as the coating agent could inhibit the efflux system, especially P-glycoprotein (Pgp) (Kreuter, 2001).

Solid lipid nanoparticle (SLN)

The solid lipid nanoparticles (SLN) can enable the transport of many essential drugs across the BBB that normally cannot cross this barrier. It has been claimed SLN that the advantages and avoid the disadvantages of other colloidal carrier. Proposed advantages include: (i) possibility of controlled drug release and drug targeting (ii) increase drug stability (iii) high drug payload (iv) incorporation of lipophillic and hydrophilic drugs feasible (v) no biotoxicity of the carrier (vi) avoidance of organic solvents (vii) no problems with respect to large scale production and sterilization (Muller and Runge, 1998).

SLN represents a colloid drug carrier system with mean particle diameter ranging from 50 up to 1000 nm. General ingredients include solid lipid(s), emulsifier and water. Many researcher have prepared SLN by various technique such as:

1. High shear homogenization and ultrasound: are dispersing techniques which were initially used for the production of solid lipid nanodispersion (Abraham, 1993, Siekmann and Westesen, 1996). Both methods are widespread and easy to handle. However, dispersion quality is often compromised by the presence of microparticles. Furthermore, metal contamination has to be considered if ultrasound is used.

2. High pressure homogenization (HPH): has emerged as a reliable and powerful technique for the preparation of SLN. Homogenizers of different sizes are commercially available from several manufacturers at reasonable prices. HPH has been used for years for the production of nanoemulsions for parenteral nutrition. In contrast to other techniques, scaling up represents no problem in most cases. HPH push a liquid with high pressure (100 – 2000 bar) through a narrow gap (in range of few microns). The fluid acceleration on a very short distance to very high velocity (over 1000 km/h). Very high shear stress and cavitation forces disrupt the particles down to the submicron range. Typical lipid contents are in the range 5-10% and represent no problem to the homogeninizer. Even higher lipid concentration (up to 40%) have been homogenized to lipid nanodispersions (Lippacher, Muller, and

Mader, 2000). Two general approaches of homogenization step, the hot and cold homogenization techniques, can be used for the production of SLN **.**

2.1 hot homogenization : is carried out at temperatures above the melting point of lipid and can therefore be regarded as the homogenization of an emulsion. A pre-emulsion of drug loaded lipid melt and the aqueous emulsifier phase (same temperature) is obtained by high-shear mixing device. The quality of pre-emulsion affects the quality of the final product to a large extent and it is desirable to obtain droplets in the size range of a few micrometers. HPH of the pre-emulsion is carried out at temperatures above the melting point of the lipid. In general, higher temperatures result in lower particle sizes due to the decreased viscosity of the inner phase (Lander et al., 2000). However, high temperatures may also increase the degradation rate of the drug and the carrier. The homogenization step can be repeated several times. It should always be kept in mind, that high pressure homogenization increases the temperature of the sample (approximately 10 °C for 500 bar). In most cases, 3-5 homogenization cycles at 500 – 1500 bar are sufficient. Increasing the homogenization pressure or the number of cycles often results in an increase of the particle size due to particle coalescence which occurs as a result of the high kinetic energy of the particles (Siekmann and Westesen, 1994). The primary product of the hot homogenization is nanoemulsion due to the liquid state of the lipid. Solid particles are expected to be formed by the following cooling of the sample to room temperature or to temperatures below. Due to the small particle size and the presence of emulsifiers, lipid crystallization may be highly retarded and the sample may remain as a supercooled melt for several months (Bunjes, Siekmann, and Westesen, 1998).

2.2 cold homogenization : is carried out with the solid lipid and represents, therefore, a high pressure milling of a suspension. Effective temperature control and regulation is needed in order to ensure the unmolten state of the lipid due to the increase in temperature during homogenization. Cold homogenization has been developed to overcome the following three problems of the hot homogenization technique: (a) temperature-induced drug degradation (b) drug distribution in to the aqueous phase during homogenization (c) complexity of the crystallization step of the nanoemulsion

leading to several modifications and/or supercooled melts. The first preparatory step is the same as in the hot homogenization procedure and includes the solubilization or dispersing of the drug in the melt of the bulk lipid. However, the following steps are different. The drug containing melt is rapidly cooled (e.g. by means of dry ice or liquid nitrogen). The high cooling rate flavors a homogeneous distribution of the drug within the lipid matrix. The solid, drug containing lipid is milled to microparticles. Typical particle sizes obtained by means of ball or mortar milling are in range 50 -100 microns. Low temperatures increase the fragility of the lipid and favor, therefore, particle comminution. The solid lipid microparticles are dispersed in a chilled emulsifier solution. The pre-suspension is subjected to high pressure homogenization at or below room temperature. In general, compared to hot homogenization, larger particle sizes and a broader size distribution are observed in cold homogenized samples (Siekmann and Westesen, 1994). The method of cold homogenization minimizes the thermal exposure of the sample, but it does not avoid it due to the melting of the lipid/drug-mixture in the initial step.

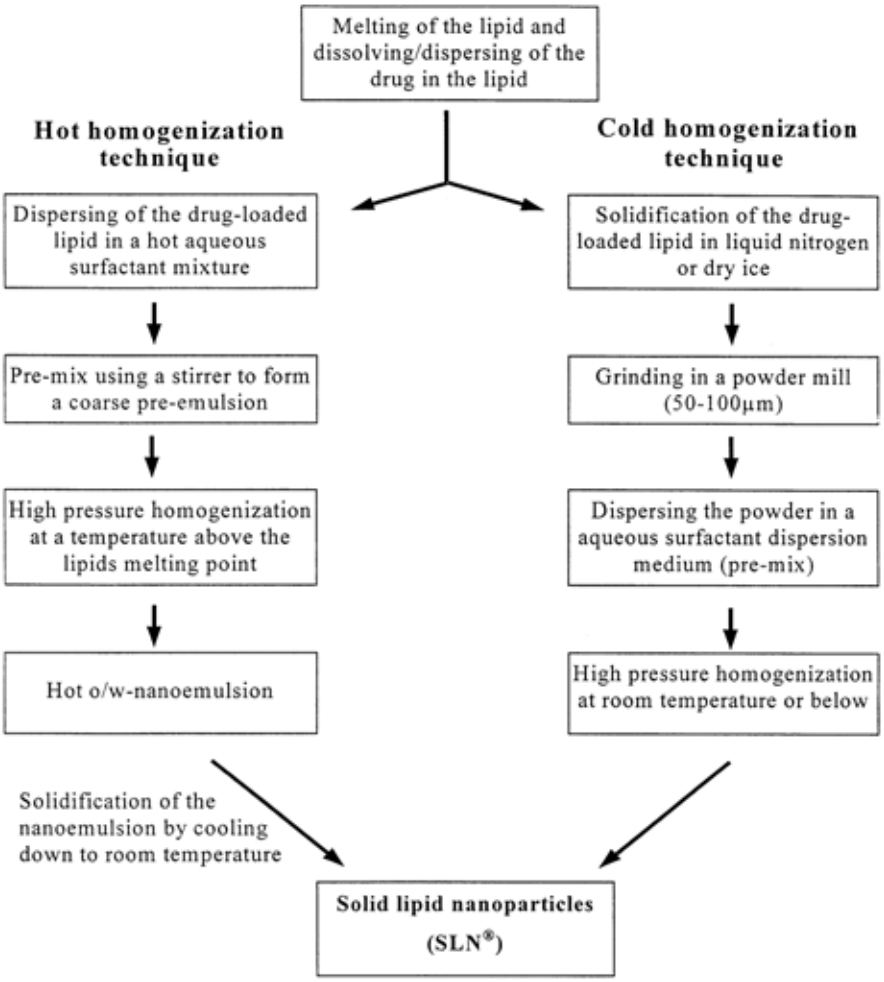

Figure 5 Schematic procedure of hot and cold homogenization techniques for SLN production (Wolfgang and Karsten, 2001).

3. Solvent emulsification / evaporation: Sjostrom and Bergenstahl described a production method to prepare nanoparticle dispersions by precipitation in o/w emulsion (Sjostrom and Westesen, 1992). The lipophillic material is dissolved in water–immiscible organic solvent (e.g. cyclohexane) that is emulsified in an aqueous phase. Upon evaporation of the solvent a nanoparticle dispersion is formed by precipitation of the lipid in the aqueous medium. The mean diameter of the obtained particles was 25 nm with cholesterol acetate as model drug and by using a lecithin/sodium glycocholate blend as emulsifier. The reproducibility of these results

is confirmed by Westesen (Siekmann and Westesen, 1996). The cholesterol acetate nanoparticles had a mean particle size of 29 nm (PCS number distribution) prepared according to Sjostrom with available equipment. Westesen prepared nanoparticles of tripalmitin by dissolving the triglyceride in chloroform. This solution was emulsified in an aqueous phase by HPH. The organic solvent was removed from the emulsion by evaporation under reduced pressure (40 – 60 mbar). The mean particle size ranged from approximately 30 to 100 nm depending on the lecithin/co-surfactant blend. Particles with average diameters as small as 30 nm were obtained by using bile salts as co-surfactants. Comparable small particle size distributions are not achievable by melt emulsification of similar composition. The mean particle size depends on the concentration of the lipid in the organic phase. Very small particles could only be obtained with low fat loads (5 % w/w) related to the organic solvent. With increasing lipid content the efficiency of the homogenization declines due to the higher viscosity of the dispersed phase. The advantage of this procedure over the cold homogenization process described before is the avoidance of any thermal stress. A clear disadvantage is the use of organic solvents.

4. Microemulsion based SLN preparations : Gasco and co-workers developed SLN preparation techniques which are based on the dilution of microemulsions (Gasco, 1993). It should be mentioned that there are different opinions in the scientific community about the structure and dynamics of microemulsion . An extended review has recently been published by Moulik and Paul (Moulik and Paul, 1998). Microemulsions as two-phase systems composed of an inner and outer phase (e.g. o/w-microemulsions). They are made by stirring an optically transparent mixture at 65–70°C which is typically composed of a low melting fatty acid (e.g. stearic acid), an emulsifier (e.g. polysorbate 20, polysorbate 60, soy phosphatidylcholine, taurodeoxycholic acid sodium salt), co emulsifiers (e.g. butanol, sodium monooctylphosphate) and water. The hot microemulsion is dispersed in cold water (2–38°C) under stirring. Typical volume ratios of the hot microemulsion to cold water are in the range of 1:25 to 1:50. The dilution process is critically determined by the composition of the microemulsion. According to the literature, the droplet structure is already contained in the microemulsion and therefore, no energy is required to

achieve submicron particle sizes. With respect to the similarities of the production procedure of polymer nanoparticles described by French scientists, different mechanisms might be considered. Fessi produced polymer particles by dilution of polymer solutions in water. According to Fessi, the particle size is critically determined by the velocity of the distribution processes. Nanoparticles were produced only with solvents which distribute very rapidly into the aqueous phase (e.g. acetone), while larger particle sizes were obtained with more lipophilic solvents. The hydrophilic cosolvents of the microemulsion might play a similar role in the formation of lipid nanoparticles as the acetone for the formation of polymer nanoparticles. Considering microemulsions, the temperature gradient and the pH value fix the product quality in addition to the composition of the microemulsion. High-temperature gradients facilitate rapid lipid crystallization and prevent aggregation. Due to the dilution step, achievable lipid contents are considerably lower compared with the HPH based formulations (Wolfgang and Karsten, 2001).

Incorporation models for the three types of SLN

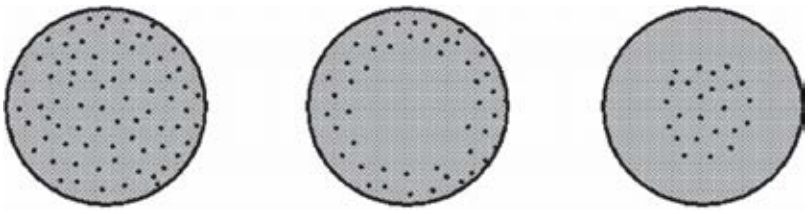

Homogenous matrix Drug-enriched shell Drug-enriched core

Figure 6 Incorporation models for the three types of SLN.

In case of model 1: Homogenous matrix of solid solution (left), a homogenous matrix, the drug is molecularly dispersed evenly in the particle matrix. Drug release takes place by diffusion from the solid lipid matrix and additionally by lipid nanoparticle degradation in the gut.

Model 2: Core-shell model with drug enriched in the shell (middle), the drug is enriched in the shell. This can be explained by a lipid precipitation mechanism occurring during particle production. After homogenization, there is a mixture of drug and lipid in each droplet. It is then being cooled. Depending on the TX solubility diagram (TX diagram: a two-dimensional graphical representation, with temperature and concentration coordinates, of the isobaric phase relationship in a binary system), the lipid can precipitate earlier than the drug to form a drug-free core or at least a core with reduced drug content. Reaching the eutectic temperature and composition, lipid and drug precipitate simultaneously in the outer shell of the particles. Drug enrichment in the shell is also a function of the solubility of the drug in the water-surfactant mixture at increased temperature during the production process. The drug partially leaves the lipid particle and dissolves in the aqueous phase during hot homogenization. Reason for this is the increased solubility for many drugs in the outer phase (surfactant solution) at elevated temperatures. Cooling of the oil/water nanoemulsion reduces the drug solubility in the aqueous phase, drug tries to repartition into the lipid particles leading to enrichment in the particle shell in case the particle core already started to solidify (Figure 2). Such particles are known to lead to a burst release. In the case of the oral cyclosporin A formulation, this was a desired effect. The dissolution rate needed to be sufficiently high to reach the therapeutic drug level but not too high to avoid nephrotoxic levels. In case of other applications, it might be necessary to have a prolonged release formulation which can be achieved by varying the production conditions during the particle production. Such conditions are low production temperature (preferably “cold homogenization”) and low surfactant concentration. Enrichment in the shell (model 2) takes place when particles are produced by hot homogenization method and the drug used shows a distinctly increased solubility in the aqueous surfactant phase at production temperature.

Model 3: Core-shell model with drug enriched in the core (right), the drug-enriched core is formed in case cooling of the hot oil/water emulsion leads to precipitation of the drug first. This takes place preferentially in lipid solutions with drug dissolved at its saturation solubility in the lipid at production temperature. During cooling, a super saturation and subsequent drug precipitation are achieved. The prolonged release of prednisolone is explained by this model (Muchow, Maincent, and Muller, 2008).

Methods to prolong brain retention of SLN

Surface characteristics size, surface hydrophobicity, surface mobility etc. The SLN have been proposed as suitable system to deliver hydrophilic drugs like diminazine and also for other BCS class IV drugs like paclitaxel, vinblastine, camptothecin, etoposide, cyclosporine etc. These carriers can gain access to the blood compartment easily (because of their small size and lipophilic nature) but the detection of these particles by the cells of the reticuloendothelial system (RES) i.e. the mononuclear phagocytic system; MPS cells of the liver (Kupffer) and that of spleen macrophages is a major limitation for their use. Uptake of nanoparticles by RES could result in therapeutic failure due to insufficient pharmacological drug concentration build up in the plasma and hence at the BBB. To overcome these limitations various researchers have tried to increase the plasma half-life of SLN by the following methods.

- Particle size :The size and the deformability of particles play a critical role in their clearance by the sinusoidal spleens of humans and rats. Particles must be either small or deformable enough to avoid the splenic filtration process at the interendothelial cell slits (IES) in the walls of venous sinuses. The IES in sinusoidal spleens provides resistance to flow through the reticular meshwork. The endothelial cells of the sinus wall have two sets of cytoplasmic filaments: a set of loosely associated tonofilaments and a set of filaments tightly organized into dense bands in the basal cytoplasm containing actin and myosin, which can probably vary the tension

in the endothelial cells and, hence, the size of IES. However, the slit size rarely exceeds 200 to 500 nm in width, even with an erythrocyte in transit. Hence, retention of blood cells and blood-borne particles at the IES depends on their bulk properties, such as size, sphericity, and deformability. These cell slits are the sites where erythrocytes containing rigid inclusions (e.g., Heinz bodies, malarial plasmodia) are believed to be “pitted” of their inclusions, which are eventually cleared by the red pulp macrophages. Therefore, the size of an engineered long circulatory particle should not exceed 200 nm ideally. If larger, then the particle must be deformable enough to bypass IES filtration. Alternatively, long-circulating rigid particles of greater than 200 nm may act as splenotropic agents and removed later on, if they are not rigid. Hence SLNs of size below 200 nm have an increased blood circulation and thus an increase in the time for which the drug remains in contact with BBB and for the drug to be taken up by the brain.

- Surface coating with hydrophilic polymers/surfactants : The high rates of RES mediated detection and clearance of colloidal carriers by liver, significantly reduce the half-life of the drug. The interaction of the colloidal carriers with blood plasma proteins (opsonins) and thus with the membranes of macrophages (opsonization) is believed to be the major criteria for clearance of these systems from the blood stream. Hence to prevent this clearance and to increase their availability at the target site the RES removal of these particulate systems should be prevented. This RES recognition can be prevented by coating the particles with a hydrophilic or a flexible polymer and/or a surfactant. The RES mediated detection and clearance by the liver is believed to be facilitated by the MPS cells. Opsonins, including complement proteins, apolipoproteins, fibronectin and Igs interact with specific membrane receptors of monocytes and tissue macrophages, resulting in their recognition and thus phagocytosis. It is generally admitted that hydrophobic surfaces promote protein adsorption and that negative surfaces activate the complement system and coagulation factors, any shielding of hydrophobic character of the nanoparticles is thus going to stearically stabilize them by providing a dense conformational cloud and thus reducing opsonization and phagocytosis as well as uptake by neutrophilic granulocytes, thus increasing the blood circulation time and hence the bioavailability.

Coating with polyethylene glycol (PEG), a polymer of hydrophilic nature showed promising results. PEG has high hydrophilicity, chain flexibility, electrical neutrality and lack of functional groups, preventing it from interacting unnecessarily with the biological components. It has been suggested that the PEG's with a molecular weight between 2000 to 5000 are necessary to suppress plasma protein adsorption; further it has been observed that the thicker the coat, the slower the clearance, and hence a better protection against liver uptake. Enlarging the molecule/particle slows down kidney ultrafiltration and, thereby allowing better accumulation into the brain and other permeable tissues by the passive enhanced permeation and retention mechanism. It also provides protein shielding which reduces proteolysis within the serum and tissues, and hinders immune surveillance of surface epitopes. Pegylation improves the pharmacokinetic profile of molecules by reducing polybutyl cyanoacrylate (PBCA) and coated with the nonionic surfactant polysorbate 80 has been intensely investigated. Similarly, polysorbates are investigated to have the highest potential to deliver the solid lipid nanoparticles to the brain.

- Use of ligands: Ligands or homing devices that specifically bind to surface epitopes or receptors on the target sites, can be coupled to the surface of the long-circulating carriers. Certain cancer cells over express certain receptors, like folic acid (over-expressed in cells of cancers with epithelial origin), LDL (B16 melanoma cell line shows higher expression of LDL receptors) and peptide receptors (such as somatostatin analogs, vasoactive intestinal peptide, gastrin related peptides, cholecystokinin, leutanising hormone releasing hormone). Attaching suitable ligands for these particular receptors on to the nanoparticles would result in their increased selectivity. Allen et al. postulated that the presence of specific ligands on the surface of nanoparticles could lead to their increased retention at the BBB and a consequent increase in nanoparticle concentration at the surface of BBB. While attempting to prove their assumption, they prepared coated nanoparticles from Brij 78, and emulsifying wax, with thiamine ligand (linked to DSPE via a PEG spacer). The authors however could not achieve prolonged nanoparticle concentration which was attributed to a number of factors including insufficient thiamine ligand coating and a preferred binding of the thiamine ligand to the blood thiamine transporters. Thole et

al. reported better interaction with brain endothelial cells and higher intracellular accumulation of stearically stabilized colloidal particles coupled to cationized albumin as compared to bovine serum albumin. Further the cationized albumin is taken up into the brain endothelia via a caveolae mediated endocytic pathway. Intact antibodies have been used as highly specific targeting agents with a high affinity towards their targets. The antibodies act as Trojan horses for delivery of nanoparticles across the BBB. The use of peptidomimetic antibodies which can bind to BBB transcytosis receptor; brain-targeted pegylated immune nanoparticles are also being proposed, such that, the delivery of entrapped actives into the brain parenchyma can be achieved without inducing BBB permeability alteration. Similarly delivery to the brain using nanoparticulate drug carriers in combination with the novel targeting principles of “differential protein adsorption (Path Finder Technology)” has been reported. The path finder technology exploits protein in the blood which adsorb onto the surface of intravenously injected carriers for targeting. Apolipoprotein E is one such targeting moiety as discussed above, for the delivery of particles to the endothelials of the BBB. These technologies can also be explored for their feasible application for improving the brain targeting of SLN. opsonization, phagocytosis and clearance by the liver and reticulao endothelial system. Other hydrophilic molecules which have been tried are Brij 78, Poloxamer F68 and Brij 68. Cavalli et al. found that parenteral administration of nanoparticles of paclitaxel was more bioavailable than an i.v. injection of the plain drug. The chemical nature of the overcoating surfactant is of importance, as only polysorbate-coated particles were found to show results in CNS pharmacological effect while a coating with poloxamers (184, 188, 388, or 407), poloxamine 908, Cremophors (EZ or RH40) or polyoxyethylene(23)-laurylether was not effective (Indu et al., 2008).

The property of material used in this study

Trimyristin

Synonyms : Dynasan 114, glyceryl trimyristate

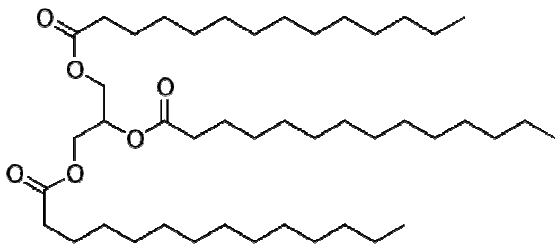

Figure 7 Structural formula of Trimyristin.

Molecular formula: $C_{45}H_{86}O_6$

Melting point : 56 – 57°C

Trimyristin is an ester. It is a saturated fat which is the triglyceride of myristic acid. Trimyristin is found naturally in many vegetable fats and oils. Trimyristin is a white to yellowish-gray solid that is insoluble in water, but soluble in ethanol, benzene, chloroform, dichloromethane, and ether.

Tristearin

Synonyms : Dynasan 118, Trioctadecanoin, Glycerol tristearate, Glyceryl tristearate

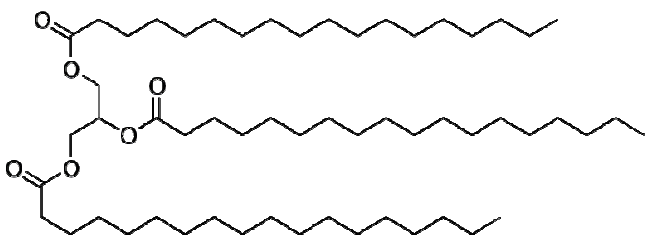

Figure 8 Structural formula of Tristearin.

Melting point : 55 °C

Molecular formula: $C_{57}H_{110}O_6$

Tristearin is a triglyceride, a glyceryl ester of stearic acid, derived from animal fats created as a byproduct of processing beef. It can also be found in tropical plants such as palm. It is used as tallow in the manufacture of candles and soap. In the manufacture of soap, tristearin is mixed with a sodium hydroxide solution in water. The following reaction gives glycerin and sodium stearate, which can be used as soap:

$$C_3H_5(C_{18}H_{35}O_2)_3 + 3\ NaOH \rightarrow C_3H_5(OH)_3 + 3\ C_{17}H_{35}COONa$$

tristearin + 3 sodium hydroxide → glycerol + 3 sodium stearate

Tristearin is also used in conjunction with aluminium flakes to help in the grinding process in making dark aluminium powder. Tristearin is a side product obtained during the extraction of cod liver oil removed during the chilling process at temperatures below -5 °C.

Glyceryl behenate (Rowe, Sheskey, and Owen, 2006)

Synonyms : Compritol 888 ATO, glycerol dibehenate

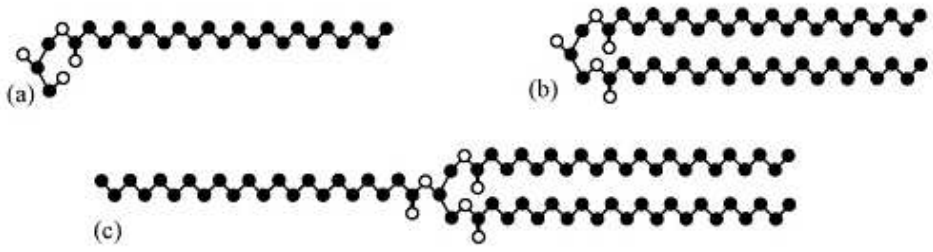

Figure 9 Structural formula of Compritol 888 ATO is (a) monobehenate, (b) is a dibehenate and (c) is a tribehenate.

HLB value : 2

Melting point : 65 – 77°C

Glyceryl behenate is a mixture of glycerides of fatty acids, mainly behenic acid. It specifies that the content of 1-monoglycerides should be 12.0 – 18.0% (USPNF 20) or a mixture of diacylglycerols, mainly dibehenoylglycerol, together with variable quantities of mono- and triacylglycerols (PhEur 2002). Glyceryl behenate is used in cosmetics, foods and oral pharmaceutical formulations. In cosmetics, it is mainly used as a viscosity-increasing agent in emulsions. Glyceryl behenate occurs as a fine white powder or hard waxy mass with faint odor. Glyceryl behenate is used in cosmetics, foods and oral pharmaceutical formulations and is generally regarded as a relatively nonirritant and nontoxic material.

Softisan 154

Synonyms : Hydrogenated Palm Oil

Melting point : 53 – 58 °C

Softisan 154 is white flake with a neutral odor and taste that is soluble in diethyl ether, toluene, acetone, insoluble in methylene chloride, water and ethanol. It is exceptionally resistant to oxidation, so there is no risk of rancidity. Softisan 154 are suitable as components for all types of cosmetics and pharmaceutical sticks.

Palmitic acid

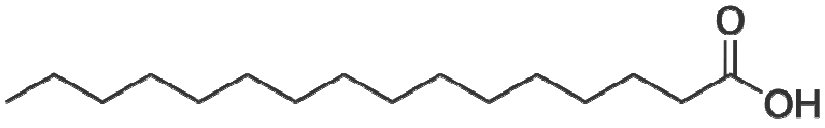

Figure 10 Structural formula of Palmitic acid.

Synonyms : Hexadecanoic acid, Cetylic acid, 1-Pentadecanecarboxylic acid, Emersol, Hexadecylic acid, Hydrofol, Hystrene, n-Hexadecoic acid

Melting point : 63 °C

Molecular formula: $C_{16}H_{32}O_2$

Palmitic acid is mainly used to produce soaps, cosmetics, and release agents. For these applications, the palmitic acid is neutralized with sodium hydroxide to give sodium palmitate. Soluble in diethyl ether, acetone. Practically insoluble in cold water. Sparingly soluble in cold alcohol or petroleum ether. Freely soluble in hot alcohol, propyl alcohol, chloroform. Soluble in aromatic, chlorinated and oxygenated solvents. Soluble in ethanol. Water solubility: 0.82 mg/ml.

Stearic acid

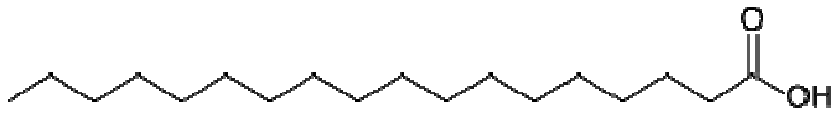

Figure 11 Structural formula of Stearic acid.

Synonyms: Ethyl Stearate, Ethyl Octadecanoate

Melting point : 69 °C

Molecular formula: $C_{18}H_{36}O_2$

Stearic acid is the saturated fatty acid with an 18 carbon chain and has the IUPAC name octadecanoic acid. It is a waxy solid, The salts and esters of stearic acid are called stearates. Generally applications of stearic acid exploit its bifunctional character, with a polar head group that can be attached to metal cations and a nonpolar

chain that confers solubility in organic solvents. The combination leads to uses as a surfactant and softening agent.

Polysorbate 80

Synonyms : Tween 80

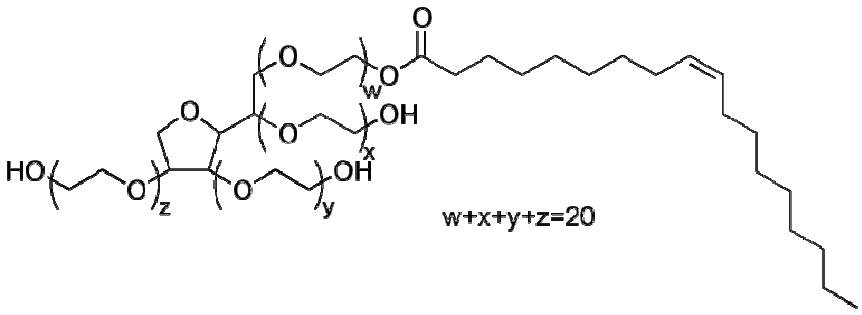

Figure 12 Structural formula of Polysorbate 80.

HLB value : 15

Molecular formula: $C_{64}H_{124}O_{26}$

Polysorbate80 is a non ionic surfactant and emulsifier derived from polyethoxylated sorbitan and oleic acid, and is often used in foods. Polysorbate 80 is a viscous, water-soluble yellow liquid. The hydrophilic groups in this compound are polyethers also known as polyoxyethylene groups which are polymers of ethylene oxide. In the nomenclature of polysorbates, the numeric designation following polysorbate refers to the lipophilic group, in this case the oleic acid (see polysorbate for more detail). Polysorbate 80 is often used in food and other products as an emulsifier.

Poloxamer 188 (Rowe, Sheskey, and Owen, 2006)

Synonyms : F-68, Lutrol, Pluronic, polyethylene-propylene glycol copolymer, polyoxyethylene- polyoxypropylene copolymer

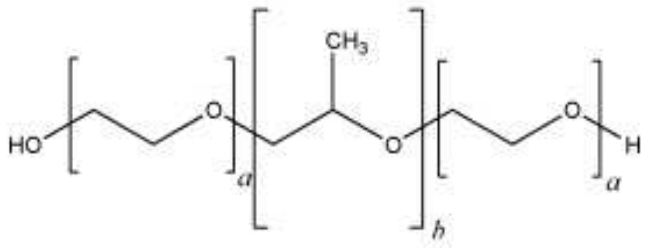

Figure 13 Structural formula of Poloxamer 188

For Poloxamer 188, a is 80 and b is 27.

Empirical formula : HO(C2H4O)*a*(C3H6O)*b*(C2H4O)*a*H

Molecular weight : 7680 – 9510

HLB value : 29

Melting point : 52 – 57°C

Poloxamer 188 is a nonionic emulsifying or solubilizing agent. It generally occurs as white, waxy, free-flowing prilled granules, or as cast solids. It is practically odorless and tasteless. Poloxamer 188 is used in a variety of oral, parenteral and topical pharmaceutical formulations and is generally regarded as nontoxic and nonirritant materials.

Span 80

Synonym : Sorbitan monooleate

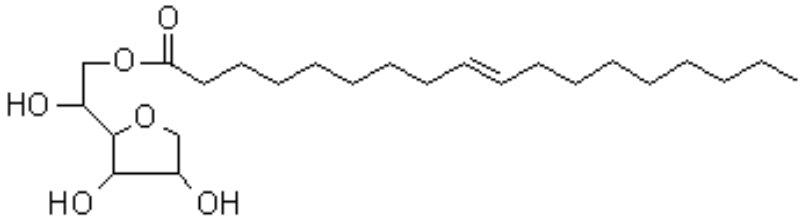

Figure 14 Structural formula of Span 80**.**

HLB value : 4.3

Molecular formula: $C_{24}H_{44}O_6$

Span 80 is amber-coloured oily viscous liquid that is a mixture of the partial esters of sorbitol and its mono- and dianhydrides with edible oleic acid (R).The constituent in greatest abundance is 1,4-sorbitan monooleate, with lesser abundance of isosorbide monooleate, sorbitan dioleate and sorbitan trioleate. It can soluble at temperatures above its melting point in ethanol, ether, ethyl acetate, aniline, toluene, dioxane, petroleum ether and carbon tetrachloride; insoluble in cold water, dispersible in warm water.

Span 85

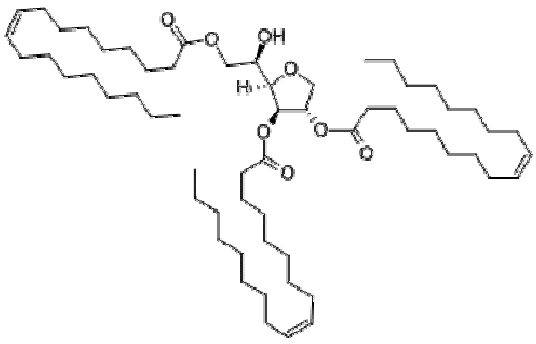

Figure 15 Structural formula of Span 85**.**

Synonym : sorbitan trioleate, emulsifier S-85

HLB value : 1.8

Molecular formula: $C_{60}H_{108}O_8$

Span 85 is amber to brown oily liquid. odorless. Slightly soluble in isopropanol, tetracarp, xylene, cotton seed oil, mineral oil**.** It is a biodegradable surfactant based on a natural fatty acid (oleic acid) and the sugar alcohol sorbitol. This sorbitan ester is highly effective at forming O/W emulsions, particularly when used in combination with its polyethoxylated derivative, Tween 80.

Solutol HS 15

Synonym **:** Polyethylene glycol-15-hydroxystearate**,** macrogol 15 hydroxystearate,

2-hydroxyethyl 12-hydroxyoctadecanoate

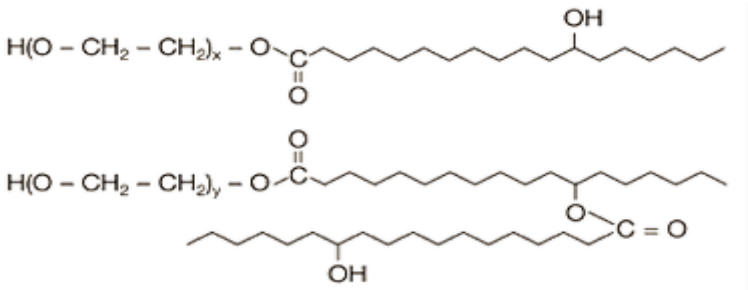

Figure 16 Structural formula of Solutol HS 15**.**

HLB value : 14- 16

Melting point : 30 °C

Molecular formula: $C_{20}H_{40}O_4$

Solutol HS 15 is a yellowish white paste at room temperature that can dissolves in water, ethanol and 2-propanol to form clear solutions. Its solubility in

water decreases with increasing temperature. It is insoluble in liquid paraffin. Solutol HS 15 consists of polyglycol mono- and di-esters of 12-hydroxystearic acid (lipophillic part) and of about 30% of free polyethylene glycol (hydrophillic part), a small part of the 12-hydroxy group can be etherified with polyethylene glycol.

Chitosan

Chitosan is a fiber-like substance derived from chitin, a homopolymer of ß-(1→4)-linked *N*-acetyl-D-glucosamine. Chitin is the second most abundant organic compound in nature after cellulose. Chitin is widely distributed in marine invertebrates, insects, fungi, and yeast. However, chitin is not present in higher plants and higher animals. Generally, the shell of selected crustacean was reported by Knorr (1984a) to consist of 30-40% protein, 30-50% calcium carbonate and calcium phosphate, and 20-30% chitin. Chitin is widely available from a variety of source among which, the principal source is shellfish waste such as shrimps, crabs, and crawfish. It also exists naturally in a few species of fungi.

Chitosan is a biopolymer of high molecular weight. Like its composition, the molecular weight of chitosan varies with the raw material sources and the method of preparation. Molecular weight of native chitin is usually larger than one million Daltons while commercial chitosan products have the molecular weight range of 100,000 – 1,200,000 Daltons, depending on the process and grades of the product. In general, high temperature, dissolved oxygen, and shear stress can cause degradation of chitosan. For instance at a temperature over 280^{o}C, thermal degradation of chotosan occurs and polymer chains rapidly break down, thereby lowering molecular weight. Also, maximal depolymerization caused by utilization of high temperature or concentrated acids, such as hydrochloric acid followed by acetic acid and sulfurous acid, results in molecular weight changes with minimal degradation with the use of EDTA (Sun and Fernandez, 2004).

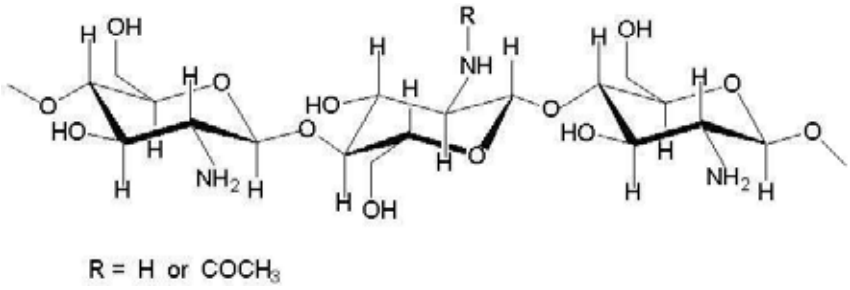

Figure 17 Structural formula of Chitosan.

Cationic polymers were probably superior mucoadhesives due to an ability to develop molecular attraction forces by electrostatic interactions with the negative charges of the mucus. The polymer is biodegradable, biocompatible and non-toxic. It possesses antimicrobial and wound-healing properties. Moreover, chitosan exhibits a pseudoplastic and viscoelastic behaviour. The mucoadhesive properties of chitosan are determined by the formation of either secondary chemical bonds such as hydrogen bonds or ionic interactions between the positively charged amino groups of chitosan and the negatively charged sialic acid residues of mucins, depending on environmental pH.

Various chitosan derivatives were synthesized not only to improve the mucoadhesion, but also to enhance the penetration of drugs and peptides through the mucosa by opening the tight junctions between epithelial cells or by intracellular routes. However, in vitro studies showed that cell surface binding and absorption-enhancing effects were reduced in mucus covered cell lines. The quaternized N-trimethyl chitosan and N-carboxymethyl chitosan have proved to be potent intestinal penetration enhancers (Annick, 2005).

CHAPTER III

MATERIALS AND METHODS

Materials

Model drug

- Asiatic acid (Batch No. AA0303612, Changzhou Natural Product Development Co., Ltd., China)

Solid lipids

- Glyceryl behenate (Compritol® ATO 888) (Lot no. 104355, Gattefosse, France)
- Hydorgenated Palm Oil (Softisan 154®) (Lot no. 810187, Sasol, Germany)
- Palmitic acid (Lot. no. 1281527, Sigma-Aldrich, USA)
- Stearic acid (Lot. no. S4751, Sigma-Aldrich, USA)
- Trimyristin (Dynasan 114®) (Lot. no 112152 , Sasol, Germany)
- Tristearin (Dynasan 118®) (Lot. no. 104576, Sasol, Germany)

Surfactants

- Polysorbate 80 (Tween 80®) (Lot. no. 809861, distributed by Srichand United dispensary Co., Ltd., Thailand)
- Poloxamer 188 (Lutrol F68®) (Lot. no. 600480, BASF, Germany)
- Sorbitan monooleate (Span 80®) (Lot. no. 61152B, distributed by Srichand United dispensary Co., Ltd., Thailand)

- Sorbitan trioleate (Lot. no. 26910B, Span 85®, distributed by Srichand United dispensary Co., Ltd., Thailand)

- Polyoxyethylene esters of 12-hydroxystearic acid (Solutol HS 15®) (Lot. no. 35286497V0, BASF; Germany)

Biomaterials

- RPMI 2650, human nasal epithelial carcinoma cell line (CCL-30 ™ , American Type Culture Collection (ATCC), VA, USA)

Chemicals

- 0.025% Trypsin in EDTA Code. 25200 (Lot. no. 939422, GIBCO®, Invitrogen, USA)

- Acetronitrile HPLC grade (Lot. no. 454A1H , Honeywell, Burdick & Jackson, USA)

- Antibiotic-Antimycotic (100X) Code. 15240 (Lot. no. 907164, GIBCO®, Invitrogen, USA)

- Dimethyl sulfoxide (DMSO) (Lot. no. K41067812045, Sigma-Aldrich, USA)

- Dipotassium hydrogen ortho-phosphate (Lot. no. F2A246, APS Chemical Limited, Australia)

- Fetal bovine serum Code. 10270 (Lot. no. 41G8397K, GIBCO®, Invitrogen, USA)

- Hanks' balance salt solution (HBSS) Code. 14025 (Lot. no. 862558, GIBCO®, Invitrogen, USA)

- Methanol HPLC grade (Lot. no. L6AG2H, Honeywell, Burdick & Jackson, USA)

- Phosphate buffer saline solution (PBS) pH 7.4 (Lot. no. 039K8200, GIBCO®, Invitrogen, USA)

- Thiazolyl blue tetrazolium bromide (MTT) Code M5655-1G (Lot. no. MKEG1611V, Sigma-Aldrich, USA)

Equipments

- Analytical Balance (Model A2000S, Sartorius, Germany)

- Centrifuge (Model 2K15, Sigma Germany)

- High pressure homogenizer (Model Emulsiflex C5®, AVESTIN, Canada)

- High performance liquid chromatography (HPLC) (Model SCL-10A VP, Shimadzu, Japan)

- High speed homogenizer (Model Polytron, PT3100, KINEMATICA, Switzerland)

- Hot Air Oven (Model 5090E Heraeus, Thermoscientific, Canada)

- HPLC Column: Luna Phenomenex® C18 (10 □m, 250 x 4.6 mm) (Phenominex, USA)

- Laminar air flow (Model HBB 2448, Holten, USA)

- Micropipette (Model Gilson® 57329H, Gilson, France)

- Micropipette (Model Socorex® ACURA 825, Socorex, Swizerland)

- Modified Franz Diffusion cells (Crown Glass, USA)

- PCS (Model Zetasizer nano-ZS, Malvern, Geramany)

- pH meter (Model 210A, Thermo Orion, Germany)

- Pipette Aid (Drummond®, USA)
- Viscometer (Model RheoWin – RV1® , HAAKE, Germany)
- Transferring pipette (Witeg, Germany)
- Transmission electron microscope (Model JSM-5410LV, JOEL, Japan)
- Vortex mixer (Model VELP, Scientifica Industries,Italy)

Laboratory supplies

- 6 Well Plate Transwell® permeable support 0.4 µm polyester membrane 3450 (Costar, USA)
- 96 Well Plate (Corning, USA)
- Aluminium foil (MMP Packing, Thailand)
- Beaker (Pyrex, USA)
- Cellulose acetate membrane 0.22 µm (Water, USA)
- Cellulose acetate membrane 0.45 µm (Whatman, UK)
- Centrifugal device, MWCO = 50 K (Amicon ultra-4®with cellulose membrane), (Millipore, USA)
- Centrifuge tubes (Corning, USA)
- Cylinder (Pyrex, USA)
- Disposible syringe and needle (Terumo, Thailand)
- Microcentrifuge tubes (Corning, USA)

- Nylon membrane filter (Water, USA)
- Parafilm (American National Can., USA)
- Tissue culture flask (Corning, USA)
- Volumetric flask (Corning, USA)

Methods

1 Preparation of solid lipid nanoparticles (SLN)

1.1 Drug-free SLN solid lipid nanoparticles (drug – free SLN)

SLN were prepared by high-pressure homogenization method (HPH method). The lipid phase (1% w/w solid lipid and acquired non-aqueous emulsifiers) was melted at above the melting point of solid lipid, and dispersed into a hot aqueous phase (acquired aqueous-emulsifiers and water) in the same temperature, then stirred in high speed homogenizer to yield pre-emulsion which was then exposed to high-pressure homogenization (Model Emulsiflex C5®;AVESTIN, Canada) at 1000 bar by five homogenization cycles and maintaining the temperature above lipid melting point. Trimyristin (TM), tristearin (TS), glyceryl behenate (GB), softisan 154 (SOF), palmitic acid (PA) and staric acid (SA) were used as solid lipids and tween 80 (TW80), span 80 (SP80), span 85 (SP85), poloxamer188 (PL188) and solutol HS 15 (SL) were used as emulsifiers (4% w/w) which containing concentration of surfactant:co-surfactants in ratio 1:9, 3:7, 5:5, 7:3 and 9:1. The drug-free SLN formulations were also observed under accelerated condition (4°C for 48 hours and 45 °C for 48 hours) for 6 cycles.

1.2 Asiatic acid loaded solid lipid nanoparticles (AA-SLN)

Asiatic acid loaded SLN (AA-SLN) were prepared by HPH method as described above by which asiatic acid (AA) was loaded in the lipid phase. The formulations of asiatic acid loaded SLN are shown in Table 1.

Table 1 The amount of AA was loaded in AA-SLN formulations.

Solid lipids	Ratio of surfactants	The amount of asiatic acid (mg/ml)
TM	TW80 : SP80 5:5	0.70
	TW80 : SP80 7:3	0.70
	TW80 : SP85 5:5	0.70
	TW80 : SP85 7:3	0.70
	TW80 : SL 5:5	0.50
	TW80 : SL 7:3	0.50
	TW80 : SL 9:1	0.50
TS	TW80 : SP80 5:5	0.70
	TW80 : SP80 7:3	0.70
	TW80 : SP85 5:5	0.70
	TW80 : SP85 7:3	0.70
	TW80 : SL 1:9	0.50
	TW80 : SL 3:7	0.50
	TW80 : SL 5:5	0.50
GB	TW80 : SP80 5:5	1.00
	TW80 : SP80 7:3	1.00
	TW80 : SP85 5:5	1.00
	TW80 : SP85 7:3	1.00
	TW80 : SL 9:1	1.00
SOF	TW80 : SP80 5:5	1.00
	TW80 : SP80 7:3	1.00
	TW80 : SP80 9:1	1.00
	TW80 : SP85 5:5	1.00
	TW80 : SP85 7:3	1.00
	TW80 : SP85 9:1	1.00

1.3 Chitosan coated asiatic acid loaded solid lipid nanoparticles (CT/AA-SLN)

After storage for 6 months, The selected AA-SLN formulations were coated by chitosan solutions in aqueous acetic acid which prepared by weighing chitosan powder and dissolving in 100 mL of 2% w/v acetic acid to obtain concentrations of 0.8 mg/ml, 2.4 mg/ml and 4 mg/ml. Each chitosan solution of 2.5 ml was dispersed in 20 ml AA-SLN and mixed overnight with constant stirring, resulting in a final concentrations of chitosan in AA-SLN of 0.1% , 0.3% and 0.5% v/v respectively.

2. Stability studies

The AA-SLN formulations were divided and kept in tightly closed glass bottles in three conditions for 6 months : at 4° C , room temperature and 45° C. The samples were withdrawn and investigated on month 0, and 6 in three batches (n=3). Physical and chemical stability of the samples was evaluated as follows:

Physical appearance

The physical appearances in term of precipitation were visually observed in comparison with their respective freshly prepared formulations.

pH

The pH of SLN was measured at room temperature using pH meter (Model 210A, Thermo Orion, Germany). The equipment was calibrated at pH 4 and 7 by using Beckman standard buffer solution before used. Each sample was examined in triplicate.

Particle size, size distribution and zeta potential

The mean particle size, particle size distribution (polydispersity index, PDI) and zeta potential, were measured by photon correlation spectroscopy, PCS (Zetasizer nano-ZS, Malvern, Geramany). The SLN dispersion was put in a quartz cuvette and placed inside the instrument chamber. The obtained value from each formulation was the average of three measurements.

Drug remaining

The total amount of AA remained in the SLN was determined by HPLC method at 210 nm as described under Topic 5.

3. Characterization of solid lipid nanoparticles

3.1 Physical appearance

The physical appearances of formulations in term of precipitation were visually observed after preparing formulation, accelerated condition and storage time.

3.2 Particle size, size distribution and zeta potential

The mean particle size, particle size distribution (polydispersity index, PDI) and zeta potential, were measured by photon correlation spectroscopy, PCS (Zetasizer nano-ZS, Malvern, Geramany). The SLN dispersion was put in a quartz cuvette and placed inside the instrument chamber. The obtained value from each formulation was the average of three measurements.

3.3 pH measurement

The pH of SLN was measured at room temperature using a pH meter (Model 210A, Thermo Orion, Germany). The equipment was calibrated at pH 4 and 7 by using Beckman standard buffer solutions before used. Each sample was examined in triplicate.

3.4 Viscosity property

Viscometer (Model RheoWin–RV1®, HAAKE, Germany) with helipath stand was used for rheological studies. The sample was placed in a plate and was allowed to equilibrate for 5 min before measuring the dial reading using a T-C spindle. At each speed, the corresponding dial reading on the viscometer was noted. The spindle speed was successively lowered and the corresponding dial reading was noted. The measurements were carried in triplicate at ambient temperature. Direct multiplication of the dial readings with factors given in the RheoWin– RV1® viscometer catalogue gave the viscosity in centipoises.

3.5 Transmission electron microscope; TEM

The drug formulations were diluted with distilled water. The morphological examination of the SLN was performed and taken under transmission electron microscope (TEM, Model JEM-1230). The samples were stained with 1% (w/v) phosphotungistic acid and placed on copper grids and dried under room temperature.

3.6 Differential scanning calorimetry (DSC)

DSC analysis was performed using Mettler DSC 822e/200 (Mettler Toledo) to evaluate lipid crystallinity and polymorphism as thermal behaviour studies. Each sample was heated from 25 to 350°C at a scanning rate of 20°C/min. Analysis was performed under a nitrogen purge (50 ml/min). A standard aluminum sample pan (40 µl) was used. About 5 mg sample was taken for analysis. An empty pan was used as reference. A physical mixture (PM) of AA and lipids, freezed dry solid lipid nanoparticles (FD SLN), the pure lipids and the pure drug were used as control. The samples were used in the same thermal cycles and prepared at the same weight ratios in SLN formulations.

3.7 Powder X-ray diffractometry (PXRD)

Powder X-ray diffractometer, Siemen's D-5000 (Germany), was used for diffraction studies. PXRD studies were performed on the samples by exposing them to a copper anode (Cu-Ka radiation (40 kV, 30 mA) and scanned from 5 to 40 Theta. Samples used for PXRD analysis were the same as those of DSC analysis.

4. Validation of HPLC method

The analytical parameters used in the assay validation for HPLC method were linearity, specificity, accuracy and precision.

- Linearity : Three sets of six standard solutions were prepared and analyzed. Linear regression analysis of the peak area versus their concentrations was performed. The linearity was determined from the coefficient of determination (R^2).

Acceptance criteria: The coefficient of determination should be more than 0.9990.

- Specificity : Under the chromatographic conditions used, The reagents were add and storage in conditions as described below for determined the decomposed products from AA. The peak of AA must be completely separated when compared with standard peak and not be interfered by the peaks of other components in the sample. Reagents and conditions were tested in 1 ml of 0.1 N NaOH and then heat 80°C for 3 hours, 1 ml of 0.1 N HCl and then heat 80°C for 3 hours, 0.5 ml 30% v/v H_2O_2 and then heat 80°C for 3 hours, 1 ml of water and then heat 80°C for 3 hours, heat 80°C for 6 hours and light for 6 hours

Accepted criteria: The resolution value should be more than 1.5 when compare with standard.

- Accuracy : The accuracy of an analytical method is the closeness of test results obtained by that method to the nominal value. The accuracy of the method was determined from the percentage of analytical recovery. Three sets of three concentrations of AA at low, medium and high (with drug-free SLN) of each nominal concentration was determined. The percentage of recovery of each concentration was calculated from the ratio of inversely estimated concentration to known concentration multiplied by 100

Acceptance criteria: The percentage of analytical recovery should be within 98.0-102.0% of each nominal concentration.

- Precision

a) Within-run precision

The within-run precision was determined by analyzing five sets of three concentrations of standard solutions of AA at 1.5, 3.5 and 4.5 μg/ml in the same analytical run. The percent of coefficient of variation (%CV) of each concentration was determined.

b) Between-run precision

The between-run precision was determined by comparing three concentrations of standard solutions of AA at 1.5, 3.5 and 4.5 μg/ml on five different analytical run. The percent coefficient of variation (%CV) of each concentration was determined.

Acceptance criteria: The percent coefficient of variation (%CV) for both within- run and between-run precision should be less than 2%.

5. Determination of AA by HPLC method

HPLC conditions

Column :	Luna Phenomenex® C18(10 μm, 250 x 4.6 mm)
Mobile phase :	0.05% Trifluoroacetic acid (TFA) in acetronitrile : 0.05% Trifluoroacetic acid (TFA) in water (45:55)
Injection volume :	20 μl
Flow rate :	1.2 ml/minutes
Detector :	UV detector at 210 nm
Temperature :	ambient
Run time :	15 minutes

The mobile phase was prepared by using 0.05% TFA in acetronitrile: 0.05% TFA in with the ratio of 45:55 %v/v. The mixture solution was thoroughly mixed, filtered through 0.45 μm membrane filter and then degassed by sonication for 30 minutes prior to use. The AA content in SLN was determined by HPLC method because of its specificity and high sensitivity.

Standard solutions of HPLC method

A standard solution of AA was prepared by accurately weighing 10 mg of AA into a 100 ml volumetric flask. The methanol:chloroform 1:1 was added to dissolve AA and adjust to the final volume. The stock solution had final concentration of AA of 100 μg/ml.

The solution of 1, 2, 3, 4, 5 and 6 ml of standard AA stock solution were added into 10 ml volumetric flasks and methanol:chloroform 1:1 was evaporated. The sample was redispersed and adjusted to final volume with methanol to give final concentrations of 1, 2, 3, 4, 5 and 6 μg/ml of AA, respectively.

Preparation of sample solution

The sample solution was prepared by pipetting 1 ml of AA-SLN into a 100 ml volumetric flask and the methanol:chloroform 1:1 was added to dissolve AA-SLN and adjust to the final volume. Then, 1 ml of this stock solution was transferred into a 10 ml volumetric flask and methanol:chloroform 1:1 was evaporated. The sample was redispersed and adjusted to volume with methanol to give the final concentration of AA and determined by HPLC method.

6. Entrapment efficiency

The entrapment efficiency of the drug was determined by measuring the concentration of free drug in the dispersion medium. Three ml of AA-SLN were purified by ultrafiltration method using centrifugal filter device (Amicon ultra-4®with cellulose membrane MWCO = 50 K was shown in Figure 18, equivalent to 15 – 30 nm that only free drug and micelle could pass this membrane), 4,000 rpm, 25°C for 30 minutes per cycle. The initial drug was finding in one ml of AA-SLN was extracted by methanol:chloroform 1:1. The extracted solvent was evaporated and the residue of AA was diluted by methanol and analyzed for content of AA using high performance liquid chromatography (HPLC) at 210 nm. The filtrates (free drug) was collected from supernatant on the bottom of Amicon ultra-4® and then analyzed for content of AA in as same as the method of finding initial drug. The entrapment efficiency (the percentage of entrapped drug) were calculated by equations below:

$$EE\ (\%) = \frac{\text{initial drug} - \text{free drug}}{\text{initial drug}} \times 100$$

Figure 18 Centrifugal device: Amicon ultra-4®.

7. Mucoadhesive property

The bioadhesive properties of formulations were determined using an adapted method described by Harikarnpakdee (Harikarnpakdee et al., 2006). The principle of this test is based on simulating a biological flow by washing a mucous membrane covered with the product to be tested. A freshly cut 4x4 cm of nasal porcine surface was obtained and cleaned by washing with PBS solution. Accurate volume of 0.5 ml SLN formulations were placed on the nasal porcine surface attached on petridish glass before study for 1 minutes, which fixed in an angle of 40° relative to the horizontal plate. After that, the nasal porcine surface was thoroughly washed with phosphate buffer solution (pH 7.4) at the rate of 5 ml/minutes using a peristaltic pump. The washed were collected at 5, 10 and 30 minutes, respectively and the concentration of the drug in the collected perfusate was determined by HPLC at 210 nm. The amount of SLN corresponding to the amount of drug in the perfusate was calculated.

Figure 19 Adaptation instrument of mucoadhesive study.

8. In vitro diffusion study

In vitro diffusion studies were performed using modification Franz diffusion cell as shown in Figure 20. The cellulose acetate membrane having pore size 0.2 μm was cut into a circular shape with a diameter of 3 cm before used. Membrane was soaked in mixture of phosphate buffer, pH 7.4 and methanol (70:30) for 12 hr before mounting in a Franz diffusion cell. The selected AA-SLN and CT/AA-SLN formulations (1.5 ml) were placed in the donor compartment and the receptor compartment was filled with mixture of phosphate buffer, pH 7.4 and methanol (70:30). A volume of 1 ml was taken from the receiver medium at certain time intervals of 30, 60, 90, 120, 150 and 180 minutes through side tube. Fresh mixture of phosphate buffer, pH 7.4 and methanol (70:30) was placed to maintain constant volume. Samples were analyzed by HPLC method at 210 nm.

Figure 20 Modification of Franz diffusion cell instrument of in vitro permeation study.

9. In vitro study in cell culture

Cell cultures

Nasal cell line (CCL-30) isolated from a human nasal septum carcinoma were maintained in minimum essential medium (MEM) alpha-medium (GIBCO Cat. No. 32571063) supplemented with 10% fetal bovine serum and 1% antibiotic-antimycotic and incubated in a humidified incubator at 37 ◦C under 5% CO_2 atmosphere. Cells were subcultured every 3 days in tissue culture flask until 70-80% confluence. The culture medium was removed, rinsed with phosphate buffer solution (PBS) pH 7.4, trypsinized by 0.025% w/v trypsin EDTA solution and cells were observed under an inverted microscope until cell layer was round up (usually within 5 to 15 minutes). To avoid clumping do not agitate the cells by hitting or shaking the flask while waiting for the cells to detach. Cells that are difficult to detach may be placed at 37°C to facilitate dispersal. Media solution was added and cells were aspirated by gently pipetting. The cells were seeded in 96-well plates for cytotoxicity study and in 6-well Transwell® plates for permeation study.

Cytotoxicity study (MTT Assay)

The cytotoxicity of asiatic acid loaded solid lipid nanoparticles in human nasal septum carcinoma cells were assessed using MTT (3-(4,5-dimethylthazol-2-yl)-2,5-diphenyl tetrazolium bromide). MTT was reduced to purple formazan in living cells by mitochondrial reductase as shown in Figure 21. This reduction occurred only when reductase enzymes were active, and therefore this conversion was used to measure viable (living) cells. The color reaction was used to measure of cell viability and proliferation. Human nasal septum carcinoma cells in culture medium were seeded in 96-well plates at a density of 4×10^5 cells/ml (Thanyamas, 2009) for 100 µl/well and incubated at 37°C in 5% CO_2 for 48 hours. One hundred microlitre of each dilution (5-fold serial dilution) of samples for each concentration were added and incubated for 48 hours (compound media was used control). After 48 hr incubation, 50 µl MTT solutions (1 mg/ ml in PBS solution pH 7.4) was added to each well after removing samples and the plates were incubated for further 3 hr. The solution in each well

containing media, unbound MTT and dead cells was removed for 50 µl. The medium was replaced with 100 µl of dimethyl sulfoxide (DMSO) in each well. The plates were then shaken for 20 minutes and the absorbance was read at 560 nm on VICTOR^3 TM microplate reader. Cytotoxicity was expressed as percentage of control (unloaded SLN). The CC50 (50% cytotoxicity concentration) value was defined as the drug concentration that cytotoxic to the cells 50% relative to controls.

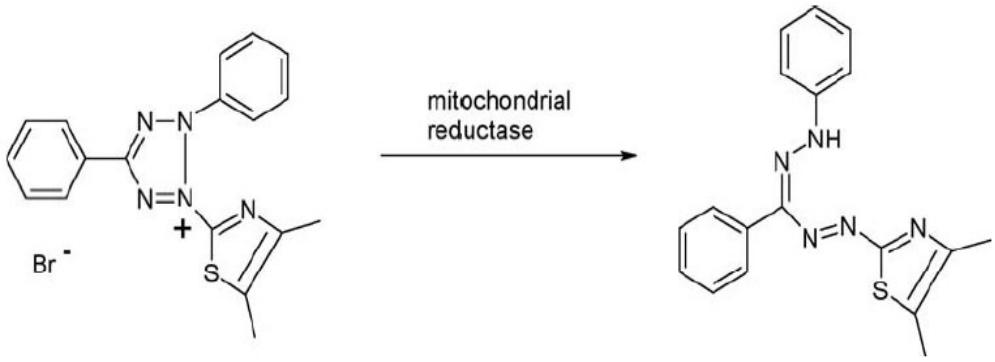

Figure 21 MTT is reduced to formazan by a mitochondrial reductase.

Cellular uptake study and permeation study

Human nasal septum carcinoma cells were seeded on six-well plate Transwell® permeable support 0.4 µm polyester membrane as shown in Figure 23 with cell density of 4×10^5 cells/cm^2 (Thanyamas, 2009). The cells were grown to a confluent monolayer within three to six days to form a multilayer cell substrate with tight junctions. The monolayer integrity was assessed firstly by inverted microscope, and confirmed again before permeation study by measurement of trans-epithelial electrical resistance (TEER). The TEER of cultured cell monolayer was measured using an electrode. The resistance values (in ohms) from the membranes were subtracted from the values for holding a human nasal septum carcinoma cells monolayer to determine the resistance across the cell monolayer. The amount of AA permeated through the cell layer and the amount retained in the cell layer were evaluated for AA-SLN. The media solution on confluent cell monolayers were

removed and rinsed with Hanks' balance salt solution (HBSS) at both compartments (apical side and basolateral side) and allowed to equilibrate for 1 hr. The 1.5 ml of sample concentration of 14 µg/ml diluted with HBSS solution composed of AA loaded TM AA-SLN, 0.3% CT/TM AA-SLN, SOF AA-SLN and 0.3% CT/SOF AA-SLN in media solution for 30 minutes (AA solution in methanol was used as control) was added to the apical compartment. At the end time point, the apical and basolateral compartment was withdrawn. The amounts of AA in both compartments were determined by HPLC method at UV absorbance 210 nm and the cells that remaining attached on membrane were washed thrice with PBS solution pH 7.4 The volume 0.5 ml of 0.025% w/v trypsin EDTA solution was added and the cell suspension was centrifuged for 3 miniutes at 4000 rpm. The supernatant was decanted and the pellets were resuspended in 10 ml of methanol:chloroform 1:1 and vortexed for 30 minutes to extract the AA. Then, the methanol:chloroform 1:1 was evaporated and the residue of AA was diluted by methanol and analyzed using HPLC method at 210 nm as described in permeation study (Gokce et al., 2008).

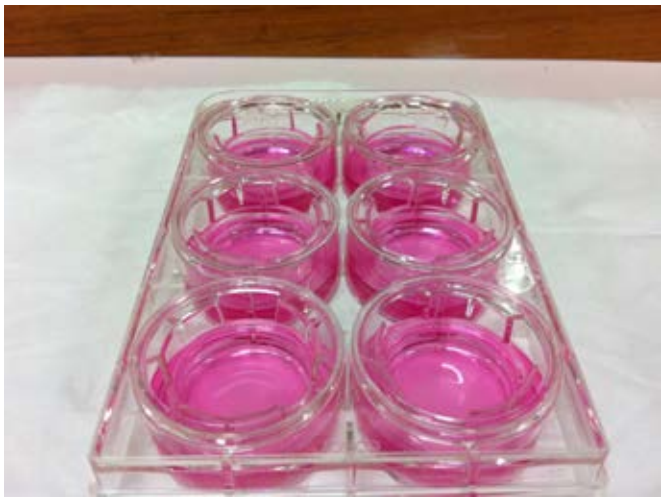

Figure 22 Six-well plate Transwell® permeable support 0.4 µm polyester membrane.

Tight junction integrity study

The trans-epithelial electrical resistance (TEER) was measured to assess the integrity of the cell substrates using a Millicell ERS-meter (Millipore Corp., Bedford, MA) as shown in Figure 22. TEER was performed before the drug permeation study. For negative control, no SLN were applied to the cell monolayers. After permeation study, the SLN were carefully removed. The complete media were applied on apical and basolateral sides. TEER was measured at the end of time (30 minutes) and again at 2 hours later. TEER values were expressed in relative values compared with TEER values before permeation experiments.

Figure 23 TEER measurement instrument: Millicell ERS-meter (Millipore, USA).

Viability of cell monolayer

Plasma membrane integrity was analyzed by performing trypan blue dye exclusion. Both the apical and basolateral sides of the cell monolayers were washed several times with PBS after finishing permeation experiment. The cell monolayer was trypsinized and diluted with the same amounts of 0.4% trypan blue solution (Sigma Aldrich, USA). Viable and non viable cells presented as absence and presence of intracellular tryptan blue were counted separately by haemocytometer and calculated as percentage of viable cells.

CHAPTER IV

RESULTS

2 Preparation of solid lipid nanoparticles (SLN)

2.1 Drug - free solid lipid nanoparticles (drug – free SLN)

In this study, drug-free SLN were prepared by the method of hot-high pressure homogenization, in order to investigate the effect of solid and surfactants on the formation and characterization of SLN and to obtain the SLN formulations with excellent stability. SLN were prepared with six different types of lipid, TM, TS, GB, SOF, PA and SA. TW80 was used as a single surfactant by varying the concentration from 1% to 5% w/w. From results shown in Table 2 only two different lipid types could produced acceptable fluid dispersion referring to TM and TS while GB, SOF, PA and SA could not obtain stabilized formulation at the same concentration of TW80. This might be due to TW80 could not decrease the surface tension and stabilize newly formed surfaces during homogenization. SLN is usually stabilized by a surfactant layer, which may consist of a single surfactant, but typically is composed of a mixture of surfactants. Combined surfactants showed advantages more than single surfactants according to previous studies. In the case of o/w emulsions, mixed surfactants have been reported to have a synergistic effect on emulsion stability in term of coalescence rate. The combination using of two emulsifying agents appeared to produce mixed surfactant film at the interface having high surfactant coverage as well as sufficient to promote stability (Michele and Francesca, 2003). If non-ionic surfactant TW80 was used only, translucent and blue opalescent emulsions with fine stability were obtained, but phase separation occurred one and several weeks later at 4◦C, respectively and lecithin was used as single emulsifier, it was easy to form vesicles to slow down the molecular movements and could not cover the naked new surface immediately due to emulsifier molecules were fixed inside the vesicles. But there was no gelating phenomenon in the samples with addition of co-emulsifier, especially good stability in combined emulsifier samples (Fei et al., 2008).

Thus, drug-free SLN were prepared with combined surfactant between TW80 and co-surfactants; SP80, SP85, SL, and PL188 in the ratios of 1:9, 3:7, 5:5, 7:3 and 9:1 as shown in Tables 3-4 by concentration of total surfactants in this study was 4% w/w similar to a previous study, an optimal particle size and good physical stability was obtained with 4% (w/w) of mixed emulsifier especially for TW:SP85, the SLN based on compritol ATO 888 (glycerol behenate) modified with 4% TW80:SP 85 and EQ1 (*N*,*N*-di-(b-stearoylethyl)-*N*,*N*-dimethyl ammonium chloride) (SII-13) were found was able to form stable complexes with DNA (Carsten et al., 2001). Drug – free SLN with PL188 was used as co-surfactant did not obtained stabilized formulation after preparation in all type of lipids (within one week, the precipitated on the bottom of container were observed). This might be due to with increasing molecular weight, the polymer adsorption layer thickness also increased, thus shifting the shear of plane to a further distance to the particle surface resulting in a decreased of the measured zeta potential may be induce, resulting in the decreasing of electric repulsion between particles and leading to particle aggregation. Thus, all of drug – free SLN formulations with PL188 did not store in accelerated conditions.

Most drug-free SLN with SP80, SP85 and SL as co-surfactants obtained stabilized formulations as shown in Table 4. After stored in accelerated conditions, formulation with TM as solid lipids obtained stabilized drug – free SLN formulations in the ratios of surfactants TW80: SP80 5:5 and 7:3, TW80:SP85 5:5 and 7:3 and all ratios of TW80:SL. Formulation with TS obtained stabilized drug – free SLN formulations in the ratios of surfactants TW80:SP80 5:5 and 7:3, TW80:SP 85 5:5 and 7:3 and TW80:SL 1:9, 3:7 and 5:5. Formulation with GB obtained stabilized drug – free SLN formulations in the ratios of surfactants TW80:SP80 5:5 and 7:3, TW80:SP85 5:5 and 7:3 and TW80:SL 9:1. For SOF in the ratios of surfactants TW80:SP80 5:5, 7:3 and 9:1, TW80:SP85 5:5, 7:3 and 9:1 would be obtained. None of the ratio of surfactants TW80:SL could stabilize drug – free SLN when using SOF as solid lipid. An explanation for the observed aggregation may involve an intrinsic thermodynamic instability of the nanoparticle system with dispersed molecules of the surfactant and co-surfactants in the lipid matrix but finally resulting in an adsorption of the surfactants to the particle surface (Goppert and Muller, 2005). The

surfactant predominantly influences the final particle size that could be achieved during the homogenization and influences the stability of the dispersions by providing sufficient repulsive interaction forces that prevent droplets from coming into close contact leading to aggregation. In addition, the surfactant plays an additional very important role in controlling the crystallization process. Because of the small size of the parent nanoemulsions, the number of lipid molecules interacting with the hydrophobic emulsifier tail groups is large enough to modulate the crystallization process. Moreover, the surfactant can subsequently improve the kinetic stability of the generated crystal structure even if that crystal structure is thermodynamically less stable than that of a corresponding alternative polymorphic form and thereby prevent re-crystallization during storage that may lead to destabilization of the dispersion during storage (Jochen et al., 2008).

The destabilized formulations of PA and SA in all ratio of surfactants might be related with higher viscosity and melting point of the PA and SA. The higher melting point of lipids could lead to a less effective homogenization process, thus resulting in bigger sizes and wider particle size distributions as resulting in particle agglomerations. The formulations of TM; TW80: SP80 5:5 and 7:3, TW80:SP85 5:5 and 7:3 and all ratios of TW80:SL. The formulations of TS; TW80:SP80 5:5 and 7:3, TW80:SP 85 5:5 and 7:3 and TW80:SL 1:9, 3:7 and 5:5. The formulations of GB; TW80:SP80 5:5 and 7:3, TW80:SP85 5:5 and 7:3 and TW80:SL 9:1. The formulations of SOF in the ratios of surfactants TW80:SP80 5:5, 7:3 and 9:1, TW80:SP85 5:5, 7:3 and 9:1 also showed a good appearance and good physical stability when freshly prepared and after stored in accelerated conditions (4°C for 48 hours and 45° C for 48 hours) for 6 cycles. Therefore, these formulations were selected to load AA and further characterized.

Table 2 Physical appearance of drug-free SLN for varying concentration of tween80 (single surfactant).

Surfactants ratios	1% GB		1% PA		1% SA		1% SOF		1%TM		1%TS	
	one week	accelerate conditions	one week	accelerate	one week	accelerate conditions	one week	accelerate conditions	one week	accelerate conditions	one week	accelerate conditions
1% TW80	P	-	P	-	P	-	P	-	+	+	+	+
2% TW80	P	-	P	-	P	-	P	-	+	+	+	+
3% TW80	P	-	P	-	P	-	P	-	+	+	+	+
4% TW80	P	-	P	-	P	-	P	-	+	+	+	+
5% TW80	P	-	P	-	P	-	P	-	+	+	+	+

+ = acceptable fluid dispersion, P = precipitation, - = not determined

Table 3 Physical appearance of drug-free SLN for varying surfactant ratios (TW80:PL188 and TW80:SP80) in various formulations (combined surfactant).

Surfactants ratios	1% GB		1% PA		1% SA		1% SOF		1%TM		1%TS	
	one week	accelerate conditions	one week	accelerate conditions	one week	accelerate conditions	one week	accelerate conditions	one week	accelerate conditions	one week	accelerate conditions
TW80 : PL188 1:9	P	-	P	-	P	-	P	-	P	-	P	-
TW80 : PL188 3:7	P	-	P	-	P	-	P	-	P	-	P	-
TW80 : PL188 5:5	P	-	P	-	P	-	P	-	P	-	P	-
TW80 : PL188 7:3	P	-	P	-	P	-	P	-	P	-	P	-
TW80 : PL188 9:1	P	-	P	-	P	-	P	-	P	-	P	-
TW80 : SP80 1:9	P	-	P	-	P	-	P	-	+	P	+	P
TW80 : SP80 3:7	+	P	P	-	P	-	+	P	+	P	+	P
TW80 : SP80 5:5	+	+	P	-	P	-	+	+	+	+	+	+
TW80 : SP80 7:3	+	+	P	-	P	-	+	+	+	+	+	+
TW80 : SP80 9:1	+	P	P	-	P	-	+	+	+	P	+	P

+ = acceptable fluid dispersion , P = precipitation, - = not determined

Table 4 Physical appearance of drug-free SLN for varying surfactant ratios (TW80:SP85 and TW80:SL) in various formulations (combined surfactant).

Surfactants ratios	1% GB		1% PA		1% SA		1% SOF		1%TM		1%TS	
	one week	accelerate conditions	one week	accelerate conditions	one week	accelerate conditions	one week	accelerate conditions	one week	accelerate conditions	one week	accelerate conditions
TW80 : SP85 1:9	P	-	P	-	P	-	P	-	+	P	+	P
TW80 : SP85 3:7	+	P	P	-	P	-	P	-	+	P	+	P
TW80 : SP85 5:5	+	+	P	-	P	-	+	+	+	+	+	+
TW80 : SP85 7:3	+	+	P	-	P	-	+	+	+	+	+	+
TW80 : SP85 9:1	+	P	P	-	P	-	+	+	+	P	+	P
TW80 : SL 1:9	P	-	P	-	P	-	P	-	P	-	+	+
TW80 : SL 3:7	+	P	P	-	P	-	P	-	P	-	+	+
TW80 : SL 5:5	+	P	P	-	P	-	P	-	+	+	+	+
TW80 : SL 7:3	+	P	P	-	P	-	P	-	+	+	P	-
TW80 : SL 9:1	+	+	P	-	P	-	P	-	+	+	P	-

+ = acceptable fluid dispersion , P = precipitation, - = not determined

1.2 Asiatic acid loaded solid lipid nanoparticles (AA-SLN)

Table 5 were shown TM and TS with 1 to 5% w/w of TW80 could not loaded an sufficient amount of AA (not more than 0.1 mg/ml) into formulations. This might be due to AA had lipophilicity characteristic when incorporated co-surfactants into lipid phase, it could promote the solubility of AA in particles to obtain higher loaded of AA concentration than single surfactant. In combined surfactants, formulations with GB and formulations with SOF obtained the highest concentration of 1 mg/ml AA in all surfactant ratios. TM and TS obtained the concentration of 0.7 mg/ml AA in TW:SP80 and TW:SP85 and obtained the lowest concentration of 0.5 mg/ml AA in TW:SL. The result concluded that the amount of AA loaded in SLN formulations depended on solubility of drug in solid lipids, surfactant and co-surfactants.

The highest amount of loading drug in GB formulations might be due to GB is a mixture of monoglycerides, diglycerides, and triglycerides of mainly C22-fatty acid chains as compared with the pure triglyceride particles (TM and TS), leading to produces less ordered lipid crystals. In the nanoparticle structure, the lipid that results in a highly crystalline structure with a perfect lattice would lead to drug expulsion. On the other hand, the imperfection (lattice defects) of the lipid structure could offer more loading space to accommodate drugs. As a result, the structure of less ordered arrangement in the nanoparticles would be beneficial to the drug loading capacity (Hou et al., 2003). SOF also displayed high AA loading in SLN, as it occurred as plate-like structure in nanodispersions leading to increasing number of contact between dispersed particles unlike the spherical shape that provides less particle and less consistency than plate-like structure with highly ordered crystal packing of SOF leading to AA could attach to SOF nanoparticles and present high loading drug (Nispa et al., 2010). However, the amount of drug to be incorporated into the delivery system is dependent on the physicochemical properties of drug and the preparation process.

Table 5 The amount of asiatic acid loaded solid lipid nanoparticles (AA-SLN) in selected formulations.

Solid lipids	Ratio of suractants	The amount of asiatic acid (mg/ml)
TM	TW80 : SP80 5:5	0.7008
	TW80 : SP80 7:3	0.7089
	TW80 : SP85 5:5	0.7023
	TW80 : SP85 7:3	0.7012
	TW80 : SL 5:5	0.5093
	TW80 : SL 7:3	0.5045
	TW80 : SL 9:1	0.5109
TS	TW80 : SP80 5:5	0.7043
	TW80 : SP80 7:3	0.7065
	TW80 : SP85 5:5	0.7023
	TW80 : SP85 7:3	0.7012
	TW80 : SL 1:9	0.5034
	TW80 : SL 3:7	0.5092
	TW80 : SL 5:5	0.5023
GB	TW80 : SP80 5:5	1.0989
	TW80 : SP80 7:3	1.0455
	TW80 : SP85 5:5	1.1023
	TW80 : SP85 7:3	1.0668
	TW80 : SL 9:1	1.0729
SOF	TW80 : SP80 5:5	1.0077
	TW80 : SP80 7:3	1.0656
	TW80 : SP80 9:1	1.0455
	TW80 : SP85 5:5	1.0304
	TW80 : SP85 7:3	1.0904
	TW80 : SP85 9:1	1.0724

1.3 Chitosan coated asiatic acid loaded solid lipid nanoparticles (CT/AA-SLN)

After storage in three conditions, 4°C, room temperature and 45°C for 6 months, the AA-SLN were selected. Optimized SLN dispersion on that showed acceptable fluid dispersion and particle size of less than 500 nm. The chitosan solution was incorporated concentration in range from 0.1, 0.3 and 0.5% w/v with respect to AA-SLN. The selected AA-SLN formulations to be coated with chitosan are shown in Table 6.

Table 6 The selected AA-SLN formulations to be coated with chitosan solution.

Solid lipids	Ratio of surfactants
TM	TW80 : SP80 5:5 TW80 : SP80 7:3 TW80 : SL 9:1
GB	TW80 : SP80 7:3 TW80 : SP85 5:5
SOF	TW80 : SP80 5:5 TW80 : SP85 5:5 TW80 : SP85 7:3

2. Stability study

One of the advantages of SLN was to protect incorporated drug from physical and chemical degradation. To prove this advantage, the physical and chemical stability of SLN containing asiatic acid was evaluated. The AA-SLN formulations were kept for 6 months in three conditions at 4° C in refrigerator, room temperature and 45° C in incubator. The physical appearance, pH measurement **,** particle size, size distribution and zeta potential and drug remaining were evaluated after 6 months compared with initial preparation.

Physical appearance

The physical appearances of AA-SLN formulations such as precipitation were visually observed compared with initial preparations as shown in Tables 7-10**.** When TM was used as solid lipid**,** non-stabilized SLN were obtained in the ratios of surfactants as TM TW80:SP80 5:5, TM TW80:SP80 7:3, TM TW80:SP85 7:3 and TM TW80:SL 1:9. For TS as solid lipid the ratios of surfactants were TS TW80:SP80 5:5, TS TW80:SP80 7:3, TS TW80:SL 1:9, TS TW80:SL 3:7 and TS TW80:SL 5:5. For SOF, the ratios of surfactants were SOF TW80:SP80 7:3, SOF TW80:SP80 9:1 and SOF TW80:SP85 9:1. All formulations of GB obtained stabilized products.

As the nanoparticles were presented with a tremendous increase in surface area and very high surface activity, aggregation and particle fusion were frequently noticed after a long period of storage of such nanoparticulate dispersions. High temperature and energy input could lead to changes in the crystalline structure of lipids resulting in the subsequent and gradual gelation and the growth of particles occurred at a faster rate than at lower temperature. The temperature at 4°C was generally the most favorable storage temperature (Freitas and Muller, 1998). At lower temperature, a high film rigidity of the emulsifier (microviscosity) avoided fusion of the film layers after particle contact. Microviscosity was a temperature dependent

factor. Increase in temperature caused indecrease in microviscosity leading to destabilization of the SLN dispersion (Schuhmann, 1995).

Table 7 The physical appearance of SLN formulations (TM as lipid) compared with initial and after storage conditions for 6 months**.**

TM was used as lipid	Initial	Appearance											
		4 ◦C				Room Temperature				45 ◦C			
		1 month	2 months	3 months	6 months	1 month	2 months	3 months	6 months	1 month	2 months	3 months	6 months
TW80 : SP80	+	+	+	+	+	+	+	+	+	P	P	P	P
TW80 : SP80	+	+	+	+	+	+	+	+	+	P	P	P	P
TW80 : SP85	+	+	+	+	+	+	+	+	+	+	+	+	+
TW80 : SP85	+	+	+	+	+	+	+	+	+	+	P	P	P
TW80 : SL 1:9	+	+	+	+	+	+	+	+	+	P	P	P	P
TW80 : SL 3:7	+	+	+	+	+	+	+	+	+	P	P	P	P
TW80 : SL 5:5	+	+	+	+	+	+	+	+	+	P	P	P	P
TW80 : SL 7:3	+	+	+	+	+	+	+	+	+	+	+	+	+
TW80 : SL 9:1	+	+	+	+	+	+	+	+	+	+	+	+	+

+ = acceptable fluid dispersion, P = precipitation

Table 8 The physical appearance of SLN formulations (TS as lipid) compared with initial and after storage conditions for 6 months**.**

TS was used as lipid	Initial	Appearance											
		4 ˚C				Room Temperature				45 ˚C			
		1 month	2 months	3 months	6 months	1 month	2 months	3 months	6 months	1 month	2 months	3 months	6 months
TW80 : SP80 5:5	+	+	+	+	+	+	+	+	+	+	+	P	P
TW80 : SP80 7:3	+	+	+	+	+	+	+	+	+	+	+	P	P
TW80 : SP85 5:5	+	+	+	+	+	+	+	+	+	+	+	+	+
TW80 : SP85 7:3	+	+	+	+	+	+	+	+	+	+	+	+	+
TW80 : SL 1:9	+	+	+	+	+	+	+	+	+	+	+	P	P
TW80 : SL 3:7	+	+	+	+	+	+	+	+	+	+	+	P	P
TW80 : SL 5:5	+	+	+	+	+	+	+	+	+	+	+	P	P

+ = acceptable fluid dispersion, P = precipitation

Table 9 The physical appearance of SLN formulations (GB as lipid) compared with initial and after storage conditions for 6 months**.**

GB was used as lipid	Initial	Appearance											
		4 ˚C				Room Temperature				45 ˚C			
		1 month	2 months	3 months	6 months	1 month	2 months	3 months	6 months	1 month	2 months	3 months	6 months
TW80 : SP80 5:5	+	+	+	+	+	+	+	+	+	+	+	+	+
TW80 : SP80 7:3	+	+	+	+	+	+	+	+	+	+	+	+	+
TW80 : SP85 5:5	+	+	+	+	+	+	+	+	+	+	+	+	+
TW80 : SP85 7:3	+	+	+	+	+	+	+	+	+	+	+	+	+
TW80 : SL 9:1	+	+	+	+	+	+	+	+	+	+	+	+	+

+ = acceptable fluid dispersion, P = precipitation

Table 10 The physical appearance of SLN formulations (SOF as lipid) compared with initial and after storage conditions for 6 months**.**

SOF was used as lipid	Initial	Appearance											
		4 ˚C				Room Temperature				45 ˚C			
		1 month	2 months	3 months	6 months	1 month	2 months	3 months	6 months	1 month	2 months	3 months	6 months
TW80 : SP80 5:5	+	+	+	+	+	+	+	+	+	+	+	+	+
TW80 : SP80 7:3	+	+	+	+	+	+	+	+	+	+	+	P	P
TW80 : SP80 9:1	+	+	+	+	+	+	+	+	+	+	+	P	P
TW80 : SP85 5:5	+	+	+	+	+	+	+	+	+	+	+	+	+
TW80 : SP85 7:3	+	+	+	+	+	+	+	+	+	+	+	+	+
TW80 : SP85 9:1	+	+	+	+	+	+	+	+	+	+	+	P	P

+ = acceptable fluid dispersion, P = precipitation

pH measurement

In this study, the pH stability of AA-SLN formulations were observed to maintain the average pH in range 4.5 – 6.5 which is suitable for use in nasal delivery route for long term duration. It was found that the pH values in all AA-SLN formulations decreased with time as shown in Table 11. Storage for 6 months in three conditions tended to obtain lower average pH than initial for all formulations. That might be due to the hydrolysis of triglycerides part of solid lipids to acquire the formation of free fatty acid (acidic activity). The pH values of most AA-SLN formulations at higher temperature (45°C) the results showed higher pH values than at lower temperature (4 °C and room temperature). These effect might due to loss activity of asiatic acid in high energy input conditions. This results were also in agreement with the drug remaining stability. Therefore pH values of AA-SLN formulations exhibited upon the storage conditions. In addition, a comparison of pH values of SOF formulations at 45°C with 4 °C and room temperature, demonstrated that the hydrolysis in SOF to produce free fatty acid did affect the pH values more than degradation of asiatic acid as a result SOF formulations tended to obtained lower average pH for high temperature conditions.

Table 11 The average pH of AA-SLN in various formulations compared with initial and after storage conditions for 6 months.

Solid lipids	Ratio of surfactants	The average pH ± SD Initial	The average pH ± SD (after storage for 6 months)		
			4 ° C	Room Temperature	45 ° C
TM	TW80 : SP80	5.11 ± 0.01	4.70± 0.01	3.63± 0.16	N
	TW80 : SP80	5.12± 0.02	4.60± 0.02	4.09± 0.01	N
	TW80 : SP85	4.99± 0.16	4.40± 0.13	3.87± 0.22	3.96± 0.16
	TW80 : SP85	4.80± 0.12	3.73± 0.15	3.20± 0.02	N
	TW80 : SL 5:5	4.79± 0.01	3.76± 0.17	3.62± 0.11	4.03 ± 0.14
	TW80 : SL 7:3	4.72± 0.01	3.75± 0.15	3.77± 0.11	4.18 ± 0.15
	TW80 : SL 9:1	4.58± 0.16	3.89± 0.17	3.79± 0.17	3.94± 0.11
TS	TW80 : SP80	5.78± 0.11	4.83± 0.01	4.96± 0.12	N
	TW80 : SP80	5.85± 0.11	4.51± 0.15	3.88± 0.17	N
	TW80 : SP85	5.35± 0.01	3.73± 0.01	3.49± 0.01	3.94± 0.01
	TW80 : SP85	5.40± 0.13	3.72± 0.13	3.38± 0.12	3.79
	TW80 : SL 1:9	4.95± 0.16	4.62± 0.11	4.51± 0.01	N
	TW80 : SL 3:7	4.84± 0.16	4.59± 0.01	4.69± 0.16	N
	TW80 : SL 5:5	4.25± 0.13	4.17± 0.15	4.05± 0.16	N
GB	TW80 : SP80	5.42± 0.02	4.83± 0.22	3.55± 0.19	4.98± 0.11
	TW80 : SP80	5.11± 0.15	4.51± 0.17	3.66± 0.22	4.47± 0.05
	TW80 : SP85	4.16± 0.02	3.71± 0.22	3.25± 0.02	3.97± 0.13
	TW80 : SP85	4.11± 0.02	3.72± 0.02	3.24± 0.13	3.79± 0.15
	TW80 : SL 9:1	4.52± 0.12	3.56± 0.12	3.62± 0.11	3.68± 0.02
SOF	TW80 : SP80	5.94± 0.17	4.91± 0.11	4.92± 0.13	4.42± 0.22
	TW80 : SP80	6.28± 0.02	5.36± 0.17	4.45± 0.15	N
	TW80 : SP80	6.42± 0.13	4.34± 0.02	4.47± 0.02	N
	TW80 : SP85	6.11± 0.01	4.28± 0.13	4.39± 0.13	4.05± 0.12
	TW80 : SP85	6.41± 0.01	4.43± 0.01	4.56± 0.02	4.08± 0.11
	TW80 : SP85	6.47± 0.17	4.99± 0.17	5.56± 0.13	N

Note: N = Not determined .

Particle size, size distribution and zeta potential

The particle size, size distribution and zeta potential of AA-SLN compared with initial and after storage for a periods of 6 months were shown in Tables 12-15. It was observed that all AA-SLN formulations were presented with no significant change in the mean particle size after storage at refrigerator and room temperature that a slight increase in average nanoparticles size was shown. This indicated that AA-SLN formulations displayed sufficient stability upon storage of six months in both conditions.

When storage at 45° C, a number of AA-SLN formulations were precipitated within 1 to 6 months correlated to the stability results of physical appearance. The dimensions of AA-SLN in some cases were not reported because destabilized formulations were observed. This instability was probably due to increased fluidity of the low transition temperature at 45° C, in conjunction with the precipitation tendency of the solid core lipids, and might be due to the high temperature could elevated surfactants diffusion from the interface of nanoparticles as a result higher solubility in the external aqueous phase rather than in the lipid matrix. Previous reports have suggested that the precipitation may be due to a mismatch between the changing solid lipid surface and the stabilizer, which must cover the surface during the phase-changing process.

The measurement of the zeta potential allowed the predictions about the storage stability of SLN dispersions. In general, particle aggregation is less likely to occur for charged particles (high zeta potential) due to electric repulsion. Most zeta potential values were found to mostly increase significantly different for all of storage conditions with respect to the initial value. The low values of zeta potential in most formulations for this study seemed to be critical and indicator for the initiation of aggregation. The particles had to overcome an energy barrier of electrostatic repulsion to approach closely and form agglomerates. The zeta potential decreased with increasing energy input such as temperature, this energy input could lead to changes in the crystalline structure of the lipid. Crystalline re-orientation could result in

changes of the charges on the particle surface (Nernst potential) and subsequently the measured zeta potential. In addition, different sides of a crystal could possess a different charge density. From these results, it was found that all SLN formulations initially possessed a potential as low as ±30 mV. This was at the lower edge of the zeta potential range required for adequate stabilization (Müller and Heinemann, 1994). The decreased in absolute zeta potential to near zero value corresponded with the increase in the particle size of the SLN formulations due to the lack of electrostatic repulsion between nanaparticles. However, the zeta potential of stabilized formulations were just below the critical value but still sufficient for stable system in combination with the sterically stabilizing effect of TW80. This indicated that in all SLN formulations regardless of the type of vehicle and their initial charge.

Table 12 Particle size (Size), size distribution (PDI) and zeta potential (ZP) of TM AA-SLN compared with initial and after storage conditions for 6 month (n=3).

Trimyristin as lipid	Initial			After storage 6 months								
				4 ° C			Room Temperature			45 ° C		
	Size ± SD (nm)	PDI ± SD	ZP± SD (MV)	Size ± SD (nm)	PDI ± SD	ZP± SD (MV)	Size ± SD (nm)	PDI ± SD	ZP± SD (MV)	Size ± SD (nm)	PDI ± SD	ZP± SD (MV)
TW80 : SP80 5:5	64.97 ±1.09	0.58 ±0.01	-16.40 ±0.61	58.73 ±1.18	0.28 ±0.02	-8.16 ±0.02	318.80 ±5.41	0.74 ±0.03	-5.34 ±0.52	N	N	N
TW80 : SP80 7:3	100.40 ±2.29	0.63 ±0.03	-10.70 ±1.33	63.08 ±0.79	0.48 ±0.03	-6.11 ±0.32	1767 ±7.94	0.53 ±0.13	-1.51 ±0.11	N	N	N
TW80 : SP85 5:5	90.60 ±1.80	0.43 ±0.03	-12.20 ±0.53	89.39 ±2.25	0.36 ±0.05	-4.81 ±0.19	89.73 ±4.05	0.34 ±0.04	-5.80 ±0.20	123.40 ±2.61	0.29 ±0.08	-4.63 ±0.28
TW80 : SP85 7:3	91.86 ±4.20	0.51 ±0.03	-5.78 ±1.30	94.70 ±6.04	0.48 ±0.03	-1.49 ±0.08	84.70 ±2.12	0.38 ±0.06	-1.61 ±0.05	N	N	N

Table 12 Particle size (Size), size distribution (PDI) and zeta potential (ZP) of TM AA-SLN compared with initial and after storage conditions for 6 month (n=3) (continuous).

Trimyristin as lipid	Initial			After storage 6 months								
				4 ◦ C			Room Temperature			45 ◦ C		
	Size ± SD (nm)	PDI ± SD	ZP± SD (MV)	Size ± SD (nm)	PDI ± SD	ZP± SD (MV)	Size ± SD (nm)	PDI ± SD	ZP± SD (MV)	Size ± SD (nm)	PDI ± SD	ZP± SD (MV)
TW80 : SL 1:9	45.90 ±3.67	0.67 ±0.04	-3.34 ±0.47	54.97 ±0.94	0.78 ±0.10	-2.23 ±0.12	55.88 ±1.09	0.72 ±0.07	-1.96 ±0.17	N	N	N
TW80 : SL 3:7	151.40 ±11.27	0.71 ±0.09	-3.16 ±1.16	137.00 ±4.84	0.52 ±0.04	-3.23 ±0.19	179.70 ±9.71	0.60 ±0.06	-1.57 ±0.12	N	N	N
TW80 : SL 5:5	163.20 ±4.09	0.78 ±0.10	-4.08 ±0.96	159.33 ±1.96	0.98 ±0.02	-2.42 ±0.13	171.37 ±2.78	0.58 ±0.02	-1.76 ±0.10	N	N	N
TW80 : SL 7:3	164.97 ±2.31	0.55 ±0.05	-4.59 ±0.41	147.43 ±5.88	0.59 ±0.04	-2.37 ±0.10	146.50 ±2.46	0.61 ±0.07	-1.37 ±0.09	121.13 ±3.01	0.37 ±0.04	-2.12 ±0.07
TW80 : SL 9:1	102.57 ±2.67	0.53 ±0.04	-6.72 ±0.22	84.59 ±3.61	0.50 ±0.03	-1.83 ±0.04	97.41 ±0.36	0.50 ±0.02	-1.43 ±0.10	139.20 ±5.77	0.30 ±0.02	-1.68 ±0.15

Note: N = Not determined.

Table 13 Particle size (size), size distribution (PDI) and zeta potential (ZP) of TS AA-SLN compared with initial and after storage conditions for 6 months (n=3).

Tristearin as lipid	Initial			After storage 6 months								
				4 ° C			Room Temperature			45 ° C		
	Size ± SD (nm)	PDI ± SD	ZP± SD (MV)	Size ± SD (nm)	PDI ± SD	ZP± SD (MV)	Size ± SD (nm)	PDI ± SD	ZP± SD (MV)	Size ± SD (nm)	PDI ± SD	ZP± SD (MV)
TW80 : SP80 5:5	120.87 ±4.79	0.46 ±0.10	-19.50 ±1.41	80.88 ±1.33	0.47 ±0.06	-9.74 ±0.15	74.85 ±2.29	0.41 ±0.03	-7.81 ±0.18	N	N	N
TW80 : SP80 7:3	170.37 ±10.89	0.61 ±0.04	-12.47 ±1.66	87.23 ±0.57	0.60 ±0.01	-5.10 ±0.38	116.57 ±2.10	0.55 ±0.07	-4.20 ±0.06	N	N	N
TW80 : SP85 5:5	119.50 ±1.87	0.38 ±0.07	-13.13 ±1.40	114.30 ±1.15	0.35 ±0.05	-2.15 ±0.01	115.27 ±0.60	0.36 ±0.03	-2.40 ±0.13	619.53 ±27.87	0.34 ±0.01	-0.84 ±2.83
TW80 : SP85 7:3	145.23 ±4.02	0.55 ±0.06	-7.10 ±1.09	110.07 ±3.80	0.60 ±0.01	-1.97 ±0.01	118.57 ±0.80	0.53 ±0.05	-1.75 ±0.10	1260 ±18.68	0.37 ±0.06	-3.39 ±0.43

Note: N = Not determined.

Table 13 Particle size (Size), size distribution (PDI) and zeta potential (ZP) of TS AA-SLN compared with initial and after storage conditions for 6 months (continuous) (n=3).

Tristearin as lipid	Initial			After storage 6 months								
				4 ° C			Room Temperature			45 ° C		
	Size ± SD (nm)	PDI ± SD	ZP± SD (MV)	Size ± SD (nm)	PDI ± SD	ZP± SD (MV)	Size ± SD (nm)	PDI ± SD	ZP± SD (MV)	Size ± SD (nm)	PDI ± SD	ZP± SD (MV)
TW80 : SL 1:9	142.30 ±2.66	0.61 ±0.01	-3.38 ±0.33	133.83 ±7.74	0.81 ±0.20	-4.06 ±0.12	141.60 ±1.91	0.60 ±0.02	-4.42 ±0.22	N	N	N
TW80 : SL 3:7	165.40 ±1.59	0.74 ±0.16	-3.77 ±0.48	165.53 ±4.65	0.72 ±0.15	-2.51 ±0.08	162.83 ±2.28	0.59 ±0.05	-2.18 ±0.07	N	N	N
TW80 : SL 5:5	186.50 ±2.23	-6.90 ±0.16	-6.98 ±0.77	143.27 ±3.09	0.59 ±0.09	-3.86 ±0.15	147.00 ±5.38	0.69 ±0.14	-1.58 ±0.05	N	N	N

Note: N = Not determined.

Table 14 Particle size (Size), size distribution (PDI) and zeta potential (ZP) of GB AA-SLN compared with initial and after storage conditions for 6 months (n=3).

Glyceryl behenate as lipid	Initial			After storage 6 months								
				4 ˚C			Room Temperature			45 ˚C		
	Size ± SD (nm)	PDI ± SD	ZP± SD (MV)	Size ± SD (nm)	PDI ± SD	ZP± SD (MV)	Size ± SD (nm)	PDI ± SD	ZP± SD (MV)	Size ± SD (nm)	PDI ± SD	ZP± SD (MV)
TW80 : SP80 5:5	151.00 ±3.65	0.53 ±0.04	-17.60 ±1.56	91.90 ±2.62	0.55 ±0.03	-9.41 ±0.08	115.83 ±3.32	0.37 ±0.12	-4.52 ±0.25	1357.67 ±11.06	0.92 ±0.13	-4.36 ±0.35
TW80 : SP80 7:3	84.93 ±10.40	0.90 ±0.18	-13.97 ±0.50	116.50 ±3.40	0.30 ±0.03	-4.73 ±0.44	137.87 ±1.92	0.27 ±0.02	-3.51 ±0.21	331.07 ±0.76	0.31 ±0.02	-3.62 ±0.10
TW80 : SP85 5:5	139.50 ±8.78	0.57 ±0.03	-15.97 ±0.95	101.47 ±2.57	0.47 ±0.05	-2.36 ±0.19	102.80 ±1.15	0.48 ±0.04	-2.36 ±0.04	274.97 ±13.76	0.24 ±0.07	-3.31 ±0.20

Note: N = Not determined.

Table 14 Particle size (Size), size distribution (PDI) and zeta potential (ZP) of GB AA-SLN compared with initial and after storage conditions for 6 months (continuous) (n=3).

Glyceryl behenate as lipid	Initial			After storage 6 months								
				4 ˚C			Room Temperature			45 ˚C		
	Size ± SD (nm)	PDI ± SD	ZP± SD (MV)	Size ± SD (nm)	PDI ± SD	ZP± SD (MV)	Size ± SD (nm)	PDI ± SD	ZP± SD (MV)	Size ± SD (nm)	PDI ± SD	ZP± SD (MV)
TW80 : SP85 7:3	142.70 ±15.20	0.58 ±0.16	-11.30 ±0.40	92.08 ±2.65	0.73 ±0.11	-1.87 ±0.02	92.04 ±1.24	0.45 ±0.02	-1.63 ±0.20	794.00 ±6.56	0.37 ±0.03	-3.32 ±0.21
TW80 : SL 9:1	34.53 ±0.81	0.74 ±0.02	-7.44 ±0.32	45.78 ±0.87	0.79 ±0.05	-2.48 ±0.19	44.52 ±0.49	0.74 ±0.03	-2.07 ±0.15	1771.33 ±6.35	0.46 ±0.20	-1.54 ±0.18

Note: N = Not determined.

Table 15 Particle size (Size), size distribution (PDI) and zeta potential (ZP) of SOF AA-SLN compared with initial and after storage conditions for 6 months (n=3)**.**

Softisan 154 as lipid	Initial			After storage 6 months								
				4 ˚C			Room Temperature			45 ˚C		
	Size ± SD (nm)	PDI ± SD	ZP± SD (MV)	Size ± SD (nm)	PDI ± SD	ZP± SD (MV)	Size ± SD (nm)	PDI ± SD	ZP± SD (MV)	Size ± SD (nm)	PDI ± SD	ZP± SD (MV)
TW80 : SP80 5:5	63.38 ±1.58	0.42 ±0.10	-6.91 ±0.23	70.55 ±1.28	0.54 ±0.03	-8.16 ±0.14	62.64 ±0.54	0.40 ±0.03	-5.66 ±0.15	158.00 ±3.18	0.16 ±0.02	-6.85 ±0.06
TW80 : SP80 7:3	120.03 ±1.06	0.66 ±0.01	-5.06 ±0.25	84.42 ±1.31	0.10 ±0.01	-5.16 ±0.17	79.24 ±0.39	0.93 ±0.08	-4.53 ±0.13	N	N	N
TW80 : SP80 9:1	123.20 ±4.95	0.79 ±0.08	-3.38 ±0.40	96.06 ± 3.18	0.85 ±0.09	-3.14 ±0.05	102.37 ±1.00	0.91 ±0.02	-2.83 ±0.11	N	N	N

Note: N = Not determined.

Table 15 Particle size (Size), size distribution (PDI) and zeta potential (ZP) of SOF AA-SLN compared with initial and after storage conditions for 6 months (continuous) (n=3)**.**

Softisan 154 as lipid	Initial			After storage 6 months								
				4 ˚C			Room Temperature			45 ˚C		
	Size ± SD (nm)	PDI ± SD	ZP± SD (MV)	Size ± SD (nm)	PDI ± SD	ZP± SD (MV)	Size ± SD (nm)	PDI ± SD	ZP± SD (MV)	Size ± SD (nm)	PDI ± SD	ZP± SD (MV)
TW80 : SP85 5:5	113.50 ±2.86	0.37 ±0.09	-4.75 ±0.81	117.57 ±2.57	0.39 ±0.05	-5.16 ±0.15	108.90 ±0.72	0.32 ±0.04	-5.66 ±0.11	117.23 ±1.36	0.15 ±0.01	-3.97 ±0.07
TW80 : SP85 7:3	145.33 ±2.45	0.47 ±0.04	-5.33 ±0.82	171.77 ±2.51	0.55 ±0.05	-5.20 ±0.08	164.47 ±1.81	0.52 ±0.02	-3.24 ± 0.03	180.93 ±7.41	0.63 ±0.01	-2.84 ±0.10
TW80 : SP85 9:1	113.40 ±7.98	0.57 ±0.14	-4.56 ±0.75	103.93 ±2.44	0.52 ±0.05	-3.69 ±0.11	113.30 ± 2.10	0.52 ±0.03	-3.72 ±0.16	N	N	N

Note: N = Not determined .

Drug remaining

The total amount of asiatic acid remaining in the formulations was analyzed by HPLC method. Tables 16-17 are shows the percentage of asiatic acid remaining in SLN and norminalized values after storage for 6 months in three conditions: at 4° C, room temperature and 45° C compared with initial preparations. The percentage of asiatic acid remaining in AA-SLN formulations decreased with time. It was shown that the degradation of asiatic acid occurred and the percentage of total asiatic acid remaining decreased upon storage. At lower temperature (4 °C and room temperature) the results showed better chemical stability than at higher temperature (45°C). Similar to the results of particle size and zeta potential, high storage temperature (high energy) induced more rapid change in the crystalline structure of lipid to more stable form resulting in drug expulsion and subsequent decrease in % entrapment, leading to more drug in the external phase which then underwent further degradation. The variation between extraction process of AA by mixed solvent leading to the percentage of drug content did not decrease upon storage in some case.

From these stability study, to select the formulations that showed appropriate appearance, particle size and good physical stability, all formulations were visually observed after preparation for 1 week and after storage conditions for 6 months at room temperate, 4° C and 45° C. For TM series as lipid, TM TW80:SP85, TM TW80:SL 7:3 and TM TW80:SL 9:1 obtained stabilized formulations. For GB as lipid, GB TW80:SP80 7:3 and GB TW80:SP85 5:5 produced stabilized formulations. For SOF as lipid, SOF TW80:SP80 5:5, SOF TW80:SP85 5:5 and SOF TW80:SP80 7:3 provided stabilized formulations. Therefore, this stabilized formulations were selected to prepare AA-SLN coated with chitosan solution in order to improve mucoadhesive property.

Table 16 The percentage of total asiatic acid remaining in SLN formulations compared with initial and after storage conditions for 6 months.

Solid lipids	Ratio of emulsifiers	The average % drug content ± SD (Initial)	The average % drug content ± SD (after storage for 6 months)		
			4 °C	Room Temperature	45 °C
TM	TW80 : SP80	86.28 ± 4.81	79.03 ±	80.97 ± 3.68	N
	TW80 : SP80	82.35 ± 1.63	70.43 ± 0.88	73.61 ± 6.53	N
	TW80 : SP85	90.90 ± 0.27	90.70 ± 1.41	91.98 ± 2.30	90.33 ± 5.67
	TW80 : SP85	82.35 ± 1.63	70.43 ± 0.88	73.61 ± 6.53	N
	TW80 : SL 1:9	89.22 ± 1.62	78.29 ± 1.89	78.34 ± 2.56	N
	TW80 : SL 3:7	90.89 ± 0.76	76.56. ±	77.98 ± 1.36	N
	TW80 : SL 5:5	90.52 ± 1.02	79.15 ± 0.21	78.99 ± 3.37	N
	TW80 : SL 7:3	91.10 ± 0.52	69.84 ± 3.76	76.71 ± 3.78	70.71 ± 7.42
	TW80 : SL 9:1	92.02 ± 2.33	70.78 ± 6.55	71.31 ± 5.10	70.52 ± 3.70
TS	TW80 : SP80	85.75 ± 5.42	80.03 ± 4.75	82.19 ± 6.92	N
	TW80 : SP80	87.01 ± 3.53	84.04 ± 2.05	86.70 ± 2.30	N
	TW80 : SP85	92.72 ± 0.60	76.95 ± 0.82	81.00 ± 5.52	79.61 ± 3.37
	TW80 : SP85	90.92 ± 1.78	78.23 ± 1.54	70.06 ± 1.66	63.80 ± 0.84
	TW80 : SL 1:9	98.49 ± 1.69	88.27 ± 1.41	88.10 ± 0.54	N
	TW80 : SL 3:7	93.28 ± 3.55	80.77 ± 6.13	85.70 ± 4.39	N
	TW80 : SL 5:5	91.36 ± 2.43	85.70 ± 2.04	76.60 ± 1.96	N
GB	TW80 : SP80	94.24 ± 1.81	91.51 ± 2.87	92.72 ± 2.68	91.20 ± 1.20
	TW80 : SP80	92.25 ± 2.09	87.36 ± 2.35	90.99 ± 2.19	87.72 ± 2.21
	TW80 : SP85	81.88 ± 4.18	76.47 ± 0.33	78.35 ± 2.33	76.66 ± 0.52
	TW80 : SP85	86.21 ± 0.86	79.71 ± 2.51	82.96 ± 1.46	80.49 ± 3.61
	TW80 : SL 9:1	63.16 ± 5.96	56.83 ± 0.91	64.61 ± 3.12	64.16 ± 2.65
SOF	TW80 : SP80	92.14 ± 1.54	85.02 ± 2.25	89.72 ± 0.85	84.87 ± 0.54
	TW80 : SP80	83.66 ± 0.29	80.83 ± 1.64	84.69 ± 2.40	N
	TW80 : SP80	86.41 ± 3.58	77.30 ± 0.93	84.60 ± 0.51	N
	TW80 : SP85	91.48 ± 0.90	82.36 ± 3.58	86.53 ± 3.88	84.00 ± 1.68
	TW80 : SP85	83.00 ± 2.95	77.36 ± 1.37	84.18 ± 0.55	77.35 ± 0.73
	TW80 : SP85	75.20 ± 1.07	61.20 ± 2.42	70.78 ± 1.62	N

Note: N = Not determined.

Table 17 Normalized the average drug content of AA-SLN in various formulations compared with initial (100%) and after storage conditions for 6 months.

Solid lipids	Ratio of surfactants	Normalized the average drug content (after storage for 6 months)		
		4 ◦C	Room Temperature	45 ◦C
TM	TW80 : SP80 5:5	91.60	93.85	N
	TW80 : SP80 7:3	85.53	89.39	N
	TW80 : SP85 5:5	99.78	101.19	99.37
	TW80 : SP85 7:3	85.53	89.39	N
	TW80 : SL 1:9	87.75	87.81	N
	TW80 : SL 3:7	84.23	85.80	N
	TW80 : SL 5:5	87.44	87.26	N
	TW80 : SL 7:3	76.66	84.20	77.62
	TW80 : SL 9:1	76.92	77.49	76.64
TS	TW80 : SP80 5:5	93.33	95.85	N
	TW80 : SP80 7:3	96.59	99.64	N
	TW80 : SP85 5:5	82.99	87.36	85.86
	TW80 : SP85 7:3	86.04	77.06	70.17
	TW80 : SL 1:9	89.62	89.45	85.50
	TW80 : SL 3:7	86.59	91.87	N
	TW80 : SL 5:5	93.80	83.84	86.95
GB	TW80 : SP80 5:5	97.10	98.39	96.77
	TW80 : SP80 7:3	94.70	98.63	95.09
	TW80 : SP85 5:5	93.39	95.69	93.62
	TW80 : SP85 7:3	92.46	96.23	93.37
	TW80 : SL 9:1	89.98	102.30	101.58
SOF	TW80 : SP80 5:5	92.27	97.37	92.11
	TW80 : SP80 7:3	96.62	101.23	N
	TW80 : SP80 9:1	89.46	97.91	N
	TW80 : SP85 5:5	90.03	94.59	91.82
	TW80 : SP85 7:3	93.20	101.42	93.19
	TW80 : SP85 9:1	81.38	94.12	N

Note: N = Not determined .

3. Characterization of solid lipid nanoparticles

3.1 Physical appearance

The physical appearance of AA-SLN formulations after stored in accelerated conditions and stability study for 6 months were shown in the topic 1.1 and 2, respectively.

3.2 Particle size, size distribution and zeta potential

Asiatic acid loaded solid lipid nanoparticles (AA-SLN)

Particle size: For AA-SLN, the particle sizes of formulations were also the nanometer range. The lowest of particle size was obtained from GB TW:SL 9:1 (34.53±0.81 nm) and the highest from TS SP80:SL 5:5 (186.5±2.23 nm). GB TW:SL 9:1 produced the smallest particle because SL has lower density than other surfactants. It had the most capacity to dissolve drug in to lipid and increased the mobility to receive high shear stress from high pressure homogenizer which led to the smallest particle size. When compared between TM (short chains triglyceride) and TS (long chains triglyceride), the particle size of TM also lower than TS in the same ratios of surfactants. Then might be that short chain triglyceride could promote high recrystallization and very high shear stress could disrupt the particle down to the submicron range when optimum ratio of combined surfactants were used. For using the hot homogenization, it has been found that the average particle size of SLN dispersions is increasing with higher melting lipids .These results are in agreement to the general theory of high pressure homogenization and can be explained by the higher viscosity of the dispersed phase. Which correlated in this experiment, TM, TS and SOF also had closed to lipid melting point in the range of 53 – 58 °C, as a results the mean particle size almost of these formulations were not difference. In contrast, GB which the highest lipid melting point was not obtained the largest mean particle size, can be explained by other critical parameters for nanoparticle formation will be different for different lipids. Examples include the velocity of lipid crystallization, the

lipid hydrophilicity (influence on self-emulsifying properties and the shape of the lipid crystals and therefore the surface area) (Wolfgang and Karsten, 2001). In the case of the effects of surfactant and co-surfactants with particle size of SLN, was found that a trend towards higher particle size with increasing amount of TW80 for almost of the SLN formulations seem to be given, might be that the asiatic acid expressed hydrophobicity property, when the concentration of lipophilicity co - surfactants were increased leading to the drug could incorporated into non-aqueous phase (solid lipids and co-surfactants), resulting in decreasing of mean particle size.

Zeta potential: for AA-SLN, The zeta potential was slightly negative charged in the range from - 3.16 to -19.50 mV. The lowest negative charged of zeta potential was for TM TW80:SL 3:7 (-3.16$\pm$1.16 mV) and the highest for TS TW80:SP80 5:5 (-19.50$\pm$1.41 mV). The analysis of the zeta potential, which is the electric potential at the plane of shear, is a useful tool to predict the physical storage stability of colloidal systems. Usually, particle aggregation is less likely to occur for charged particles with high absolute value of zeta potential was above 30 mV due to the electric repulsion between particles, indicating the better stability of this colloidal system. Despite the zeta potential below the critical value of $\pm$ 30 mV, nanoparticles can have the same long-term stability, because the steric stabilization resulting from the non-ionic surfactant (TW80, SP80, SP85 and SL) are another additional effect that increases the particle stability for relatively long periods. As a results from Table 18 was shown almost of the zeta potential of AA-SLN in the ratios of TW80:SL lower than in the ratios of TW80:SP80 and TW80:SP85, might be cause the synergistic effect of steric stabilization of TW80:SL higher than TW80:SP80 and TW80:SP85. It should be noted that adsorption of a steric stabilizer layer leads to a reduction of the measured zeta potential, which is however not an indication of a reduced electrostatic repulsion. The adsorption layer of the stabilizer shifts the plain of shear, at which the zeta potential is measured, to a larger distance from the particle surface. Consequently the measured zeta potential is lower (Mehnert and Mader, 2001).

Table 18 Particle size, size distribution and zeta potential of AA-SLN in various formulations (n = 6).

Type of lipids	Ratio of surfactants	Initial		
		Z-average ± SD (nm)	PDI ± SD	Zeta potential ± SD (mV)
Trimyristin	TW80 : SP80 5:5	64.97±1.09	0.58±0.01	-16.40±0.61
	TW80 : SP80 7:3	100.40±2.29	0.63±0.03	-10.70±1.33
	TW80 : SP85 5:5	90.60±1.80	0.43±0.03	-12.20±0.53
	TW80 : SP85 7:3	91.86±4.20	0.51±0.03	-5.78±1.30
	TW80 : SL 1:9	45.90±3.67	0.67±0.04	-3.34±0.47
	TW80 : SL 3:7	151.40±11.27	0.71±0.09	-3.16±1.16
	TW80 : SL 5:5	163.20±4.09	0.78±0.10	-4.08±0.96
	TW80 : SL 7:3	164.97±2.31	0.55±0.05	-4.59±0.41
	TW80 : SL 9:1	102.57±2.67	0.53±0.04	-6.72±0.22
Tristearin	TW80 : SP80 5:5	120.87±4.79	0.46±0.10	-19.5±1.41
	TW80 : SP80 7:3	170.37±10.89	0.61±0.04	-12.47±1.66
	TW80 : SP85 5:5	119.50±1.87	0.38±0.07	-13.13±1.40
	TW80 : SP85 7:3	145.23±4.02	0.55±0.06	-7.10±1.09
	TW80 : SL 1:9	142.30±2.66	0.61±0.01	-3.38±0.33
	TW80 : SL 3:7	165.40±1.59	0.74±0.16	-3.77±0.48
	TW80 : SL 5:5	186.5±2.23	0.69±0.16	-6.98±0.77

Table 18 Particle size, size distribution and zeta potential of AA-SLN in various formulations (n = 6) (continous).

Type of lipids	Ratio of surfactants	Initial		
		Z-average ± SD (nm)	PDI ± SD	Zeta potential ± SD (mV)
Glyceryl behenate	TW80 : SP80 5:5	151±3.65	0.53±0.04	-17.6±1.56
	TW80 : SP80 7:3	84.93±10.40	0.90±0.18	-13.97±0.50
	TW80 : SP85 5:5	139.5±8.78	0.57±0.03	-15.97±0.95
	TW80 : SP85 7:3	142.7±15.20	0.58±0.16	-11.3±0.40
	TW80 : SL 9:1	34.53±0.81	0.74±0.02	-7.44±0.32
Softisan 154	TW80 : SP80 5:5	63.38±1.58	0.42±0.10	-6.91±0.23
	TW80 : SP80 7:3	120.03±1.06	0.66±0.01	-5.06±0.25
	TW80 : SP80 9:1	123.20±4.95	0.79±0.08	-3.38±0.40
	TW80 : SP85 5:5	113.50±2.86	0.37±0.09	-4.75±0.81
	TW80 : SP85 7:3	145.33+2.45	0.47±0.04	-5.33±0.82
	TW80 : SP85 9:1	113.40±7.98	0.57±0.14	-4.56±0.75

Chitosan coated asiatic acid loaded solid lipid nanoparticles (CT/AA-SLN)

Particle size: for CT/AA-SLN, the particle size were observed in the range of 94.41 – 568.9 nm, 144.4 – 817.6 nm and 169.20 – 1547.67 nm for the chitosan concentration of 0.1%, o.3% and 0.5% w/v, respectively. The increase in chitosan concentration, was determine an important increase in the mean particle size of SLN formulation. All of various concentrations of chitosan (0.1%, 0.3% and 0.5% w/v) were incorporated into SLN showed significant increase in dimensions of particle size for all of SLN formulations. In analogy with results previously, after chitosan coating, SLN presented a mean particle size around 470 nm. Such increase of the mean particle size is attributable to the chitosan coating around the surface of SLN. Also, possible aggregation caused by the stickiness of the polymer may have contributed to partial agglomeration of SLN (Pedro Fonte et al, 2011). Whereas the 0.5% w/v chitosan solution was obtained the highest mean particle size. That behaviour was probably due to the viscosity of chitosan solution employed for SLN preparation. For higher concentrations, viscosity probably became more crucial and SLN size increased.

Zeta potential: for CT/AA-SLN, the zeta potential were observed in the range of 4.37 to 13.57 mV, 10.83 to 17.8 mV and 8.73 to 20.23 mV for the chitosan concentration of 0.1%, o.3% and 0.5% w/v, respectively. It can described to the higher availability of protonated amine groups with increasing chitosan concentration. When chitosan solution were incorporated in AA-SLN, The positive charged of zeta potential were obtained, these results due to the cationic character of chitosan. The positively charged amino groups are capable of neutralizing the negative charge at the surface of these particles and change the zeta potential (the higher availability of protonated amine groups with increasing chitosan concentration). As a consequence of the charge reversal to the positive value of zeta potential, the particles are highly instable around the point of zero charged and aggregation is facilitated, as it could be observed after particle size analysis. The results were shown in Table 19.

Table 19 Particle size, size distribution and zeta potential of AA-SLN and CT/AA-SLN (n = 6).

Formulation	No chitosan			With chitosan								
				0.1%			0.3%			0.5%		
	Z-average ± SD (nm)	PDI ± SD	Zeta potential ± SD (mV)	Z-average ± SD (nm)	PDI ± SD	Zeta potential ± SD (mV)	Z-average ± SD (nm)	PDI ± SD	Zeta potential ± SD (mV)	Z-average ± SD (nm)	PDI ± SD	Zeta potential ± SD (mV)
TM TW80:SP855:5	102.60±1.65	0.43±0.06	-11.83±1.33	133.90±2.23	0.44±0.04	13.57±0.39	221.57±3.23	0.48±0.06	16.60±0.17	254.40±4.26	0.49±0.11	11.67±0.59
TM TW80: SL 7:3	76.76±2.93	0.52±0.05	-5.53±0.27	97.64±3.35	0.58±0.04	4.37±0.39	154.17±0.99	0.72±0.12	10.14±0.59	205.97±5.16	0.73±0.12	8.73±0.39
TM TW80:SL 9:1	71.78±1.69	0.55±0.04	-6.78±0.24	94.41±3.37	0.62±0.05	8.26±0.13	144.47±2.21	0.60±0.02	11.77±0.23	169.20±1.31	0.65±0.10	12.8±0.44
GB TW80:SP80 7:3	87.97±1.16	0.97±0.02	-13.76±0.26	342.30±1.18	0.47±0.08	6.52±0.25	770.70±10.92	0.64±0.08	10.83±0.58	1475±62.60	0.77±0.10	14.57±0.38
GB TW80:SP85 5:5	133.07±2.50	0.63±0.07	-15.03±1.06	195.33±3.72	0.55±0.04	12.63±0.12	345.53±6.04	0.63±0.05	15.50±0.17	483.20±9.58	0.66±0.05	19.63±0.38
SOF TW80:SP80 5:5	68.77±4.72	0.53±0.04	-6.43±1.12	568.97±14.55	0.55±0.08	6.33±0.21	817.67±3.19	0.62±0.06	12.43±0.35	1547.67±37.07	0.86±0.22	20.23±2.01
SOF TW80:SP85 5:5	122.63±1.58	0.34±0.01	-4.53±1.23	157.90±2.25	0.49±0.01	8.80±0.12	252.97±22.40	0.55±0.06	17.80±0.92	283.93±3.80	0.55±0.06	20.03±0.90
SOF TW80:SP85 7:3	133.00±3.68	0.54±0.04	-5.43±0.17	157.97±2.28	0.55±0.04	7.56±0.16	239.27±15.26	0.62±0.02	12.47±0.60	356.87±6.71	0.74±0.16	15.20±0.89

3.3 pH measurement

The pH of the formulation, as well as that of nasal surface, can affect to permeation of drugs. To avoid nasal irritation, the pH of the nasal formulation should be adjusted to 4.5–6.5. In addition to avoiding irritation, it results in obtaining efficient drug permeation and prevents the growth of bacteria. The average pH of AA-SLN and CT/AA-SLN were shown in Table 20. The average pH of all formulations were moderately to highly acidic acid in range of 3.5 – 6.5. In the case of AA-SLN, the average pH in range 4.5 – 6.5, which suitable formulations for use in nasal delivery route. The pH values of SLN formulations in the case of TM AA-SLN and TS AA-SLN were used SL as co-surfactants (0.5 mg/ml) obtained the lower average pH compared with SP80 and SP85 were used as co-surfactants (0.7 mg/ml). This might be due to the higher amount of asiatic acid was incorporated into formulations, resulting in the acidic property of asiatic acid which could dissolve in dispersion medium partially and affecting with pH values to SLN formulations in the same type of solid lipids. However, the acidic property of asiatic acid were not affected by vary type of solid lipids. SOF AA-SLN obtained the higher pH value because of the lipid characteristic. Similarity in previous study, with SLN formulation with softisan154 and hydrogenated lecithin (lipid matrix), 1% oleyl alcohol was used as surfactant by hot high pressure homogenization method, the pH value of samples were always between 6.20 ± 0.9 (Nagi et al., 2009).

The pH values of SLN formulations coated with chitosan exhibited upon the concentration of chitosan. As the amount of chitosan was increased, the average pH of CT/AA-SLN formulations increased. The results were presented that the order of the pH values for AA-SLN > 0.5% CT/AA-SLN > 0.3% CT/AA-SLN > 0.1% CT/AA-SLN as follow in Table 21. Chitosan is capable of being hydrolyzed due to the presence of glycoside bond in the molecule; this bond is rather unstable when treated with hydrolyzing agents, for example, aqueous solutions of acids. Glycoside bonds are cleaved during hydrolysis, and the molecular weight of chitosan decreases. At the site of cleavage of β-1,4-glycoside bonds, a new alcohol hydroxyl is formed at one

fragment of the chain (at C4 carbon atom) and a free glycoside hydroxyl, that is, an aldehyde group, at the other (at C1 carbon atom). An exhaustive hydrolysis of chitosan, as a rule, produces a mixture of N-acetylglucosamine and glucosamine which expressed alkaline activity (Ilina and Varlamov, 2004). Therefore, it can be assumed that the 0.5% CT/AA-SLN obtained the highest pH compared with other formulations that coated with chitosan, because of the highest pH values in 0.5% chitosan solution were added.

Table 20 The average pH of AA-SLN in various formulations.

Solid lipids	Ratios of surfactants	The average pH + SD Initial
Trimyristin	TW80 : SP80 5:5	5.11 ± 0.01
	TW80 : SP80 7:3	5.12± 0.02
	TW80 : SP85 5:5	4.99± 0.16
	TW80 : SP85 7:3	4.80± 0.12
	TW80 : SL 5:5	4.79± 0.01
	TW80 : SL 7:3	4.72± 0.01
	TW80 : SL 9:1	4.58± 0.16
Tristearin	TW80 : SP80 5:5	5.78± 0.11
	TW80 : SP80 7:3	5.85± 0.11
	TW80 : SP85 5:5	5.35± 0.01
	TW80 : SP85 7:3	5.40± 0.13
	TW80 : SL 1:9	4.95± 0.16
	TW80 : SL 3:7	4.84± 0.16
	TW80 : SL 5:5	4.25± 0.13
Glyceryl behenate	TW80 : SP80 5:5	5.42± 0.02
	TW80 : SP80 7:3	5.11± 0.15
	TW80 : SP85 5:5	4.16± 0.02
	TW80 : SP85 7:3	4.11± 0.02
	TW80 : SL 9:1	4.52± 0.12
Softisan 154	TW80 : SP80 5:5	5.94± 0.17
	TW80 : SP80 7:3	6.28± 0.02
	TW80 : SP80 9:1	6.42± 0.13
	TW80 : SP85 5:5	6.11± 0.01
	TW80 : SP85 7:3	6.41± 0.01
	TW80 : SP85 9:1	6.47± 0.17

Table 21 The average pH of AA-SLN and CT/AA-SLN in various formulations.

Solid lipids	Ratio of surfactants	The average pH ± SD			
		No chitosan	With chitosan		
			0.1%	0.3%	0.5%
Trimyristin	TW80 : SP85 5:5	5.25± 0.08	3.67± 0.12	3.94± 0.22	4.34± 0.04
	TW80 : SL 7:3	4.82± 0.14	3.62± 0.05	4.11± 0.22	4.35± 0.12
	TW80 : SL 9:1	4.65± 0.12	3.57± 0.22	3.94± 0.02	4.23± 0.04
Glyceryl behenate	TW80 : SP80 7:3	5.31± 0.15	3.58± 0.04	4.00± 0.04	4.24± 0.06
	TW80 : SP85 5:5	5.26± 0.02	3.42± 0.02	3.87± 0.22	4.15± 0.02
Softisan 154	TW80 : SP80 5:5	5.87± 0.11	3.56± 0.14	3.96± 0.12	4.23± 0.13
	TW80 : SP85 5:5	6.05± 0.09	3.55± 0.07	3.94± 0.11	4.19± 0.14
	TW80 : SP85 7:3	6.23± 0.06	3.63± 0.08	4.06± 0.02	4.28± 0.09

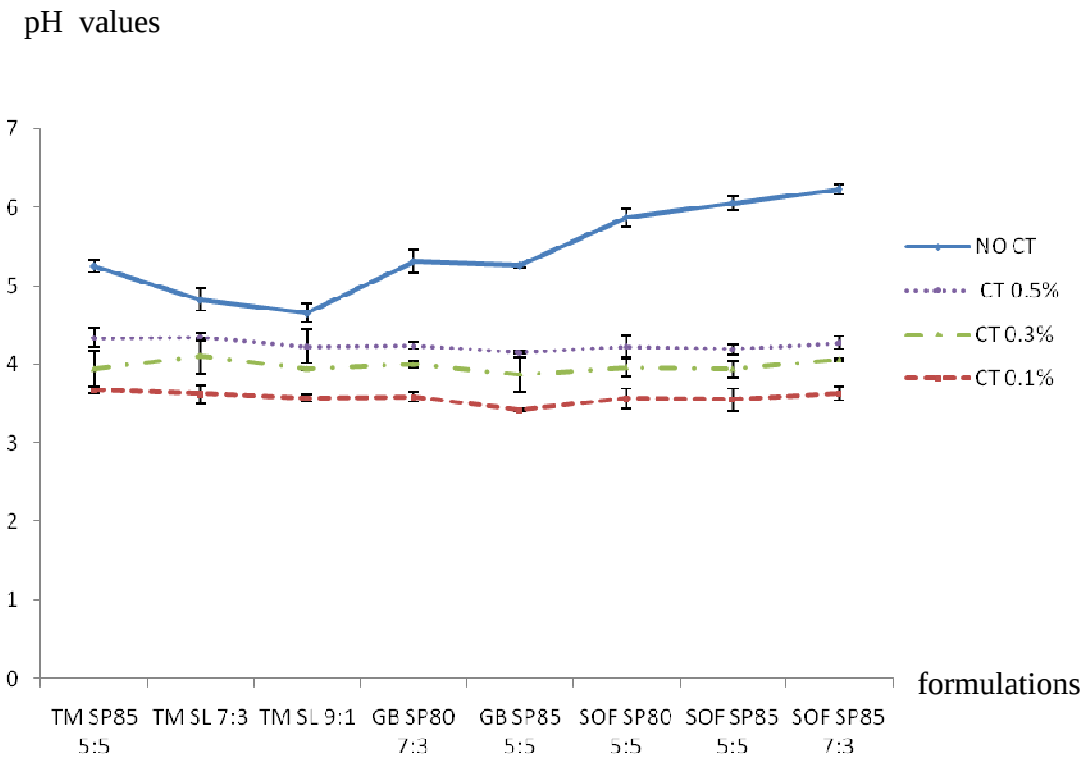

Figure 24 The average pH of AA-SLN and CT/AA-SLN in various formulations.

3.4 Viscosity property

The viscosity measurements were performed with a viscometer (RheoWin – RV1®, HAAKE, Germany) were shown in Table 22. The AA-SLN exhibited viscosity in the range of 0.90 ± 0.07 to 1.39 ± 0.07 cps. Formulations with GB were shown the highest viscosity and formulations with SOF had the lowest viscosity. This might be due to the longer chain of GB could promote more sensitive network structure to get tangled up in each other particles similar to spaghetti. The number hydrocarbon chain of lipids was ranged GB > TM > SOF.

The major limiting factor for drug delivery to the nasal mucosa has been the mucociliary clearance. A higher viscosity of the formulation increased contact time between the drug and the nasal mucosa thereby increasing the time for absorption. At the same time, highly viscous formulations interfere with the normal functions like ciliary beating or mucociliary clearance (Ghada and Rania, 2009). Thus, the purpose of chitosan coated SLN in this study for increased viscosity of formulations to enhance adhesion property, decreasing rate of mucociliary clearance and prolong stability of formulations. The viscosity of SLN dispersions that added with chitosan solution of 0.1%, 0.3% and 0.5% possessed a low viscosity, viscous liquid dispersions with a consistency like parenteral nanosuspensions when compared with AA-SLN. This results exhibited the effect of chitosan concentration. As the concentration of chitosan increased, the viscosity of CT/AA-SLN formulations was increased. The viscosity were ranked 0.5% CT/AA-SLN > 0.3% CT/AA-SLN > 0.1% CT/AA-SLN > AA-SLN as shown in Table 12. Thus, 0.5% CT AA-SLN showed the highest viscosity property compared with other concentrations of chitosan solution.

Besides the viscosity properties of CT/AA-SLN were studied, the flow properties and its deformation termed as rheology were of concern. In previous study, it was reported that non-newtonian solutions containing methylcellulose derivatives lowered the clearance rate and enhanced the bioavailability of the drugs administered through the nose by immobilizing the virus on the airway epithelia and the rheological profiles of commercial corticosteroid nasal spray suspensions made of

phosphoinositide 3-kinase demonstrated that they were shear-thinning to varying degrees (Chi, Venkat, and Yugyung, 2009). Continuous shear rheometry displayed pseudoplastic flow characteristics for both the systems tested. SLN A and SLN B formulations exhibited pseudoplastic rheology (shear thinning) and an increase in the shear stress with increased shear rate and viscosity that is high under the low shear rate, and low under the high shear rate conditions (enhance corneal retention) are appropriate for ophthalmic use due to the fact that the ocular shear rate is very high particularly during the blinking period (Mohd et al., 2010).

In this study, continuous shear rheometry investigations displayed newtonian flow characteristics for all AA-SLN and CT/AA-SLN formulations tested, where a newtonian fluid which a direct proportionality exists between shear stress and shear rate, for all values of shear. This phenomenon was more emphasized for incorporation of chitosan solution into AA-SLN formulations.

Viscosity represents the resistance to the relative motion of adjacent liquid layers and the reciprocal of viscosity is termed as fluidity. The viscosity of the fluid varies with the shear stress and the consistency depends upon the duration and rate of shear.

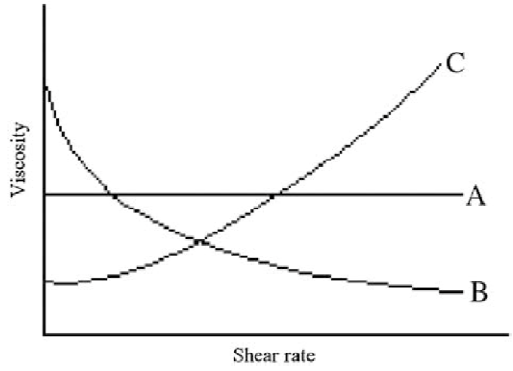

Figure 25 Effect of shear rate on the viscosity of (A) newtonian liquids, (B) shear-thinning systems and (C) shear thickening systems.

The graphs representing the flow properties are termed as rheograms and in case of newtonian systems the flow curves (shear stress vs. shear rate) are straight

lines passing through origin, indicating that shear stress (τ) varies directly with the shear rate as described in the following equations.

Newton's equation for the flow of a liquid is

$$\tau = \eta D$$

Shear stress (dyn/cm^2) = Viscosity (mPa s) × Rate of shear (s^{-1})

Where, τ = Shear stress, D = Shear rate and η = viscosity

The shear stress and shear rate are directly proportional, and the proportionality constant is the co-efficient of viscosity. If we plot graph of shear stress verses shear rate, the slope gives the viscosity. The curve always passes through the origin.

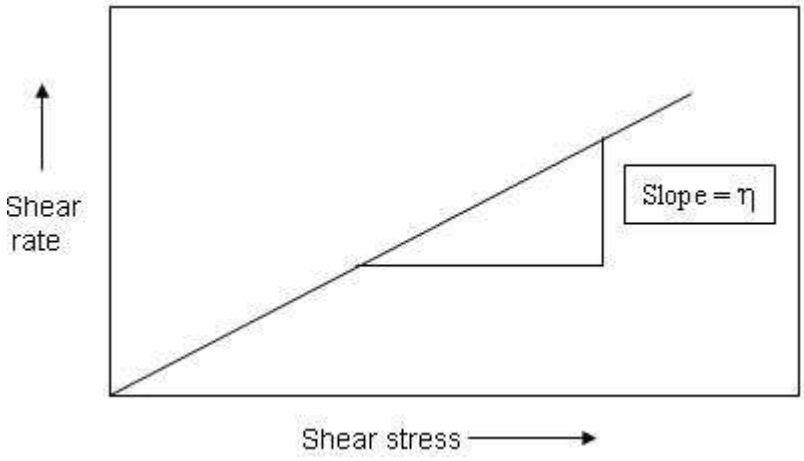

Figure 26 Rheogram of newtonian fluid in term of shear stress verses shear rate.

.

Table 22 The average viscosity of AA-SLN and CT /AA-SLN (n = 3).

Formulation	Viscosity (Cp) ± SD			
	No chitosan	With chitosan		
		0.1%	0.3%	0.5%
TM SP85 5:5	1.02 ± 0.11	1.73 ± 0.09	3.367 ± 0.12	5.46± 0.14
TM SL 7:3	1.07 ± 0.12	1.90 ± 0.18	2.98 ± 0.12	3.73 ± 0.02
TM SL 9:1	1.09 ± 0.13	2.18 ± 0.01	3.48 ± 0.10	4.90 ± 0.04
GB SP80 7:3	1.30 ± 0.11	2.38 ± 0.08	3.70 ± 0.02	5.44 ± 0.04
GB SP85 5:5	1.39 ± 0.07	2.36 ± 0.06	3.83 ± 0.07	5.60± 0.17
SOF SP80 5:5	1.05 ± 0.07	2.24 ± 0.18	3.56 ± 0.06	5.20 ± 0.11
SOF SP85 5:5	0.97 ± 0.09	1.80 ± 0.07	2.88 ± 0.11	4.49 ± 0.07
SOF SP85 7:3	0.90 ± 0.07	2.06 ± 0.12	3.15± 0.13	4.42 ± 0.13

The average viscosity

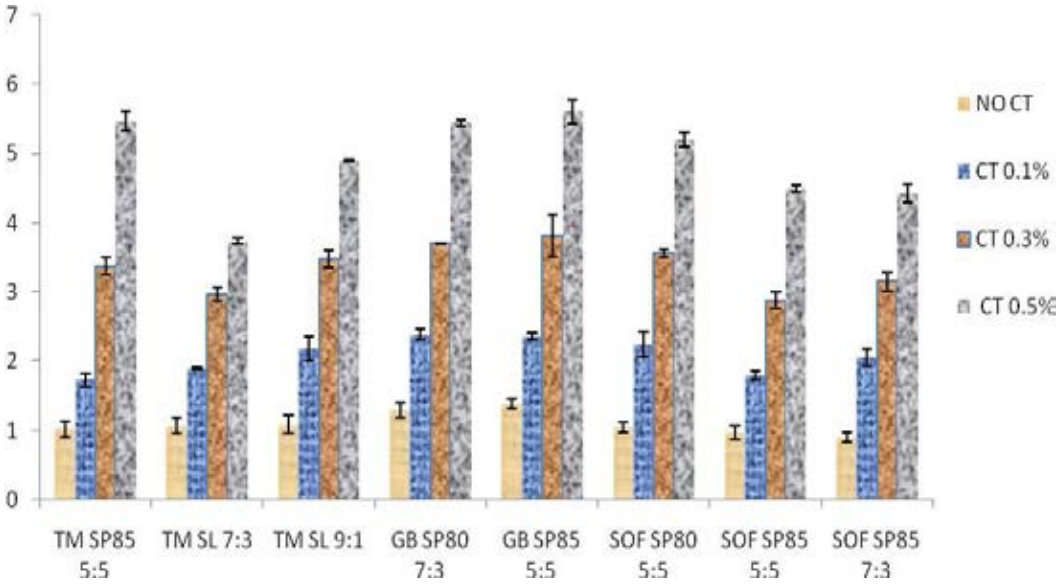

Figure 27 The average viscosity of AA-SLN and CT/AA-SLN.

3.5 Transmission electron microscope; TEM

The morphological feature of AA-SLN formulations were investigated using transmission electron microscope (TEM). The observation of size and shape is shown in Figures 28-35. The particles of AA-SLN in various formulations exhibited almost uniform nanospheres and were homogenous in size distribution. From the images, we also conclude that drug incorporation did not affect particle shape. The TEM studies agreed with the results from particle size determination by photon correlation spectroscopy (PCS). In this study, it was found that the particle size of AA-SLN was around 200 nm. In analogy with results previously obtained with podophyllotoxin-loaded solid lipid nanoparticles, the TEM photographs detection showed that the SLN were homogeneous and spherical in shape, The particle size and size distribution was in accordance with the PCS result (Zhu et al., 2008).

TEM observation were also obtained to study CT/AA-SLN in comparison with AA-SLN. Chitosan solution was added to selected SLN formulations by various ratios of chitosan solution 0.1 and 0.5% v/v. It was found that a particle size of CT/AA-SLN was larger and showed broad size distribution than AA-SLN. The reason of broad size distribution might be an aggregation of chitosan nanoparticle, some particles interacted with each other. Particle size observed in TEM photos was almost similar to the results of particle size. On the other hand, the shape of CT / AA-SLN were not expressd uniformity and spherical shape. The nanoparticles was discrete, which may be due to the presence of positive surface charge in formulations. The slightly negative charged on SLN surface was not enough to attach chitosan particles on their surface, as a result the remaining chitosan nanoparticle were suspended in liquid phase of SLN (external surfaces). For the ratios of chitosan solution 0.5% v/v , was found that the shape of nanopaticles can not expected, were agglomerated together was increased more than 0.1% v/v CT/AA-SLN can be described to the higher concentration of the chitosan in SLN formulations. In contrary to previous study , SLN was uniformly distributed in chitosan-SLN microparticles of PIETC along the internal planes in the particle and no heterogeneous localization was observed at the particle surface, indicating that SLN was compatibly and

homogeneously loaded in chitosan-SLN microparticles (Kiran et al., 2008). It was possible that chitosan solution was incorporated to SLN formulations in the part of liquid phase between the process of mixing before to obtain SLN formulations, which different in these experiment the chitosan solution was added to SLN formulations after the SLN formulations were obtained. As a result, the shape and distribution of particles were agglomerated. For the objective of adding the chitosan solution after preparation of SLN because chitosan particles were coated on the surface of SLN by the charged properties between chitosan particles (positive charged) and SLN (negative charged).

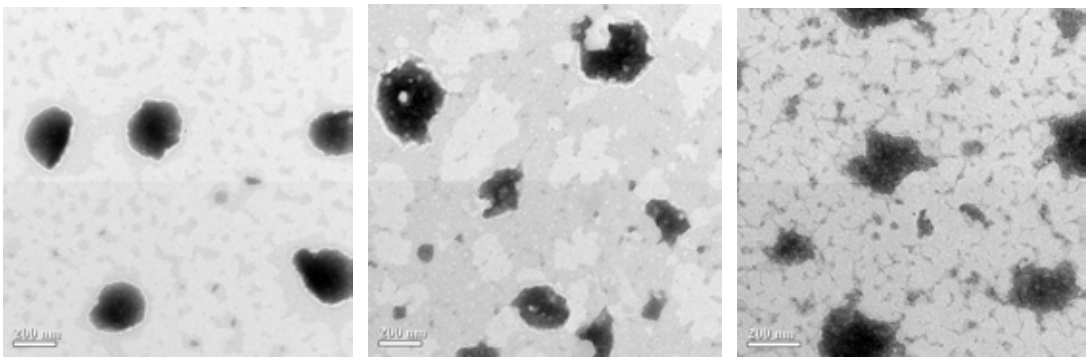

Figure 28 TEM micrograph of AA-SLN: (a) TM SP85 5:5; no chitosan, (b) 0.1% CT/AA-SLN and (c) 0.5% CT/AA-SLN.

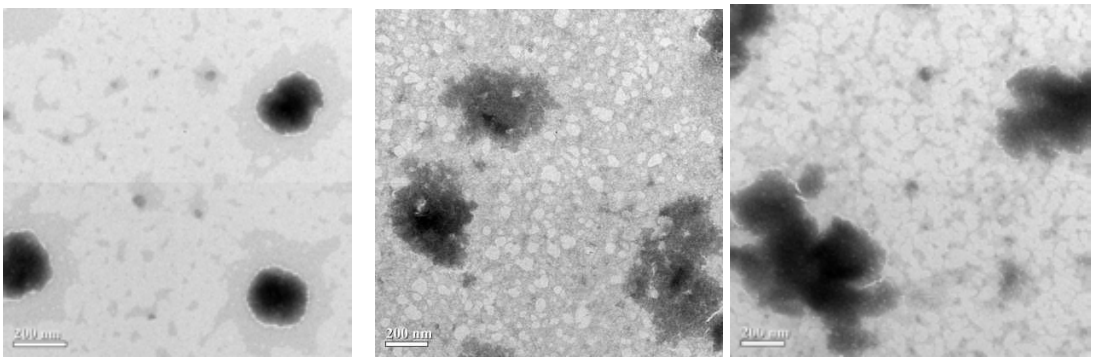

Figure 29 TEM micrograph of AA-SLN : (a) TM SL 7:3; no chitosan, (b) 0.1% CT/AA-SLN and (c) 0.5% CT/AA-SLN.

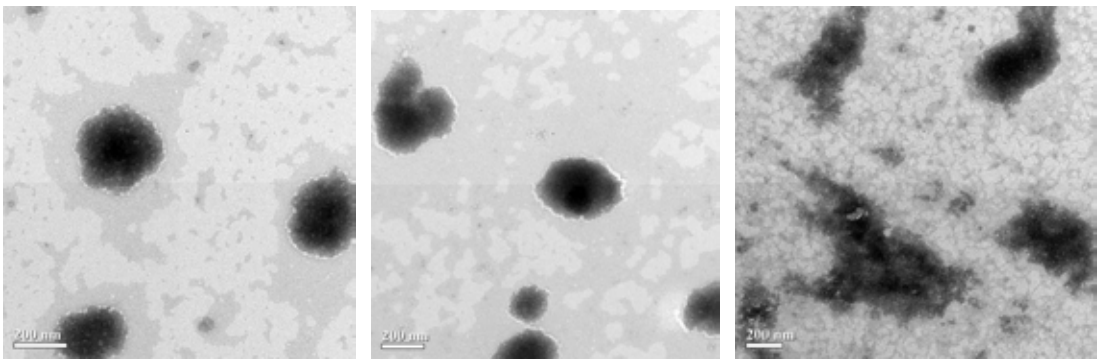

Figure 30 TEM micrograph of AA-SLN : (a) TM SL 9:1; no chitosan, (b) 0.1% CT/AA-SLN and (c) 0.5% CT/AA-SLN.

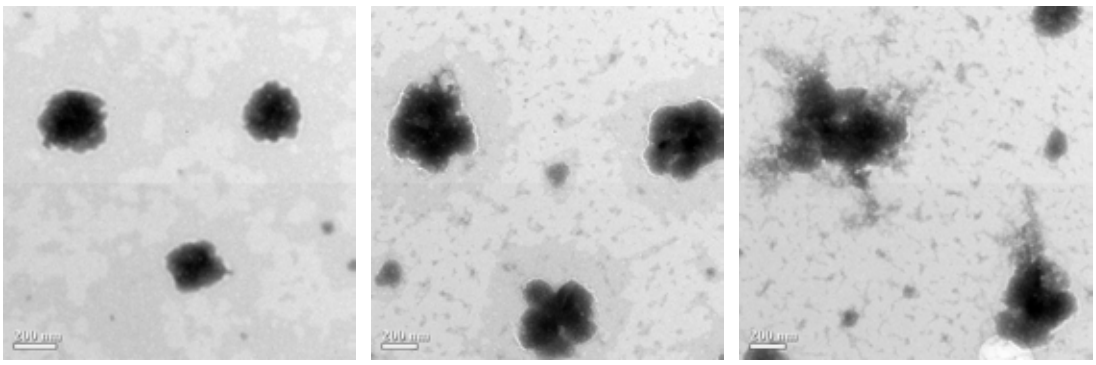

Figure 31 TEM micrograph of AA-SLN : (a) GB SP80 5:5; no chitosan, (b) 0.1% CT/AA-SLN and (c) 0.5% CT/AA-SLN.

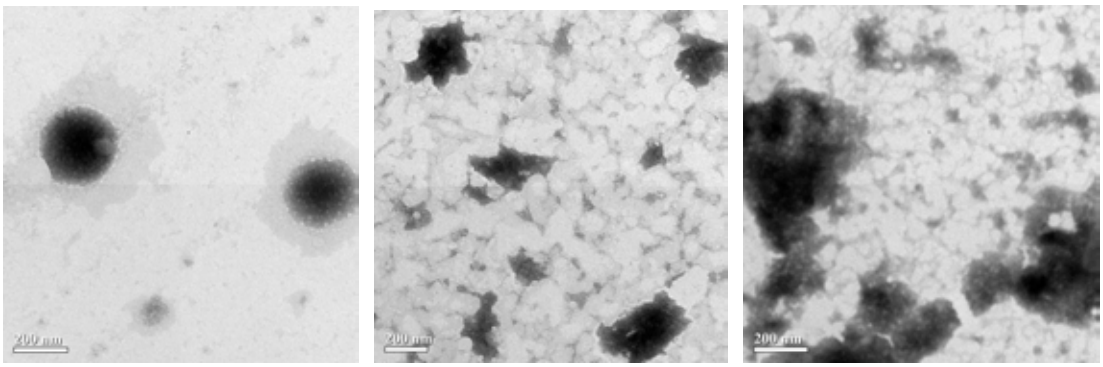

Figure 32 TEM micrograph of AA-SLN : (a) GB SP85 5:5; no chitosan, (b) 0.1% CT/AA-SLN and (c) 0.5% CT/AA-SLN.

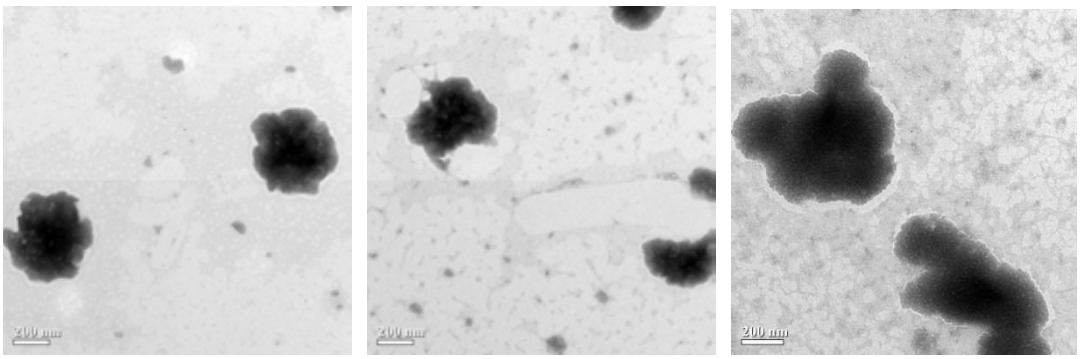

Figure 33 TEM micrograph of AA-SLN : (a) SOF SP80 5:5; no chitosan, (b) 0.1% CT/AA-SLN and (c) 0.5% CT/AA-SLN.

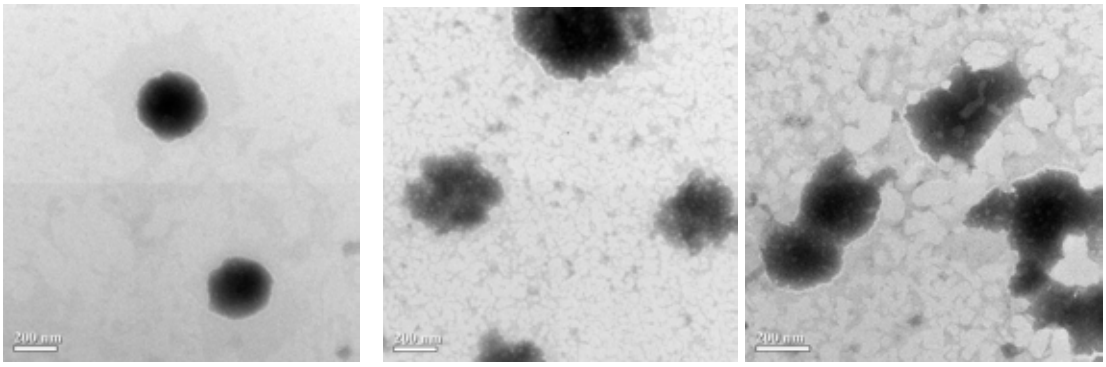

Figure 34 TEM micrograph of AA-SLN: (a) SOF SP85 5:5; no chitosan, (b) 0.1% CT/AA-SLN and (c) 0.5% CT/AA-SLN.

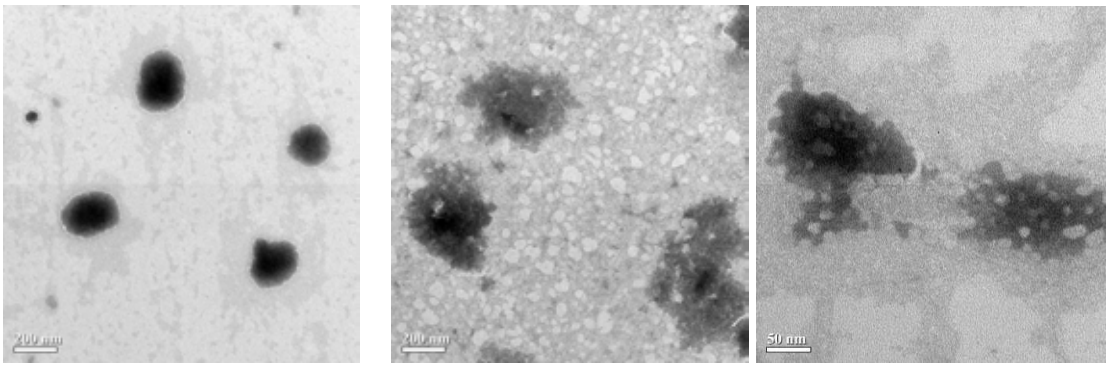

Figure 35 TEM micrograph of AA-SLN : (a) SOF SP85 7:3 ; no chitosan, (b) 0.1% CT/AA-SLN and (c) 0.5% CT/AA-SLN.

3.6 Differential scanning calorimetry (DSC)

Due to lipid crystalline nature, polymorphism is their typical feature. Moreover, melting and recrystallization of the majority of the lipids can lead to the occurrence of transitions between their multiple polymorphic states: unstable (α), metastable (β') and stable (β). For glyceride mixtures intermediate states between β and β' form usually appear. This should be considered for production and long-term storage of SLN, in order to predict if there are influences in their stability and capability for drug incorporation. DSC was a tool to investigate the melting and recrystallization behavior of crystalline materials like SLN. Figures 36-39 show DSC thermograms of AA, TM, TS, GB and SOF, physical mixtures of asiatic acid with trimyristin (PM AA-TM), tristearin (PM AA-TS), glyceryl behenate (PM AA-GB) and softisan154 (PM AA-SOF), freeze-dried asiatic acid with trimyristin (FD AA-TM) , tristearin (FD AA-TS), glyceryl behenate (FD AA-GB) and softisan154 (FD AA-SOF). For the bulk asiatic acid, the melting process took place at 342 °C.

The thermograms of SLN containing asiatic acid in FD AA-TM, FD AA-TS, FD AA-GB and FD AA-SOF did not show the melting peak for the asiatic acid around 342 °C. This indicated that asiatic acid was not in crystalline state but it was in amorphous state. Similar results were reported by S.C. Yang et al. DSC analysis of camptothecin solid lipid nanoparticle prepared by high pressure homogenization showed that camptothecin was in amorphous state (Yang and Zhu, 2002) and Lian Dong Hu et al were reported the thermograms of the lyophilized ATRA-SLN did not show the melting peak for ATRA at around 182 °C. The disappearance of the endothermic peak of the lyophilized ATRA-SLN demonstrates that ATRA dispersed homogeneously in an amorphous state and no ATRA crystallized out of the dispersion (Lian, Xing, and Fu, 2004). However, this was confirmed by the presence of melting peak of asiatic acid in the physical mixtures all of formulations. All of physical mixtures and freeze dried SLN formulations showed a significant reduction in melting temperature as compared to bulk asiatic acid . This shift could be taken as an indication of the interference of SLN formation in the crystallization of solid lipid. This result could be correlated with the impurities or less ordered crystal lattice, so the

substance required less energy than perfect crystalline material. Furthermore, small particle size of SLN leads to high surface energy and the presence of surfactants, which creates an energetically suboptimal state causing a decrease in the melting point (Vivek, Reddy, and Murthy, 2007). When compared to bulk lipid, the melting points and the onset temperatures of SLN formulations are lower. However, they remain higher than 40 ◦C, which is required to obtain solid nanoparticles at body temperature, avoiding the presence of supercooled melts. Thermodynamic stability of lipid nanoparticles depends upon their existing lipid modification. Polymorphic transitions after crystallization of triglyceride nanoparticles were slower for longer chain triglycerides (tristearin) than for shorter chain triglycerides (trimyristin) whereas these transitions were faster for small size of crystallites (Bunjes, 1996).

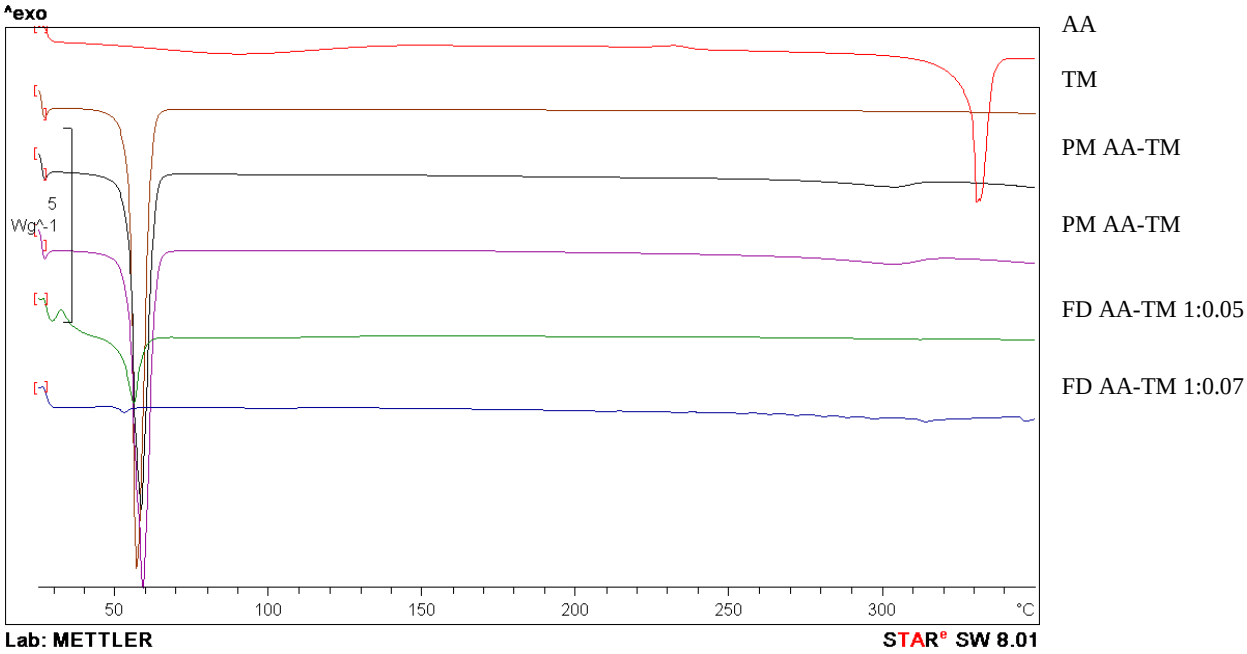

Figure 36 DSC thermograms of trimyristin was used as lipid in SLN: AA, TM, PM AA-TM (1:0.05) and PM AA-TM (1:0.07), FD AA-TM (1:0.05) and FD AA-TM (1:0.07), respectively.

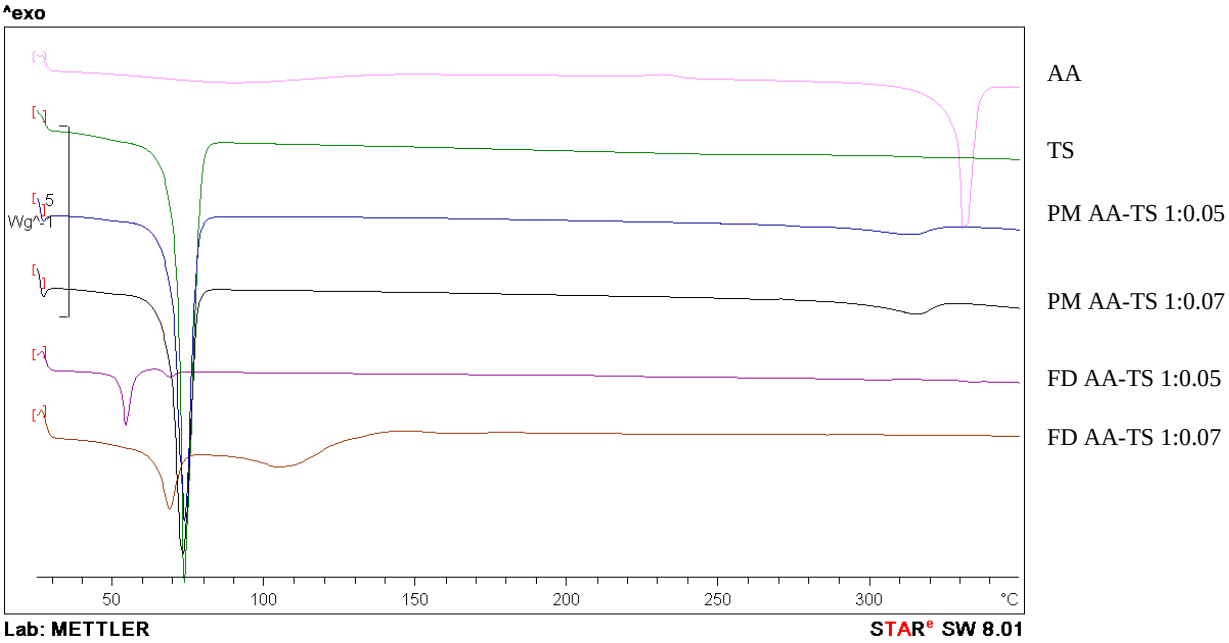

Figure 37 DSC thermograms of tristearin was used as lipid in SLN : AA, TS, PM AA-TS (1:0.05) and PM AA-TS (1:0.07), FD AA-TS (1:0.05) and FD AA-TS (1:0.07), respectively.

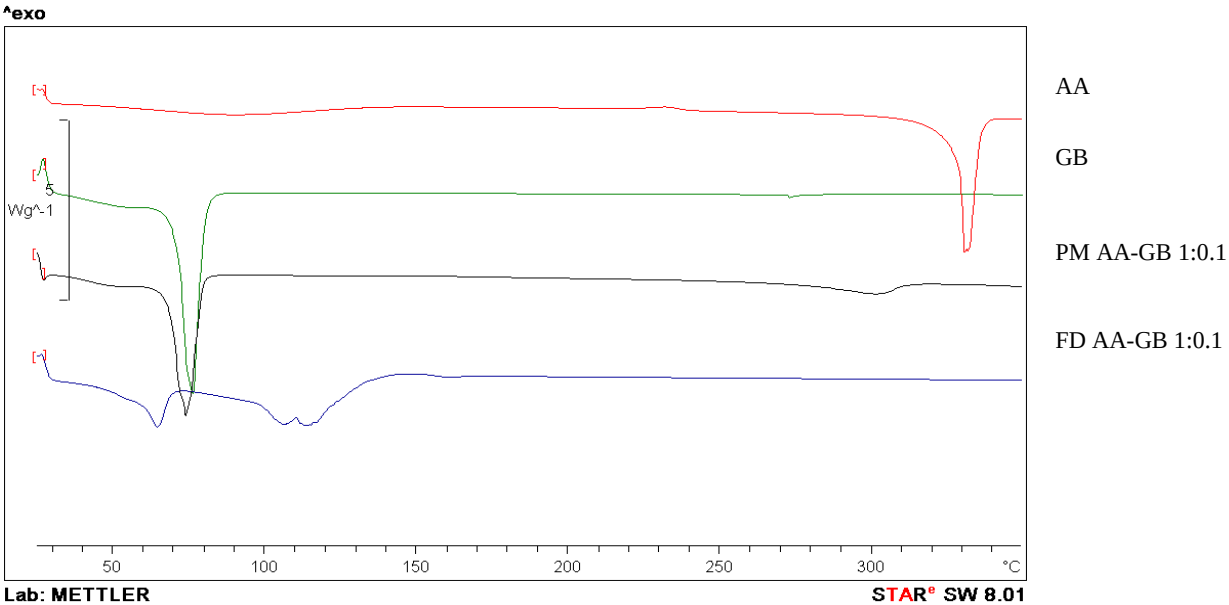

Figure 38 DSC thermograms of glyceryl behenate was used as lipid in SLN: AA, GB, PM AA-GB (1: 0.1) and FD AA-GB (1: 0.1), respectively.

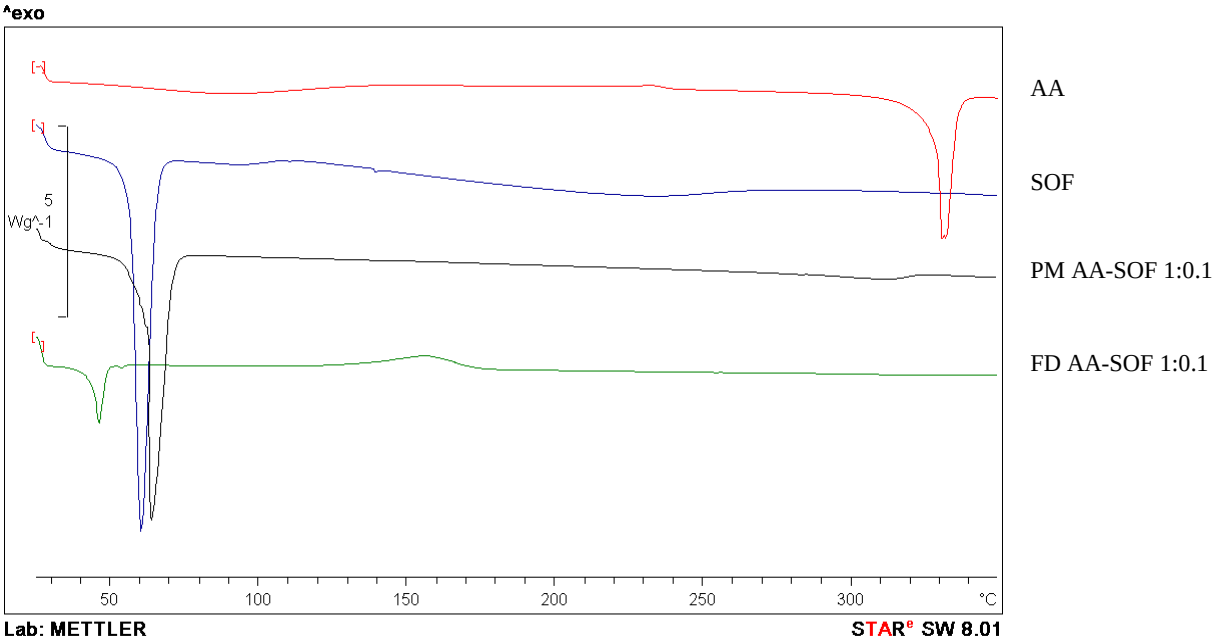

Figure 39 DSC thermograms of softisan 154 was used as lipid in SLN: AA, SOF, PM AA-SOF (1: 0.1) and FD AA-SOF (1: 0.1), respectively.

3.7 Powder X-ray diffractometry (PXRD)

Overlaid PXRD patterns of AA, AA-TM, AA-TS, AA-GB , AA-SOF, PM AA-TM, PM AA-TS, PM AA-GB , PM AA-SOF, FD AA-TM, FD AA-TS, FD AA-GB and FD AA-SOF were shown in Figures 40-43. These studies are useful to investigate crystallinity of the drug in solid lipids. The lipid crystalline structure related to the chemical nature of lipid was a key factor to determine whether a drug would be expelled or firmly incorporated into the carrier systems. It is proposed that the structure of less ordered arrangement in the nanoparticles would be beneficial to the drug loading capacity. The PXRD patterns of asiatic acid exhibits sharp peaks at 2Ɵ scattered angles 7.6, 12.5, 12.8, 13.6 and 15.1 indicated crystalline nature. In physical mixtures of all four types of solid lipids (TM, TS, GB and SOF), decreased peak intensities were observed. This shows that degree of crystallinity of asiatic acid reduced in physical mixtures. However, there were no characteristic peaks for asiatic acid in all freeze-dried AA-SLN, indicating that asiatic acid was entrapped in the lipid core of SLN and in amorphous or molecular dispersion form. Similar results were reported previously. The crystallographic properties of them were characterized by X-ray diffraction (XRD). It was found that PEG-S did not exist in crystallline state in the SLN, both surface-modified and non-modified SLN existed in the amorphous state (Xin et al., 2007). The decrease in crystallinity indicates an enhanced solubility of asiatic acid in solid lipids in the analyzed ratio. Polymorphic crystalline changes occur in the lipid structure, which upon heating it will convert to stable form. From this analysis it is clear the influence of drug in the crystallinity of particles, confirms that asiatic acid was encapsulated in the lipid matrix and increasing the more amorphous modifications, because the typical crystalline drug peaks are not detected. (Alex et al., 2011), which in good agreement with the results established by DSC analysis.

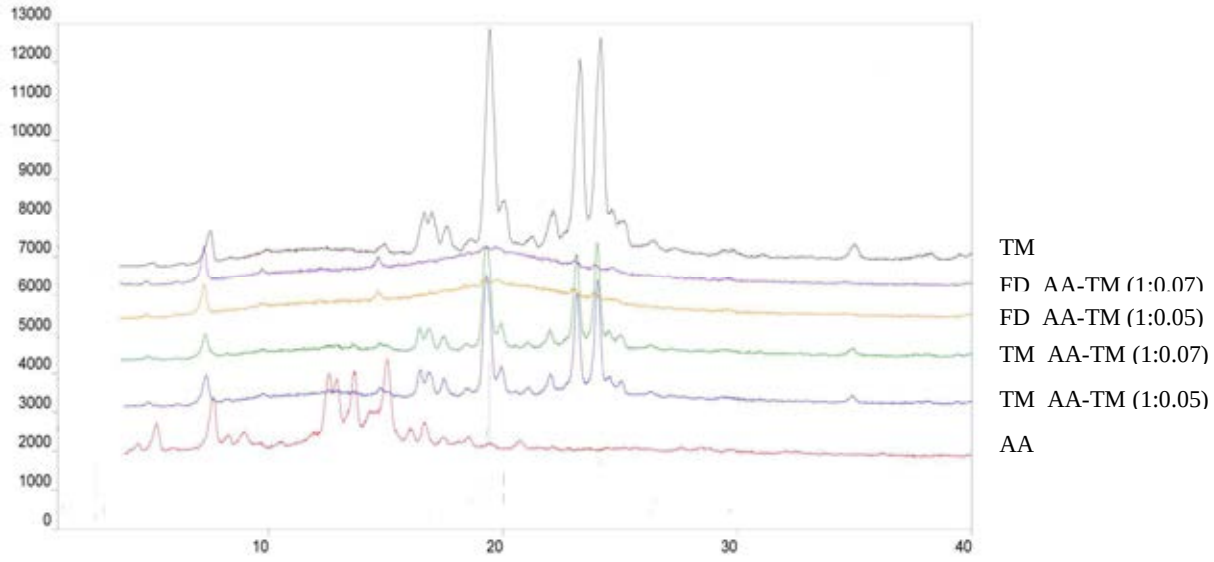

Figure 40 PXRD patterns of trimyristin was used as lipid in SLN: TM, FD AA-TM (1:0.07), FD AA-TM (1:0.05), PM AA-TM (1:0.07), PM AA-TM (1:0.05) and AA, respectively.

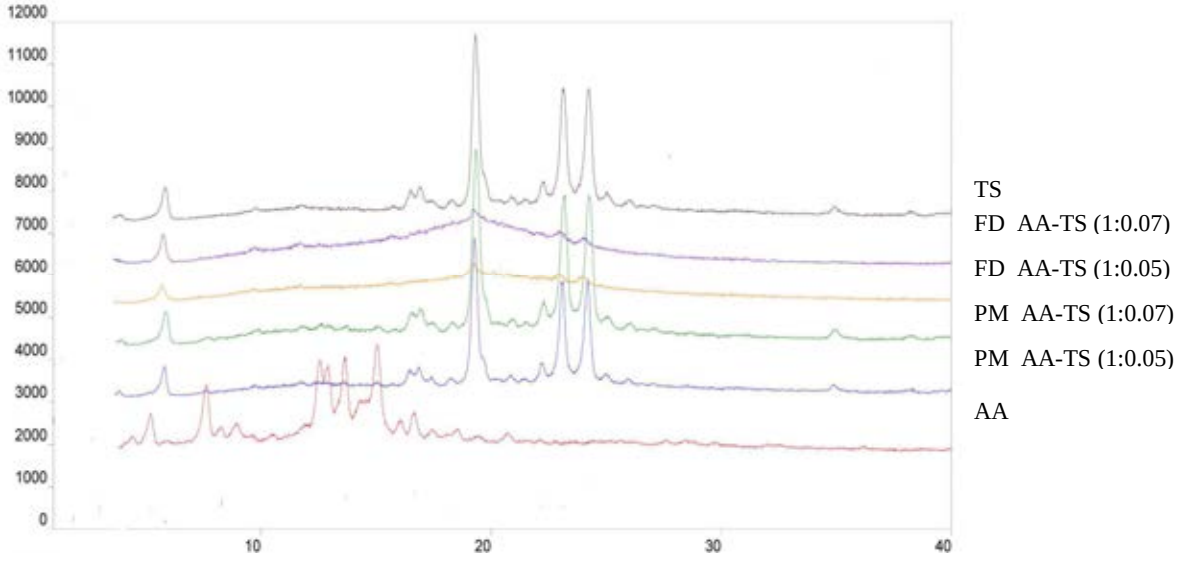

Figure 41 PXRD patterns of tristearin was used as lipid in SLN: TS, FD AA-TS (1:0.07), FD AA-TS (1:0.05), PM AA-TS (1:0.07), PM AA-TS (1:0.05) and AA, respectively.

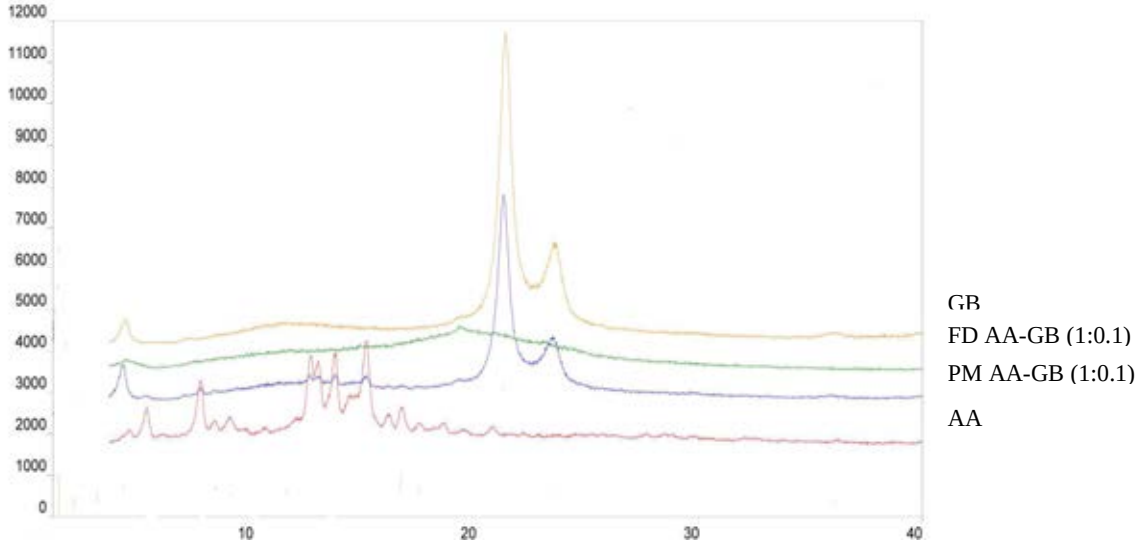

Figure 42 PXRD patterns of glyceryl behenate was used as lipid in SLN: GB, FD AA-GB (1:0.1), PM AA-GB (1:0.1) and AA, respectively.

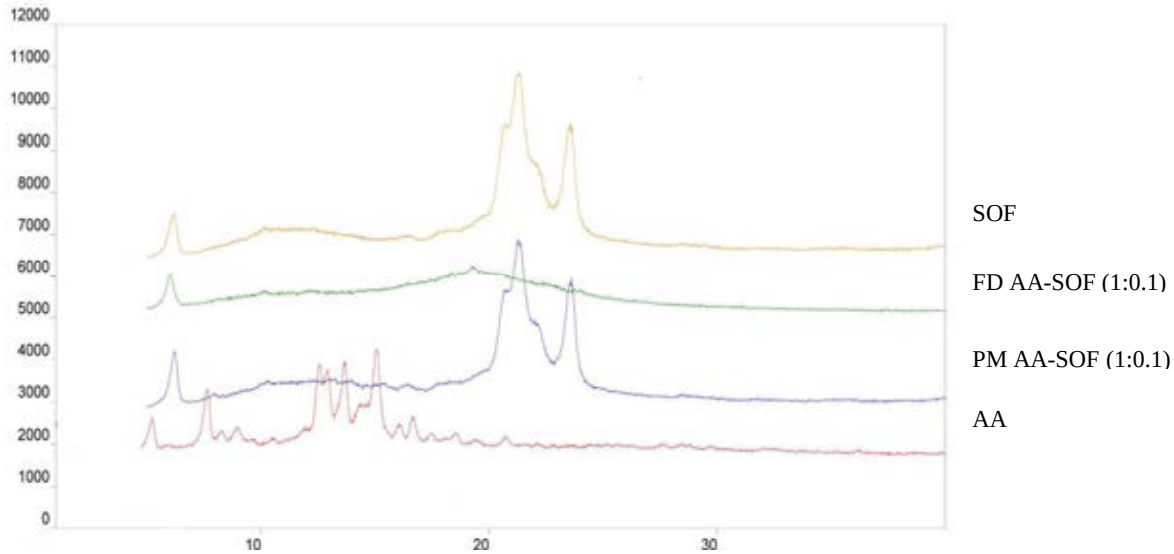

Figure 43 PXRD patterns of softisan 154 was used as lipid in SLN: SOF, FD AA-SOF (1:0.1), PM AA-SOF (1:0.1) and AA, respectively.

4. Validation of HPLC method

The developed HPLC system was applied to analyze the asiatic acid content in SLN formulations. The method validation was performed in the topic below. Validation of the analytical method is the process by which it is established that the performance characteristics of the method meet the requirements for the intended analytical applications. The performance characteristics are expressed in terms of analytical parameters. For HPLC assay validation, these include linearity, specificity accuracy and precision.

Linearity

The linearity of an analytical method is the ability of the method to elicit test results that are directly, or by a well-defined mathematical transformation, proportional to the concentration of analyte in the samples within a given range. The representative calibration curve data of asiatic acid standard solutions are shown in Table 39. The coefficient of determination (R^2) of this line was 0.9993. These results indicated that the HPLC method was acceptable for quantitative analysis of asiatic acid in the range studied.

Specificity

The specificity of an analytical method is its ability to measure the analyte accurately and with specificity in the presence of other components in the sample. The 0.05% Trifluoroacetic acid (TFA) in acetronitrile : 0.05% Trifluoroacetic acid (TFA) in water (45:55) was used as the mobile phase. It was found that there was no interference from other components in the chromatogram after the reagents were added and storage in each conditions. The resolution value of each peak not more than 1.5 when compare with the closed peak. So, the HPLC method was acceptable for specificity. The typical chromatograms of asiatic standard solution and blank SLN for all ratios of surfactants are shown in Figures 56 - 82. All chromatograms are shown under the same attenuation and scale.

Accuracy

The determination of accuracy was performed by analyzing fives sets of three concentrations (1.5, 3.5 and 4.5 μg/ml) of asiatic acid in SLN formulations. The inversely estimated concentrations and percentage of analytical recovery for each concentration, respectively. The percentages of analytical recovery were in the range of 98.79 - 101.04%, (within range 98 – 102%) which indicated that this method could be used for analysis of asiatic acid at all concentrations studied with high accuracy. The data for acuracy are shown in Tables 41-51.

Precision

The precision of an analytical method is the degree of agreement among individual test results when the method is applied repeatedly to multiple samplings of a homogenous sample. The precision of an analytical method is usually expressed as the standard deviation or relative standard deviation (coefficient of variation, % CV) of a series of measurements.

Tables 52 -53 illustrate the data of within-run precision and between-run precision, respectively, of asiatic acid in SLN formulations. All coefficient of variation values were in range 0.80 to 0.91% and 0.72 to 1.12%, respectively. The coefficient of variation of an analytical method should generally be less than 2%. Therefore, the HPLC method was precise for the quantitative analysis of asiatic acid in the range studied.

In conclusion, the analysis of asiatic acid content in SLN formulations by HPLC method developed in this study showed good specificity, linearity, accuracy and precision. Thus, this method was used for determination of the content of asiatic acid in SLN formulations to evaluate its stability.

6. Entrapment efficiency and % drug content

Entrapment efficiency: The percentage of drug incorporation in the lipid matrix (entrapment efficiency) was evaluated after preparation for one week. The formulations studied demonstrated high % entrapment efficiency (% EE) of more than 93% (w/w) using the centrifugation method. The results are shown in Table 23. After statistical analysis by one-way ANOVA, it was found that most of AA-SLN formulations were not significantly different in the entrapment efficiency among various formulations ($P > 0.05$). Incorporation of AA showed high entrapment efficiency, probably because of the highly lipophilic character of drug, high compatibility between drug and solid lipids and high solubility in solid lipids which in this experiments the concentration of AA was added into melted solid lipids was well near its saturation. As a result, AA particles can distribute and entrap into the solid lipids. The high entrapment efficiency might be beneficial to reduce the nasal irritation of drug due to avoid the direct contact between drug and nasal surface. For SLN formulations, the concentration of the drug in the melted lipid is well below its saturation solubility. As a result, SLN show a drug-enriched shell model. A drug-enriched core model is formed when the drug in the melted lipid is closed to its saturation solubility. The cooling process leads to supersaturation of the drug and subsequently to drug crystallization prior to lipid crystallization. Another explanation for increased entrapment of AA could be due to small particle size (particle size of all formulations in this experiment were not more than 200 nanometers), thus the overall surface area was increased. It was possible that some AA molecules might distribute to the surface of the particles and could be stabilized at the surfactant layer on the surface of SLN. Therefore, when the surface area increased, more AA could be trapped at the nanoparticles surface (Tiyaboonchai, Tungpradit, and Plianbangchang, 2007). Moreover, TW80 that used as surfactant in this experiments might form micells beside lipids. Also, the micellar structure in pharmaceutical formulations was able to solubilize drug. The addition of co-surfactants in oil phase and surfactant in aqueous external phase might stabilize the lipid particles, reduce the diffusion speed of the drug therefore increase the entrapment efficiency. For this reason, AA-SLN

with their solid lipids, surfactants and co-surfactants showed higher entrapment efficiency.

The chemical nature of the lipid was also important because lipids which form highly crystalline particles with a perfect lattice (e.g. monostearin) led to drug expulsion. More complex lipids being mixtures of mono-, di- and triglycerides (e.g. GB) formed less perfect crystals with many imperfections offering space to accommodate the drugs (Muller, Mader, and Gohla, 2000). The entrapment efficiency of formulations containing TS was a little higher than that of formulations containing TM, GB and SOF. These results may be contributed to the higher solubilization of TS compared with TM, GB and SOF in the solid system for asiatic acid.

% Drug content: it was found that the percentage of drug in AA-SLN formulations were in wide range from 63.16 to 98.49 % , that the highest and lowest percentages of drug content was found in TS TW80:SL 1:9 and GB TW80:SL 9:1 formulations, respectively. Most formulations showed low amount of AA might be due to loss of activity between hot-high pressure homogenization process that AA was added into lipid phase and heated until acquired clear solution above lipid melting point. Moreover, part of AA might remained in narrow gap and some part of high pressure homogenizer and high speed homogenizer especially for the high viscosity formulations and in type of formulations with containing low melting point of solid lipids. Thus, TW80 probably provided high viscosity in AA-SLN formulations compared with other surfactants leading to the quite low percentage of drug in AA-SLN formulations and most of TM and TS formulations (low melting point of solid lipids).

Table 23 The average % drug content, % entrapment efficiency and normalized of entrapment efficiency of various AA-SLN formulations (n=3).

Solid lipids	Ratio of surfactants	The average % drug content ± SD (Initial)	%Entrapment efficiency	Normalized of Entrapment efficiency
TM	TW80 : SP80 5:5	86.28 ± 4.81	96.11 ± 0.37	111.39
	TW80 : SP80 7:3	82.35 ± 1.63	96.83 ± 0.37	117.58
	TW80 : SP85 5:5	90.90 ± 0.27	96.20 ± 0.49	105.83
	TW80 : SP85 7:3	82.35 ± 1.63	94.44 ± 1.14	114.68
	TW80 : SL 1:9	89.22 ± 1.62	97.66 ± 0.46	109.46
	TW80 : SL 3:7	90.89 ± 0.76	97.27 ± 0.13	107.02
	TW80 : SL 5:5	90.52 ± 1.02	97.79 ± 0.08	108.03
	TW80 : SL 7:3	91.10 ± 0.52	96.32 ± 0.70	105.73
	TW80 : SL 9:1	92.02 ± 2.33	95.77 ± 0.96	104.08
TS	TW80 : SP80 5:5	85.75 ± 5.42	98.38 ± 0.31	114.73
	TW80 : SP80 7:3	87.01 ± 3.53	97.64 ± 0.50	112.22
	TW80 : SP85 5:5	92.72 ± 0.60	98.43 ± 0.84	106.16
	TW80 : SP85 7:3	90.92 ± 1.78	97.23 ± 0.10	106.94
	TW80 : SL 1:9	98.49 ± 1.69	96.82 ± 0.53	98.30
	TW80 : SL 3:7	93.28 ± 3.55	96.88 ± 2.05	103.86
	TW80 : SL 5:5	91.36 ± 2.43	97.04 ± 0.77	106.22
GB	TW80 : SP80 5:5	94.24 ± 1.81	97.69 ± 0.36	103.66
	TW80 : SP80 7:3	92.25 ± 2.09	96.81 ± 1.14	104.94
	TW80 : SP85 5:5	81.88 ± 4.18	97.55 ± 0.57	119.14
	TW80 : SP85 7:3	86.21 ± 0.86	96.82 ± 0.33	112.31
	TW80 : SL 9:1	63.16 ± 5.96	95.50 ± 0.55	151.20
SOF	TW80 : SP80 5:5	92.14 ± 1.54	97.78 ± 0.54	106.12
	TW80 : SP80 7:3	83.66 ± 0.29	97.41 ± 0.16	116.44
	TW80 : SP80 9:1	86.41 ± 3.58	95.45 ± 1.00	110.46
	TW80 : SP85 5:5	91.48 ± 0.90	97.11 ± 1.47	106.15
	TW80 : SP85 7:3	83.00 ± 2.95	93.72 ± 0.54	112.92
	TW80 : SP85 9:1	75.20 ± 1.07	95.33 ± 0.67	126.77

7. Muoadhesive property

In this experiment, mucoadhesive property of AA-SLN and CT/AA-SLN were examined by the percentage of washed AA-SLN particles after all of formulations were attached on porcine nasal mucosa for 30 minutes because of these are normal defence mechanisms of the nasal cavity that clear mucus as well as substances adhering to the nasal mucosa (bacteria, allergens, and so on) and drain them into the nasopharnyx for eventual discharge into the gastrointestinal tract. A substance is nasally administered, it is cleared from the nasal cavity in about 21 mininutes (Marttin et al., 1998). Differences in mucoadhesive characteristics were expected by compared between selected AA-SLN formulations (TM AA-SLN, SOF AA-SLN) and selected AA-SLN formulations coated with chitosan (0.1%, 0.3% CT for TM AA-SLN and 0.1%, 0.3% , 0.5% CT for SOF AA-SLN). The AA solution was used as reference.

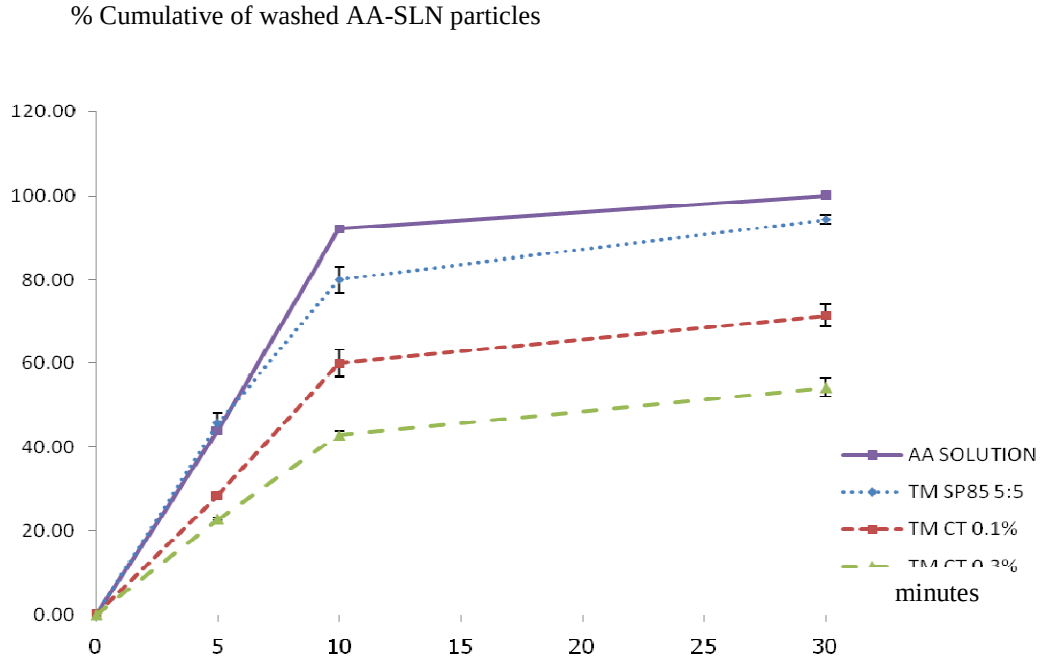

Figure 44 The percentage of washed AA-SLN particles representing the adhesion property on porcine nasal tissue of AA solution, TM AA-SLN, 0.1% and 0.3% CT/TM AA-SLN.

From Figure 44, the results showed the adhesion property in the represent of the percentage of washed AA-SLN particles could be remark ; 0.3% CT/TM AA-SLN > 0.1% CT/TM AA-SLN > TM AA-SLN > AA solution, respectively. It indicated that high concentration of chitosan could adhere on nasal tissue surface for a long period of time compared to low concentraton of chitosan and also SLN formulations. When the end of time (30 minutes), only the AA solution that the percentage of washed AA-SLN particles reached 100%. In contrast with other SLN formulations (both of non-containing chitosan SLN and containing chitosan SLN). The results suggested that SLN formulations and SLN coated with chitosan could improve mucoadhesive property than AA solution.

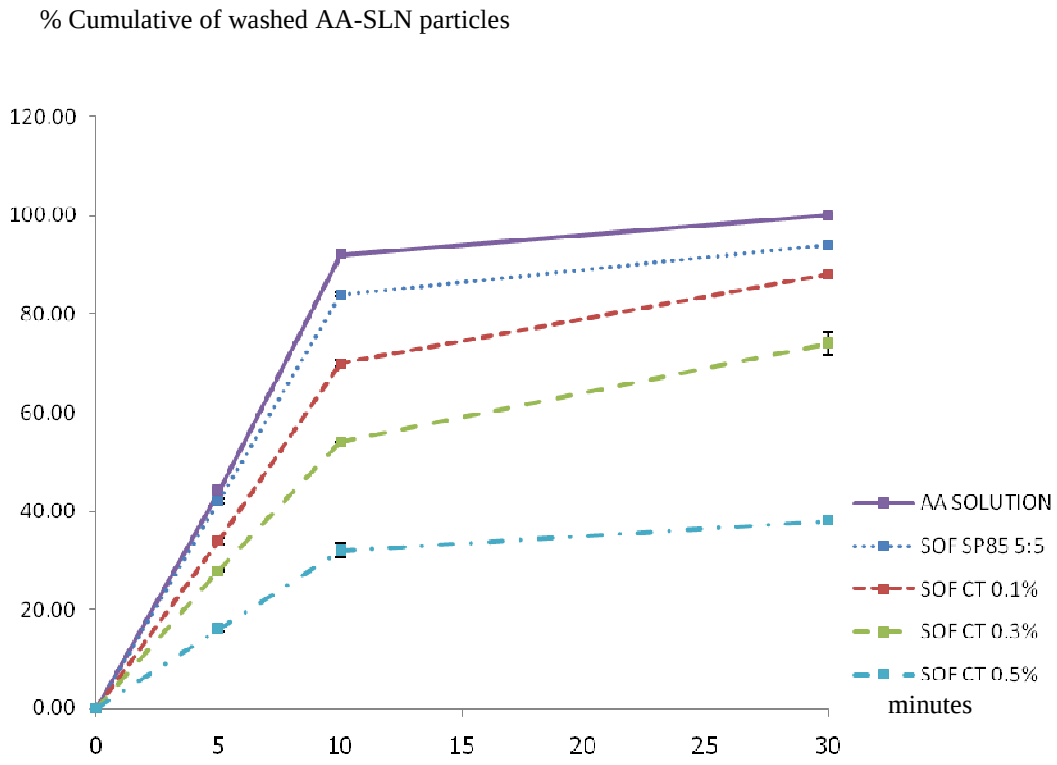

Figure 45 The percentage of washed AA-SLN particles representing the adhesion property on porcine nasal tissue of AA solution, SOF AA-SLN, 0.1% , 0.3% and 0.5% CT/SOF AA-SLN.

The diffusion theory states that inter-penetration of the chains of polymer and mucus may lead to sustained mucoadhesion and mechanical interlocking between mucin and mucoadhesive agents, because of its greater ability to penetrate within the mucus chains. Chitosan obtained by deacetylation of chitin (a naturally occurring polymer) has been shown to possess mucoadhesive properties owing to the molecular attractive forces formed by electrostatic interaction between positively charged chitosan and negatively charged mucosal surfaces. Chitosan has 1 primary amino and 2 free hydroxyl groups for each C6 building unit. Due to the easy availability of free amino groups in chitosan, it carries a positive charge and thus, in turn, reacts with many negatively charged surfaces. The contribution of physical entanglement to the adhesion phenomenon between 0.3% chitosan solution and the surface of mucin particles was clearly much stronger than 0.1% chitosan solution in TM AA-SLN formulations and 0.5% chitosan solution was clearly much stronger than 0.3% and 0.1% chitosan solution in SOF AA-SLN formulations. This results also indicated that higher chitosan concentrations produced more mucoadhesion, which was due to the presence of a greater amount of polymer in the same volume of liquid droplets, and thus provided a greater positive charge to interact with the negative mucin surface. The positive surface charge also confirmed the deposition of the positively charged chitosan on the surface of SLN, which make it able to further interact with the negatively charged membrane of nasal cells. From these results, we can conclude that 0.1% CT/AA-SLN are less useful for preparing mucoadhesive property when compared with 0.3% and 0.5% CT/AA-SLN which have excellent mucoadhesive properties. Consequently, we can expect that these AA-SLN containing chitosan solution will reduce the mucociliary clearance and prolong the contact time with the nasal mucosal surface. Similary in previous study about the adhesive properties of high, medium and low molecular weight (HMW, MMW and LMW, respectively) microspheres of chitosan, differences in mucoadhesive characteristics were expected by changing the chitosan concentrations. The significant differences were seen between LMW and MMW ($p < 0.01$) and between LMW and HMW ($p < 0.01$). LMW microspheres showed a significantly lower binding to mucin than the other types of chitosan. A statistically higher adhesion of MMW microspheres was observed compared with HMW microspheres studied at the same concentration ($p < 0.05$) (Yu

et al., 2009). For other reason to explain the increasing adhesion property of CT/AA-SLN, regarding to the large size of particles required more force in order to eliminate particles from mucosal surface. Thus, large size of particles appeared to be adhered on mucosal surface for a longer period of time. In this experiment, the large particle size of CT/AA-SLN were obtained when compared with AA-SLN varying to the concentration of chitosan solution was added.

Table 24 The percentage cumulative of washed AA-SLN particles of AA solution, TM AA-SLN, 0.1% and 0.3% CT/TM AA-SLN.

Time (minutes)	% cumulative of washed AA-SLN particles			
	AA solution	TM AA-SLN	0.1% CT	0.3% CT
5	44.97 ± 0.02	47.13 ± 0.36	27.47 ± 0.65	23.04 ± 2.40
10	91.56 ± 0.001	79.72 ± 1.00	60.76 ± 3.32	42.30 ± 3.09
30	100.97 ± 0.003	93.58 ± 2.21	72.01 ± 2.56	53.90 ± 1.05

Table 25 The percentage cumulative of washed AA-SLN particles of SOF AA-SLN, 0.1% , 0.3% and 0.5% CT/SOF AA-SLN.

Time (minutes)	% cumulative of washed AA-SLN particles			
	SOF AA-SLN	0.1% CT	0.3% CT	0.5% CT
5	41.24 ± 0.45	34.42 ± 0.58	28.46 ± 0.16	16.41 + 0.38
10	83.92 ± 0.30	69.21 ± 0.72	53.62 ± 0.04	31.03 + 1.56
30	93.32 ± 0.32	88.02 ± 0.23	73.57 ± 2.37	37.39 + 0.51

From Tables 24-25 were shown to compared the adhesion property among SLN formulations in different type of lipid (TM and SOF). The percentage cumulative of washed AA-SLN particles of TM AA-SLN were no considerable difference to SOF AA-SLN. For 0.1 % and 0.3 % CT/TM AA-SLN formulations, The percentage cumulative of washed AA-SLN particles lower than 0.1 % and 0.3 % CT/SOF AA-SLN formulations which may be because the zeta potential of 0.1 % and 0.3 %

CT/TM AA-SLN (13.57±0.39 and 16.60±0.17, respectively) expressed positive charged more than 0.1 % and 0.3 % CT/SOF AA-SLN (8.80±0.12 and 11.80±0.92, respectively). As the process of mucoadhesion is a consequence of interaction between the mucus layer on mucosa and mucoadhesive polymer, it is greatly dependent upon mucus and polymer structure including their charges, a salt bridge effect for the interaction of positively charged chitosan microspheres with the negatively charged mucus glycoprotein, but subsequently it was demonstrated that positive charge on the surface of chitosan could give rise to a strong electrostatic interaction with mucus or with a negatively charged mucosal surface (He et al., 1998).

8. In vitro diffusion study

In order to assess the nasal epithelial cells diffusion of AA from SLN, the in vitro diffusion ability through 0.2 µm cellulose acetate were performed using modified Franz diffusion cells. The AA solution (in methanol) was used as reference to evaluate the nasal targeting ability of the AA-SLN formulations. The results were obtained as shown in Figure 46 , the % cumulative diffusion of AA were performed for 3 hours, AA solution, TM AA-SLN, SOF AA-SLN, 0.3% CT/TM A-SLN and 0.3% CT/SOF AA-SLN were 73.07 $\pm$ 0.44, 60.90 $\pm$ 0.31, 55.24 $\pm$ 0.61, 14.61 $\pm$ 1.76 and 9.48 $\pm$ 0.74, respectively. The high diffusion rate of AA solution might be due to the significant diffusion enhancement effect of methanol. In addition, during the diffusion studies, the loss of methanol can enhance the concentration of AA, also followed by the increase of the thermodynamic activity of AA. These factors might contribute to the diffusion through nasal cell from methanol. At the end of time, when compared between TM AA-SLN and SOF AA-SLN there was significantly different in % cumulative diffusion ($p<0.05$), might be a reason for TM AA-SLN had a smaller diameter than SOF AA-SLN which were advantageous to improve the diffusion of nanoparticles into nasal membrane (102.60 $\pm$ 1.65 and 122.63 $\pm$ 1.58 nm, respectively) as similar as in the case of 0.3%CT/TM AA-SLN and 0.3% CT/SOF AA-SLN (221.57$\pm$3.23 and 252.97$\pm$22.40 nm, respectively). It was relatively with previous study the ex vivo evaluation of $Al(OH_3)$ and chitosan conjugated PLGA microparticles as nasal vaccine carriers in porcine nasal mucosa. The results represented the small size of 1 µm particles was more preferred to be take up and permeated through porcine nasal tissue compared to the large particles of 5 and 15 µm (Amolnat, 2011). For the larger particle size of CT/AA-SLN formulations leading to obtained lower diffusion activity compared with AA-SLN formulations, due to chitosan might stay on the cellulose acetate membrane surface and did not go through the membrane due to its high molecular weight and other reason for explained that the low aqueous solubility might be obtained the slow diffusion of AA from the CT/AA-SLN formulations.

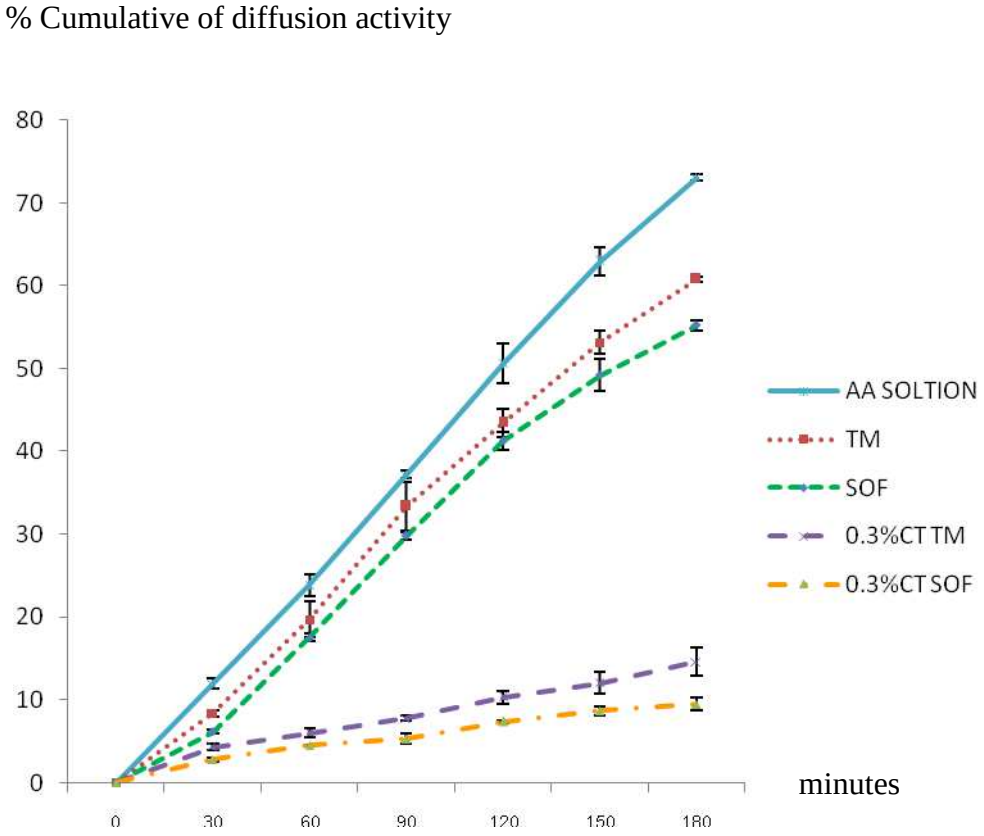

Figure 46 The diffusion profiles of AA from selected SLN formulations.

9. In vitro study in cell culture

Cell culture

Morphological characteristics of a human nasal epithelial carcinoma cell line (CCL-30 nasal cells) were very small, densely cell clumbs, firstly formed small colonies, grew within 5-8 days to a confluent monolayer and then multilayered cell aggregates as shown in Figure 47.

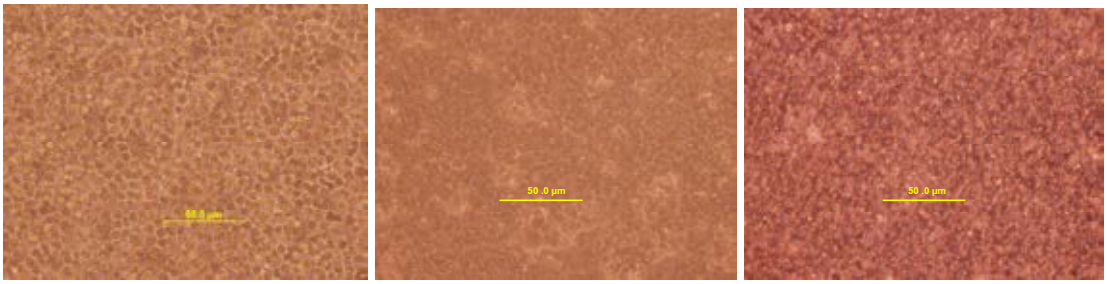

Figure 47 Photographs observed from inverted microscope of human nasal epithelial carcinoma cell line: a = day 1, b = day 3, c = confluent growth.

Cytotoxicity study (MTT Assay)

For the reason that the cytotoxicity study of SLN is an essential product parameter with regard to a prospective in vivo tolerance evaluation in humans and/or animals. The cytotoxicity of asiatic acid loaded solid lipid nanoparticles in human nasal epithelial carcinoma cell line was assessed using MTT (3-(4,5-dimethylthazol-2-yl)-2,5-diphenyl tetrazolium bromide). MTT was reduced to purple formazan in living cells by mitochondrial reductase. This reduction occurred only when reductase enzymes were active, and therefore this conversion was used as to measure of viable (living) cells. The results obtained in cytotoxicity assays were presented in Table 26. In order to compare cytotoxicity of various formulations The 50% cytotoxicity concentration (CC_{50}) of SLN were obtained depending on the asiatic acid in each formulations. The CC_{50} values were determined by intersection of the dose response curves with the y-axis at a viability of 50% and a subsequent transfer of the interception point to the x-axis representing the respective SLN concentrations and

were determined by insert y value = 50% in linear regression equation, x value was calculated for CC_{50} values (R^2 of linear regression equation should more than 0.95 for represents the true value of CC_{50}). The AA-SLN formulations possessed a good reproducibility and a low standard deviation for all the investigated systems and the dose dependent reduce of viability displayed the typical inverse sigmoid curve.

In this experiment, were evaluated after 48 hours exposure of cell with selected AA-SLN formulations composed of TM SP85 5:5, TM SL 7:3, TM SL 9.1, SOF SP80 5:5, SOF SP85 5:5, SOF SP85 7:3, GB SP80 7:3 and GB SP85 5:5. The concentrations of AA-SLN formulations varied from 0.036 to 100 μg/ml for TM SL 7:3 and TM SL 9.1 formulations, varied from 0.112 to 350 μg/ml for TM SP85 5:5 and varied from 0.16 to 500 μg/ml for SOF SP80 5:5, SOF SP85 5:5, SOF SP85 7:3, GB SP80 7:3 and GB SP85 5:5, respectively. In this experiments, CC_{50} values of asiatic acid was not determined because of the cytotoxicity of the corresponding concentration of methanol solvent. The results are mean values $\pm$ SD of three independent experiments performed in triplicate. The CC_{50} value for AA-SLN were in the range of 4.09 - 4.18 μg/ml.

Table 26 The CC_{50} values determined in human nasal epithelial carcinoma cell line of AA-SLN.

Formulation	CC_{50} (μg/ml)
TM SP85 5:5	4.16 $\pm$ 0.56
TM SL 7:3	4.12 $\pm$ 1.98
TM SL 9.1	4.07 $\pm$ 2.88
SOF SP80 5:5	4.09 $\pm$ 0.92
SOF SP85 5:5	4.13 $\pm$ 1.91
SOF SP85 7:3	4.09 $\pm$ 0.56
GB SP80 5:5	4.18 $\pm$ 1.16
GB SP85 5:5	4.09 $\pm$ 2.34

From Tables 27- 31, the %cell viability of AA-SLN were evaluated after 48 hours compared with drug-free SLN. The concentrations of AA-SLN formulations varied from 0.032 to 4 μg/ml for TM SL 7:3 and TM SL 9.1 formulations, varied from 0.112 to 14 μg/ml for TM SP85 5:5 and varied from 0.16 to 20 μg/ml for SOF SP80 5:5, SOF SP85 5:5, SOF SP85 7:3, GB SP80 7:3 and GB SP85 5:5, respectively. The ratios of dilution in drug-free SLN also similar with AA-SLN formulations. In this experiments. The results are mean values $\pm$ SD of three independent experiments performed in triplicate. The results showed the %cell viability of AA-SLN was not higher than drug-free SLN formulations. These suggested that the cytotoxicity of SLN formulations did not depended on the concentration of asiatic acid. However, the extent of SLN cytotoxicity was not different from that in the aqueous phase. Therefore, it can be assumed that the cytotoxicity of the SLN can be mainly attributed to components of the aqueous phase, especially to the nonionic emulsifier and the preservative. It analog with results from previous study on viability and cytokine production by macrophages. Cytotoxicity, as assessed MTT test, was strongly influenced by the surfactant used being marked with cetylpyridinium chloride (CPC) coated SLN at a concentration of 0.001% and further increased at SLN concentrations of 0.01 and 0.1%. All other SLN formulations containing poloxamine 908 (P908), poloxamer 407 (P407), poloxamer 188 (P188), solutol HS15 (HS15), tween 80 (T80), lipoid S75 (S75), sodium cholate (SC), or sodium dodecylsulfate (SDS) when used at the same concentrations reduced cell viability only slightly (Schler et al, 2001).

Table 27 The %cell viability of Drug-free TM TW80:SL 9:1, TM TW80:SL 9:1, Drug-free TM TW80:SL 7:3 and TM TW80:SL 7:3.

Concentration	% Cell viability			
	Drug-free TM TW80:SL 9:1	TM TW80:SL 9:1	Drug-free TM TW80:SL 7:3	TM TW80:SL 7:3
0.032 µg/ml	100.52 ± 0.72	105.89 ± 2.35	95.13 ± 1.82	95.62 ± 0.47
0.160 µg/ml	96.73 ± 4.08	92.22 ± 3.66	90.46 ± 3.99	92.92 ± 3.13
0.800 µg/ml	78.79 ± 1.30	86.73 ± 1.52	82.84 ± 1.30	82.04 ± 4.13
4.000 µg/ml	13.56 ± 0.95	20.42 ± 0.49	14.07 ± 5.10	20.1 ± 1.04

Table 28 The %cell viability of Drug-free TM TW80:SP85 5:5 and TM TW80:SP85 5:5.

Concentration	% Cell viability	
	Drug-free TM TW80:SP80 5:5	TM TW80:SP80 5:5
0.112 µg/ml	101.27 ± 0.92	105.8 ± 3.27
0.560 µg/ml	93.32 ± 4.35	92.28 ± 5.02
2.800 µg/ml	78.12 ± 1.82	80.9 ± 2.90
14.000 µg/ml	13.60 ± 0.17	33.79 ± 3.92

Table 29 The %cell viability of Drug-free GB TW80:SP80 7:3, GB TW80:SP80 7:3, Drug free GB TW80:SP85 5:5 and GB TW80:SP85 5:5.

Concentration	% Cell viability			
	Drug-free GB SP80 7:3	GB SP80 7:3	Drug-free GB SP85 5:5	GB SP85 5:5
0.16 µg/ml	95.15 ± 2.98	105.00 ± 1.92	95.38 ± 6.04	96.26 ± 1.82
0.80 µg/ml	84.53 ± 1.70	95.43 ± 7.18	89.92 ± 5.83	94.23 ± 1.39
4.00 µg/ml	83.28 ± 0.18	80.04 ± 5.64	73.34 ± 0.94	88.57 ± 8.83
20.00 µg/ml	28.33 ± 2.29	29.13 ± 4.10	25.19 ± 4.83	24.62 ± 0.11

Table 30 The %cell viability of Drug-free SOF TW80:SP80 5:5, SOF TW80:SP80 5:5, Drug-free SOF TW80:SP85 5:5 and SOF TW80:SP85 5:5.

Concentration	% Cell viability			
	Drug-free SOF TW80:SP80 5:5	SOF TW80:SP80 5:5	Drug-free SOF TW80:SP85 5:5	SOF TW80:SP85 5:5
0.16 μg/ml	92.83 ± 7.88	101.50 ± 0.45	95.69 ± 0.80	98.43 ± 1.75
0.80 μg/ml	88.73 ± 3.72	99.58 ± 0.81	92.51 ± 3.42	97.38 ± 2.00
4.00 μg/ml	83.22 ± 11.96	85.73 ± 0.11	78.97 ± 3.05	88.39 ± 8.97
20.00 μg/ml	19.28 ± 7.88	18.33 ± 5.28	34.18 ± 0.04	35.82 ± 2.01

Table 31 The %cell viability of Drug-free SOF TW80:SP85 7:3 and SOF TW80:SP85 7:3.

Concentration	% Cell viability	
	Drug-free SOF TW80:SP85 7:3	SOF TW80:SP85 7:3
0.16 μg/ml	93.99 ± 1.83	95.30 ± 2.05
0.80 μg/ml	87.39 ± 3.36	88.89 ± 2.02
4.00 μg/ml	70.72 ± 7.65	78.14 ± 13.62
20.00 μg/ml	28.26 ± 3.54	30.42 ± 4.88

The selected CT/AA-SLN formulations (CT/TM SP85 5:5 and CT/SOF SP85 5:5) in the concentration of chitosan solution 0.1%, 0.3% and 0.5% w/v were examined and reported as the percentage of cell viability compared with TM AA-SLN. The concentrations of TM AA-SLN and CT/TM AA-SLN formulations varied from 0.112 to 14 μg/ml and varied from 0.16 to 20 μg/ml for SOF AA-SLN and CT/SOF AA-SLN formulations. The results of MTT assays for all prepared formulations were presented in Figures 48-49 The results showed the percentage of cell viability were no significant different ($p > 0.05$: ANOVA) in both of SLN formulations 0.1% and 0.3% CT/AA-SLN formulations compared with AA-SLN formulations with two type solid lipids. These suggested that the formulations did not

damage cell membrane and were characterized by good biocompatibility with nasal cell in the appropriate concentration. In contrast to the 0.5% CT/AA-SLN formulations, it might be correlated with the higher percentage of cellular uptake. The 0.5% CT/AA-SLN formulations with two type solid lipids showed the lowest CC_{50} value, indicating that the 0.5% CT/AA-SLN formulations were more cytotoxic to nasal cell than other formulations. Thus, AA-SLN containing 0.3% w/v chitosan solution was chosen to continue the study in the next step.

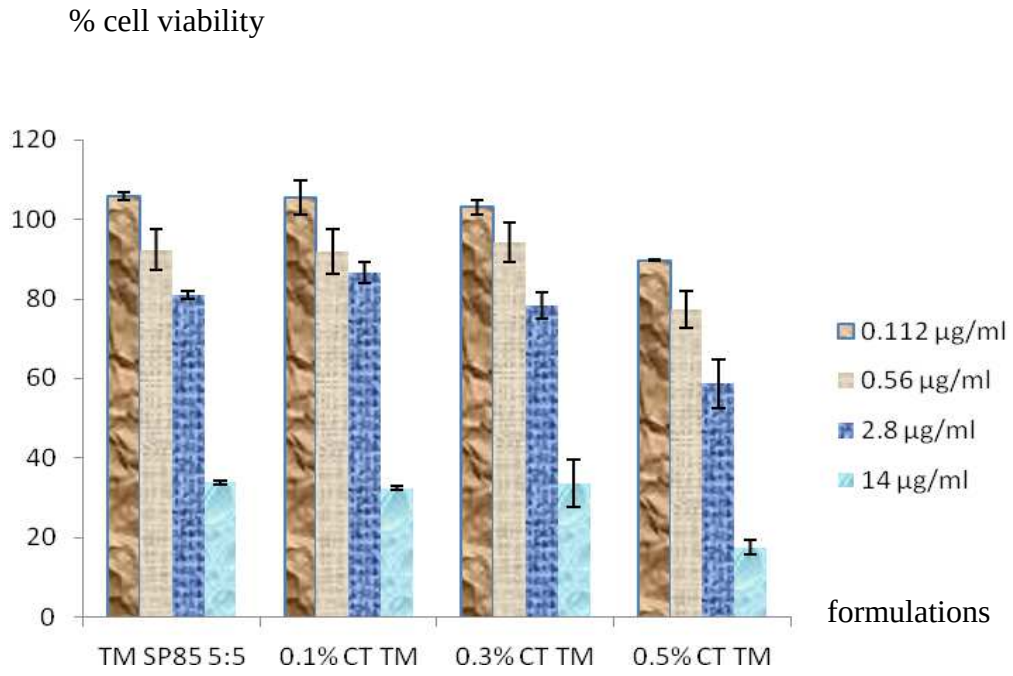

Figure 48 The %cell viability of TM AA-SLN and CT/TM AA-SLN in human nasal epithelial carcinoma cell line.

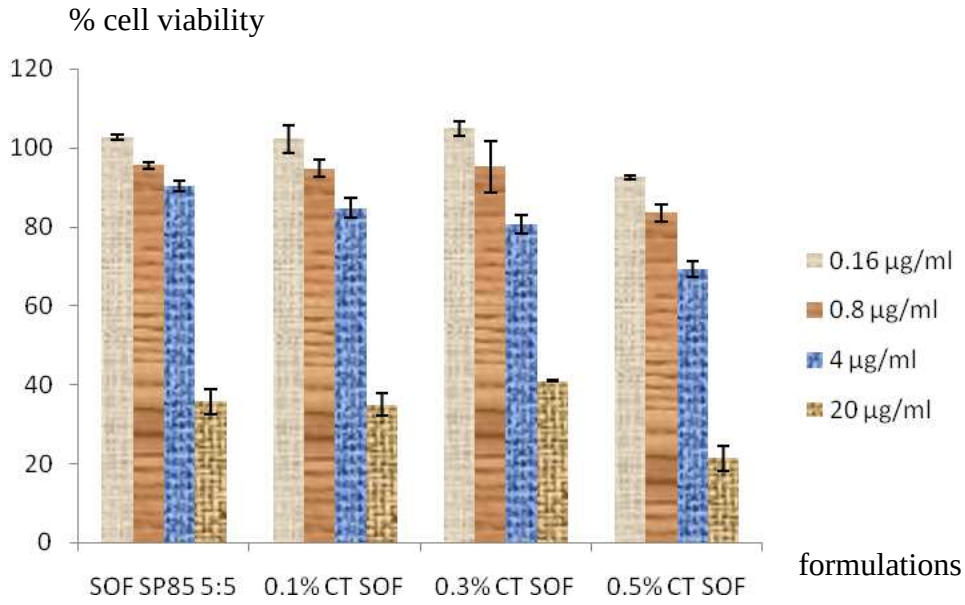

Figure 49 The %cell viability of SOF AA-SLN and CT/SOF AA-SLN in human nasal epithelial carcinoma cell line.

Table 32 The CC_{50} values obtained in human nasal epithelial carcinoma cell line of TM AA-SLN, SOF AA-SLN and coated with chitosan solution for both formulations in various concentrations.

Formulations	CC50 µg/ml (50% cytotoxic concentration)			
	AA-SLN	0.1% chitosan	0.3% chitosan	0.5% chitosan
TM SP85 5:5	4.16 ± 0.56	4.26 ± 1.54	4.22 ± 0.93	3.89 ± 1.03
SOF SP85 5:5	4.13 ± 1.91	4.21 ± 0.76	4.17 ± 1.72	3.84 ± 1.21

The previous results showed the low concentration of asiatic acid in all SLN formulations biocompatible with human nasal epithelial carcinoma cell line, which could not be appropriate for use in permeation and cellular uptake study. The contact time of formulations to human nasal epithelial carcinoma cell line used in these study was only 30 minutes . Thus, inverted microscope was used to evaluate preliminary nasal cell cytotoxicity in methanol, TM AA-SLN, SOF AA-SLN, 0.3% CT/ TM AA-SLN and 0.3% CT SOF AA-SLN as shown in Tables 33-35.

Table 33 Evaluation of cytotoxicity in human nasal epithelial carcinoma cell line of TM AA-SLN and 0.3% CT/TM AA-SLN by inverted microscope.

Duration / Formulations	**Concentration (µg/ml)**					
TM SP85 5:5	**175**	**35**	**7**	**1.4**	**0.28**	**0.056**
initial	4	4	4	4	4	4
30 minutes	1	2	4	4	4	4
60 minutes	1	2	3	4	4	4
120 minutes	1	1	3	4	4	4
180 minutes	1	1	2	4	4	4
24 hours	1	1	1	4	4	4
0.3% CT/TM SP85 5:5						
initial	4	4	4	4	4	4
30 minutes	1	2	4	4	4	4
60 minutes	1	2	4	4	4	4
120 minutes	1	2	3	4	4	4
180 minutes	1	1	2	4	4	4
24 hours	1	1	1	4	4	4

Note: 1 = cell viability $\leq$ 25%, 2 = cell viability 26-50%, 3 = cell viability 51- 75% and 4 = cell viability 76 - 100% cell viability.

Table 34 Evaluation of cytotoxicity in human nasal epithelial carcinoma cell line of SOF AA-SLN and 0.3% CT/SOF AA-SLN by inverted microscope.

Duration / Formulations	**Concentration (µg/ml)**					
SOF SP85 5:5	**250**	**50**	**10**	**2**	**0.4**	**0.08**
initial	4	4	4	4	4	4
30 minutes	2	3	4	4	4	4
60 minutes	1	2	4	4	4	4
120 minutes	1	2	3	4	4	4
180 minutes	1	2	2	4	4	4
24 hours	1	1	2	4	4	4
0.3% CT/SOF SP85 5:5						
initial	4	4	4	4	4	4
30 minutes	2	3	4	4	4	4
60 minutes	2	3	4	4	4	4
120 minutes	1	2	3	4	4	4
180 minutes	1	2	2	4	4	4
24 hours	1	1	2	4	4	4

Note: 1 = cell viability $\leq$ 25%, 2 = cell viability 26-50%, 3 = cell viability 51- 75% and 4 = cell viability 76 - 100% cell viability.

Table 35 Evaluation of cytotoxicity in human nasal epithelial carcinoma cell line of methanol by inverted microscope.

Duration / Formulations	**Concentration (% v/v)**					
Methanol	**50**	**10**	**8**	**4**	**2**	**1**
initial	4	4	4	4	4	4
30 minutes	3	4	4	4	4	4
60 minutes	3	4	4	4	4	4
120 minutes	3	4	4	4	4	4
180 minutes	3	4	4	4	4	4
24 hours	2	3	4	4	4	4

Note: 1 = cell viability $\leq$ 25%, 2 = cell viability 26-50%, 3 = cell viability 51- 75% and 4 = cell viability 76 - 100% cell viability.

After human nasal epithelial carcinoma cell line were contacted with all formulations for 30 minutes, the cytotoxicity were obtained with inverted microscope, in the case of TM AA-SLN and 0.3% CT/TM AA-SLN, the concentration of asiatic acid that less cytotoxic to human nasal epithelial carcinoma cell line was in the range of 10 – 50 µg/ml, for SOF AA-SLN and 0.3%CT/SOF AA-SLN in the range of 7 – 35 µg/ml and for methanol less than 50%v/v. These concentrations were confirmed by MTT assay and were reported as percentage of cell viability showed in Figures 50-52. The highest concentration of asiatic acid that showed 90% cell viability in TM AA-SLN and 0.3%CT/TM AA-SLN were 20 µg/ml and for SOF AA-SLN, 0.3%CT/SOF AA-SLN were 14 µg/ml and for methanol were 50% v/v . Thus, the concentration of asiatic acid at 14 µg/ml in all formulations, were selected to examine the permeation and cellular uptake study in the next step that the 50% v/v methanol was used to dilute asiatic acid for reference.

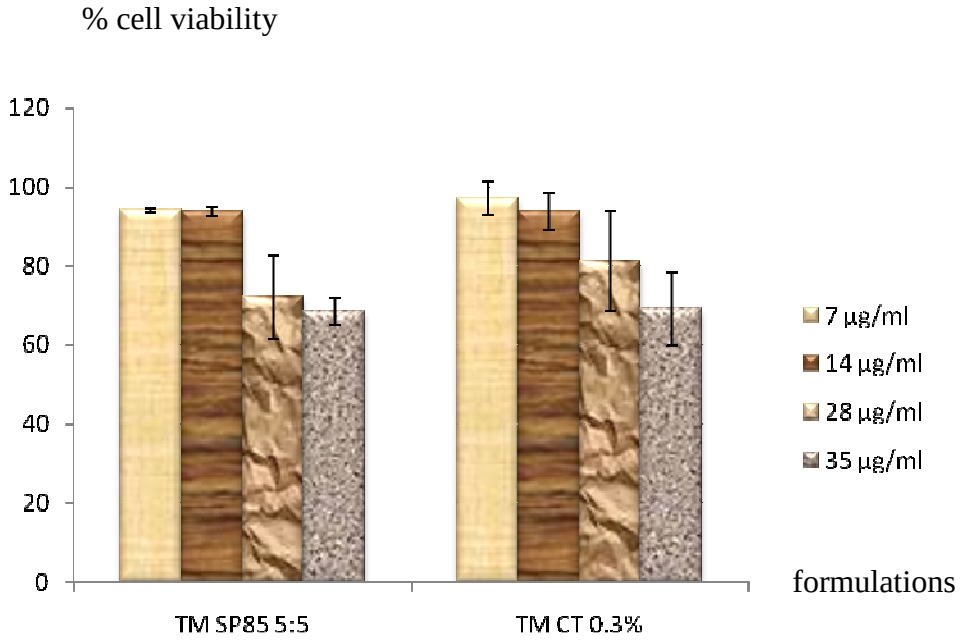

Figure 50 The % cell viability of TM AA-SLN and 0.3% CT/TM AA-SLN in human nasal epithelial carcinoma cell line.

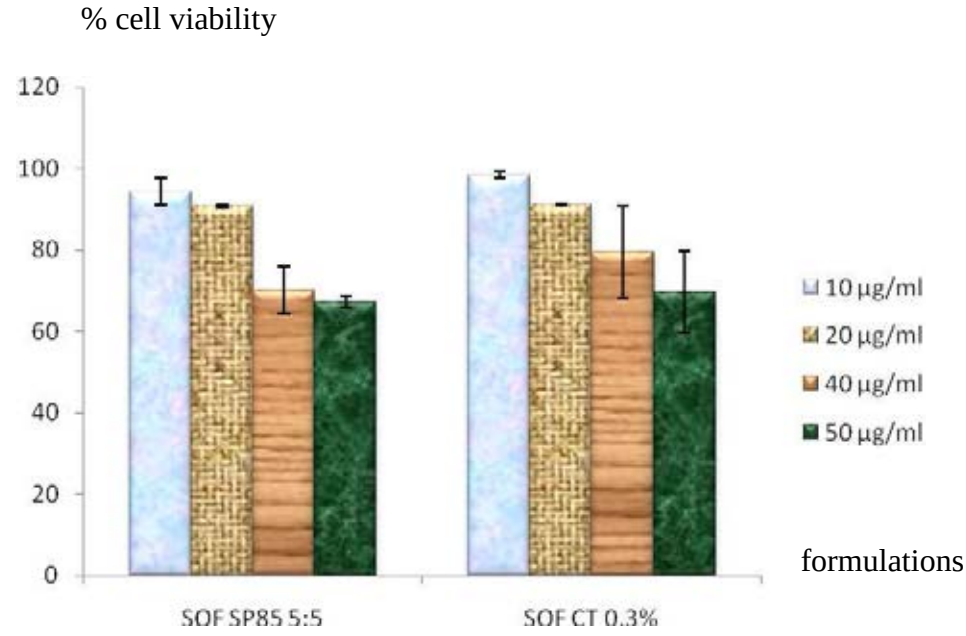

Figure 51 The % cell viability of SOF AA-SLN and 0.3%CT/SOF AA-SLN in human nasal epithelial carcinoma cell line.

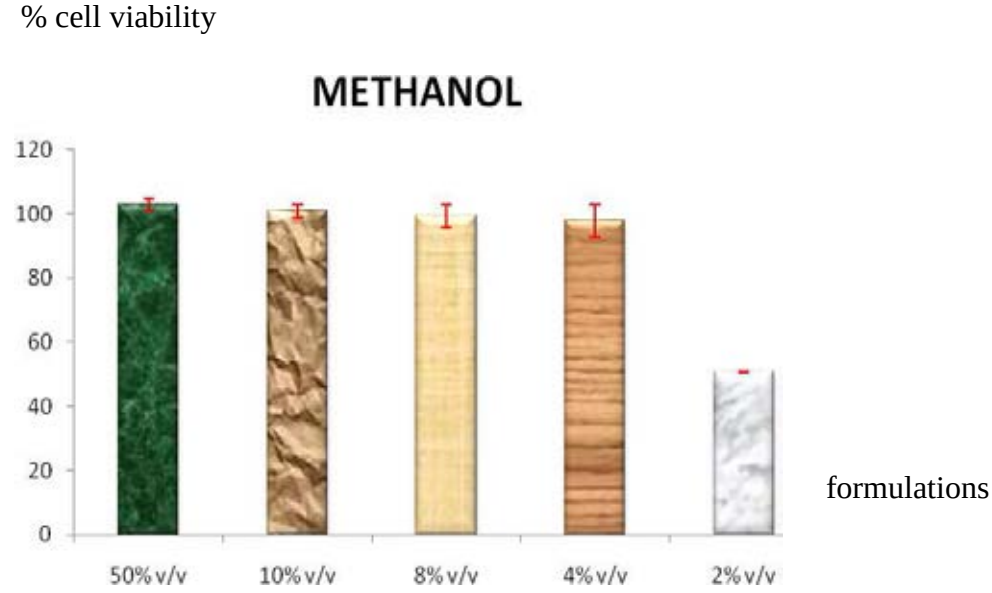

Figure 52 The % cell viability of methanol in human nasal epithelial carcinoma cell line.

Cellular uptake study and permeation study

Cellular uptake study:

The cellular uptake study of SLN formulations were illustrated by the percentage analytical of drug amount in human nasal epithelial carcinoma cell line. When a drug contact with the epithelial cells of the nasal membranes, it can be absorbed by one of two pathways, transcellular transport and paracellular pathways. Transcellular permeation takes place across cell membrane whereas paracellular absorption takes place through the tight junction between cells. Chitosan can be considered as one of cationic polymer which normally had the ability to enhance the paracellular permeability of mucosal epithelia by the dilation of paracellular space and reduction of TEER values with their charge excluding the damage of cell membrane, as a result of transiently opening the tight junctions, and increasing the paracellular absorption of hydrophilic and macromolecular drugs. Nanoparticles are generally internalized into cells through fluid phase endocytosis , receptor-mediated endocytosis or phagocytosis (Hans E et al., 1998). In addition, the chitosan was shown to open tight junction of epithelial cell and also is known to interact with cell membranes by adsorptive endocytosis, which is preceded by nonspecific interaction of ligand with the cell membrane. For the past decades, significant effort has been devoted to surface modification of various drug carriers with polymer such as chitosan, polyethylene glycol to improve their internalization efficiency. It can be seen that the order of cellular uptake ability for AA-SLN formulations were AA solution > 0.3% CT/TM AA-SLN > 0.3% CT/SOF AA-SLN > TM AA-SLN > SOF AA-SLN as indicated in Figure 53. The asiatic acid solution (in methanol) showed the highest cellular uptake activity. This might be due to the significant permeation enhancement effect of methanol which was used as reference. 0.3%CT/AA-SLN showed the higher cellular uptake ability which was significantly different compared with AA-SLN ($p < 0.05$), it might be that the surface of 0.3%CT/AA-SLN formulations showed a great deal of roughness after coated with chitosan solution, and could accelerate the endocytosis of SLN formulations by human nasal epithelial carcinoma cell line leading to the higher cellular uptake ability compared with AA-

SLN formulations. Moreover, the enhancing mucoadhesion properties of 0.3%CT/AA-SLN can be explored to promote the contact of 0.3%CT/AA-SLN formulations with nasal epithelium, increasing the concentration at the site of absorption and enlarge its cellular uptake. Viscosity affected to the nasal permeability, a higher viscosity of 0.3%CT/AA-SLN formulations increased contact time between the substrance and a nasal mucosa, leading to decreasing the nasal clearance than AA-SLN formulations. The slightly higher cellular uptake ability of TM AA-SLN than SOF AA-SLN might be due to the smaller particle size of TM AA-SLN (102.60 $\pm$ 1.65) than SOF AA-SLN (122.63 $\pm$ 1.58) that was correlated with results from previous study, the effect of particle size on the cellular uptake of the oleoyl-chitosan nanoparticles by A549 cells as a results showed the nanoparticles were taken up by the cells, and levels of binding and uptake increased with the decrease of particle size of nanoparticles (Jing Zhang et, 2008).

Permeation study

The percentage of permeation activity after 30 minutes of contact time was shown in Table 36. TM AA-SLN showed permeation profile that was slightly higher than that of SOF AA-SLN. This confirmed the results obtained from in vitro experiments diffusion study used 0.2 µm cellulose acetate membrane (0.2 CA) as barrier. In this study, the permeation activity of both groups of AA-SLN formulation (with chitosan and without chitosan) were quite low. This revealed that the presence of solid lipids composed of TM and SOF (longer chain length) formed less perfect crystals with many imperfections in the lattice and not only modified the drug entrapment efficiency (highly entrapment efficiency) but also modified the drug release profile. This results represented more sustained release of the drug from solid lipid nanoparticle. Especially, the 0.3%CT/AA-SLN of both types of solid lipids showed lower permeation across nasal epithelium membrane although they were rapidly taken up by nasal cell and thereafter behaved as a sustained release formulations. This might be due to that the asiatic acid not released completely from the chitosan coated SLN formulations inside the cells within 30 minutes compared with AA-SLN formulations. The slightly higher permeation ability of TM AA-SLN

than SOF AA-SLN might be due to the smaller particle size of TM AA-SLN as same as in cellular uptake study.

The difference of permeation rate between AA-SLN formulation and 0.3%CT/AA-SLN formulation was applied by the unionized species were absorbed better compared with ionized species and be consistent in the case of nasal absorption. As shown in results, TM AA-SLN and SOF AA-SLN formulations (pH 5.11± 0.16 and 6.11± 0.01, respectively) would be in unionized form in nasal cavity (pH 4.5-6.5) than 0.3%CT/ TM AA-SLN and 0.3%CT/ SOF AA-SLN (pH 3.94± 0.22 and 3.94± 0.11, respectively). As a result, AA-SLN formulations were obtained a higher permeability activity than 0.3%CT AA-SLN formulations that was correlated with previous study of the permeation of GTX from Gatiquin solution, the results of the permeation profiles it was found that the SLN-B showed more sustained release of GTX as compared to SLN-A and both SLN showed sustained release of GTX as that of the marketed eye drop, which showed immediate release of most of the drug from its solution form, might be due to the fact that most of the drug would be in unionized form at the higher pH (6.8) of the Gatiquin eye drops solution (Mohd. Abul Kalam et al., 2010).

The difference for the in vitro experiments (0.2 µm cellulose acetate membrane) and in vitro cell (human nasal epithelial carcinoma cell line) were considerable due to the differences in the structures of the biological substrates: human nasal epithelial carcinoma cell line were highly differentiated and forming tight junction while in cellulose acetate membrane alls were not. Moreover it could be proposed that the major factor determining the drug permeate from nanoparticles is its solubilization or dissolution rate in the permeate medium. The medium penetrates into the particles and dissolves the entrapped AA-SLN formulations and, therefore, in vitro permeation study by human nasal epithelial carcinoma cell line the amount of permeate medium (13 ml) was much more than in vitro diffusion study by 0.2 µm cellulose acetate membrane (2.6 ml). As a result, the permeation activity of SLN formulations in human nasal epithelial carcinoma cell line were lower than that in 0.2 µm cellulose acetate membrane.

% cellular uptake and % permeation

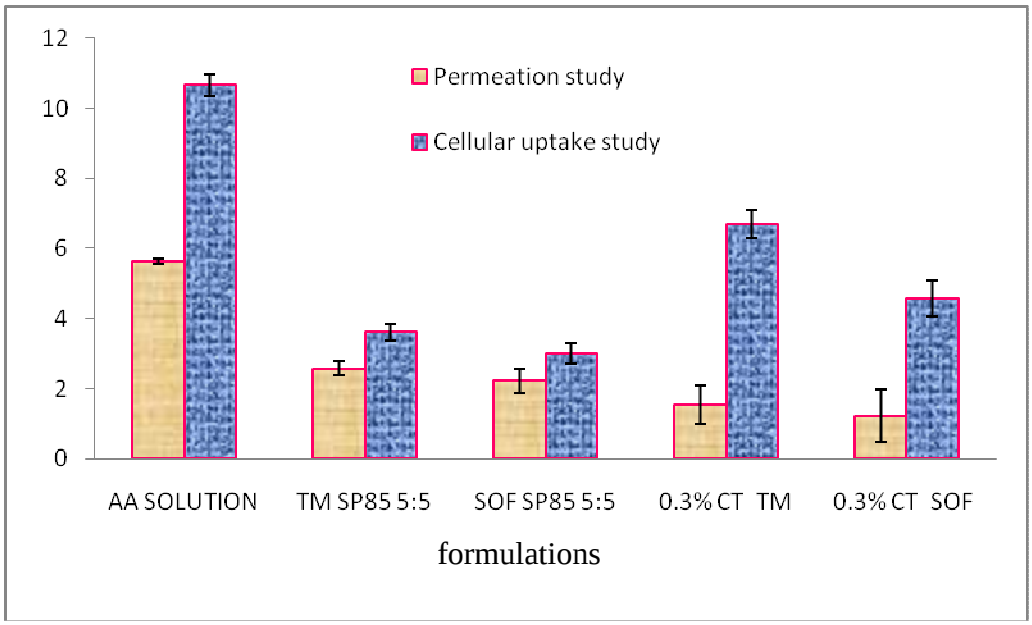

Figure 53 The cellular uptake and permeation activity of selected AA-SLN formulations.

Table 36 The cellular uptake and permeation for selected AA-SLN formulations.

Formulations	% Permeation of drug	% Cellular uptake of drug
Asiatic acid solution	5.63 ± 0.06	10.66 ± 0.30
TM SP85 5:5	2.58 ± 0.21	3.61 ± 0.24
SOF SP85 5:5	2.23 ± 0.35	3.02 ± 0.29
0.3% CT/TM SP85 5:5	1.54 ± 0.54	6.7 ± 0.39
0.3% CT/SOF SP85 5:5	1.23 ± 0.76	4.59 ± 0.51

Tight junction integrity study

The Trans-epithelial electrical resistance (TEER) profiles as shown in Table 37. The confluent monolayers of human nasal epithelial carcinoma cell line were obtained within six days. The TEER values of AA solution, TM SP85 5:5, SOF SP85 5:5, 0.3% CT/TM SP85 5:5 and 0.3% CT/SOF SP85 5:5 were reached 125.67 $\pm$ 1.70 $\Omega.cm^2$, 127.44$\pm$ 1.64 $\Omega.cm^2$, 124.67 $\pm$ 2.60 $\Omega.cm^2$, 121.67 $\pm$ 2.89 $\Omega.cm^2$ and 123.44 $\pm$ 2.88 $\Omega.cm^2$, respectively. Thus, the TEER values of nasal epithelial carcinoma cell cultured on porous membranes were in the same range of previous report (Boucher et al., 1987).

After experiments for 30 minutes, the TEER values obtained 126.44 $\pm$ 1.22 $\Omega.cm^2$, 128.44 $\pm$ 2.03 $\Omega.cm^2$, 125.44 $\pm$ 1.76 $\Omega.cm^2$, 122.11 $\pm$ 1.24 $\Omega.cm^2$ and 124.11 $\pm$ 1.98 $\Omega.cm^2$, respectively. And after experiments for 120 minutes, the TEER values obtained 129.22 $\pm$ 1.02 $\Omega.cm^2$, 129.55 $\pm$ 2.80 $\Omega.cm^2$, 127.11 $\pm$ 1.68 $\Omega.cm^2$, 122.67 $\pm$ 1.00 $\Omega.cm^2$ and 125.44 $\pm$ 2.14 $\Omega.cm^2$, respectively.

The TEER values in all SLN formulations after experiments for 30 minutes and 120 minutes slightly increased compared with initial value. The results indicated that all of selected SLN formulations did not modify the human nasal epithelial carcinoma cell line substrate integrity and the integrity of the nasal cells were maintained. An increase of TEER was observed when some epithelial mucosa were exposed to hyperosmotic condition, which is probably due to the collapse of the epithelial intercellular space (Madara, 1983). Although in the previous literature, chitosan solution is reported to be capable of opening tight junctions and causing a TEER decrease. However, in these experiments the chitosan-associated SLN did not produce a widening of tight junctions correlated with the results from permeation and cellular uptake experiments**.** It might be due to less of duration in cellular uptake and permeation study (30 minutes), correlated with previous study; the effect of chitosan to absorption of desmopressin. The results showed no apparent difference ($P > 0.05$) in absorption rate and extent was observed between CS group and the control group in the initial 40 min, irrespective of chitosan concentration. Compared to the control

group, significant absorption increase was shown at 60 min and the absorption amount increased with increasing chitosan concentration, with an absorption increase of 16.4%, 23.9% and 22.7% for 0.1%, 0.5% and 1% chitosan group, respectively (Dan et al., 2008).

Table 37 The TEER values of human nasal epithelial carcinoma cell line in various SLN formulations compared between before (initial) and after experiments (for 30 minutes and 120 minutes).

Formulations	Duration		
	Initial	30 mins	120 mins
AA SOLUTION	125.67 ± 1.70	126.44 ± 1.22	129.22 ± 1.02
TM SP85 5:5	127.44 ± 1.64	128.44 ± 2.03	129.55 ± 2.80
SOF SP85 5:5	124.67 ± 2.60	125.44 ± 1.76	127.11 ± 1.68
0.3% CT TM	121.67 ± 2.89	122.11 ± 1.24	122.67 ± 1.00
0.3% CT SOF	123.44 ± 2.88	124.11 ± 1.98	125.44 ± 2.14

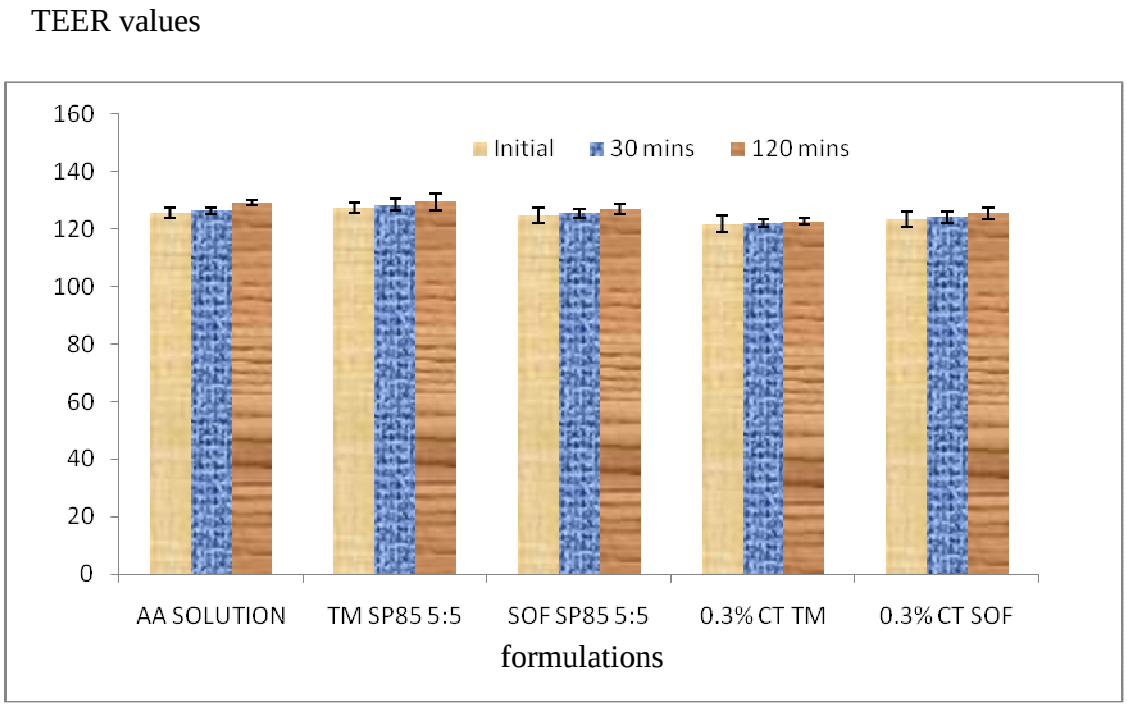

Figure 54 The TEER values of human nasal epithelial carcinoma cell line in various SLN formulations compared between before (initial) and after experiments (for 30 minutes and 120 minutes).

Viability of cell monolayer

The results from trypan blue dye exclusion and haemotocytometer showed the percentage of cell viability (% cell viability) after exposure to all of selected SLN formulations for 120 minutes for permeation and uptake experiments as shown in Table 38. The results of % cell viability up to 94% for all formulations. Indicated that all SLN formulations did not damage cell membrane and were characterized by good biocompatibility with nasal cell for all permeation and uptake experiments duration that were correlated with the results from cytotoxicity study**.**

Table 38 The percentage of cell viability after permeation experiment.

Types of SLN	% Cell viability $\pm$ SD
TM TW80 : SP85 5:5	95.34 $\pm$ 2.12
0.3% CT TM TW80 : SP85 5:5	94.82 $\pm$ 3.71
SOF TW80 : SP85 5:5	94.26 $\pm$ 2.61
0.3% CT SOF TW80 : SP85 5:5	96.12 $\pm$ 1.21

CHAPTER V

CONCLUSIONS

From the results, drug-free SLN were prepared to investigate the optimal SLN for incorporation of AA into formulations by hot-high pressure homogenization method in varying types of lipids; TM, TS, GB, SOF, PA and SA . TW80 used as single surfactant could obtain stabilized SLN formulations and displayed a low AA loading. This was due to TW80 could not decrease the surface tension and stabilize newly formed surfaces during homogenization to smaller droplets, thus destabilized formulations were obtained. In the case of combined surfactants were used. TW80:PL188 produced destabilized formulation in all type of lipids, might be due to decreasing of zeta potential which induced particle aggregation.

Particle size of AA-SLN as also in the nanometer range. The mean particle sizes of TM, TA and SOF formulations were not different, this might be due to closed melting point of lipids. Although, GB which has the highest melting point but the formulation did not obtain the largest mean particle size. The explainatoin is by other critical parameters for example velocity of lipid crystallization. I n the case of SOL as surfactant, a trend towards small particle size was seen . Low density and melting point supported to increase the mobility to receive high shear from high pressure homogenizer. In addition, when AA-SLN were coated with chitosan, the particle size was affected upon the concentration of chitosan. As the concentration of chitosan was increased, the mean particle size of CT/AA-SLN formulations increased. The zeta potentials in all AA-SLN were slightly negative. When coated chitosan, positive values of zeta potential were obtained as a results from its cationic character. The positively charged amino groups of chitosan were capable of neutralizing the negative charge at the surface of SLN. Although, the zeta potential values were not above absolute 30mv but stabilized formulations were obtained because of steric stabilization of non-ionic surfactants.

In the case of AA-SLN, the average pH was in the range 4.5 – 6.5, which was suitable for use in nasal delivery route . For chitosan coated, lower pH values were obtained when compared with AA-SLN. The results were presented that the order of the pH values: AA-SLN > 0.5% CT/AA-SLN > 0.3% CT/AA-SLN > 0.1% CT/AA-SLN, respectively. The lower pH value of 0.1% CT/AA-SLN might be due to hydrolysis reaction of chitosan producing alkali mixures of N-acetylglucosamine and glucosamine.

TEM photographs showed that all AA-SLN seemed uniform nanospheres, when chitosan was added, they was not expressd uniformity and spherical shape. The increasing of chitosan concentration led to particles aggregation, might be due to not enough negative charged on SLN surface to interact with chitosan particles on leading to an aggregation of chitosan nanoparticle.

The results of DSC and X-RAY were correspondingly that after AA was incorporated into SLN, it was not in crystalline state but in amorphous state DSC thermograms and PRXD patterns did not show the melting peak for the AA in FD AA-SLN. Whereas by the presence of melting peak of AA in the physical mixtures of all formulations was clearly seen.

Chitosan was added to enhance mucoadhesion property and to decrease mucociliary clearance. Formulations with high concentration of chitosan could adhere on nasal tissue surface for a longer period of time than those of low concentraton also SLN formulations. This was due to the presence of greater amount of chitosan in the same volume of liquid droplets, thus providing more positive charge to interact with the negative mucin surface. Thus, 0.5% CT AA-SLN showed the highest adhesive property compared with other concentrations of chitosan solution added relating to the highest viscosity of formulations. This result was confirmed by viscosity study.

The rheology of AA-SLN and CT/AA-SLN displayed newtonian flow characteristic, indicating that a direct proportionality existed between shear stress and shear rate, for all values of shear.

In vitro permeation through 0.2 µm cellulose acetate were performed using modified Franz diffusion cells. The results were shown the order of the % cumulative permeation of AA; AA solution > TM AA-SLN > SOF AA-SLN > 0.3% CT/TM A-SLN > 0.3% CT/SOF AA-SLN, respectively. The possible was that smaller diameter was more advantageous to improve the penetration of nanoparticles into nasal membrane. CT/AA-SLN obtained lower permeation activity compared with AA-SLN was attributed to the large particles of chitosan (more than 200 nm) were attached on membrane surface and did not pass through the membrane. Further, the good advantage that chitosan may stay on the membrane surface and not go through the membrane due to its high molecular weight, resulting in less severe damage. CT/AA-SLN formulations were prepared in this study showed the potential as a carrier for controlling drug release rate.

In stability studies particle sizes, % drug content and physicochemical stability of AA-SLN was determined after certain condition. In high temperature, the mean particle size and zeta potential significantly increased as a result that TW80 might diffuse from the interface leading to higher solubility in aqueous phase. Less of stabilizer adhering on the solid lipids would produce larger particles from small particles aggregation. In addition, high input energy of high temperature could also lead to change in the charges on the particle surface. Moreover, the obtained pH values were lower than initial. That might be due to the hydrolysis of triglyceride part of solid lipids to acquire the formation of free fatty acid (acidic activity). The percentage of AA remaining was decreased with time. It was possible that the degradation of asiatic acid be occur.

TM TW80:SP85 5:5 and SOF TW80:SP85 5:5 had the best ability to physical stabilization of SLN, thus were selected that both formulations was further study for biocompatibly, capability to enhance cellular uptake and in vitro permeation through CCL-30 nasal cells compared with SLN formulation coated by chitosan. The CC_{50} of AA-SLN were in range 4 µg/ml. The TEER values were not different after permeation in all AA-SLN and CT/AA--SLN compared with initial, indicating that the tight junction did not open. However, the cellular uptake and permeation of AA in

basolateral were detected due to small particles size and lipophilic charator of AA-SLN to promote transcellular absorption in nasal cells. The cell viability with trypan blue dye exclusion of nasal cells after permeation study was more than 90%. This result was in good agreement with data from cytotoxicity by MTT assay.

The high pressure homogenization method is still the most suitable method for SLN production. In academic research, due to the ease of preparation and low cost of the required apparatus. Furthermore, the idea behind the present work is to show the positive effect of the coating of the SLN nanoparticles with chitosan. Moreover, these findings indicate that future clinical use of the generated SLN will require that the preparations should be stored and maintained at temperature below that caused phase transition. It was suggested that additional work have to be establish the optimum stabilizer composition for generation of stable SLN, study in %entrapment efficiency after storage for confirmed stability of AA-SLN formulations, study in vitro nasal mucosa by modification of Franz cell to evaluated permeation study compared with in vitro permeation study of a human nasal epithelial carcinoma cell line.

REFERENCES

Abraham, J. D. 1993. Lipospheres for controlled delivery of sub stances. United States Patent, USS 188837.

Annick, L. 2005. The use of mucoadhesive polymers in ocular drug delivery**.** Advanced Drug Delivery Reviews 57: 1595– 1639**.**

Begly, D.J. 1996. The blood-brain barrier: Principles for targeting peptides and drugs to the central nervous system. Journal of Pharmacy and Pharmacology 48: 136-146.

Begly, D.J. 2004. Delivery of therapeutic agents to the central nervous system: The problems and possibilities. Pharmacology & Therapeutics 104: 29-45.

Bunjes, H., Siekmann, B., and Westesen, K. 1998. Emulsions of super-cooled melts - a novel drug delivery system, in: S. Benita (Ed.), Submicron Emulsions in Drug Targeting and Delivery, Harwood Academic Publishers, Amsterdam. pp.175– 204.

Carsten, O., et al., 2001. Cationic solid-lipid nanoparticles can efficiently bind and transfect plasmid DNA. Journal of Controlled Release 77: 345–355.

Channarong, M. 2007. Bioaccessibility, cellular uptake, and angiotensin I converting enzyme (ACE) inhibitory activity of triterpenoids from Centella asiatica (Linn.) Urban. Master's thesis. Department of science, Graduate School, Mahidol University.

Chen, X.Q., Fawcett, J.R., Rahman, Y.E., Ala, T.A., and Frey, W.H. 1998. Delivery of nerve growth factor to the brain via the olfactory pathway. Journal of Alzheimer's Disease 1: 35–44.

Chi, H. L., Venkat, M., and Yugyung, L. 2009. Thixotropic property in pharmaceutical formulations. Journal of Controlled Release 136: 88–98.

Fei, H., Sanming, L., Ran, Y., Hongzhuo L., and Lu X. 2008. Effect of surfactants on the formation and characterization of a new type of colloidal drug delivery system:Nanostructured lipid carriers. Colloids and Surfaces A: Physicochemical. 210–216.

Frey, W.H., Thorne, R.G., and Pronk, G. 2000. Delivery of Insulin like growth factor-1 to the brain and spinal cord along olfactory and trigeminal pathways following intranasal administration: a noninvasive method for bypassing the blood brain barrier. Society for Neuroscience 26:1365–1370.

Gasco, M.R. 1993. Method for producing solid lipid microspheres having a narrow size distribution. United States Patent, USS 188837.

Ghada, A., and Rania H. F. 2009. Diazepam-Loaded Solid Lipid Nanoparticles: Design and Characterization. Journal of the American Association of Pharmaceutical Scientists. Vol. 10, No. 1.

Gokce, E.H., et al. 2008. Cyclosporine A loaded SLNs: Evaluation of cellular uptake and corneal cytotoxicity. International Journal of Pharmaceutics 364: 76–86.

Goppert, T., and Muller, R. 2005. Protein adsorption patterns on poloxamer- and poloxamine-stabilized solid lipid nanoparticles (SLN). European Journal of Pharmaceutics and Biopharmaceutics 60: 361–372.

Gummerloch, M.K., and Neuwelt, E.A. 1992. Drug entry into the brain and its pharmacologic manipulation. Bradbury MWB (ed). Physiology and Pharmacology of the Blood-Brain Barrier. Handbook of Experimental Pharmacology 103: 525-542.

Hou, D., Xie, C., Huang, K., and Zhu, C. 2003. The production and characteristics of solid lipid nanoparticles (SLNs). Biomaterials 24:1781–1785.

Indu, P. K., Rohit, B., Swati, B., and Vandita, K. 2008. Potential of solid lipid nanoparticles in brain targeting. Journal of Controlled Release 127: 97–109.

Jochen W., et al. 2008. Solid Lipid Nanoparticles as Delivery Systems for Bioactive Food Components. Food Biophysics 3:146–154.

Kiran, D., Jin, W., Yoo, C., and Lee H. 2008. Development of Chitosan–SLN Microparticles for chemotherapy: In vitro approach through efflux-transporter modulation. Journal of Controlled Release 131: 190–197.

Krishnamurthy, RG., et al., 2009. Asiatic acid, a pentacyclic triterpene from Centella asiatica, is neuroprotective in a mouse model of focal cerebral ischemia. Journal of Neuroscience Research 87: 2541-2550.

Kreuter, J. 2001. Nanoparticulate systems for brain delivery of drugs. Advance Drug Delivery 47: 65-81.

Kreuter, J. 2002. Transport of drugs across the blood-brain barrier by nanoparticles. Current Medicinal Chemistry-Central Nervous System Agents 2: 241-249.

Lander, R., et al. 2000. Gaulin homogenization: a mechanistic study, Biotechnology Progress. 16: 80–85.

Lee, M., et al. 2000. Asiatic acid derivatives protect cultured cortical neurons from glutamate-induced excitotoxicity. Research Communications in Molecular Pathology and Pharmacology 108: 75-86.

Lian, D.H., Xing, T., and Fu D.C. 2004. Solid lipid nanoparticles (SLNs) to improve oral bioavailability of poorly soluble drugs. Journal of Biomedicine and Biotecnology 56: 1527–1535.

Lippacher, A., Muller, R.H., and Mader, K. 2000. Investigation on the viscoelastic properties of lipid based colloidal drug carriers, International Journal of Pharmaceutical 196: 227–230.

Ilina, A. V., and Varlamov, V. P. 2004. Hydrolysis of Chitosan in Lactic Acid. Biochemistry and Microbiology 3: 300–303.

Illum, L. 2000. Review Transport of drugs from the nasal cavity to the central nervous system. European Journal of Pharmaceutical Sciences 11: 1–18.

Illum, L. 2003. Nasal drug delivery – possibilities, problems and solutions. Journal of Controlled Release 87:187–198.

Madara, J.L. 1983. Increases in guinea pig small intestinal transepithelial resistance induced by osmotic loads are accompanied by rapid alterations in absorptive-cell tight junction structure. Journal of Cell Biology 97: 125–136.

Mathison, S., Nagilla, R., and Kompella, U.B. 2007. Nasal route for direct delivery of solutes to the central nervous system: fact or fiction? Journal of controlled release 87: 187-198.

Mehnert, W., and Mader, K. 2001. Solid lipid nanoparticles: production, characterization and applications, Advanced Drug Delivery Reviews 47: 165–196.

Michele, T., Francesca, D., and Otto, C. 2003. Preparation of solid lipid nanoparticles by a solvent emulsification–diffusion technique. International Journal of Pharmaceutics 257:153–160.

Mohd, A.K., et al. 2010. Preparation, characterization, and evaluation of gatifloxacin loaded solid lipid nanoparticles as colloidal ocular drug delivery system. Journal of Drug Targeting 18: 191–204.

Moulik, S.P., and Paul, B.K. 1998. Structure, dynamics and transport properties of microemulsions, Advances in Colloid and Interface Science 78: 99–195.

Muller, R.H., and Runge, S.A. 1998. Solid lipid nanoparticles (SLN) for controlled drug delivery, in: S. Benita (Ed.), Submicron Emulsions in Drug Targeting and Delivery. Harwood Academic Publishers, Amsterdam. pp. 219–234.

Muller, R.H., Karsten, M., and Sven, G. 2000. Solid lipid nanoparticles (SLN) for controlled drug delivery - a review of the state of the art. European Journal of Pharmaceutics and Biopharmaceutics 50: 161-177.

Muchow, M., Maincent, P., and Muller R.H. 2008. Lipid Nanoparticles with a Solid Matrix (SLN®, NLC®, LDC®) for Oral Drug Delivery. Drug Development and Industrial Pharmacy 34: 1394–1405.

Nagi, A., et al. 2008. Tamoxifen Drug Loading Solid Lipid Nanoparticles Prepared by Hot High Pressure Homogenization Techniques. American Journal of Pharmacology and Toxicology 3: 219-224.

Nispa, S., Piyawan B., Wanwisa, S., Satit, P., and Uracha R. 2010. Nondestructive rheological measurement of aqueous dispersions of solid lipid nanoparticles: effects of lipid types and concentrations on dispersion consistency. Drug Development and Industrial Pharmacy 36: 1005–1015.

Priyanka, A., Shringi, S., and Sanjay, G. 2002. Permeability issues in nasal drug delivery. Drug Discoveries &Therapeutics. Vol. 7, No.18.

Ramanathan, M., Sivakumar, S., Anandvijayakumar, P. R., Saravanababu, C., and Pandian P.R. 2007. Neuroprotective evaluation of standardized extract of Centella asiatica in monosodium glutamate treated rats. Indian Journal of Experimental Biology 45: 425-431.

Rowe, R. C., Sheskey, P. J., and Owen, S. C. 2006. Handbook of Pharmaceutical Excipients, 4th ed. London: The Pharmaceutical Press.

Siekmann, B., and Westesen, K. 1994. Melt-homogenized solid lipid nanoparticles stabilized by the nonionic surfactant tyloxapol. Pharmaceutical and Pharmacological Letters 3: 194–197.

Siekmann, B., and Westesen, K. 1996. Investigations on solid lipid nanoparticles prepared by precipitation in o/w emulsions, European Journal of Pharmaceutics and Biopharmaceutics. 43: 104–109.

Sjostrom, B., and Bergenstahl, B. 1992. Preparation of submicron drug particles in lecithin-stabilized o/w emulsions. I. Model studies of the precipitation of cholesteryl acetate. International Journal of Pharmaceutical Sciences 88: 53–62.

Soumyanath, A., et al. 2005. Centella asiatica accelerates nerve regeneration upon oral administration and contains multiple active fractions increasing neurite elongation in- vitro. Journal of Pharmacy and Pharmacology 57: 1221-1229.

Sun, O., and Fernandez, K. 2004. Physicochemical and functional properties of crawfish chitosan as affected by different process protocol. Master's thesis. Department of Food Science, Louisiana State University.

Thorne, R.G., Emory, C.R., Ala, T.A., and Frey, W.H. 1995. Quantitative analysis of the olfactory pathway for drug delivery to brain. Brain Research 692: 278–282.

Thorne, R.G., and Frey, W.H., 2001. Delivery of neurotrophic factors to the central nervous system: pharmacokinetic considerations. Clinical Pharmacokinetics 40: 907–946.

Tiyaboonchai, W., Tungpradit, W., and Plianbangchang, P. 2007. Formulation and characterization of curcuminoids loaded solid lipid nanoparticles. International Journal of Pharmaceutics 337: 299-306.

Vivek, K., Reddy, H., and Murthy, R.S. 2007. Investigations of the Effect of the lipid matrix on drug entrapment, in vitro release, and physical stability of olanzapine-loaded solid lipid nanoparticles. American Association of Pharmaceutical Scientists 8: E1-E9.

Ward, P., et al. 2000. Enhancing paracellular permeability by modulating epithelial tight junctions. Pharmaceutical Science and Technology 3: 346-358.

Wattanathorn, J., et al. 2008. Positive modulation of cognition and mood in the healthy elderly volunteer following the administration of *Centella asiatica*. Journal of Ethnopharmacology 116: 325–332.

Wolfgang, M., and Karsten, M. 2001. Solid lipid nanoparticles production, characterization and application. Advanced Drug Delivery Reviews 47: 165-196.

Xiong, Y., Ding, H., Xu, M., Gao, J. 2009. Protective Effects of Asiatic Acid on Rotenone- or H_2O_2-Induced Injury in SH-SY5Y Cells. Neurochemical Reserch 34: 746-754.

Yang, S.C., and Zhu, J.B. 2002. Preparation and characterization of camptothecin solid lipid nanoparticles. Drug Devevelopment and Industrial Pharmacy 28: 265– 274.

Yashpal, C., Pragati, K., and Kapoor, A.K. 2009. Review article intranasal drug delivery :a novel approach. Indian Journal of Otolaryngology Head Neck Surgery 61: 90-94.

YiFan, L., DaWei, C., LiXiang, R., XiuLi, Z., and Jing Q. 2006. Solid lipid nanoparticles for enhancing vinpocetine's oral bioavailability. Journal of Controlled Release 114: 53–59.

APPENDICES

APPENDIX A

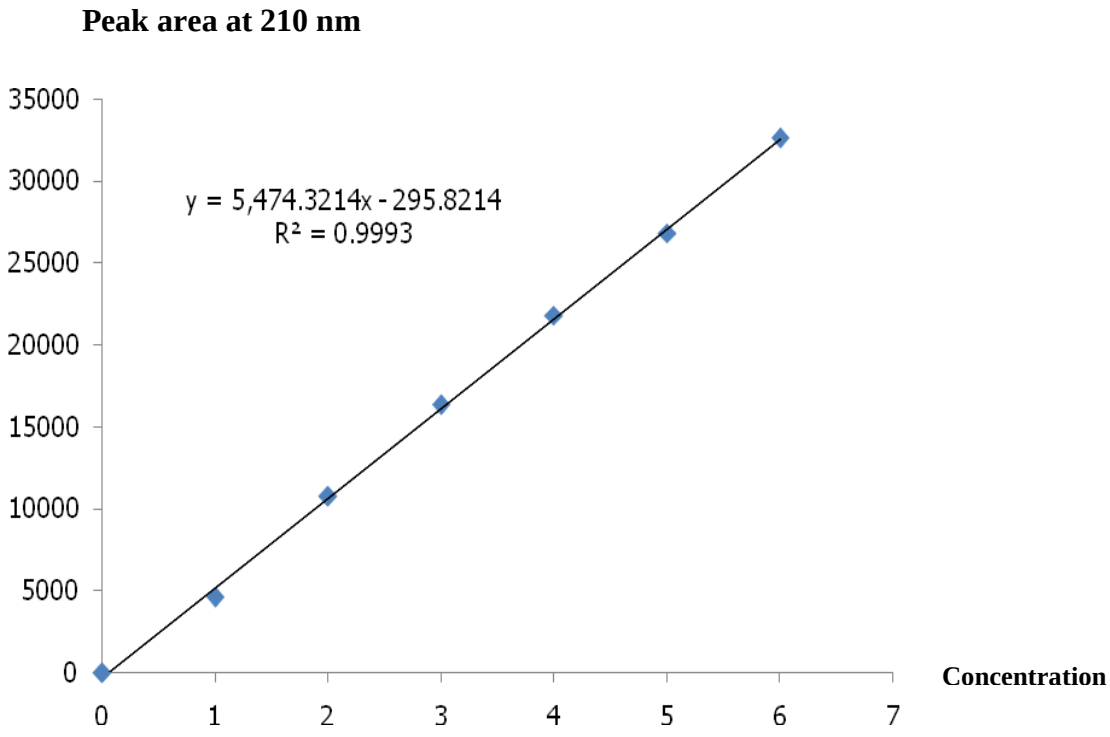

Figure 55 Calibration curve of asiatic acid by HPLC method.

Table 39 Data for calibration curve of asiatic acid by HPLC method.

Concentration (μg/ml)	Peak area 210 nm			Mean	SD	%CV
	1st day	2nd day	3rd day			
1	4602	5255	4537	4798	397	0.08
2	10758	12216	10498	11157	926	0.08
3	16318	18275	16365	16986	1117	0.07
4	21793	25014	21423	22743	1975	0.09
5	26807	31067	26752	28209	2476	0.09
6	32612	38122	32884	34539	3106	0.09
R^2	0.9993	0.9992	0.9994	0.9993	-	-
Intercept	295.8214	591.7143	435.1786	440.9643	-	-
Slope	5474.3214	6385.2857	5500.25	5786.6071	-	-

Table 40 Data for specificity validation after the reagents were added for HPLC method.

Conditions	**Retention Time**	**peak Area**	**Resolution**
Standard	9.711	320724	10.870
0.1 NaOH	9.667	306951	8.350
0.1 HCl	9.687	296147	8.362
35% H_2O_2	9.684	313961	8.051
Water	9.712	179226	8.678
Heat	9.697	279652	8.706
Light	9.624	278488	8.667

Table 41 The percentages of analytical recovery of low, medium and high concentration of asiatic acid with blank SLN formulations (TM SP80 5:5 and TM SP80 7:3) by HPLC method.

Formulations	**concentration (µg/ml)**	**Estimated concentration (µg/ml)**	**% Accuracy**	**Mean ± SD**
TM : SP80 5:5	1.5	1.5193 1.5081 1.4869 1.4908 1.5040	101.29 100.54 99.13 99.39 100.27	100.12 ± 0.88
	3.5	3.5629 3.5527 3.4698 3.4754 3.5067	101.80 101.51 99.14 99.30 100.19	100.39 ± 1.23
	4.5	4.5806 4.5092 4.5134 4.4626 4.5440	101.79 100.20 100.30 99.17 100.98	100.49 ± 0.97
TM : SP80 7:3	1.5	1.4886 1.4910 1.4755 1.4879 1.4984	99.24 99.40 98.37 99.19 99.90	99.22 ± 0.55
	3.5	3.4509 3.5069 3.4562 3.4864 3.4750	98.60 100.20 98.75 99.61 99.29	99.29 ± 0.65
	4.5	4.5776 4.5794 4.5440 4.5431 4.4866	101.72 101.76 100.98 100.96 99.70	101.03 ± 0.84

Table 42 The percentages of analytical recovery of low, medium and high concentration of asiatic acid with blank SLN formulations (TM SP85 5:5 and TM SP85 7:3) by HPLC method

Formulations	**concentration (µg/ml)**	**Estimated concentration (µg/ml)**	**% Accuracy**	**Mean ± SD**
TM : SP85 5:5	1.5	1.4928 1.5022 1.5037 1.5079 1.5091	99.52 100.14 100.25 100.53 100.61	100.21 ± 0.43
	3.5	3.5634 3.4662 3.4811 3.5067 3.5222	101.81 99.03 99.46 100.19 100.63	100.23 ± 1.08
	4.5	4.5813 4.5682 4.4468 4.5353 4.5102	101.81 101.52 98.82 100.78 100.23	100.63 ± 1.19
TM : SP85 7:3	1.5	1.4796 1.4833 1.4984 1.5059 1.4867	98.64 98.89 99.90 100.39 99.12	99.39 ± 0.73
	3.5	3.5624 3.4881 3.5239 3.5351 3.5222	101.78 99.66 100.68 101.00 100.63	100.75 ± 0.76
	4.5	4.5250 4.5022 4.5611 4.5587 4.4329	100.56 100.05 101.36 101.31 98.51	100.36 ± 1.17

Table 43 The percentages of analytical recovery of low, medium and high concentration of asiatic acid with blank SLN formulations (TM SL 1:9 and TM SL 9:1) by HPLC method

Formulations	**concentration (µg/ml)**	**Estimated concentration (µg/ml)**	**% Accuracy**	**Mean ± SD**
TM : SL 1:9	1.5	1.5181 1.5204 1.5004 1.4989 1.5022	101.21 101.36 100.03 99.93 100.15	100.53 ± 0.69
	3.5	3.5063 3.5264 3.5616 3.5023 3.4913	100.18 100.75 101.76 100.07 99.75	100.50 ± 0.79
	4.5	4.4686 4.5044 4.4651 4.5074 4.4862	99.30 100.10 99.23 100.16 99.69	99.70 ± 0.43
TM : SL 9.1	1.5	1.5231 1.5283 1.5191 1.4932 1.4897	101.54 101.89 101.27 99.55 99.31	100.71 ± 1.19
	3.5	3.5249 3.5416 3.5095 3.4858 3.5150	100.71 101.19 100.27 99.59 100.43	100.44 ± 0.59
	4.5	4.5680 4.5241 4.4945 4.5241 4.4782	101.51 100.53 99.88 100.53 99.51	100.39 ± 0.76

Table 44 The percentages of analytical recovery of low, medium and high concentration of asiatic acid with blank SLN formulations (TS SP80 5:5 and TS SP80 7:3) by HPLC method

Formulations	**concentration (µg/ml)**	**Estimated concentration (µg/ml)**	**% Accuracy**	**Mean ± SD**
TS : SP80 5:5	1.5	1.5189 1.4949 1.5208 1.4837 1.4845	101.26 99.66 101.38 98.91 98.97	100.04 ± 1.21
	3.5	3.4888 3.5581 3.4928 3.5275 3.5018	99.68 101.66 99.79 100.79 100.05	100.39 ± 0.83
	4.5	4.4812 4.4912 4.5618 4.4314 4.5069	99.58 99.80 101.37 98.48 100.15	99.88 ± 1.05
TS : SP80 7:3	1.5	1.5231 1.5101 1.5021 1.4880 1.4964	101.54 100.67 100.14 99.20 99.76	100.26 ± 0.89
	3.5	3.5390 3.4649 3.5265 3.4946 3.4519	101.12 99.00 100.76 99.85 98.63	99.87 ± 1.08
	4.5	4.5838 4.5077 4.4366 4.4783 4.4571	101.86 100.17 98.59 99.52 99.05	99.84 ± 1.27

Table 45 The percentages of analytical recovery of low, medium and high concentration of asiatic acid with blank SLN formulations (TS SP85 5:5 and TM SP85 7:3) by HPLC method

Formulations	**concentration (µg/ml)**	**Estimated concentration (µg/ml)**	**% Accuracy**	**Mean ± SD**
TS : SP85 5:5	1.5	1.4986 1.4839 1.4879 1.5231 1.4912	99.90 98.92 99.19 101.54 99.41	99.79 ± 1.04
	3.5	3.4876 3.5075 3.5230 3.5242 3.5284	99.65 100.21 100.66 100.69 100.81	100.40 ± 0.48
	4.5	4.4725 4.4725 4.5798 4.5241 4.5090	99.39 99.39 101.77 100.53 100.20	100.26 ± 0.99
TS : SP85 7:3	1.5	1.4857 1.4872 1.5171 1.5029 1.5046	99.05 99.15 101.14 100.19 100.30	99.97 ± 0.87
	3.5	3.5636 3.4708 3.5135 3.5063 3.4819	101.82 99.16 100.39 100.18 99.48	100.21 ± 1.03
	4.5	4.5282 4.5449 4.4893 4.4930 4.5301	100.63 101.00 99.76 99.84 100.67	100.38 ± 0.55

Table 46 The percentages of analytical recovery of low, medium and high concentration of asiatic acid with blank SLN formulations (TS SL 1:9 and TS SL 5:5) by HPLC method

Formulations	**concentration (µg/ml)**	**Estimated concentration (µg/ml)**	**% Accuracy**	**Mean ± SD**
TS : SL 1:9	1.5	1.5046 1.5231 1.4870 1.5286 1.5221	100.30 101.54 99.14 101.91 101.47	100.87 ± 1.14
	3.5	3.4337 3.5375 3.5390 3.4634 3.4853	98.11 101.07 101.12 98.95 99.58	99.77 ± 1.32
	4.5	4.5282 4.5613 4.5052 4.4366 4.4172	100.63 101.36 100.12 98.59 98.16	99.11 ± 1.18
TS : SL 5:5	1.5	1.4857 1.4785 1.5156 1.5064 1.5193	99.05 98.57 101.04 100.43 101.28	100.07 ± 1.21
	3.5	3.5038 3.4988 3.5227 3.5451 3.4748	100.11 99.97 100.65 101.29 99.28	100.26 ± 0.75
	4.5	4.5282 4.4725 4.4354 4.5241 4.5301	100.63 99.39 98.56 100.53 100.67	99.96 ± 0.94

Table 47 The percentages of analytical recovery of low, medium and high concentration of asiatic acid with blank SLN formulations (COM SP80 5:5 and COM SP80 7:3) by HPLC method

Formulations	**concentration (µg/ml)**	**Estimated concentration (µg/ml)**	**% Accuracy**	**Mean ± SD**
COM : SP80 5:5	1.5	1.4849 1.4971 1.5156 1.5171 1.5209	98.99 99.80 101.04 101.14 101.40	100.47 ± 1.03
	3.5	3.5210 3.5259 3.5636 3.4703 3.4557	100.60 100.74 101.82 99.15 98.74	100.21 ± 1.26
	4.5	4.5838 4.4666 4.4134 4.5060 4.5576	101.86 99.26 98.07 100.13 101.28	100.12 ± 1.53
COM : SP80 7:3	1.5	1.4804 1.4912 1.5031 1.5208 1.4986	98.69 99.41 100.20 101.38 99.90	99.92 ± 1.00
	3.5	3.5247 3.5579 3.4482 3.4612 3.4668	100.71 101.65 98.52 98.89 99.05	99.76 ± 1.35
	4.5	4.5433 4.5615 4.4967 4.4870 4.4317	100.96 101.37 99.93 99.71 98.48	100.09 ± 1.13

Table 48 The percentages of analytical recovery of low, medium and high concentration of asiatic acid with blank SLN formulations (COM SP85 5:5 and COM SP85 7:3) by HPLC method

Formulations	**concentration (µg/ml)**	**Estimated concentration (µg/ml)**	**% Accuracy**	**Mean ± SD**
COM : SP85 5:5	1.5	1.4710 1.4854 1.4774 1.4842 1.4915	98.07 99.02 98.49 98.95 99.44	98.79 ± 0.53
	3.5	3.4893 3.5544 3.5284 3.4910 3.5227	99.69 101.55 100.81 99.74 100.65	100.49 ± 0.78
	4.5	4.5262 4.4499 4.4923 4.5241 4.5765	100.58 98.89 99.83 100.53 101.70	100.31 ± 1.04
COM : SP85 7:3	1.5	1.4874 1.5156 1.5209 1.5024 1.5064	99.16 101.04 101.40 100.16 100.43	100.44 ± 0.87
	3.5	3.4673 3.5078 3.5038 3.5060 3.5636	99.06 100.22 100.11 100.17 101.82	100.28 ± 0.99
	4.5	4.5282 4.5653 4.4905 4.4169 4.5241	100.63 101.45 99.79 98.15 100.53	100.11 ± 1.24

Table 49 The percentages of analytical recovery of low, medium and high concentration of asiatic acid with blank SLN formulations (COM SL 9:1) by HPLC method

Formulations	**concentration (µg/ml)**	**Estimated concentration (µg/ml)**	**% Accuracy**	**Mean ± SD**
COM : SL 9:1	1.5	1.4824 1.5009 1.5174 1.5211 1.5009	98.82 100.06 101.16 101.41 100.06	100.30 ± 1.03
	3.5	3.5244 3.5038 3.5636 3.5245 3.5654	100.70 100.11 101.82 100.70 101.87	101.04 ± 0.77
	4.5	4.4524 4.5301 4.5229 4.4718 4.4129	98.94 100.67 100.51 99.37 98.06	99.51 ± 1.09

Table 50 The percentages of analytical recovery of low, medium and high concentration of asiatic acid with blank SLN formulations (SOF SP80 5:5 and SOF SP80 9:1) by HPLC method

Formulations	**concentration (µg/ml)**	**Estimated concentration (µg/ml)**	**% Accuracy**	**Mean ± SD**
SOF : SP80 5:5	1.5	1.4785 1.4986 1.5171 1.5029 1.4899	98.57 99.90 101.14 100.19 99.33	99.83 ± 0.96
	3.5	3.5210 3.5451 3.5038 3.4668 3.4482	100.60 101.29 100.11 99.05 98.52	99.91 ± 1.13
	4.5	4.4723 4.5259 4.5648 4.4870 4.5653	99.38 100.58 101.44 99.71 101.45	100.51 ± 0.96
SOF : SP80 9:1	1.5	1.4867 1.4931 1.5061 1.5116 1.5196	99.11 99.54 100.40 100.77 101.31	100.23 ± 0.90
	3.5	3.5038 3.5063 3.5601 3.4477 3.4723	100.11 100.18 101.72 98.51 99.21	99.94 ± 1.21
	4.5	4.5055 4.5079 4.5204 4.4870 4.4902	100.12 100.17 100.45 99.71 99.78	100.05 ± 0.30

Table 51 The percentages of analytical recovery of low, medium and high concentration of asiatic acid with blank SLN formulations (SOF SP85 5:5 and SOF SP85 9:1) by HPLC method

Formulations	**concentration (µg/ml)**	**Estimated concentration (µg/ml)**	**% Accuracy**	**Mean ± SD**
SOF : SP85 5:5	1.5	1.4857 1.5082 1.5213 1.5134 1.4819	99.05 100.55 101.42 100.89 98.79	100.14 ± 1.16
	3.5	3.5280 3.5596 3.5038 3.5042 3.5245	100.80 101.70 100.11 100.12 100.70	100.69 ± 0.65
	4.5	4.4314 4.5282 4.4925 4.5082 4.4875	98.48 100.63 99.83 100.18 99.72	99.77 ± 0.80
SOF : SP85 9:1	1.5	1.5019 1.4849 1.5054 1.5066 1.5151	100.13 98.99 100.36 100.44 101.01	100.18 ± 0.74
	3.5	3.5205 3.5602 3.5038 3.4708 3.5290	100.59 101.72 100.11 99.16 100.83	100.48 ± 0.94
	4.5	4.5409 4.4898 4.4239 4.4673 4.5130	100.91 99.77 98.31 99.27 100.29	99.71 ± 0.99

Table 52 Data of within-run precision by HPLC method.

Concentration (μg/ml)	Estimated concentration (μg/ml)					Mean	SD	%CV
	1	2	3	4	5			
1.5	1.4854	1.4800	1.4971	1.5108	1.4966	1.4940	0.0119	0.80
3.5	3.4896	3.5081	3.5034	3.5653	3.5137	3.5160	0.0290	0.82
4.5	4.5209	4.4987	4.4712	4.4208	4.4429	4.4709	0.0405	0.91

Table 53 Data of between-run precision by HPLC method.

Concentration(μg/ml)	Estimated concentration (μg/ml)					Mean	SD	%CV
	1	2	3	4	5			
1.5	1.4854	1.4769	1.5186	1.4979	1.5076	1.4973	0.0167	1.12
3.5	3.4896	3.5097	3.5379	3.5532	3.5068	3.5194	0.0256	0.73
4.5	4.5209	4.4755	4.4306	4.4688	4.466	4.4724	0.0323	0.72

APPENDIX B

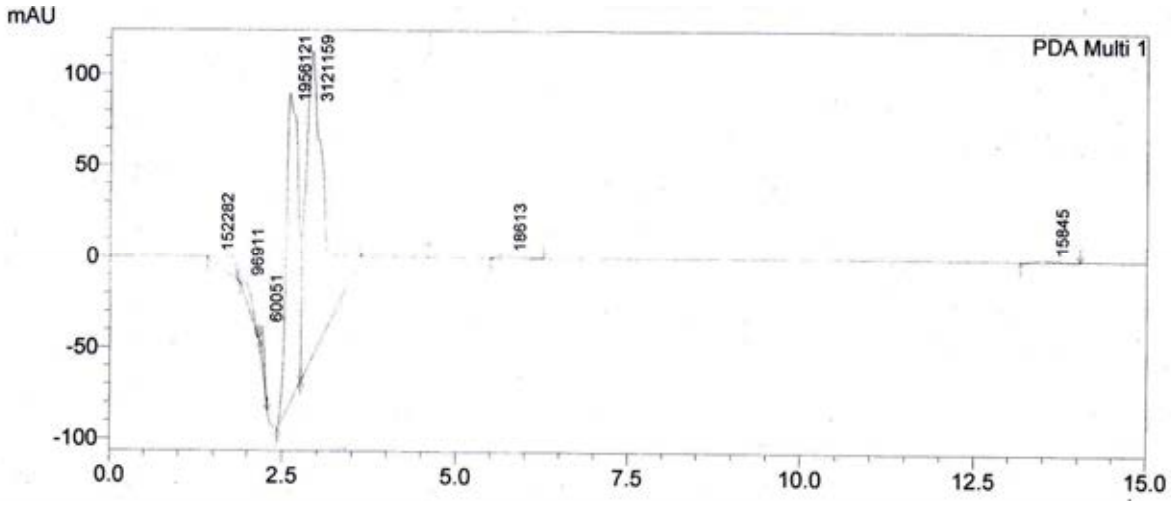

Figure 56 HPLC chromatogram of standard solution of AA (1 µg/ml).

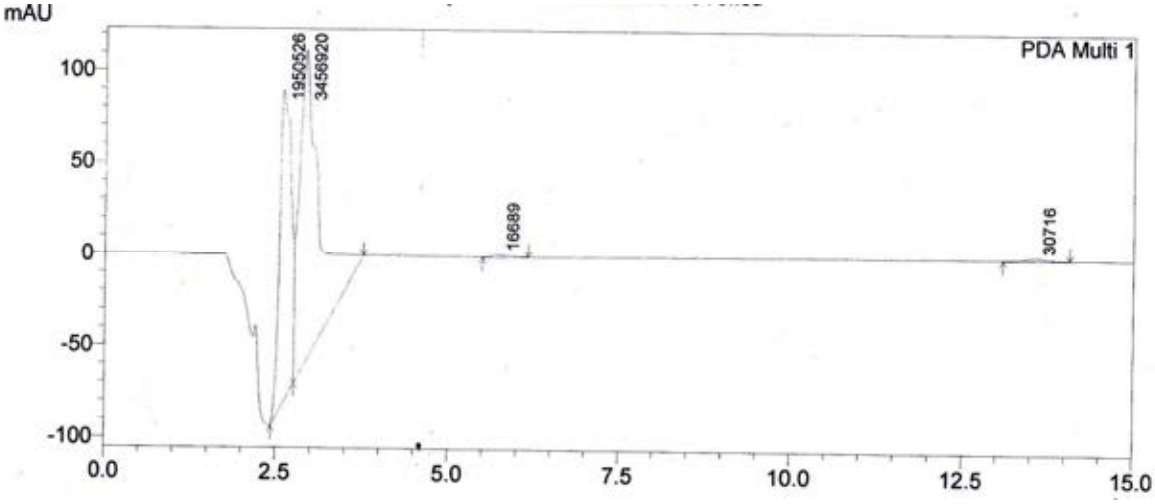

Figure 57 HPLC chromatogram of standard solution of AA (2 µg/ml).

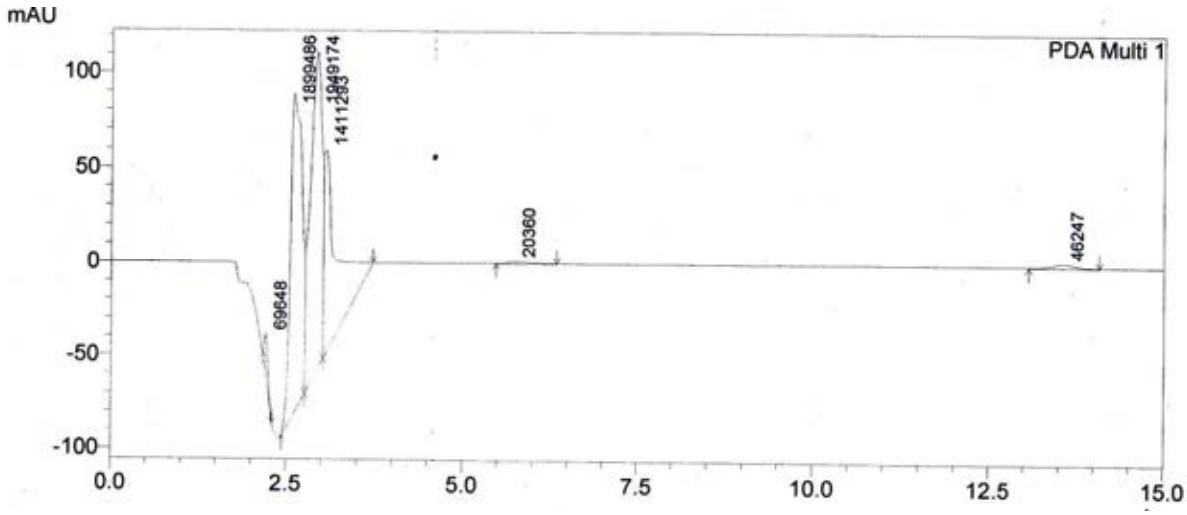

Figure 58 HPLC chromatogram of standard solution of AA (3 µg/ml).

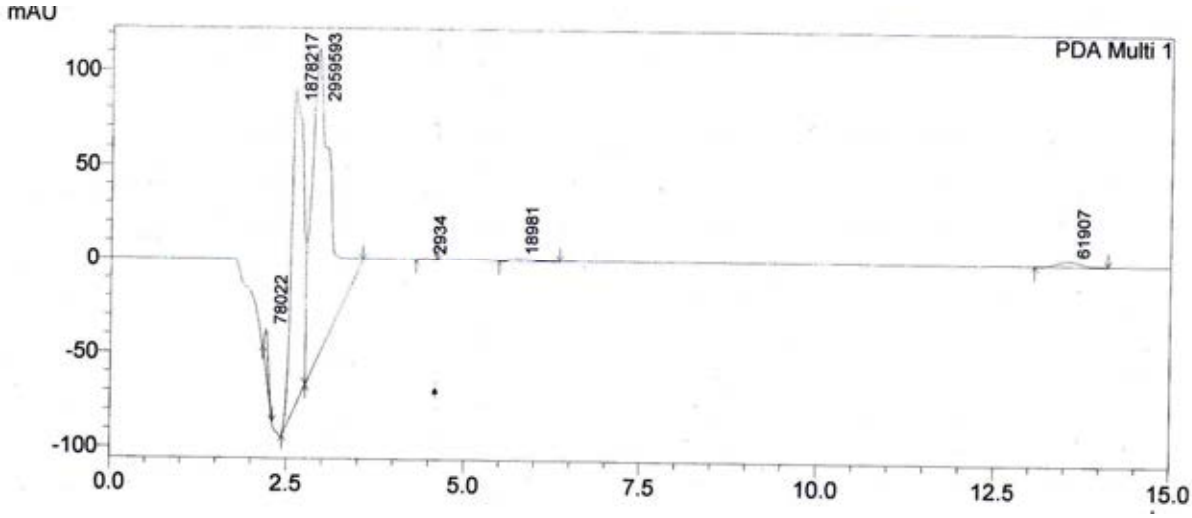

Figure 59 HPLC chromatogram of standard solution of AA (4 µg/ml).

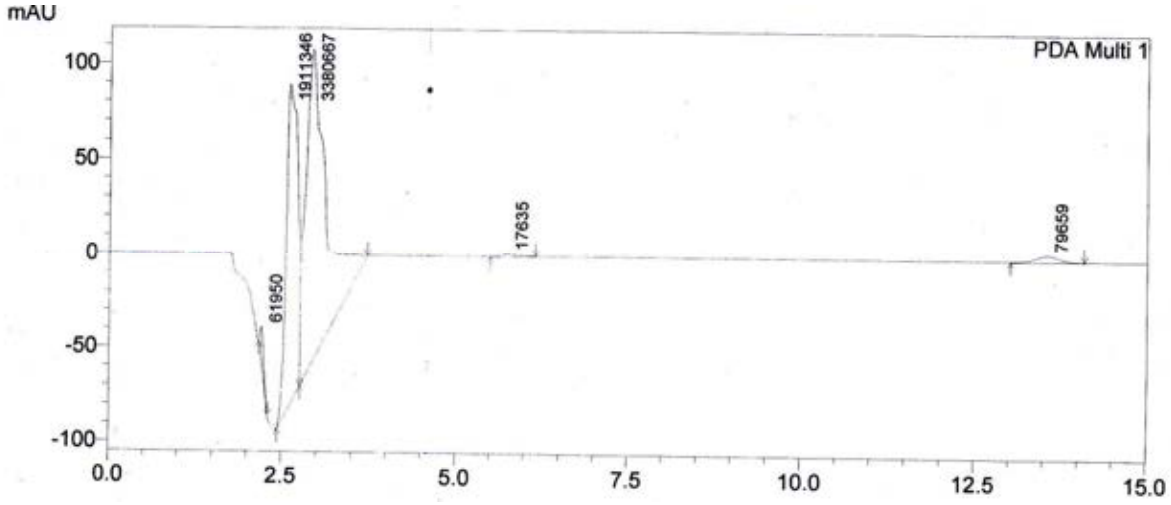

Figure 60 HPLC chromatogram of standard solution of AA (5 µg/ml).

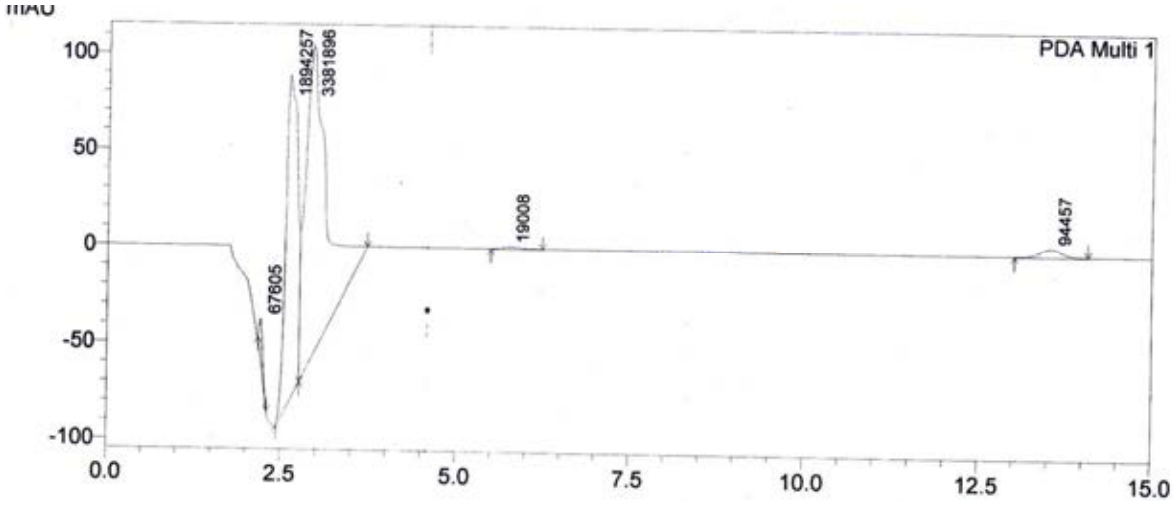

Figure 61 HPLC chromatogram of standard solution of AA (6 µg/ml).

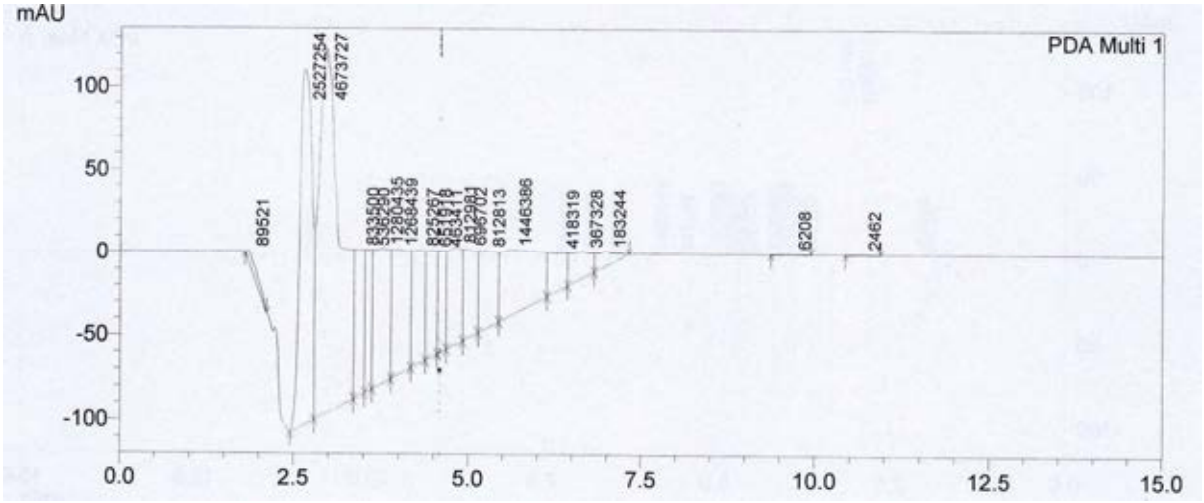

Figure 62 HPLC chromatogram of blank GB TW80:SP80 5:5.

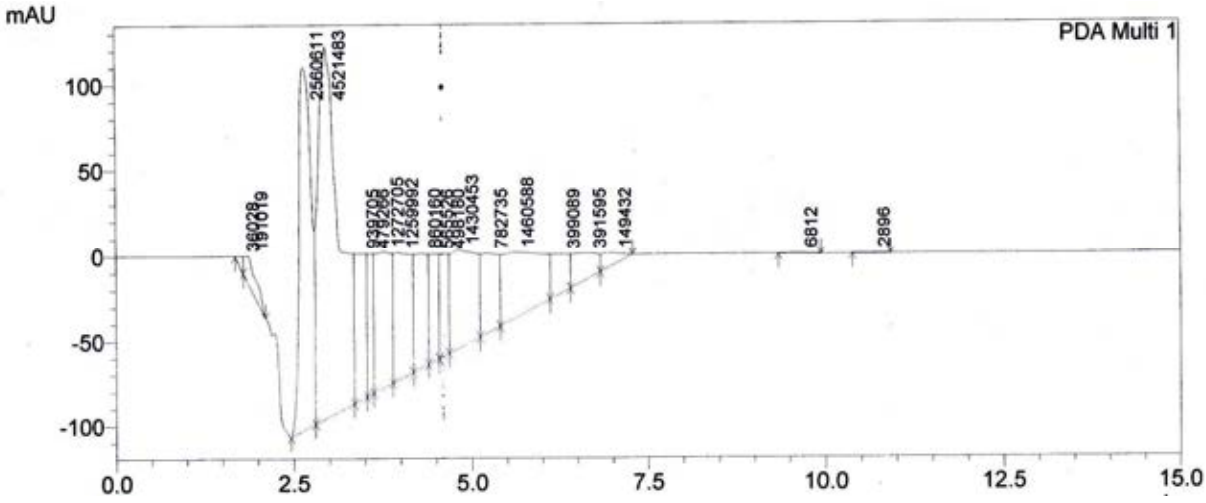

Figure 63 HPLC chromatogram of blank GB TW80:SP80 7:3.

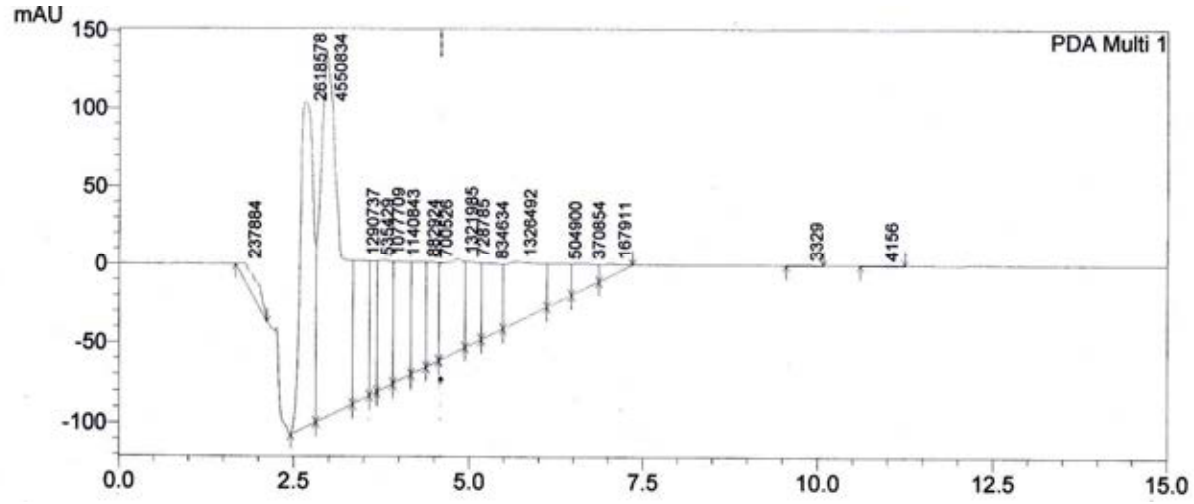

Figure 64 HPLC chromatogram of blank GB TW80:SP85 5:5**.**

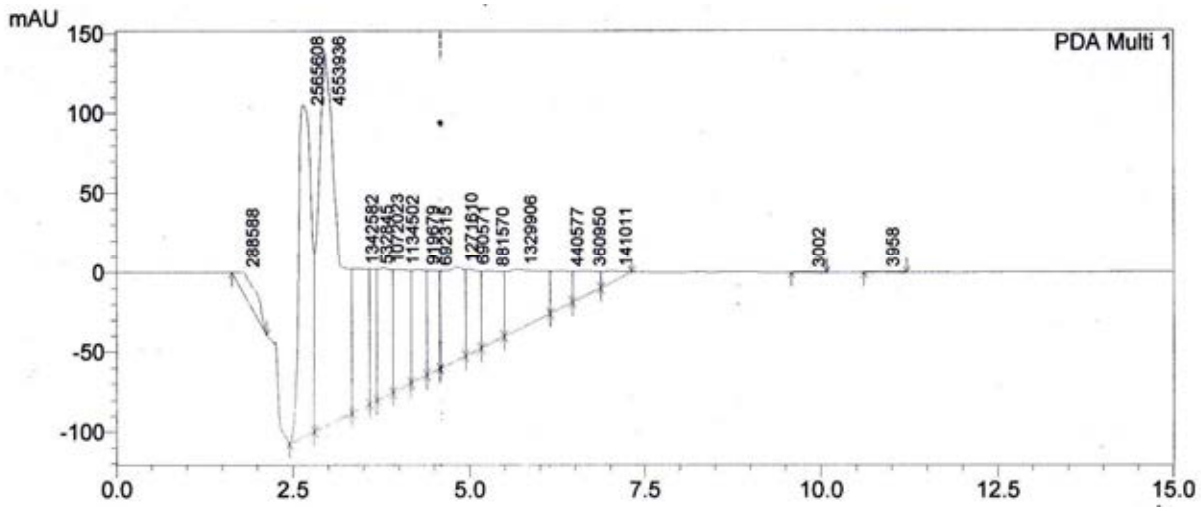

Figure 65 HPLC chromatogram of blank GB TW80:SP85 7:3**.**

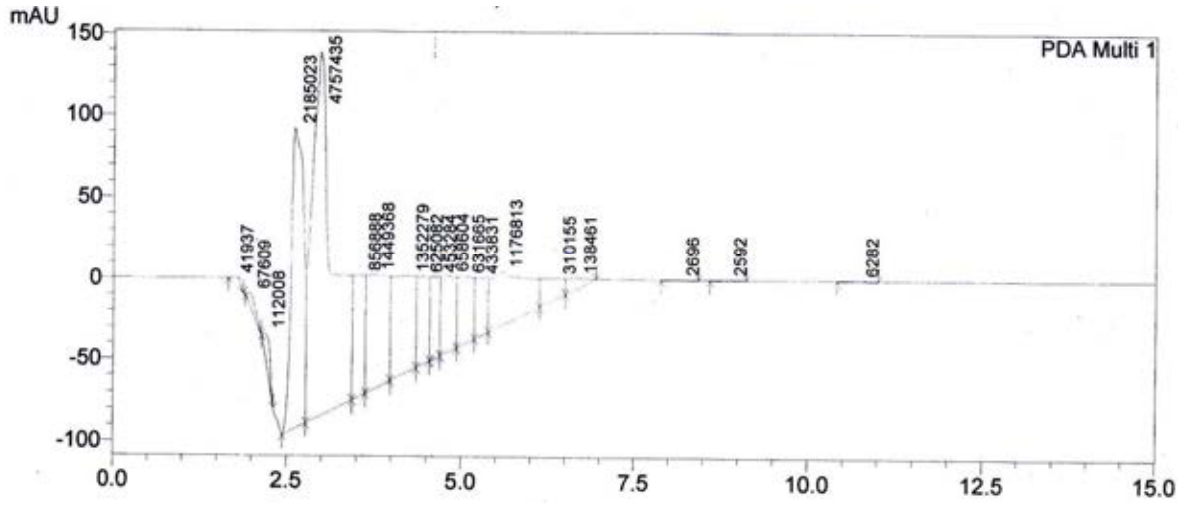

Figure 66 HPLC chromatogram of blank GB SL 9:1.

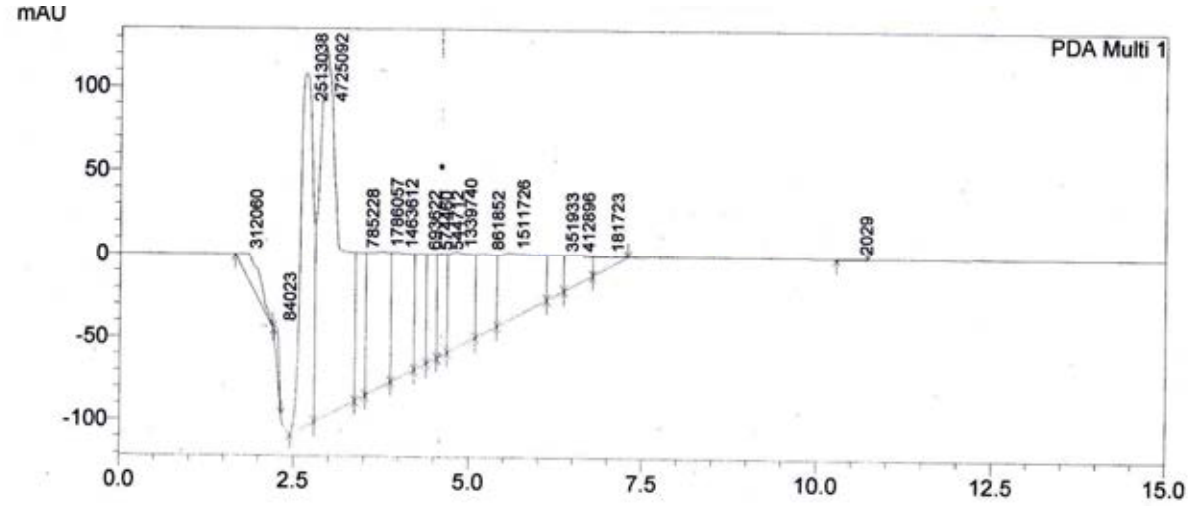

Figure 67 HPLC chromatogram of blank SOF TW80:SP80 5:5**.**

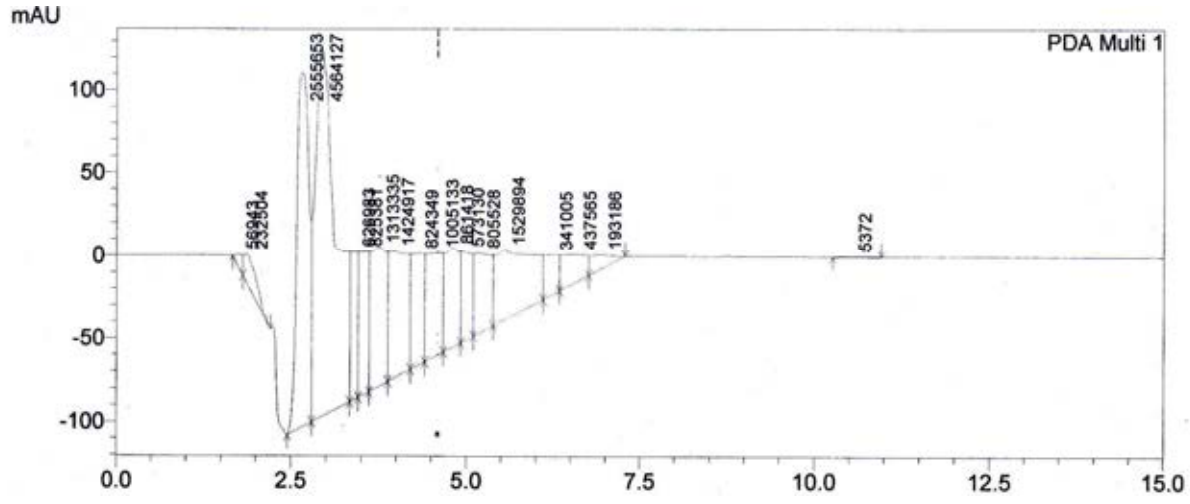

Figure 68 HPLC chromatogram of blank SOF TW80:SP80 9:1.

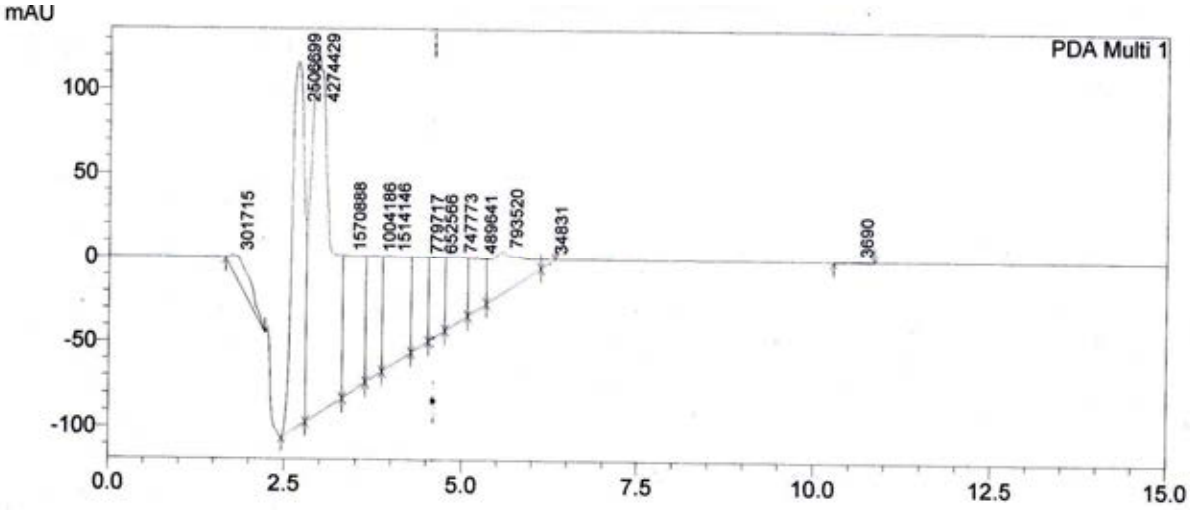

Figure 69 HPLC chromatogram of blank SOF TW80:SP85 5:5.

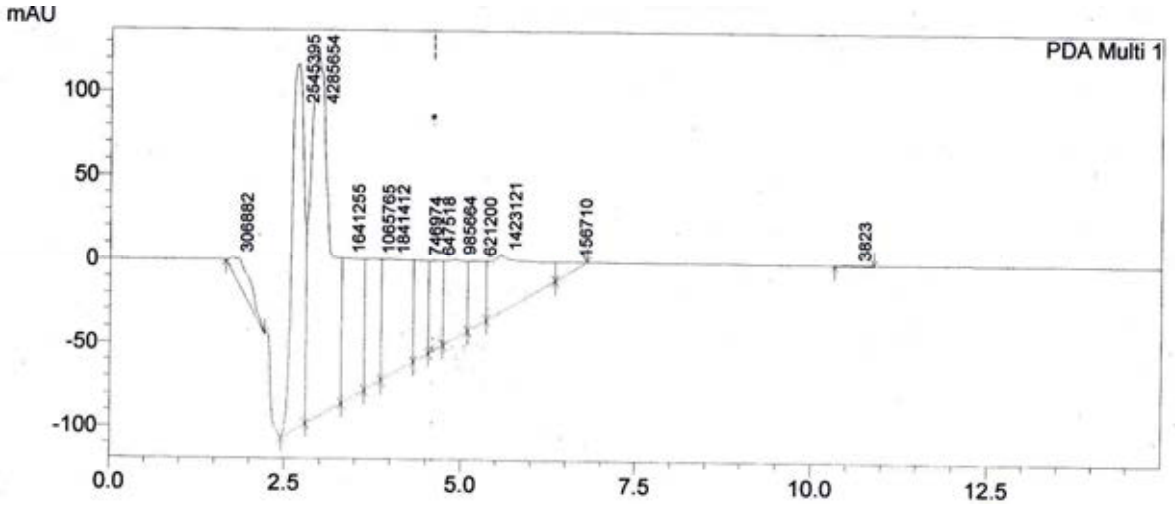

Figure 70 HPLC chromatogram of blank SOF TW80:SP85 9:1**.**

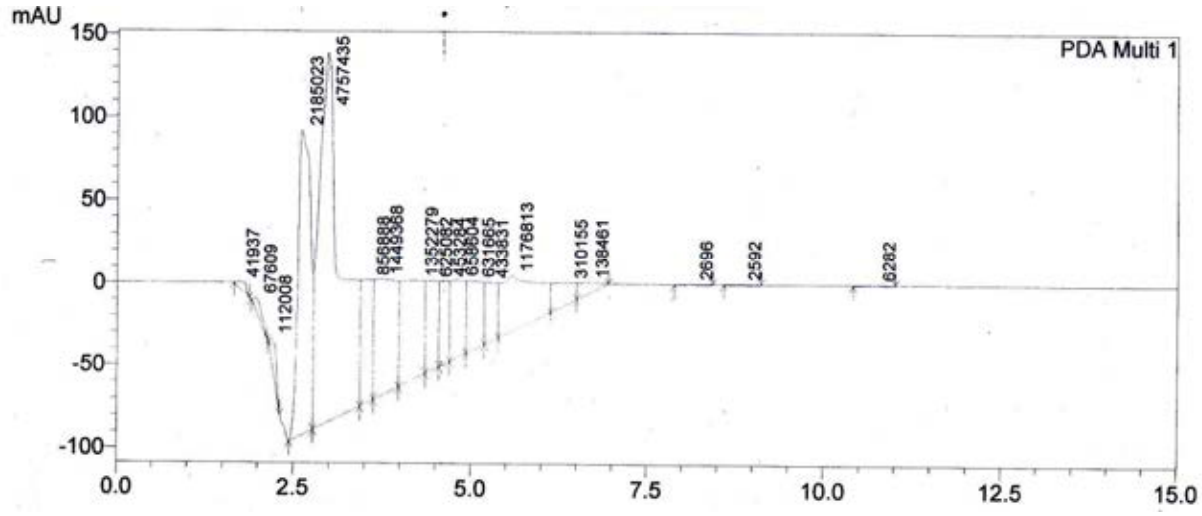

Figure 71 HPLC chromatogram of blank TM TW80:SP80 5:5.

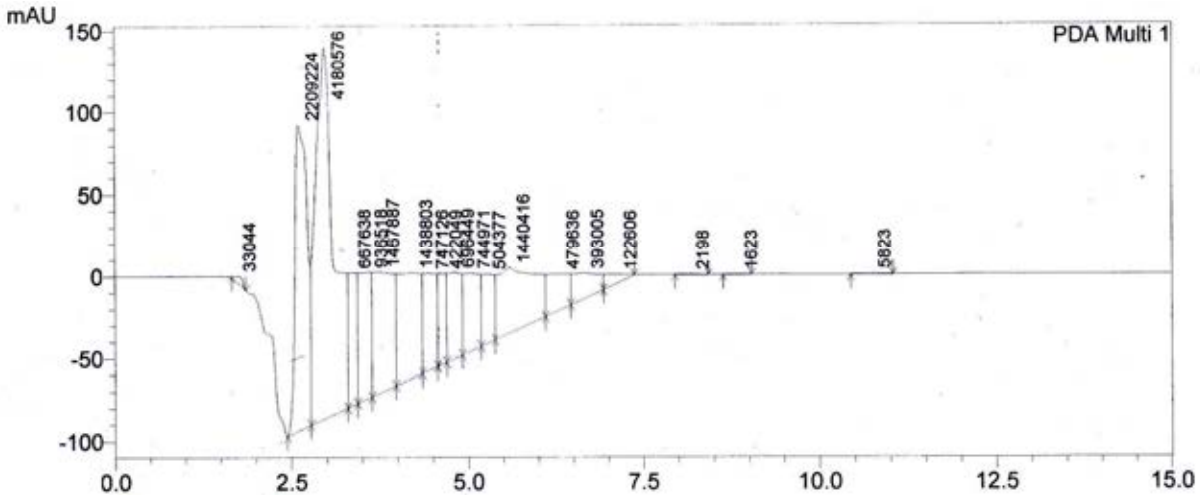

Figure 72 HPLC chromatogram of blank TM TW80:SP80 7:3.

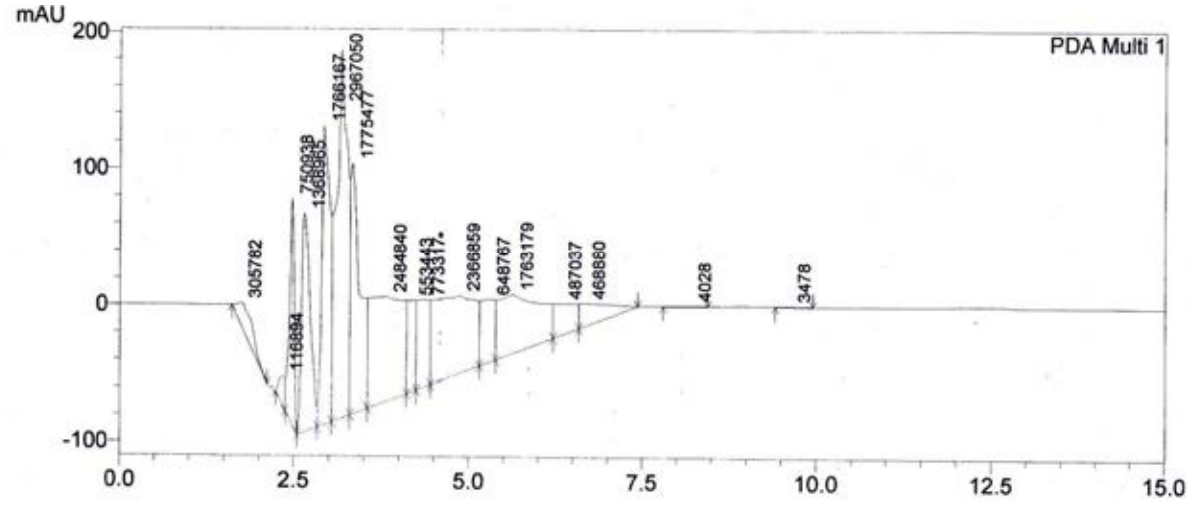

Figure 73 HPLC chromatogram of blank TM TW80:SP85 5:5.

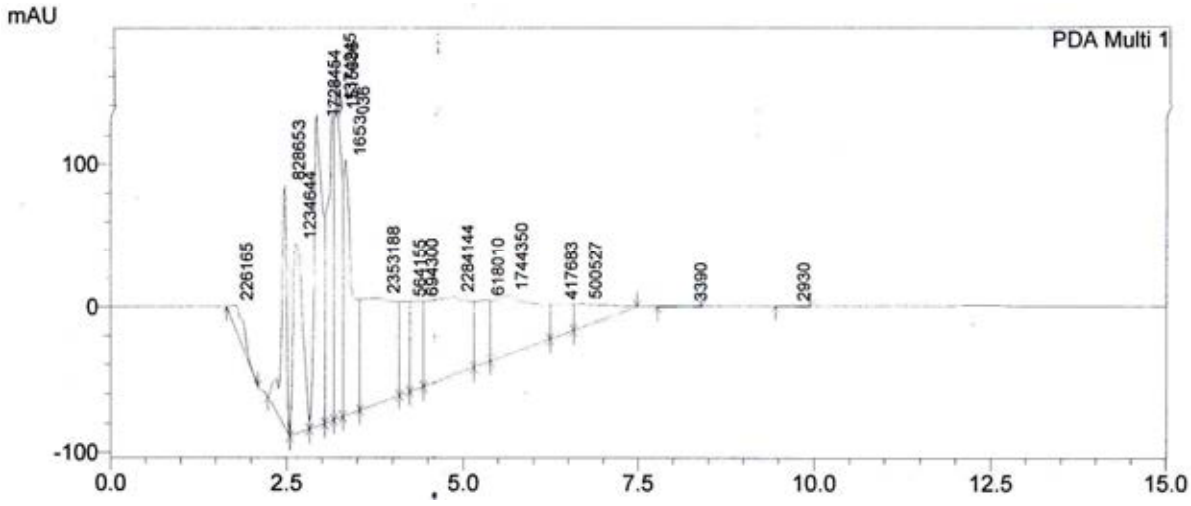

Figure 74 HPLC chromatogram of blank TM TW80:SP85 7:3.

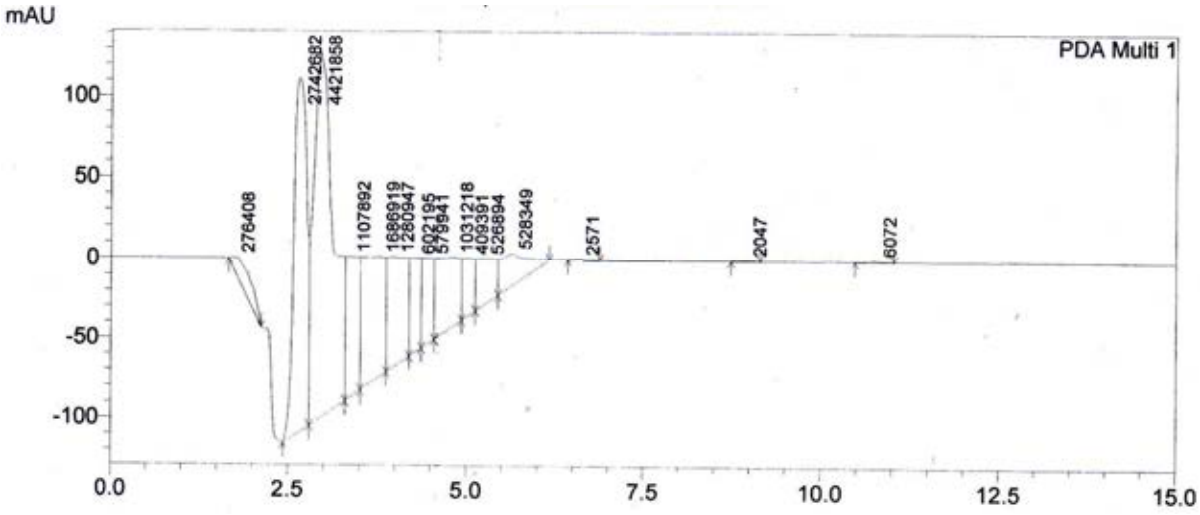

Figure 75 HPLC chromatogram of blank TM TW80:SL 5:5.

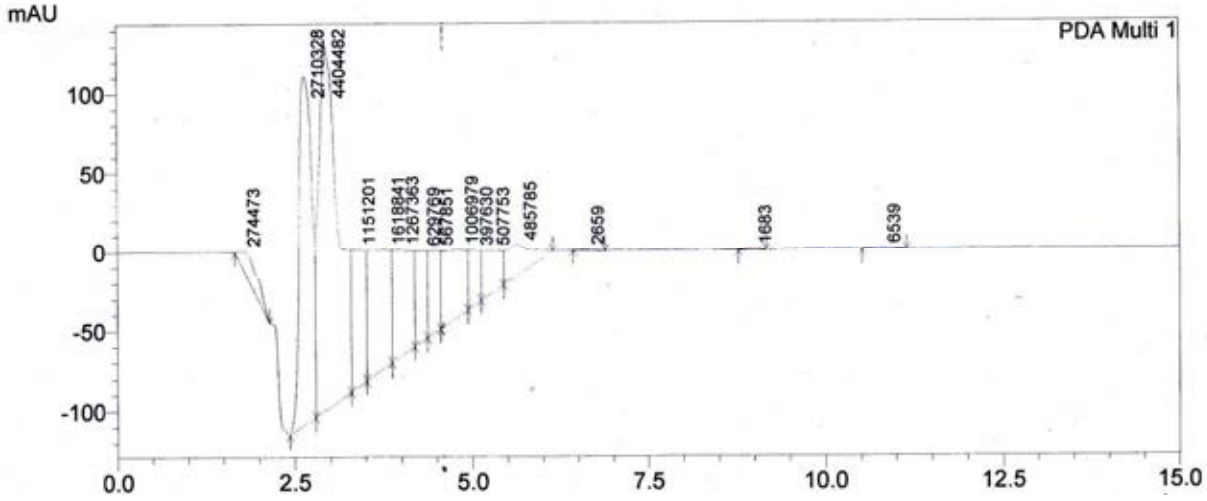

Figure 76 HPLC chromatogram of blank TM TW80:SL 9:1.

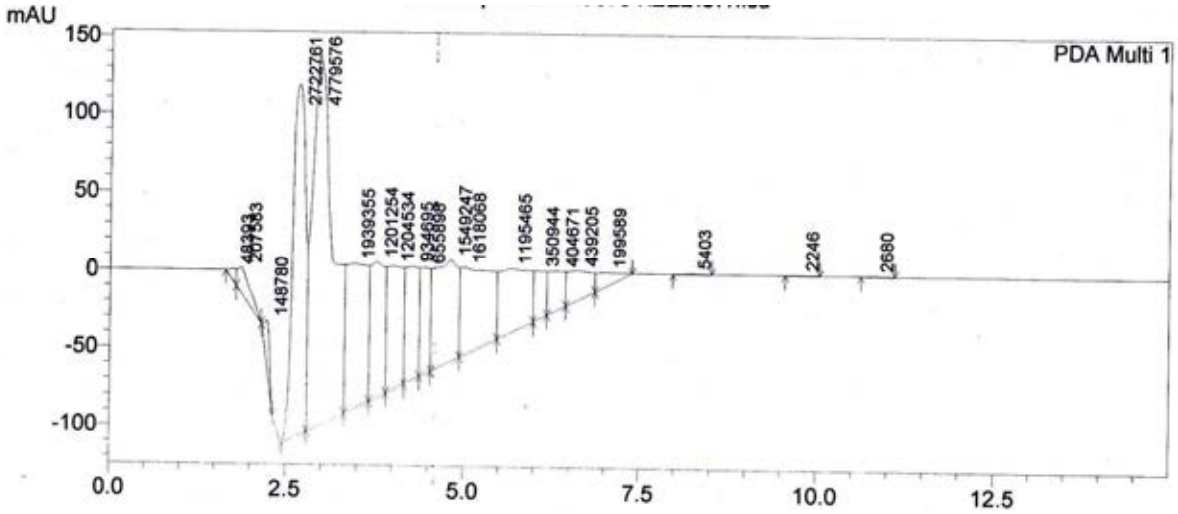

Figure 77 HPLC chromatogram of blank TS TW80:SP80 5:5.

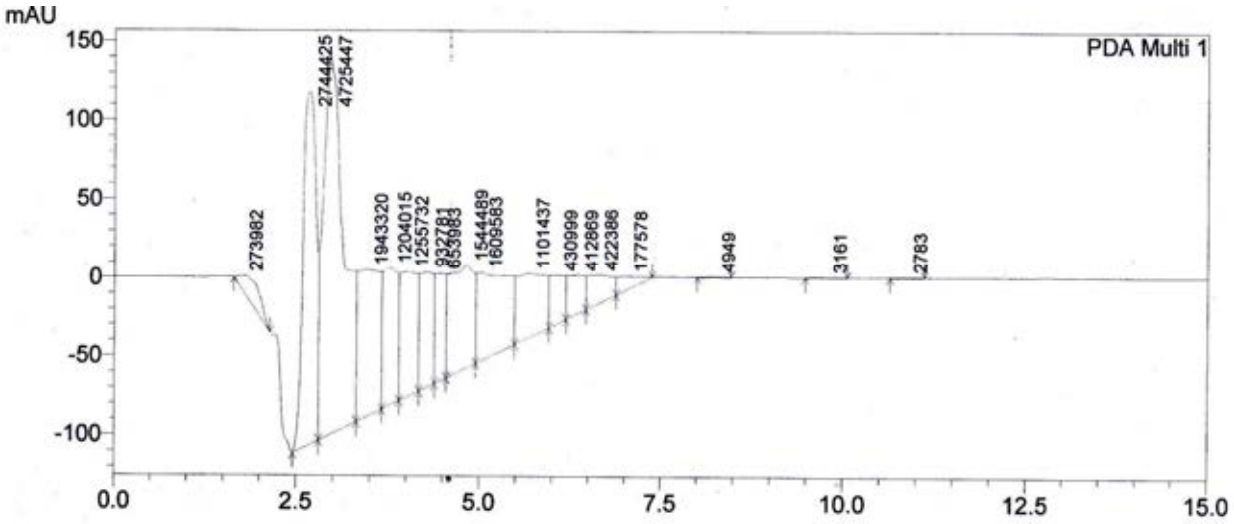

Figure 78 HPLC chromatogram of blank TS TW80:SP80 7:3**.**

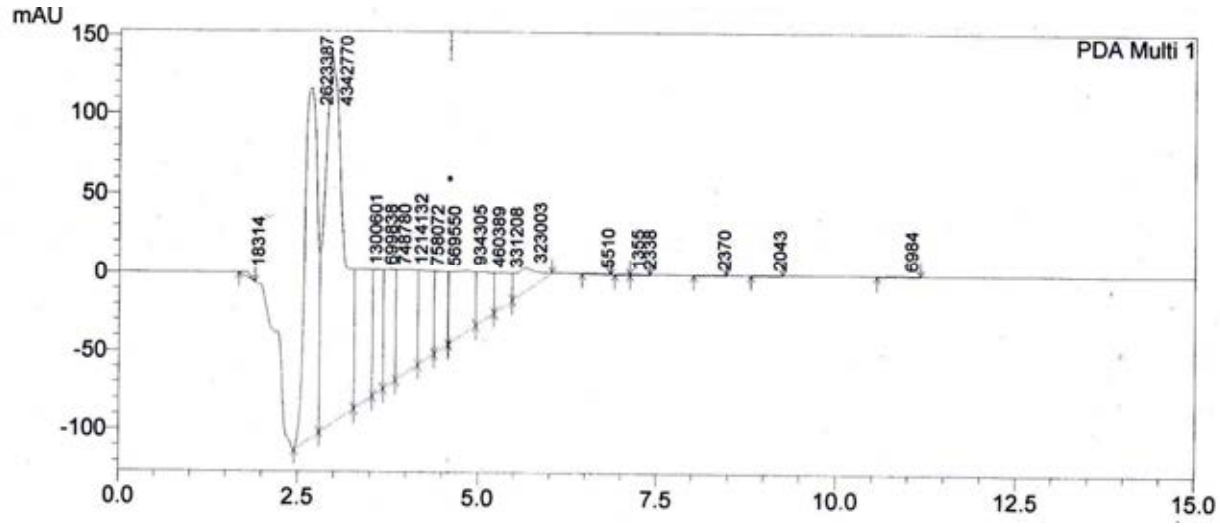

Figure 79 HPLC chromatogram of blank TS TW80:SP85 5:5.

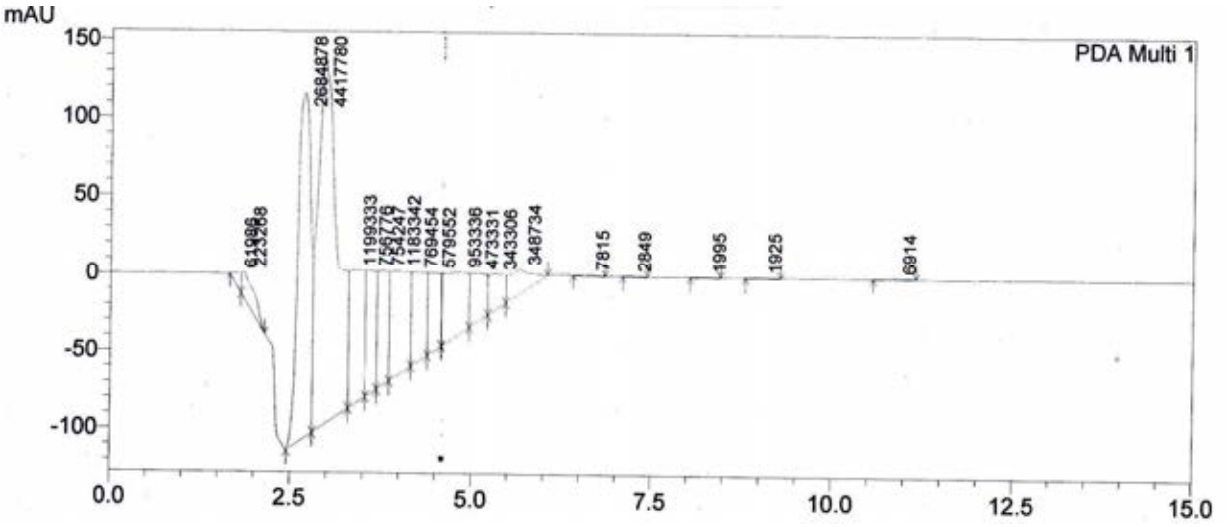

Figure 80 HPLC chromatogram of blank TS TW80:SP85 7:3**.**

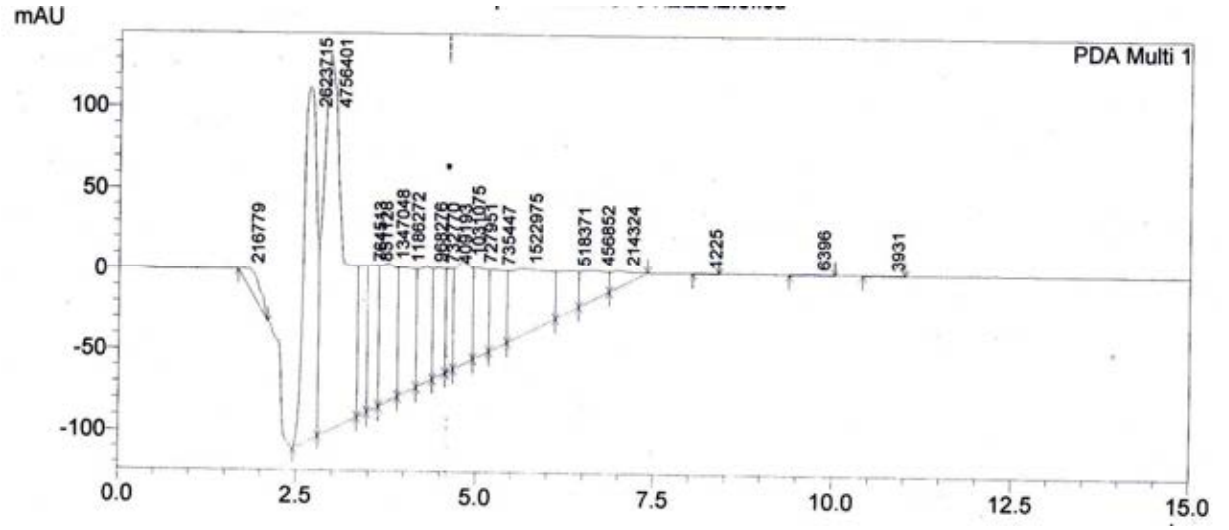

Figure 81 HPLC chromatogram of blank TS TW80:SL 1:9**.**

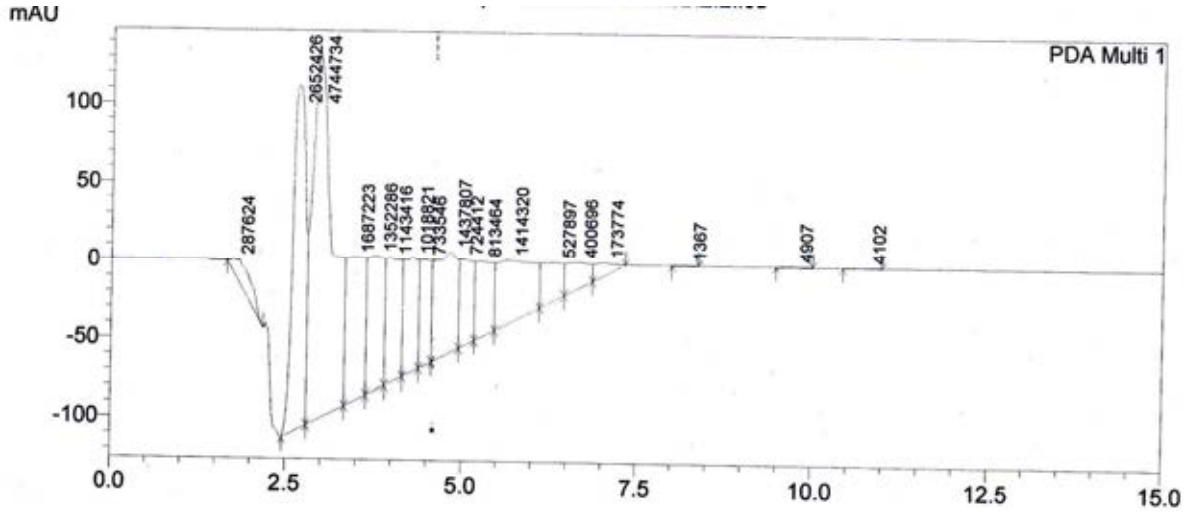

Figure 82 HPLC chromatogram of blank TS TW80:SL 5:5**.**

APPENDIX C

Table 54 Various of SLN formulations for CC_{50} values by ANOVA test.

Formulations	Code
TM SP85 5:5	1
0.1% TM SP85 5:5	2
0.3% TM SP85 5:5	3
0.5% TM SP85 5:5	4
SOF SP85 5:5	5
0.1% SOF SP85 5:5	6
0.3% SOF SP85 5:5	7
0.5% SOF SP85 5:5	8

Table 55 Test of homogeneity of variance of CC_{50} values in TM AA-SLN, CT TM AA-SLN,SOF AA-SLN and CT SOF AA-SLN (data specified in Table 32, page 131).

Test of Homogeneity of Variances

CC50

Levene Statistic	df1	df2	Sig.
2.164	7	16	.095

Result: Homogeneity of variance (p= 0.095 > α = .05), implying that variances are equal and homogeneity of variance assumption Of ANOVA has been showed, then ANOVA could test.

Table 56 One way analysis of variance of CC_{50} values in TM AA-SLN, CT TM AA-SLN, SOF AA-SLN and CT SOF AA-SLN (data specified in Table 32, page 131).

ANOVA

CC50

Source of variation	Sum of Squares	df	Mean Square	F	Sig.
Between Groups	4.700	7	.671	25.621	p< 0.05
Within Groups	.419	16	.026		
Total	5.119	23			

Result: significant at the 0.5 level ($p < 0.05$), there is sufficient evidence to claim that at least one pair of the means might be the difference from each other. So, Turkey's test was used to compare between groups.

Table 57 Multiple comparison of CC_{50} values in TM AA-SLN, CT TM AA-SLN, SOF AA-SLN and CT SOF AA-SLN (data specified in Table 32, page 131).

Multiple Comparisons

Dependent Variable: CC50
Tukey HSD

(I) FORMULATION	(J) FORMULATION	Mean Difference (I-J)	Std. Error	Sig.	95% Confidence Interval	
					Lower bound	Upper bound
1	2	-.06333	0.13217	1.000	-.5209	.3943
	3	.04667	0.13217	1.000	-.4109	.5043
	4	1.02000(*)	0.13217	p<0.05	.5624	1.4776
	5	-.00333	0.13217	1.000	-.4609	.4543
	6	.13000	0.13217	.970	-.3276	.5876
	7	.02000	0.13217	1.000	-.4376	.4776
	8	1.05333(*)	0.13217	p<0.05	.5957	1.5109
2	1	.06333	0.13217	1.000	-.3943	.5209
	3	.11000	0.13217	.988	-.3476	.5676
	4	1.08333(*)	0.13217	p<0.05	.6257	1.5409
	5	.06000	0.13217	1.000	-.3976	.5176
	6	.19333	0.13217	.815	-.2643	.6509
	7	.08333	0.13217	.998	-.3743	.5409
	8	1.11667(*)	0.13217	p<0.05	.6591	1.5743
3	1	-.04667	0.13217	1.000	-.5043	.4109
	2	-.11000	0.13217	.988	-.5676	.3476
	4	.97333(*)	0.13217	p<0.05	.5157	1.4309
	5	-.05000	0.13217	1.000	-.5076	.4076
	6	.08333	0.13217	.998	-.3743	.5409
	7	-.02667	0.13217	1.000	-.4843	.4309
	8	1.00667(*)	0.13217	p<0.05	.5491	1.4643
4	1	-1.02000(*)	0.13217	p<0.05	-1.4776	-.5624
	2	-1.08333(*)	0.13217	p<0.05	-1.5409	-.6257
	3	-.97333(*)	0.13217	p<0.05	-1.4309	-.5157
	5	-1.02333(*)	0.13217	p<0.05	-1.4809	-.5657
	6	-.89000(*)	0.13217	p<0.05	-1.3476	-.4324
	7	-1.00000(*)	0.13217	p<0.05	-1.4576	-.5424
	8	.03333	0.13217	1.000	-.4243	.4909
5	1	.00333	0.13217	1.000	-.4543	.4609
	2	-.06000	0.13217	1.000	-.5176	.3976
	3	.05000	0.13217	1.000	-.4076	.5076
	4	1.02333(*)	0.13217	p<0.05	.5657	1.4809
	6	.13333	0.13217	.966	-.3243	.5909
	7	.02333	0.13217	1.000	-.4343	.4809
	8	1.05667(*)	0.13217	p<0.05	.5991	1.5143

Table 57 Multiple comparison of CC_{50} values in TM AA-SLN, CT TM AA-SLN, SOF AA-SLN and CT SOF AA-SLN (continous) (data specified in Table 32, page 131).

Dependent Variable: CC50
Tukey HSD

(I) FORMULATION	(J) FORMULATION	Mean Difference (I-J)	Std. Error	Sig.	95% Confidence Interval	
					Lower bound	Upper bound
5	1	0.00333	0.13217	1.000	-0.4543	0.4609
	2	-0.06	0.13217	1.000	-0.5176	0.3976
	3	0.05	0.13217	1.000	-0.4076	0.5076
	4	1.02333(*)	0.13217	p<0.05	0.5657	1.4809
	6	0.13333	0.13217	0.966	-0.3243	0.5909
	7	0.02333	0.13217	1.000	-0.4343	0.4809
	8	1.05667(*)	0.13217	p<0.05	0.5991	1.5143
6	1	-0.13	0.13217	0.97	-0.5876	0.3276
	2	-0.19333	0.13217	0.815	-0.6509	0.2643
	3	-0.08333	0.13217	0.998	-0.5409	0.3743
	4	.89000(*)	0.13217	p<0.05	0.4324	1.3476
	5	-0.13333	0.13217	0.966	-0.5909	0.3243
	7	-0.11	0.13217	0.988	-0.5676	0.3476
	8	.92333(*)	0.13217	p<0.05	0.4657	1.3809
7	1	-0.02	0.13217	1.000	-0.4776	0.4376
	2	-0.08333	0.13217	0.998	-0.5409	0.3743
	3	0.02667	0.13217	1.000	-0.4309	0.4843
	4	1.00000(*)	0.13217	p<0.05	0.5424	1.4576
	5	-0.02333	0.13217	1.000	-0.4809	0.4343
	6	0.11	0.13217	0.988	-0.3476	0.5676
	8	1.03333(*)	0.13217	p<0.05	0.5757	1.4909
8	1	-1.05333(*)	0.13217	p<0.05	-1.5109	-0.5957
	2	-1.11667(*)	0.13217	p<0.05	-1.5743	-0.6591
	3	-1.00667(*)	0.13217	p<0.05	-1.4643	-0.5491
	4	-0.03333	0.13217	1.000	-0.4909	0.4243
	5	-1.05667(*)	0.13217	p<0.05	-1.5143	-0.5991
	6	-.92333(*)	0.13217	p<0.05	-1.3809	-0.4657
	7	-1.03333(*)	0.13217	p<0.05	-1.4909	-0.5757

* The mean difference is significant at the .05 level.

Table 58 Various of SLN formulations for celluar uptake activity by ANOVA test .

Formulations	Code
AA solution	1
TM SP85 5:5	2
0.3% TM SP85 5:5	3
SOF SP85 5:5	4
0.3% SOF SP85 5:5	5

Table 59 Test of homogeneity of variance of celluar uptake activity in AA solution, TM AA-SLN, 0.3% CT TM AA-SLN, SOF AA-SLN and 0.3% CT SOF AA-SLN (data specified in Table 36, page 139).

Test of Homogeneity of Variances

UPTAKE

Levene Statistic	df1	df2	Sig.
4.139	4	10	.031

Result: Heterogeneity of variance ($p = 0.031 < \alpha = .05$), implying that variances are not equal. ANOVA is still performed and Dunnett's test is used for multiple comparison instead of Turkey's test

Table 60 One way analysis of variance of celluar uptake activity in AA solution, TM AA-SLN, 0.3% CT TM AA-SLN, SOF AA-SLN and 0.3% CT SOF AA-SLN (data specified in Table 36, page 139).

ANOVA

UPTAKE

Source of variation	Sum of Squares	df	Mean Square	F	Sig.
Between Groups	141.732	4	35.433	190.200	$p < 0.05$
Within Groups	1.863	10	.186		
Total	143.595	14			

Table 61 Multiple comparison of cellular uptake in AA solution, TM AA-SLN, 0.3% CT TM AA-SLN, SOF AA-SLN and 0.3% CT SOF AA-SLN (data specified in Table 36, page 139).

Multiple Comparisons

Dependent Variable: UPTAKE
Dunnett T3

(I) FORMULATION	(J) FORMULATION	Mean Difference (I-J)	Std. Error	Sig.	95% Confidence Interval	
					Lower bound	Upper bound
1	2	7.84333(*)	0.49509	0.013	3.7694	11.9172
	3	8.48333(*)	0.49734	0.011	4.4723	12.4943
	4	4.88333(*)	0.53614	0.019	1.5397	8.2269
	5	7.02667(*)	0.50301	0.014	3.1590	10.8944
2	1	-7.84333(*)	0.49509	0.013	-11.9172	-3.7694
	3	.64000(*)	0.10408	0.024	.1266	1.1534
	4	-2.96000(*)	0.22568	0.012	-4.5722	-1.3478
	5	-.81667(*)	0.12850	0.032	-1.5208	-.1125
3	1	-8.48333(*)	0.49734	0.011	-12.4943	-4.4723
	2	-.64000(*)	0.10408	0.024	-1.1534	-.1266
	4	-3.60000(*)	0.23058	0.006	-5.1344	-2.0656
	5	-1.45667(*)	0.13691	0.004	-2.1509	-.7625
4	1	-4.88333(*)	0.53614	0.019	-8.2269	-1.5397
	2	2.96000(*)	0.22568	0.012	1.3478	4.5722
	3	3.60000(*)	0.23058	0.006	2.0656	5.1344
	5	2.14333(*)	0.24258	0.016	.7262	3.5604
5	1	-7.02667(*)	0.50301	0.014	-10.8944	-3.1590
	2	.81667(*)	0.12850	0.032	.1125	1.5208
	3	1.45667(*)	0.13691	0.004	.7625	2.1509
	4	-2.14333(*)	0.24258	0.016	-3.5604	-.7262

* The mean difference is significant at the .05 level.

Table 62 Various of SLN formulations for permeation activity by ANOVA test.

Formulations	Code
AA solution	1
TM SP85 5:5	2
0.3% TM SP85 5:5	3
SOF SP85 5:5	4
0.3% SOF SP85 5:5	5

Table 63 Test of homogeneity of variance of permeation activity in AA solution, TM AA-SLN, 0.3% CT TM AA-SLN, SOF AA-SLN and 0.3% CT SOF AA-SLN (data specified in Table 36, page 139).

Test of Homogeneity of Variances

PERMEATION

Levene Statistic	df1	df2	Sig.
.583	4	10	.682

Result: Homogeneity of variance ($p = 0.682 > \alpha = .05$), implying that variances are equal and homogeneity of variance assumption Of ANOVA has been showed, then ANOVA could test.

Table 64 One way analysis of variance of permeation activity in AA solution, TM AA-SLN, 0.3% CT TM AA-SLN, SOF AA-SLN and 0.3% CT SOF AA-SLN (data specified in Table 36, page 139).

ANOVA

PERMEATION

Source of variation	Sum of Squares	df	Mean Square	F	Sig.
Between Groups	39.949	4	9.987	1348.421	$p < 0.05$
Within Groups	.074	10	.007		
Total	40.023	14			

Result: significant at the 0.5 level ($p < 0.05$), there is sufficient evidence to claim that at least one pair of the means might be the difference from each other. So, Turkey's test was used to compare between groups.

Table 65 Multiple comparison of permeation activity in AA solution, TM AA-SLN, 0.3% CT TM AA-SLN, SOF AA-SLN and 0.3% CT SOF AA-SLN (data specified in Table 36, page 139).

Multiple Comparisons

Dependent Variable: PERMEATION
Tukey HSD

(I) FORMULATION	(J) FORMULATION	Mean Difference (I-J)	Std. Error	Sig.	95% Confidence Interval	
					Lower bound	Upper bound
1	2	3.19333(*)	0.07027	p < 0.05	2.9621	3.4246
	3	3.60667(*)	0.07027	p < 0.05	3.3754	3.8379
	4	4.23667(*)	0.07027	p < 0.05	4.0054	4.4679
	5	4.56667(*)	0.07027	p < 0.05	4.3354	4.7979
2	1	-3.19333(*)	0.07027	p < 0.05	-3.4246	-2.9621
	3	.41333(*)	0.07027	.001	.1821	.6446
	4	1.04333(*)	0.07027	p < 0.05	.8121	1.2746
	5	1.37333(*)	0.07027	p < 0.05	1.1421	1.6046
3	1	-3.60667(*)	0.07027	p < 0.05	-3.8379	-3.3754
	2	-.41333(*)	0.07027	.001	-.6446	-.1821
	4	.63000(*)	0.07027	p < 0.05	.3987	.8613
	5	.96000(*)	0.07027	p < 0.05	.7287	1.1913
4	1	-4.23667(*)	0.07027	p < 0.05	-4.4679	-4.0054
	2	-1.04333(*)	0.07027	p < 0.05	-1.2746	-.8121
	3	-.63000(*)	0.07027	p < 0.05	-.8613	-.3987
	5	.33000(*)	0.07027	.006	.0987	.5613
5	1	-4.56667(*)	0.07027	p < 0.05	-4.7979	-4.3354
	2	-1.37333(*)	0.07027	p < 0.05	-1.6046	-1.1421
	3	-.96000(*)	0.07027	p < 0.05	-1.1913	-.7287
	4	-.33000(*)	0.07027	.006	-.5613	-.0987

* The mean difference is significant at the .05 level.

Table 66 Various of SLN formulations for entrapment efficiency by ANOVA test.

Formulations	Code
TW80 : SP80 5:5	1
TW80 : SP80 7:3	2
TW80 : SP85 5:5	3
TW80 : SP85 7:3	4
TW80 : SL 1:9	5
TW80 : SL 3:7	6
TW80 : SL 5:5	7
TW80 : SL 7:3	8
TW80 : SL 9:1	9
TW80 : SP80 5:5	10
TW80 : SP80 7:3	11
TW80 : SP85 5:5	12
TW80 : SP85 7:3	13
TW80 : SL 1:9	14
TW80 : SL 3:7	15
TW80 : SL 5:5	16
TW80 : SP80 5:5	17
TW80 : SP80 7:3	18
TW80 : SP85 5:5	19
TW80 : SP85 7:3	20
TW80 : SL 9:1	21
TW80 : SP80 5:5	22
TW80 : SP80 7:3	23
TW80 : SP80 9:1	24
TW80 : SP85 5:5	25
TW80 : SP85 7:3	26
TW80 : SP85 9:1	27

Table 67 Test of homogeneity of variance of entrapment efficiency in SLN formulations (data specified in Table 23, page 117).

Test of Homogeneity of Variances

Levene Statistic	df1	df2	Sig.
2.761	26	54	.001

Result: Heterogeneity of variance ($p = 0.001 < \alpha = .05$), implying that variances are not equal. ANOVA is still performed and Dunnett's test is used for multiple comparison instead of Turkey's test.

Table 68 One way analysis of variance of entrapment efficiency in SLN formulations (data specified in Table 23, page 117).

ANOVA

ENTRAPMENT

Source of variation	Sum of Squares	df	Mean Square	F	Sig.
Between Groups	89.719	26	3.451	12.917	$p < 0.05$
Within Groups	14.426	54	.267		
Total	104.146	80			

Table 69 Multiple comparison of permeation activity in various formulations (data specified in Table 23, page 117).

Multiple Comparisons

Dependent Variable: ENTRAPMENT
Dunnett T3

(I) FORMULATION	(J) FORMULATION	Mean Difference (I-J)	Std. Error	Sig.	95% Confidence Interval	
					Lower bound	Upper bound
1	1	-.89297(*)	0.09858	0.048	-1.7761	-.0098
	3	-.04542	0.11446	1.000	-1.1647	1.0738
	4	1.71082	0.27119	0.207	-1.7975	5.2192
	5	.68551	0.31126	0.861	-3.4123	4.7834
	6	-1.11334(*)	0.05551	0.004	-1.5991	-.6276
	7	-1.16176	0.49032	0.818	-7.8386	5.5150
	8	-.17176	0.15581	1.000	-1.9311	1.5876
	9	.38042	0.20696	0.942	-2.1655	2.9263
	10	-1.59218	0.39756	0.453	-6.9414	3.7570
	11	-1.53489	0.42961	0.532	-7.3443	4.2745
	12	-1.32125	0.67581	0.915	-10.6258	7.9833
	13	-1.07809	0.21651	0.309	-3.7687	1.6125
	14	-.66483	0.11379	0.181	-1.7739	.4442
	15	-.72735	0.42477	0.958	-6.4674	5.0127
	16	-.88877	0.16979	0.270	-2.8648	1.0872
	17	-1.25585	0.19111	0.179	-3.5600	1.0483
	18	-.66056	0.20392	0.596	-3.1602	1.8390
	19	-1.04416	0.44337	0.822	-7.0506	4.9623
	20	-.66884	0.08705	0.064	-1.3924	.0547
	21	.65095	0.17301	0.479	-1.3748	2.6767
	22	-1.02820	0.47887	0.873	-7.5418	5.4854
	23	-1.25800(*)	0.06025	0.002	-1.7333	-.7827
	24	.70497	0.22884	0.635	-2.1717	3.5816
	25	-.95908	0.31286	0.641	-5.0803	3.1621
	26	2.92053	0.40255	0.166	-2.5004	8.3414
	27	.82103	0.17915	0.348	-1.2995	2.9416
2	1	.89297(*)	0.09858	0.048	0.0098	1.7761
	3	0.84755	0.13501	0.099	-0.1947	1.8898
	4	2.60379	0.28049	0.078	-0.5646	5.7722
	5	1.57848	0.31939	0.303	-2.192	5.3489
	6	-0.22037	0.0906	0.807	-1.2409	0.8002
	7	-0.26879	0.49552	1.000	-6.6938	6.1562
	8	0.72121	0.17147	0.346	-0.7842	2.2266
	9	-1.27339	0.21900	0.191	-0.9408	3.4876
	10	-0.69921	0.40396	0.959	-5.7583	4.3599
	11	-0.64192	0.43554	0.986	-6.1751	4.8913
	12	-0.42828	0.67959	1.000	-9.5383	8.6818
	13	-0.18512	0.22804	1.000	-2.5388	2.1685
	14	0.22814	0.13444	0.984	-0.8081	1.2644
	15	0.16562	0.43076	1.000	-5.2961	5.6273
	16	0.0042	0.18427	1.000	-1.6857	1.6941
	17	-0.36288	0.20409	0.963	-2.3491	1.6233
	18	0.23241	0.21613	1.000	-1.9376	2.4025
	19	-0.15119	0.44911	1.000	-5.8872	5.5848
	20	0.22413	0.11272	0.943	0.6427	1.091
	21	1.54392	0.18724	0.069	-0.1897	3.2775
	22	-0.13522	0.48419	1.000	-6.3926	6.1222
	23	-0.36502	0.09358	0.431	-1.3149	0.5848
	24	1.59794	0.23979	0.149	-0.9377	4.1336
	25	-0.0661	0.32095	1.000	-3.8605	3.7283
	26	3.8135	0.40887	0.093	-1.3195	8.9465
	27	1.714	0.19293	0.059	-0.1042	3.5322

Table 69 Multiple comparison of permeation activity in various formulations (continuous) (data specified in Table 23, page 117).

Dependent Variable: ENTRAPMENT
Dunnett T3

(I) FORMULATION	(J) FORMULATION	Mean Difference (I-J)	Std. Error	Sig.	95% Confidence Interval	
					Lower bound	Upper bound
3	1	0.04542	0.11446	1.000	-1.0738	1.1647
	2	-0.84755	0.13501	0.099	-1.8898	0.1947
	4	1.75624	0.28645	0.178	-1.2587	4.7712
	5	0.73093	0.32464	0.855	-2.8778	4.3396
	6	-1.06792	0.10767	0.075	-2.3523	0.2164
	7	-1.11634	0.49892	0.854	-7.3938	5.1611
	8	-0.12634	0.18107	1.000	-1.5957	1.343
	9	0.42584	0.22659	0.95	-1.6759	2.5276
	10	-1.54676	0.40813	0.477	-6.4459	3.3524
	11	-1.48946	0.4394	0.561	-6.8665	3.8875
	12	-1.27583	0.68208	0.933	-10.2654	7.7137
	13	-1.03267	0.23534	0.333	-3.2646	1.1993
	14	-0.6194	0.14649	0.305	-1.7266	0.4878
	15	-0.68193	0.43467	0.979	-5.9868	4.623
	16	-0.84335	0.19323	0.309	-2.4711	0.7844
	17	-1.21043	0.21221	0.170	-3.1025	0.6817
	18	-0.61513	0.22382	0.718	-2.6759	1.4456
	19	-0.99874	0.45286	0.863	-6.5804	4.5829
	20	-0.62342	0.12684	0.222	-1.6538	0.4069
	21	0.69637	0.19607	0.481	-0.9697	2.3625
	22	-0.98277	0.48767	0.906	-7.0909	5.1254
	23	-1.21257(*)	0.11019	0.049	-2.42	-0.0052
	24	0.7504	0.24674	0.633	-1.6536	3.1544
	25	-0.91365	0.32617	0.704	-4.5462	2.7189
	26	2.96595	0.41298	0.150	-2.0076	7.9395
	27	0.86645	0.20151	0.326	-0.8745	2.6074
4	1	-1.71082	0.27119	0.207	-5.2192	1.7975
	2	-2.60379	0.28049	0.078	-5.7722	0.5646
	3	-1.75624	0.28645	0.178	-4.7712	1.2587
	5	-1.02531	0.40723	0.799	-4.1408	2.0902
	6	-2.82416	0.26839	0.083	-6.4669	0.8186
	7	-2.87258	0.55621	0.221	-7.8938	2.1486
	8	-1.88258	0.30534	0.141	-4.6195	0.8544
	9	-1.3304	0.33435	0.367	-3.977	1.3162
	10	-3.303	0.47646	0.085	-7.2227	0.6167
	11	-3.24571	0.50351	0.113	-7.5245	1.0331
	12	-3.03207	0.72503	0.385	-10.6108	4.5466
	13	-2.78891(*)	0.34034	0.042	-5.4461	-0.1317
	14	-2.37565	0.28619	0.089	-5.3967	0.6454
	15	-2.43817	0.49938	0.237	-6.6611	1.7847
	16	-2.59959	0.3127	0.055	-5.2852	0.0861
	17	-2.96667(*)	0.32477	0.035	-5.6135	-0.3198
	18	-2.37138	0.33247	0.071	-5.0162	0.2735
	19	-2.75498	0.51529	0.192	-7.1956	1.6856
	20	-2.37966	0.27665	0.101	-5.6713	0.912
	21	-1.05987	0.31446	0.529	-3.7367	1.6169
	22	-2.73901	0.54614	0.235	-7.615	2.1369
	23	-2.96881	0.26942	0.073	-6.5605	0.6228
	24	-1.00585	0.34832	0.672	-3.6881	1.6764
	25	-2.66989	0.40845	0.085	-5.7976	0.4578
	26	1.20971	0.48062	0.794	-2.7641	5.1835
	27	-0.88979	0.31789	0.702	-3.5527	1.7731

Table 69 Multiple comparison of permeation activity in various formulations (continuous) (data specified in Table 23, page 117).

Dependent Variable: ENTRAPMENT
Dunnett T3

(I) FORMULATION	(J) FORMULATION	Mean Difference (I-J)	Std. Error	Sig.	95% Confidence Interval	
					Lower bound	Upper bound
5	1	-0.68551	0.31126	0.861	-4.7834	3.4123
	2	-1.57848	0.31939	0.303	-5.3489	2.192
	3	-0.73093	0.32464	0.855	-4.3396	2.8778
	4	1.02531	0.40723	0.799	-2.0902	4.1408
	6	-1.79885	0.30882	0.25	-6.0175	2.4198
	7	-1.84727	0.5768	0.576	-6.7321	3.0375
	8	-0.85728	0.34142	0.79	-4.1272	2.4127
	9	-0.30509	0.36759	1.000	-3.3689	2.7587
	10	-2.27769	0.50035	0.261	-6.2002	1.6449
	11	-2.2204	0.52617	0.323	-6.449	2.0082
	12	-2.00676	0.74095	0.73	-9.2856	5.2721
	13	-1.7636	0.37305	0.248	-4.8149	1.2877
	14	-1.35034	0.32441	0.399	-4.9656	2.2649
	15	-1.41286	0.52222	0.734	-5.5933	2.7675
	16	-1.57428	0.34802	0.304	-4.7639	1.6153
	17	-1.94136	0.35891	0.187	-5.0435	1.1608
	18	-1.34607	0.36589	0.447	-4.4156	1.7234
	19	-1.72967	0.53746	0.568	-6.0989	2.6396
	20	-1.35435	0.31602	0.396	-5.2476	2.5389
	21	-0.03456	0.3496	1.000	-3.2082	3.1391
	22	-1.71371	0.5671	0.631	-6.4681	3.0407
	23	-1.94351	0.30971	0.217	-6.1167	2.2297
	24	0.01946	0.38034	1.000	-3.0267	3.0656
	25	-1.64459	0.43609	0.404	-4.9406	1.6515
	26	2.23501	0.50432	0.281	-1.733	6.2031
	27	0.13552	0.35269	1.000	-3.0105	3.2815
6	1	1.11334(*)	0.05551	0.004	0.6276	1.5991
	2	0.22037	0.0906	0.807	-0.8002	1.2409
	3	1.06792	0.10767	0.075	-0.2164	2.3523
	4	2.82416	0.26839	0.083	-0.8186	6.4669
	5	1.79885	0.30882	0.25	-2.4198	6.0175
	7	-0.04842	0.48878	1.000	-6.8066	6.7098
	8	0.94158	0.15089	0.21	-0.9955	2.8787
	9	1.49376	0.20329	0.16	-1.2122	4.1998
	10	-0.47884	0.39566	0.998	-5.9264	4.9687
	11	-0.42155	0.42785	1.000	-6.3227	5.4796
	12	-0.20791	0.67469	1.000	-9.5726	9.1568
	13	0.03525	0.21299	1.000	-2.8114	2.8819
	14	0.44852	0.10695	0.405	-0.8249	1.7219
	15	0.38599	0.42299	1.000	-5.4467	6.2187
	16	0.22457	0.16528	0.993	-1.9257	2.3749
	17	-0.14251	0.18712	1.000	-2.6132	2.3282
	18	0.45278	0.20019	0.846	-2.2082	3.1138
	19	0.06918	0.44166	1.000	-6.0265	6.1648
	20	0.4445	0.0779	0.209	-0.3786	1.2676
	21	1.76429	0.16859	0.078	-0.4348	3.9633
	22	0.08515	0.47729	1.000	-6.5116	6.6819
	23	-0.14465	0.04606	0.589	-0.5073	0.218
	24	1.81831	0.22552	0.136	-1.2093	4.8459
	25	0.15427	0.31044	1.000	-4.0873	4.3958
	26	4.03387	0.40067	0.092	-1.4843	9.552
	27	1.93437	0.17489	0.071	-0.3573	4.2261

Table 69 Multiple comparison of permeation activity in various formulations (continuous) (data specified in Table 23, page 117).

Dependent Variable: ENTRAPMENT
Dunnett T3

(I) FORMULATION	(J) FORMULATION	Mean Difference (I-J)	Std. Error	Sig.	95% Confidence Interval	
					Lower bound	Upper bound
7	1	1.16176	0.49032	0.818	-5.515	7.8386
	2	0.26879	0.49552	1.000	-6.1562	6.6938
	3	1.11634	0.49892	0.854	-5.1611	7.3938
	4	2.87258	0.55621	0.221	-2.1486	7.8938
	5	1.84727	0.57680	0.576	-3.0375	6.7321
	6	0.04842	0.48878	1.000	-6.7098	6.8066
	8	0.99	0.51000	0.926	-4.8862	6.8662
	9	1.54218	0.52788	0.669	-3.8802	6.9646
	10	-0.43042	0.62760	1.000	-5.3026	4.4418
	11	-0.37313	0.64837	1.000	-5.3269	4.5807
	12	-0.15949	0.83219	1.000	-6.8363	6.5173
	13	0.08367	0.53169	1.000	-5.2656	5.4329
	14	0.49694	0.49877	1.000	-5.7869	6.7808
	15	0.43441	0.64517	1.000	-4.5044	5.3732
	16	0.27299	0.51444	1.000	-5.471	6.0169
	17	-0.09409	0.52187	1.000	-5.6471	5.4589
	18	0.50121	0.52669	1.000	-4.9454	5.9478
	19	0.1176	0.65757	1.000	-4.8838	5.119
	20	0.49292	0.49336	1.000	-6.0327	7.0186
	21	1.81271	0.51551	0.523	-3.9014	7.5269
	22	0.13357	0.68201	1.000	-5.023	5.2901
	23	-0.09623	0.48934	1.000	-6.8244	6.6319
	24	1.86674	0.53683	0.518	-3.3946	7.1281
	25	0.20269	0.57767	1.000	-4.6785	5.0839
	26	4.08229	0.63077	0.091	-0.7998	8.9644
	27	1.98279	0.51761	0.456	-3.6754	7.641
8	1	0.17176	0.15581	1.000	-1.5876	1.9311
	2	-0.72121	0.17147	0.346	-2.2266	0.7842
	3	0.12634	0.18107	1.000	-1.343	1.5957
	4	1.88258	0.30534	0.141	-0.8544	4.6195
	5	0.85728	0.34142	0.790	-2.4127	4.1272
	6	-0.94158	0.15089	0.210	-2.8787	0.9955
	7	-0.99	0.51000	0.926	-6.8662	4.8862
	9	0.55218	0.25004	0.889	-1.4424	2.5467
	10	-1.42042	0.42159	0.554	-5.9231	3.0822
	11	-1.36312	0.45194	0.645	-6.3377	3.6115
	12	-1.14949	0.69022	0.968	-9.781	7.482
	13	-0.90633	0.25799	0.483	-2.9988	1.1861
	14	-0.49306	0.18065	0.725	-1.9629	0.9767
	15	-0.55559	0.44734	0.998	-5.4586	4.3474
	16	-0.71701	0.22025	0.549	-2.3907	0.9567
	17	-1.08409	0.23708	0.256	-2.9289	0.7607
	18	-0.48879	0.24752	0.943	-2.4533	1.4757
	19	-0.8724	0.46504	0.940	-6.0507	4.3059
	20	-0.49708	0.16512	0.640	-2.0661	1.072
	21	0.82272	0.22275	0.425	-0.8743	2.5197
	22	-0.85643	0.49900	0.964	-6.5622	4.8493
	23	-1.08623	0.15269	0.155	-2.9495	0.777
	24	0.87674	0.26843	0.556	-1.3498	3.1032
	25	-0.78731	0.34288	0.851	-4.0793	2.5046
	26	3.09229	0.42630	0.125	-1.4835	7.668
	27	0.99279	0.22756	0.285	-0.7513	2.7369

Table 69 Multiple comparison of permeation activity in various formulations (continuous) (data specified in Table 23, page 117).

Dependent Variable: ENTRAPMENT
Dunnett T3

(I) FORMULATION	(J) FORMULATION	Mean Difference (I-J)	Std. Error	Sig.	95% Confidence Interval	
					Lower bound	Upper bound
9	1	-0.38042	0.20696	0.942	-2.9263	2.1655
	2	-1.27339	0.21900	0.191	-3.4876	0.9408
	3	-0.42584	0.22659	0.950	-2.5276	1.6759
	4	1.3304	0.33435	0.367	-1.3162	3.977
	5	0.30509	0.36759	1.000	-2.7587	3.3689
	6	-1.49376	0.20329	0.160	-4.1998	1.2122
	7	-1.54218	0.52788	0.669	-6.9646	3.8802
	8	-0.55218	0.25004	0.889	-2.5467	1.4424
	10	-1.9726	0.44306	0.319	-6.1051	2.1599
	11	-1.91531	0.47203	0.393	-6.4823	2.6517
	12	-1.70167	0.70353	0.809	-9.8511	6.4478
	13	-1.45851	0.29175	0.192	-3.6667	0.7497
	14	-1.04524	0.22626	0.294	-3.1509	1.0604
	15	-1.10777	0.46762	0.831	-5.6082	3.3927
	16	-1.26919	0.25898	0.211	-3.2796	0.7412
	17	-1.63627	0.27344	0.111	-3.712	0.4395
	18	-1.04097	0.28254	0.426	-3.1768	1.0948
	19	-1.42458	0.48458	0.662	-6.1822	3.3331
	20	-1.04926	0.21406	0.291	-3.3713	1.2728
	21	0.27053	0.26110	1.000	-1.7467	2.2878
	22	-1.40861	0.51726	0.726	-6.6672	3.85
	23	-1.63841	0.20463	0.131	-4.2816	1.0048
	24	0.32455	0.30102	1.000	-1.9661	2.6152
	25	-1.33949	0.36895	0.458	-4.4213	1.7423
	26	2.54011	0.44754	0.185	-1.659	6.7392
	27	0.44061	0.26522	0.987	-1.5928	2.474
10	1	1.59218	0.39756	0.453	-3.757	6.9414
	2	0.69921	0.40396	0.959	-4.3599	5.7583
	3	1.54676	0.40813	0.477	-3.3524	6.4459
	4	3.303	0.47646	0.085	-0.6167	7.2227
	5	2.27769	0.50035	0.261	-1.6449	6.2002
	6	0.47884	0.39566	0.998	-4.9687	5.9264
	7	0.43042	0.62760	1.000	-4.4418	5.3026
	8	1.42042	0.42159	0.554	-3.0822	5.9231
	9	1.9726	0.44306	0.319	-2.1599	6.1051
	11	0.05729	0.58140	1.000	-4.3536	4.4682
	12	0.27093	0.78114	1.000	-6.5636	7.1054
	13	0.51409	0.44759	1.000	-3.5688	4.597
	14	0.92736	0.40794	0.846	-3.9785	5.8333
	15	0.86483	0.57783	0.996	-3.5146	5.2442
	16	0.70341	0.42696	0.977	-3.6818	5.0887
	17	0.33633	0.43588	1.000	-3.8927	4.5653
	18	0.93163	0.44164	0.901	-3.2181	5.0814
	19	0.54802	0.59164	1.000	-3.957	5.053
	20	0.92334	0.40130	0.837	-4.2492	6.0959
	21	2.24313	0.42825	0.242	-2.1167	6.6029
	22	0.56399	0.61869	1.000	-4.2125	5.3405
	23	0.33419	0.39635	1.000	-5.0768	5.7452
	24	2.29715	0.45369	0.228	-1.731	6.3253
	25	0.63311	0.50134	1.000	-3.2915	4.5577
	26	4.51271(*)	0.56170	0.04	0.2669	8.7586
	27	2.41321	0.43077	0.205	-1.8998	6.7262

Table 69 Multiple comparison of permeation activity in various formulations (continuous) (data specified in Table 23, page 117).

Dependent Variable: ENTRAPMENT
Dunnett T3

(I) FORMULATION	(J) FORMULATION	Mean Difference (I-J)	Std. Error	Sig.	95% Confidence Interval	
					Lower bound	Upper bound
11	1	1.53489	0.42961	0.532	-4.2745	7.3443
	2	0.64192	0.43554	0.986	-4.8913	6.1751
	3	1.48946	0.43940	0.561	-3.8875	6.8665
	4	3.24571	0.50351	0.113	-1.0331	7.5245
	5	2.2204	0.52617	0.323	-2.0082	6.449
	6	0.42155	0.42785	1.000	-5.4796	6.3227
	7	0.37313	0.64837	1.000	-4.5807	5.3269
	8	1.36312	0.45194	0.645	-3.6115	6.3377
	9	1.91531	0.47203	0.393	-2.6517	6.4823
	10	-0.05729	0.58140	1.000	-4.4682	4.3536
	12	0.21364	0.79793	1.000	-6.5298	6.9571
	13	0.4568	0.47629	1.000	-4.0508	4.9644
	14	0.87006	0.43923	0.914	-4.5136	6.2537
	15	0.80754	0.60033	0.999	-3.7302	5.3453
	16	0.64612	0.45695	0.993	-4.2038	5.496
	17	0.27904	0.46529	1.000	-4.399	4.9571
	18	0.87433	0.47070	0.95	-3.7128	5.4615
	19	0.49073	0.61363	1.000	-4.1501	5.1316
	20	0.86605	0.43307	0.908	-4.7762	6.5083
	21	2.18584	0.45815	0.301	-2.6366	7.0083
	22	0.50669	0.63976	1.000	-4.3642	5.3776
	23	0.27689	0.42849	1.000	-5.5903	6.1441
	24	2.23986	0.48202	0.288	-2.1994	6.6791
	25	0.57581	0.52712	1.000	-3.6527	4.8044
	26	4.45541(*)	0.58482	0.049	0.0235	8.8874
	27	2.35592	0.46051	0.258	-2.4155	7.1274
12	1	1.32125	0.67581	0.915	-7.9833	10.6258
	2	0.42828	0.67959	1.000	-8.6818	9.5383
	3	1.27583	0.68208	0.933	-7.7137	10.2654
	4	3.03207	0.72503	0.385	-4.5466	10.6108
	5	2.00676	0.74095	0.730	-5.2721	9.2856
	6	0.20791	0.67469	1.000	-9.1568	9.5726
	7	0.15949	0.83219	1.000	-6.5173	6.8363
	8	1.14949	0.69022	0.968	-7.482	9.781
	9	1.70167	0.70353	0.809	-6.4478	9.8511
	10	-0.27093	0.78114	1.000	-7.1054	6.5636
	11	-0.21364	0.79793	1.000	-6.9571	6.5298
	13	0.24316	0.70640	1.000	-7.8168	8.3032
	14	0.65643	0.68196	1.000	-8.3385	9.6513
	15	0.5939	0.79533	1.000	-6.1608	7.3486
	16	0.43248	0.69351	1.000	-8.0689	8.9339
	17	0.0654	0.69904	1.000	-8.2341	8.3649
	18	0.6607	0.70264	1.000	-7.5175	8.8388
	19	0.27709	0.80542	1.000	-6.4394	6.9936
	20	0.65241	0.67801	1.000	-8.537	9.8418
	21	1.9722	0.69430	0.695	-6.4988	10.4432
	22	0.29306	0.82549	1.000	-6.3861	6.9722
	23	0.06326	0.67510	1.000	-9.2794	9.4059
	24	2.02622	0.71028	0.690	-5.9198	9.9723
	25	0.36218	0.74162	1.000	-6.9059	7.6302
	26	4.24178	0.78369	0.188	-2.5759	11.0595
	27	2.14228	0.69586	0.634	-6.2707	10.5552

Table 69 Multiple comparison of permeation activity in various formulations (continuous) (data specified in Table 23, page 117).

Dependent Variable: ENTRAPMENT
Dunnett T3

(I) FORMULATION	(J) FORMULATION	Mean Difference (I-J)	Std. Error	Sig.	95% Confidence Interval	
					Lower bound	Upper bound
13	1	1.07809	0.21651	0.309	-1.6125	3.7687
	2	0.18512	0.22804	1.000	-2.1685	2.5388
	3	1.03267	0.23534	0.333	-1.1993	3.2646
	4	2.78891(*)	0.34034	0.042	0.1317	5.4461
	5	1.7636	0.37305	0.248	-1.2877	4.8149
	6	-0.03525	0.21299	1.000	-2.8819	2.8114
	7	-0.08367	0.53169	1.000	-5.4329	5.2656
	8	0.90633	0.25799	0.483	-1.1861	2.9988
	9	1.45851	0.29175	0.192	-0.7497	3.6667
	10	-0.51409	0.44759	1.000	-4.597	3.5688
	11	-0.4568	0.47629	1.000	-4.9644	4.0508
	12	-0.24316	0.70640	1.000	-8.3032	7.8168
	14	0.41326	0.23502	0.967	-1.8231	2.6496
	15	0.35074	0.47192	1.000	-4.0916	4.7931
	16	0.18932	0.26667	1.000	-1.9073	2.2859
	17	-0.17776	0.28073	1.000	-2.3221	1.9666
	18	0.41753	0.28960	0.998	-1.7767	2.6117
	19	0.03393	0.48873	1.000	-4.6607	4.7285
	20	0.40925	0.22330	0.948	-2.0566	2.8751
	21	1.72904	0.26873	0.095	-0.3717	3.8298
	22	0.0499	0.52115	1.000	-5.1377	5.2375
	23	-0.1799	0.21428	1.000	-2.9657	2.6059
	24	1.78306	0.30766	0.122	-0.5471	4.1132
	25	0.11902	0.37439	1.000	-2.9494	3.1874
	26	3.99862	0.45203	0.055	-0.1492	8.1464
	27	1.89912	0.27273	0.071	-0.2127	4.0109
14	1	0.66483	0.11379	0.181	-0.4442	1.7739
	2	-0.22814	0.13444	0.984	-1.2644	0.8081
	3	0.6194	0.14649	0.305	-0.4878	1.7266
	4	2.37565	0.28619	0.089	-0.6454	5.3967
	5	1.35034	0.32441	0.399	-2.2649	4.9656
	6	-0.44852	0.10695	0.405	-1.7219	0.8249
	7	-0.49694	0.49877	1.000	-6.7808	5.7869
	8	0.49306	0.18065	0.725	-0.9767	1.9629
	9	1.04524	0.22626	0.294	-1.0604	3.1509
	10	-0.92736	0.40794	0.846	-5.8333	3.9785
	11	-0.87006	0.43923	0.914	-6.2537	4.5136
	12	-0.65643	0.68196	1.000	-9.6513	8.3385
	13	-0.41326	0.23502	0.967	-2.6496	1.8231
	15	-0.06252	0.43449	1.000	-5.3741	5.2491
	16	-0.22394	0.19283	1.000	-1.8533	1.4054
	17	-0.59102	0.21185	0.705	-2.4861	1.3041
	18	0.00427	0.22347	1.000	-2.0602	2.0688
	19	-0.37933	0.45269	1.000	-5.9676	5.2089
	20	-0.00401	0.12624	1.000	-1.0268	1.0187
	21	1.31578	0.19568	0.101	-0.3521	2.9837
	22	-0.36337	0.48752	1.000	-6.478	5.7512
	23	-0.59317	0.10949	0.24	-1.7897	0.6034
	24	1.3698	0.24643	0.204	-1.039	3.7786
	25	-0.29425	0.32594	1.000	-3.9334	3.3449
	26	3.58535	0.41280	0.101	-1.395	8.5657
	27	1.48586	0.20113	0.080	-0.2574	3.2291

Table 69 Multiple comparison of permeation activity in various formulations (continuous) (data specified in Table 23, page 117).

Dependent Variable: ENTRAPMENT
Dunnett T3

(I) FORMULATION	(J) FORMULATION	Mean Difference (I-J)	Std. Error	Sig.	95% Confidence Interval	
					Lower bound	Upper bound
15	1	0.72735	0.42477	0.958	-5.0127	6.4674
	2	-0.16562	0.43076	1.000	-5.6273	5.2961
	3	0.68193	0.43467	0.979	-4.623	5.9868
	4	2.43817	0.49938	0.237	-1.7847	6.6611
	5	1.41286	0.52222	0.734	-2.7675	5.5933
	6	-0.38599	0.42299	1.000	-6.2187	5.4467
	7	-0.43441	0.64517	1.000	-5.3732	4.5044
	8	0.55559	0.44734	0.998	-4.3474	5.4586
	9	1.10777	0.46762	0.831	-3.3927	5.6082
	10	-0.86483	0.57783	0.996	-5.2442	3.5146
	11	-0.80754	0.60033	0.999	-5.3453	3.7302
	12	-0.5939	0.79533	1.000	-7.3486	6.1608
	13	-0.35074	0.47192	1.000	-4.7931	4.0916
	14	0.06252	0.43449	1.000	-5.2491	5.3741
	16	-0.16142	0.45240	1.000	-4.9407	4.6178
	17	-0.5285	0.46083	1.000	-5.138	4.081
	18	0.06679	0.46628	1.000	-4.4534	4.587
	19	-0.31681	0.61025	1.000	-4.9345	4.3009
	20	0.05851	0.42827	1.000	-5.5129	5.6299
	21	1.3783	0.45362	0.637	-3.3737	6.1303
	22	-0.30085	0.63651	1.000	-5.1549	4.5532
	23	-0.53065	0.42364	0.996	-6.329	5.2677
	24	1.43232	0.47771	0.642	-2.9436	5.8083
	25	-0.23173	0.52318	1.000	-4.4124	3.9489
	26	3.64788	0.58127	0.095	-0.7535	8.0492
	27	1.54838	0.45600	0.544	-3.1532	6.25
16	1	0.88877	0.16979	0.270	-1.0872	2.8648
	2	-0.0042	0.18427	1.000	-1.6941	1.6857
	3	0.84335	0.19323	0.309	-0.7844	2.4711
	4	2.59959	0.31270	0.055	-0.0861	5.2852
	5	1.57428	0.34802	0.304	-1.6153	4.7639
	6	-0.22457	0.16528	0.993	-2.3749	1.9257
	7	-0.27299	0.51444	1.000	-6.0169	5.471
	8	0.71701	0.22025	0.549	-0.9567	2.3907
	9	1.26919	0.25898	0.211	-0.7412	3.2796
	10	-0.70341	0.42696	0.977	-5.0887	3.6818
	11	-0.64612	0.45695	0.993	-5.496	4.2038
	12	-0.43248	0.69351	1.000	-8.9339	8.0689
	13	-0.18932	0.26667	1.000	-2.2859	1.9073
	14	0.22394	0.19283	1.000	-1.4054	1.8533
	15	0.16142	0.45240	1.000	-4.6178	4.9407
	17	-0.36708	0.24650	0.996	-2.2486	1.5144
	18	0.22821	0.25655	1.000	-1.756	2.2124
	19	-0.15539	0.46990	1.000	-5.2066	4.8959
	20	0.21993	0.17837	0.999	-1.55	1.9899
	21	1.53972	0.23274	0.079	-0.2198	3.2993
	22	-0.13942	0.50354	1.000	-5.7138	5.435
	23	-0.36922	0.16693	0.861	-2.4486	1.7101
	24	1.59374	0.27678	0.140	-0.6227	3.8102
	25	-0.0703	0.34945	1.000	-3.2809	3.1403
	26	3.8093	0.43160	0.074	-0.6477	8.2663
	27	1.7098	0.23735	0.059	-0.0878	3.5074

Table 69 Multiple comparison of permeation activity in various formulations (continuous) (data specified in Table 23, page 117).

Dependent Variable: ENTRAPMENT
Dunnett T3

(I) FORMULATION	(J) FORMULATION	Mean Difference (I-J)	Std. Error	Sig.	95% Confidence Interval	
					Lower bound	Upper bound
17	1	1.25585	0.19111	0.179	-1.0483	3.56
	2	0.36288	0.20409	0.963	-1.6233	2.3491
	3	1.21043	0.21221	0.170	-0.6817	3.1025
	4	2.96667(*)	0.32477	0.035	0.3198	5.6135
	5	1.94136	0.35891	0.187	-1.1608	5.0435
	6	0.14251	0.18712	1.000	-2.3282	2.6132
	7	0.09409	0.52187	1.000	-5.4589	5.6471
	8	1.08409	0.23708	0.256	-0.7607	2.9289
	9	1.63627	0.27344	0.111	-0.4395	3.712
	10	-0.33633	0.43588	1.000	-4.5653	3.8927
	11	-0.27904	0.46529	1.000	-4.9571	4.399
	12	-0.0654	0.69904	1.000	-8.3649	8.2341
	13	0.17776	0.28073	1.000	-1.9666	2.3221
	14	0.59102	0.21185	0.705	-1.3041	2.4861
	15	0.5285	0.46083	1.000	-4.081	5.138
	16	0.36708	0.24650	0.996	-1.5144	2.2486
	18	0.59529	0.27114	0.897	-1.46	2.6506
	19	0.21169	0.47802	1.000	-4.6623	5.0857
	20	0.58701	0.19878	0.661	-1.4976	2.6716
	21	1.90680(*)	0.24873	0.049	0.0137	3.7999
	22	0.22766	0.51112	1.000	-5.1585	5.6138
	23	-0.00214	0.18858	1.000	-2.4067	2.4024
	24	1.96082	0.29035	0.078	-0.2817	4.2034
	25	0.29677	0.36030	1.000	-2.8246	3.4182
	26	4.17638	0.44043	0.054	-0.1217	8.4744
	27	2.07688(*)	0.25304	0.038	0.1587	3.995
18	1	0.66056	0.20392	0.596	-1.839	3.1602
	2	-0.23241	0.21613	1.000	-2.4025	1.9376
	3	0.61513	0.22382	0.718	-1.4456	2.6759
	4	2.37138	0.33247	0.071	-0.2735	5.0162
	5	1.34607	0.36589	0.447	-1.7234	4.4156
	6	-0.45278	0.20019	0.846	-3.1138	2.2082
	7	-0.50121	0.52669	1.000	-5.9478	4.9454
	8	0.48879	0.24752	0.943	-1.4757	2.4533
	9	1.04097	0.28254	0.426	-1.0948	3.1768
	10	-0.93163	0.44164	0.901	-5.0814	3.2181
	11	-0.87433	0.47070	0.950	-5.4615	3.7128
	12	-0.6607	0.70264	1.000	-8.8388	7.5175
	13	-0.41753	0.28960	0.998	-2.6117	1.7767
	14	-0.00427	0.22347	1.000	-2.0688	2.0602
	15	-0.06679	0.46628	1.000	-4.587	4.4534
	16	-0.22821	0.25655	1.000	-2.2124	1.756
	17	-0.59529	0.27114	0.897	-2.6506	1.46
	19	-0.3836	0.48329	1.000	-5.1625	4.3953
	20	-0.00828	0.21112	1.000	-2.2846	2.268
	21	1.31151	0.25870	0.189	-0.6804	3.3034
	22	-0.36764	0.51605	1.000	-5.6498	4.9145
	23	-0.59744	0.20155	0.665	-3.1949	2.0001
	24	1.36553	0.29894	0.251	-0.9141	3.6452
	25	-0.29852	0.36725	1.000	-3.3862	2.7892
	26	3.58108	0.44614	0.078	-0.6357	7.7979
	27	1.48159	0.26285	0.136	-0.5282	3.4913

Table 69 Multiple comparison of permeation activity in various formulations (continuous) (data specified in Table 23, page 117).

Dependent Variable: ENTRAPMENT
Dunnett T3

(I) FORMULATION	(J) FORMULATION	Mean Difference (I-J)	Std. Error	Sig.	95% Confidence Interval	
					Lower bound	Upper bound
19	1	1.04416	0.44337	0.822	-4.9623	7.0506
	2	0.15119	0.44911	1.000	-5.5848	5.8872
	3	0.99874	0.45286	0.863	-4.5829	6.5804
	4	2.75498	0.51529	0.192	-1.6856	7.1956
	5	1.72967	0.53746	0.568	-2.6396	6.0989
	6	-0.06918	0.44166	1.000	-6.1648	6.0265
	7	-0.1176	0.65757	1.000	-5.119	4.8838
	8	0.8724	0.46504	0.94	-4.3059	6.0507
	9	1.42458	0.48458	0.662	-3.3331	6.1822
	10	-0.54802	0.59164	1.000	-5.053	3.957
	11	-0.49073	0.61363	1.000	-5.1316	4.1501
	12	-0.27709	0.80542	1.000	-6.9936	6.4394
	13	-0.03393	0.48873	1.000	-4.7285	4.6607
	14	0.37933	0.45269	1.000	-5.2089	5.9676
	15	0.31681	0.61025	1.000	-4.3009	4.9345
	16	0.15539	0.46990	1.000	-4.8959	5.2066
	17	-0.21169	0.47802	1.000	-5.0857	4.6623
	18	0.3836	0.48329	1.000	-4.3953	5.1625
	20	0.37532	0.44672	1.000	-5.4678	6.2184
	21	1.69511	0.47108	0.501	-3.328	6.7182
	22	0.01597	0.64907	1.000	-4.908	4.94
	23	-0.21383	0.44228	1.000	-6.2765	5.8488
	24	1.74913	0.49432	0.498	-2.8721	6.3703
	25	0.08509	0.53839	1.000	-4.2832	4.4534
	26	3.96469	0.59500	0.078	-0.5587	8.4881
	27	1.86519	0.47337	0.429	-3.1055	6.8358
20	1	0.66884	0.08705	0.064	-0.0547	1.3924
	2	-0.22413	0.11272	0.943	-1.091	0.6427
	3	0.62342	0.12684	0.222	-0.4069	1.6538
	4	2.37966	0.27665	0.101	-0.912	5.6713
	5	1.35435	0.31602	0.396	-2.5389	5.2476
	6	-0.4445	0.07790	0.209	-1.2676	0.3786
	7	-0.49292	0.49336	1.000	-7.0186	6.0327
	8	0.49708	0.16512	0.640	-1.072	2.0661
	9	1.04926	0.21406	0.291	-1.2728	3.3713
	10	-0.92334	0.40130	0.837	-6.0959	4.2492
	11	-0.86605	0.43307	0.908	-6.5083	4.7762
	12	-0.65241	0.67801	1.000	-9.8418	8.537
	13	-0.40925	0.22330	0.948	-2.8751	2.0566
	14	0.00401	0.12624	1.000	-1.0187	1.0268
	15	-0.05851	0.42827	1.000	-5.6299	5.5129
	16	-0.21993	0.17837	0.999	-1.9899	1.55
	17	-0.58701	0.19878	0.661	-2.6716	1.4976
	18	0.00828	0.21112	1.000	-2.268	2.2846
	19	-0.37532	0.44672	1.000	-6.2184	5.4678
	21	1.31979	0.18144	0.111	-0.4972	3.1368
	22	-0.35936	0.48198	1.000	-6.719	6.0002
	23	-0.58915	0.08135	0.100	-1.3532	0.1749
	24	1.37381	0.23528	0.212	-1.2783	4.0259
	25	-0.29024	0.31760	1.000	-4.2074	3.6269
	26	3.58937	0.40624	0.108	-1.6564	8.8351
	27	1.48987	0.18731	0.092	-0.4174	3.3971

Table 69 Multiple comparison of permeation activity in various formulations (continuous) (data specified in Table 23, page 117).

Dependent Variable: ENTRAPMENT
Dunnett T3

(I) FORMULATION	(J) FORMULATION	Mean Difference (I-J)	Std. Error	Sig.	95% Confidence Interval	
					Lower bound	Upper bound
21	1	-0.65095	0.17301	0.479	-2.6767	1.3748
	2	-1.54392	0.18724	0.069	-3.2775	0.1897
	3	-0.69637	0.19607	0.481	-2.3625	0.9697
	4	1.05987	0.31446	0.529	-1.6169	3.7367
	5	0.03456	0.34960	1.000	-3.1391	3.2082
	6	-1.76429	0.16859	0.078	-3.9633	0.4348
	7	-1.81271	0.51551	0.523	-7.5269	3.9014
	8	-0.82272	0.22275	0.425	-2.5197	0.8743
	9	-0.27053	0.26110	1.000	-2.2878	1.7467
	10	-2.24313	0.42825	0.242	-6.6029	2.1167
	11	-2.18584	0.45815	0.301	-7.0083	2.6366
	12	-1.9722	0.69430	0.695	-10.4432	6.4988
	13	-1.72904	0.26873	0.095	-3.8298	0.3717
	14	-1.31578	0.19568	0.101	-2.9837	0.3521
	15	-1.3783	0.45362	0.637	-6.1303	3.3737
	16	-1.53972	0.23274	0.079	-3.2993	0.2198
	17	-1.90680(*)	0.24873	0.049	-3.7999	-0.0137
	18	-1.31151	0.25870	0.189	-3.3034	0.6804
	19	-1.69511	0.47108	0.501	-6.7182	3.328
	20	-1.31979	0.18144	0.111	-3.1368	0.4972
	22	-1.67915	0.50463	0.566	-7.2241	3.8658
	23	-1.90895	0.17021	0.063	-4.0378	0.2199
	24	0.05402	0.27877	1.000	-2.1633	2.2713
	25	-1.61003	0.35103	0.294	-4.8044	1.5844
	26	2.26958	0.43288	0.243	-2.1616	6.7008
	27	0.17008	0.23966	1.000	-1.6429	1.9831
22	1	1.0282	0.47887	0.873	-5.4854	7.5418
	2	0.13522	0.48419	1.000	-6.1222	6.3926
	3	0.98277	0.48767	0.906	-5.1254	7.0909
	4	2.73901	0.54614	0.235	-2.1369	7.615
	5	1.71371	0.56710	0.631	-3.0407	6.4681
	6	-0.08515	0.47729	1.000	-6.6819	6.5116
	7	-0.13357	0.68201	1.000	-5.2901	5.023
	8	0.85643	0.49900	0.964	-4.8493	6.5622
	9	1.40861	0.51726	0.726	-3.85	6.6672
	10	-0.56399	0.61869	1.000	-5.3405	4.2125
	11	-0.50669	0.63976	1.000	-5.3776	4.3642
	12	-0.29306	0.82549	1.000	-6.9722	6.3861
	13	-0.0499	0.52115	1.000	-5.2375	5.1377
	14	0.36337	0.48752	1.000	-5.7512	6.478
	15	0.30085	0.63651	1.000	-4.5532	5.1549
	16	0.13942	0.50354	1.000	-5.435	5.7138
	17	-0.22766	0.51112	1.000	-5.6138	5.1585
	18	0.36764	0.51605	1.000	-4.9145	5.6498
	19	-0.01597	0.64907	1.000	-4.94	4.908
	20	0.35936	0.48198	1.000	-6.0002	6.719
	21	1.67915	0.50463	0.566	-3.8658	7.2241
	23	-0.2298	0.47786	1.000	-6.7959	6.3363
	24	1.73317	0.52640	0.564	-3.3697	6.836
	25	0.06912	0.56798	1.000	-4.6823	4.8205
	26	3.94872	0.62191	0.095	-0.8397	8.7371
	27	1.84922	0.50677	0.492	-3.6404	7.3389

Table 69 Multiple comparison of permeation activity in various formulations (continuous) (data specified in Table 23, page 117).

Dependent Variable: ENTRAPMENT
Dunnett T3

(I) FORMULATION	(J) FORMULATION	Mean Difference (I-J)	Std. Error	Sig.	95% Confidence Interval	
					Lower bound	Upper bound
23	1	1.25800(*)	0.06025	0.002	0.7827	1.7333
	2	0.36502	0.09358	0.431	-0.5848	1.3149
	3	1.21257(*)	0.11019	0.049	0.0052	2.42
	4	2.96881	0.26942	0.073	-0.6228	6.5605
	5	1.94351	0.30971	0.217	-2.2297	6.1167
	6	0.14465	0.04606	0.589	-0.218	0.5073
	7	0.09623	0.48934	1.000	-6.6319	6.8244
	8	1.08623	0.15269	0.155	-0.777	2.9495
	9	1.63841	0.20463	0.131	-1.0048	4.2816
	10	-0.33419	0.39635	1.000	-5.7452	5.0768
	11	-0.27689	0.42849	1.000	-6.1441	5.5903
	12	-0.06326	0.67510	1.000	-9.4059	9.2794
	13	0.1799	0.21428	1.000	-2.6059	2.9657
	14	0.59317	0.10949	0.240	-0.6034	1.7897
	15	0.53065	0.42364	0.996	-5.2677	6.329
	16	0.36922	0.16693	0.861	-1.7101	2.4486
	17	0.00214	0.18858	1.000	-2.4024	2.4067
	18	0.59744	0.20155	0.665	-2.0001	3.1949
	19	0.21383	0.44228	1.000	-5.8488	6.2765
	20	0.58915	0.08135	0.100	-0.1749	1.3532
	21	1.90895	0.17021	0.063	-0.2199	4.0378
	22	0.2298	0.47786	1.000	-6.3363	6.7959
	24	1.96297	0.22674	0.115	-1.0062	4.9322
	25	0.29892	0.31132	1.000	-3.8974	4.4952
	26	4.17852	0.40135	0.085	-1.3035	9.6606
	27	2.07902	0.17646	0.058	-0.1438	4.3019
24	1	-0.70497	0.22884	0.635	-3.5816	2.1717
	2	-1.59794	0.23979	0.149	-4.1336	0.9377
	3	-0.7504	0.24674	0.633	-3.1544	1.6536
	4	1.00585	0.34832	0.672	-1.6764	3.6881
	5	-0.01946	0.38034	1.000	-3.0656	3.0267
	6	-1.81831	0.22552	0.136	-4.8459	1.2093
	7	-1.86674	0.53683	0.518	-7.1281	3.3946
	8	-0.87674	0.26843	0.556	-3.1032	1.3498
	9	-0.32455	0.30102	1.000	-2.6152	1.9661
	10	-2.29715	0.45369	0.228	-6.3253	1.731
	11	-2.23986	0.48202	0.288	-6.6791	2.1994
	12	-2.02622	0.71028	0.690	-9.9723	5.9198
	13	-1.78306	0.30766	0.122	-4.1132	0.5471
	14	-1.3698	0.24643	0.204	-3.7786	1.039
	15	-1.43232	0.47771	0.642	-5.8083	2.9436
	16	-1.59374	0.27678	0.140	-3.8102	0.6227
	17	-1.96082	0.29035	0.078	-4.2034	0.2817
	18	-1.36553	0.29894	0.251	-3.6452	0.9141
	19	-1.74913	0.49432	0.498	-6.3703	2.8721
	20	-1.37381	0.23528	0.212	-4.0259	1.2783
	21	-0.05402	0.27877	1.000	-2.2713	2.1633
	22	-1.73317	0.52640	0.564	-6.836	3.3697
	23	-1.96297	0.22674	0.115	-4.9322	1.0062
	25	-1.66405	0.38165	0.298	-4.7262	1.3981
	26	2.21555	0.45807	0.256	-1.8752	6.3064
	27	0.11606	0.28262	1.000	-2.106	2.3381

Table 69 Multiple comparison of permeation activity in various formulations (continuous) (data specified in Table 23, page 117).

Dependent Variable: ENTRAPMENT
Dunnett T3

(I) FORMULATION	(J) FORMULATION	Mean Difference (I-J)	Std. Error	Sig.	95% Confidence Interval	
					Lower bound	Upper bound
25	1	0.95908	0.31286	0.641	-3.1621	5.0803
	2	0.0661	0.32095	1.000	-3.7283	3.8605
	3	0.91365	0.32617	0.704	-2.7189	4.5462
	4	2.66989	0.40845	0.085	-0.4578	5.7976
	5	1.64459	0.43609	0.404	-1.6515	4.9406
	6	-0.15427	0.31044	1.000	-4.3958	4.0873
	7	-0.20269	0.57767	1.000	-5.0839	4.6785
	8	0.78731	0.34288	0.851	-2.5046	4.0793
	9	1.33949	0.36895	0.458	-1.7423	4.4213
	10	-0.63311	0.50134	1.000	-4.5577	3.2915
	11	-0.57581	0.52712	1.000	-4.8044	3.6527
	12	-0.36218	0.74162	1.000	-7.6302	6.9059
	13	-0.11902	0.37439	1.000	-3.1874	2.9494
	14	0.29425	0.32594	1.000	-3.3449	3.9334
	15	0.23173	0.52318	1.000	-3.9489	4.4124
	16	0.0703	0.34945	1.000	-3.1403	3.2809
	17	-0.29677	0.36030	1.000	-3.4182	2.8246
	18	0.29852	0.36725	1.000	-2.7892	3.3862
	19	-0.08509	0.53839	1.000	-4.4534	4.2832
	20	0.29024	0.31760	1.000	-3.6269	4.2074
	21	1.61003	0.35103	0.294	-1.5844	4.8044
	22	-0.06912	0.56798	1.000	-4.8205	4.6823
	23	-0.29892	0.31132	1.000	-4.4952	3.8974
	24	1.66405	0.38165	0.298	-1.3981	4.7262
	26	3.8796	0.50530	0.054	-0.0902	7.8494
	27	1.7801	0.35410	0.234	-1.3861	4.9463
26	1	-2.92053	0.40255	0.166	-8.3414	2.5004
	2	-3.8135	0.40887	0.093	-8.9465	1.3195
	3	-2.96595	0.41298	0.150	-7.9395	2.0076
	4	-1.20971	0.48062	0.794	-5.1835	2.7641
	5	-2.23501	0.50432	0.281	-6.2031	1.733
	6	-4.03387	0.40067	0.092	-9.552	1.4843
	7	-4.08229	0.63077	0.091	-8.9644	0.7998
	8	-3.09229	0.42630	0.125	-7.668	1.4835
	9	-2.54011	0.44754	0.185	-6.7392	1.659
	10	-4.51271(*)	0.56170	0.040	-8.7586	-0.2669
	11	-4.45541(*)	0.58482	0.049	-8.8874	-0.0235
	12	-4.24178	0.78369	0.188	-11.0595	2.5759
	13	-3.99862	0.45203	0.055	-8.1464	0.1492
	14	-3.58535	0.41280	0.101	-8.5657	1.395
	15	-3.64788	0.58127	0.095	-8.0492	0.7535
	16	-3.8093	0.43160	0.074	-8.2663	0.6477
	17	-4.17638	0.44043	0.054	-8.4744	0.1217
	18	-3.58108	0.44614	0.078	-7.7979	0.6357
	19	-3.96469	0.59500	0.078	-8.4881	0.5587
	20	-3.58937	0.40624	0.108	-8.8351	1.6564
	21	-2.26958	0.43288	0.243	-6.7008	2.1616
	22	-3.94872	0.62191	0.095	-8.7371	0.8397
	23	-4.17852	0.40135	0.085	-9.6606	1.3035
	24	-2.21555	0.45807	0.256	-6.3064	1.8752
	25	-3.8796	0.50530	0.054	-7.8494	0.0902
	27	-2.0995	0.43537	0.285	-6.4832	2.2842

Table 69 Multiple comparison of permeation activity in various formulations (continuous) (data specified in Table 23, page 117).

Dependent Variable: ENTRAPMENT
Dunnett T3

(I) FORMULATION	(J) FORMULATION	Mean Difference (I-J)	Std. Error	Sig.	95% Confidence Interval	
					Lower bound	Upper bound
27	1	-0.82103	0.17915	0.348	-2.9416	1.2995
	2	-1.714	0.19293	0.059	-3.5322	0.1042
	3	-0.86645	0.20151	0.326	-2.6074	0.8745
	4	0.88979	0.31789	0.702	-1.7731	3.5527
	5	-0.13552	0.35269	1.000	-3.2815	3.0105
	6	-1.93437	0.17489	0.071	-4.2261	0.3573
	7	-1.98279	0.51761	0.456	-7.641	3.6754
	8	-0.99279	0.22756	0.285	-2.7369	0.7513
	9	-0.44061	0.26522	0.987	-2.474	1.5928
	10	-2.41321	0.43077	0.205	-6.7262	1.8998
	11	-2.35592	0.46051	0.258	-7.1274	2.4155
	12	-2.14228	0.69586	0.634	-10.5552	6.2707
	13	-1.89912	0.27273	0.071	-4.0109	0.2127
	14	-1.48586	0.20113	0.080	-3.2291	0.2574
	15	-1.54838	0.45600	0.544	-6.25	3.1532
	16	-1.7098	0.23735	0.059	-3.5074	0.0878
	17	-2.07688(*)	0.25304	0.038	-3.995	-0.1587
	18	-1.48159	0.26285	0.136	-3.4913	0.5282
	19	-1.86519	0.47337	0.429	-6.8358	3.1055
	20	-1.48987	0.18731	0.092	-3.3971	0.4174
	21	-0.17008	0.23966	1.000	-1.9831	1.6429
	22	-1.84922	0.50677	0.492	-7.3389	3.6404
	23	-2.07902	0.17646	0.058	-4.3019	0.1438
	24	-0.11606	0.28262	1.000	-2.3381	2.106
	25	-1.7801	0.35410	0.234	-4.9463	1.3861
	26	2.0995	0.43537	0.285	-2.2842	6.4832

* The mean difference is significant at the .05 level.

VITA

Miss Pilaiporn Khunathum was born on October 13th, 1981 in Roi-ed, Thailand. She received Bachelor of Pharmacy from Faculty of Pharmacy, Mahidol University in 2005. she worked as a Production pharmacist supervisor at the Vesco Pharmaceutical Co., Ltd. From 2005 – 2007.